Therapeutic drug monitoring of mycophenolic acid and *para*-cresol in human plasma and dried blood spots: analytical assay development and validation

by

Yashita Singh

A thesis submitted in partial fulfillment of the requirements for the degree of

Master of Science

in

Pharmaceutical Sciences

Faculty of Pharmacy and Pharmaceutical Sciences
University of Alberta

Abstract

Background/Hypothesis/Objectives: Kidneys are amongst the most transplanted organs in pediatric, adult, and geriatric populations. Post transplantation, the recipients are prescribed a regimen of immunosuppressants to avoid or decrease the chances of graft rejection. Mycophenolic acid (MPA) is one of the widely prescribed immunosuppressant that works as a selective and reversible inhibitor of inosine monophosphate dehydrogenase (IMPDH), thereby causing a reduction in the proliferation of T and B-lymphocytes. *p*-Cresol is a protein-bound uremic toxin (PBUTs) that is accumulated to high concentrations in patients with renal dysfunction and is primarily metabolized to *p*-cresol sulfate (*p*CS) and *p*-cresol glucuronide (*p*CG). Both *p*-cresol and its metabolites are associated with multi-organ toxicities. In this thesis, we have initially conducted a literature review that summarizes various biological matrices (i.e., dried blood spots, saliva, and urine) that have been employed for the concentration monitoring of MPA, and it was determined that dried blood spot may be a suitable alternative matrix for MPA therapeutic drug monitoring. The **overall hypothesis** of this thesis is that it is feasible to conduct MPA and *p*C TDM using highly sensitive and high throughput UPLC analytical assays in plasma and DBS. The objective of this thesis was to i) develop high-throughput ultra-high performance liquid chromatography assays for measuring MPA and *p*C in the plasma; ii) to validate these assays in human plasma in accordance with the US Food and Drug Administration (U.S.F.D.A) guidelines; and iii) to conduct a proof-of-concept feasibility study to assess the applicability of our assays using the dried blood spot (DBS) matrix.

Methods: The assays for quantifying MPA and *p*-cresol were developed on a Shimadzu® ultra-high performance liquid chromatography with ultraviolet detector (UPLC, LC-2040C Plus) coupled with a fluorescence detector (RF-20Axs) respectively. Chromatographic separation was

obtained by using a reversed-phase Agilent® Eclipse XDB-C18 column (5µm, 4.6×250mm). The detection methods (i.e., absorbance or fluorescence) and chromatographic conditions such as organic solvents (i.e., methanol or acetonitrile), additives (i.e., ammonium acetate or formic acid), mobile phase flow rate, and injection volume were systematically optimized for each compound. MPA carboxybutoxy ether and 2',6'-dimethyl phenol were utilized as the internal standards for MPA and *p*C assays, respectively.

Results: The MPA assay (final condition consisting of 40:60 acetonitrile: water, 0.1% v/v formic acid, 2 mM ammonium acetate; 0.5 mL/min flow rate; 10 µL injection volume; UV wavelengths 305 & 295 nm; run time of 24 minutes) had a calibration range in plasma between 0.3003 to 10 µg/mL (r^2 =0.99). The *p*C assay (final conditions consisted of 80:20 acetonitrile: water; 0.5 mL/min flow rate; 20 µL injection volume; excitation & emission wavelengths of 268 & 300 nm; run time of 10 minutes) had a calibration range in plasma from 0.723 to 31.25 µg/mL (r^2 =0.99). Both analytical assays could capture these analytes at their respective physiological ranges in plasma humans. The accuracy & precision values for these assays were within 15% of the nominal values, and both assays were stable at the following storage conditions: long-term (6-week for MPA and 1-week for *p*C at -80°C), benchtop (3h at room temperature), freeze-thaw (3 cycles), and autosampler (24h at 4°C). Furthermore, our validated protocols were successfully translated to the DBS matrix, and the calibration ranges for the MPA (3.794 to 28.57 µg/mL) and *p*C (0.723 to 31.25 µg/mL) assays were also linear within known physiological concentrations, illustrating a successful proof-of-concept to measure these analytes using this alternative approach for both analytes. However, further optimizations are required for the DBS matrix, including improving the assay sensitivity, precision, accuracy, and recovery for both MPA and *p*C, prior to further laboratory and clinical validation of our DBS protocols.

In **conclusion**, we have successfully developed and validated physiologically relevant analytical assays quantifying MPA and *p*-cresol with acceptable accuracy and precision in the human plasma. These assays have been successfully applied, as proof-of-concept, to a novel micro sampling matrix, DBS, proving their potential applicability in the clinic. To our knowledge, this is the first report indicating the suitability of measuring *p*-cresol using the DBS approach. These minimally invasive assays, once further validated, can have significant impacts to transplant patient care.

Preface

This thesis is an original work by Yashita Singh. Currently, there are no parts of this thesis published in peer-reviewed journals. I have submitted two abstracts to the Faculty of Pharmacy and Pharmaceutical Sciences Research Day in 2021 and 2022.

The abstract submitted in year 2021 was titled "*Development of a High-Throughput and Sensitive Ultra-High Performance Liquid Chromatography with Florescence Detection Assay for the Quantification of p-Cresol and Its Metabolites*".

The abstract submitted for year 2022 was titled "*Development and Validation of High-Throughput and Sensitive Ultra-High Performance Liquid Chromatography Assays for the Quantifications of Mycophenolic acid and p-Cresol for Drug-Interaction Studies*".

Both submitted abstracts were a collaborative effort of my supervisor, Dr. Tony KL Kiang, myself and, Dr. Yan Rong (post-doctoral fellow in Dr. Kiang's lab).

The principal investigator of this project was Dr. Tony KL Kiang who guided me through the development and advancement of this study and shared his knowledge in the field of toxicology and pharmacokinetics. No ethics approval was required for the completion of this thesis.

Dedication

This work is dedicated to my family and friends. I would like to thank my sister, Ms. Preet Kaur from the bottom of my heart, who supported me when times were challenging. She is and will always be the source of my happiness and inspiration. I would also like to thank my Mother, Mrs. Paramjit Kaur and Father, Mr. Kirpal Singh who supported my dreams and encouraged me to pursue my graduate studies in Canada. Regardless of how challenging things have been for my parents, both emotionally and physically, they have always been able to brighten my day.

I would also like extend my gratitude to each person who helped me during my journey here at the Faculty of Pharmacy and Pharmaceutical Sciences, University of Alberta.

To all the friends who I met in Edmonton, I am greatly honored to be a part of your life and will forever cherish your friendships that supported me and enabled me to successfully progress as a graduate student.

Acknowledgements

Firstly, I would also like to thank the members of my examining committee, Dr. Raimar Löbenberg, Dr. Nese Yuksel, and Dr. Mark Makowsky for sparing their precious times in reviewing, evaluating, and providing invaluable feedback regarding this work.

Also, I would like to extend my thanks to my colleague and friend, Dr. Yan Rong, in our lab for her constant support and advice. I am sincerely thankful to you for all the time and effort you have put towards my studies here as a Master's student.

I would like to thank the Faculty of Pharmacy and Pharmaceutical Sciences for accepting me into this graduate program and helping me widen my knowledge, interpersonal, communication, and teamwork skills.

Lastly, I would like to extend my deepest appreciation and most sincere gratitude to my supervisor, Dr. Tony KL Kiang, for his invaluable expertise and knowledge as well as immense guidance and support through my Master's program. I am grateful to him for giving me this opportunity to be a part of his lab group where I learned and harnessed my research skills.

Table of Contents

List of Tables

List of Figures

List of Abbreviations

AUC	area under the concentration-time curve
ACN	acetonitrile
%R.E.	[(found conc-theoretical conc)/theoretical conc * 100]
ADME	absorption, distribution, metabolism, and excretion
AR	acute organ rejection
b/w	between
F	bioavailability
BCRP	breast cancer resistance protein
CIHI	Canadian Institute for Health Information
CEDIA	cloned enzyme donor immunoassay
%C.V.	coefficient of variation
Conc	concentration
Cn	concentration at time ‘n’
CI	confidence interval
DMP	di-methyl phenol
DBS	dried blood spot
ESI	electrospray ionization
EC-MPS	enteric coated mycophenolate sodium
EDTA	ethylene diamine tetra acetate
fMPA	free fraction of MPA
GFR	glomerular filtration rate

Hct	hematocrit
HPLC	high performance liquid chromatography
HPLC-DAD	high performance liquid chromatography with diode array detector
h	hours
HCL	hydrochloric acid
∞	infinity
IMPDH	inosine monophosphate dehydrogenase
IUPAC	International Union of Pure and Applied Chemistry
LSS	limited sampling strategy
LC/ESI-MS/MS	liquid chromatography electrospray ionization with tandem mass spectrometry
LC-MS	liquid chromatography mass spectrometry
LC-MS/MS	liquid chromatography tandem mass spectrometry
Log P	logarithmic partition coefficient
LLA	lower limit of agreement
LLOQ	lower limit of quantification
Cmax	maximum concentration
MPPE	mean prediction percentage error
Cmin	minimum concentration
min	minute
sMPA	MPA levels in saliva
MMF	mycophenolate mofetil
MPA	mycophenolic acid

MPAC	mycophenolic acid carboxybutoxy ether
MPAG	mycophenolic acid glucuronide
NADPH	nicotinamide adenine dinucleotide phosphate
N	number of people in the study
Obs	observed concentration
PETINIA	particle-enhanced turbidimetric inhibition immunoassay
pCG	p-cresol glucuronide
pCS	p-cresol sulfate
Tmax	peak time
POC	point-of-care
PVDF	polyvinylidene difluoride
Pred	predicted concentration
RT	room temperature
RMSE	root mean square value
SPE	solid phase extraction
S.D.	standard deviation
SULT	sulfotransferases
TDM	therapeutic drug monitoring
tMPA	total MPA
UPLC-UV	ultra-high performance liquid chromatography with ultraviolet detection
UPLC-MS/MS	ultra-performance liquid chromatography tandem mass spectrometry
ULA	upper limit of agreement
UGTs	uridine diphosphate glucuronosyltransferases

VAMS	volumetric absorptive micro sampling
W	watts
WB	whole blood
yrs.	years

Chapter 1

1.1 Background

1.1.1 Renal transplantation

The three main components of our renal system include kidneys, ureters, and the urinary bladder [1]. Kidneys are responsible for the excretion of waste and toxins that get accumulated inside the body. For a healthy individual, the kidneys should be able to filter and excrete the toxins that are produced because of our metabolic activities. However, when the kidneys failed to function properly, transplantation may become necessary if other treatments (e.g., dialysis) cannot maintain the kidney functions. According to the statistics reported by the Kidney Foundation of Canada, 10% of the Canadian population suffers from kidney disease, and the number of end-stage kidney disease patients has increased drastically by 35% since 2009 [2]. For the patients with end-stage kidney disease, approximately 40% will end up receiving kidney transplantation [2]. In fact, renal transplantation is the most common solid organ transplantation performed in North America including Canada [2]. A total of 1,406 adult and 43 pediatric renal transplantations have been conducted as per the Canadian Institute for Health Information (CIHI) in the year 2021 [3]. Based on the data reported by the Kidney Foundation of Canada, approximately 72% of patients received organ donation from deceased donors, and the median waiting time is 3 years and 10 months [3].

After kidney transplantation, patients are required to visit their doctors as a part of the post-operative care assessment at multiple post-transplant periods (e.g., 2-3 times per week during the first month post-transplant, 1-2 times per week at 2-3 month post-transplant, 1-2 times per month at 4-6 month post-transplant, and every 4-6 weeks during 6-12 month post-transplant

[4]). During the post-transplant visits, one of the major outcomes assessed by the doctors are signs and symptoms of graft rejection [5]. Graft rejection is of major concern for kidney transplantations, as the introduction of a "foreign" kidney to the recipient can trigger the immune response which in turn causes the body to react and destroy the grafted organ. To prevent the immune system from causing graft rejection, transplant patients are prescribed immunosuppressive therapies [5]. In general, immunosuppressive therapy consisted of two types, that is, induction therapy and maintenance therapy [6]. Induction therapy could be considered as initial treatment that are given to significantly suppress the immunosuppression system and is given to the transplant patients as soon as they receive the tissue/organ in order to decrease the risks of acute organ rejection (AR) [5]. On the other hand, the maintenance anti-rejection therapy is administered throughout the entire life of the transplant recipients, maintaining the grafted organ/tissues [5]. The most prescribed maintenance immunosuppressants for kidney transplant patients include mycophenolic acid (MPA), tacrolimus or cyclosporin A, sirolimus, and Everolimus [7]. Today, the most used immunosuppressants in Canada are MPA in combination with tacrolimus, given with or without corticosteroids [8]. However, proper dosage regimen needs to be followed since excess immunosuppression could also lead to the individual being at a higher risk of getting other infections or more severe consequences, such as cancers [9].

Overall, there have been significant advancements in the field of renal transplantation that have led to higher patient compliance and overall survival rate. Moreover, pharmacotherapy has become the cornerstone of anti-rejection management. However, therapeutic drug monitoring of immunosuppressants is still warranted for optimizing the precision dosing of these drugs, to improve the efficacy, minimize side effects, and monitor potential drug interactions, thereby further improving the quality-of-life of transplant patients.

1.2 Mycophenolic acid

1.2.1 Drug regimen and use in clinics

Immunosuppressants are widely prescribed to patients after solid organ transplantation, which can reduce the host body's ability to reject the new grafts. Nowadays in Canada, MPA (the chemical structure as shown in Figure 1.1), in combination of tacrolimus, with or without corticosteroids are the most prescribed immunosuppressive regimens to the kidney transplant patients[10]. Specifically, MPA is commercially available in two oral formulations, mycophenolate mofetil (MMF) and enteric coated mycophenolate sodium (EC-MPS). Upon oral administration, both formulations release the active MPA extensively, which acts as a selective and reversible inhibitor of inosine monophosphate dehydrogenase (IMPDH), thereby causing a reduction in the proliferation of T and B-lymphocytes [11]. The MMF formulation is supplied as 250 mg capsules, 500 mg tablets, and a powder for suspension (200 mg/mL when dissolved) [11]. To increase the patient compliance in situations where the patient has difficulty taking the oral drug (e.g., in a coma), MMF can also be given via the intravenous (i.v.) route. On the other hand, EC-MPS is typically available in 180 mg or 360 mg tablets [11].

The dose of MPA varies based on the type of transplantation [11], for example, the dose recommendation for adult liver transplant recipients is 1g of MMF twice a day i.v. or 1.5g oral MMF twice a day. For heart transplant recipients, MMF is recommended to be used as a 1.5g i.v. dose or an oral dose of 1.5g two times a day. For adult kidney transplant recipients, a dose of 1g of MMF two times daily or a 720 mg dose of the EC-MPS two times daily should be administered. For pediatric transplant patients, MMF is administered as an oral 600 mg/m^2 suspension to be taken twice a day [12]. The dosing guidelines of MPA for kidney transplant

recipients are usually standardized/empiric across the different transplant centers but can be varied with physiological factors and specific patient demographics (e.g., age, sex, other health conditions, medical history, genetics etc.).

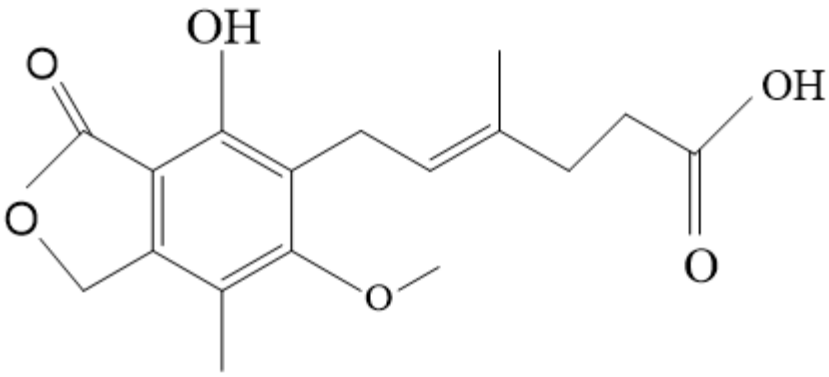

Figure 1.1 The chemical structure of mycophenolic acid (MPA)

1.2.2 Other indications of mycophenolic acid

According to *Jayne* [13], MMF has other off-label usages in addition to its primary indication as immunosuppressants post-transplantation. MMF has shown better efficacy in a clinical model for the treatment of lupus nephritis in comparison to azathioprine or cyclophosphamide that have higher toxicities [13]. MMF can also be used to treat conditions including rheumatoid arthritis, psoriasis, inflammatory eye diseases, etc. [13]. Additionally, MMF is also used for the treatment of Crohn's disease as compared to the much more toxic azathioprine [13].

The use of MPA has increased over the years owing to its efficacy and safety over other agents such as azathioprine [14]. However, MPA is associated with large pharmacokinetic

variability (i.e., up to 10-fold in exposure is commonly observed [11] in patients prescribed the same dosage). Various factors have been correlated with MPA pharmacokinetic variability (see section 1.2.3.2). In addition, MPA can be associated with frequent and serious adverse effects such as gastrointestinal disorders, hematological toxicity, and infections (see section 1.2.3.1.1).

1.2.3 Pharmacology of mycophenolic acid

According to *Currie et al.* [15], *"Pharmacology is the scientific study of the action and effects of drugs on living systems and the interaction of drugs with living systems"*. To explain it briefly, pharmacology can be divided into two major categories – pharmacodynamics and pharmacokinetics. Pharmacodynamics is the study of what the drug does to the body, whereas pharmacokinetics is the study of what the body does to the drug. A few other branches of pharmacology include pharmacogenetics, pharmacogenomics, pharmacoepidemiology, pharmacoeconomics, and lastly pharmacovigilance [15]. In this thesis, pharmacodynamics and pharmacokinetic will be discussed in detail as below.

1.2.3.1 *Pharmacodynamics of mycophenolic acid*

When a drug is administered, it goes into the systemic circulation where it undergoes various processes of drug disposition including absorption, distribution, metabolism, and excretion (which will be discussed in the following section 1.2.3.2). These processes together convert the drug into its active form which then binds to the receptors in the body thereby forming a receptor-drug complex and activating or initiating their therapeutic effects [15]. The drug causes immunosuppression in the body by acting on IMPDH enzymes. According to *Jayne*

et al. [13], the enzyme IMPDH-2 particularly is essential for the *de novo* synthesis of guanine nucleotides in T and B-lymphocytes. When the enzyme IMPDH is inhibited by MPA, the nucleic acid synthesis ceases since the proliferation of the lymphocytes is inhibited [13]. This in turn helps the host body get adjusted to the new graft and therefore prevent rejections by the host body.

To explain the *de novo* synthesis in detail, *Allison et al.* [14] explained that the ribose-5P in the system gets converted to 5-phosphoribosyl-1-pyrophosphate (PRPP) which further forms inosine monophosphate (IMP). Now, IMP gets converted to guanosine monophosphate (GMP) mediated by IMPDH enzymes, which is the key compound in the formation of DNA, RNA, and proteins. MPA works by inhibiting the IMPDH enzymes and hence causes a cessation in the formation of downstream proteins [14]. An increased expression of IMPDH has been observed in patients who have been taking MMF for a long time [11]. To optimize the biological activity of IMPDH inhibitor (i.e., MPA), dose optimization/individualization of mycophenolate therapy should be conducted based on the IMPDH activities. However, to date, monitoring of IMPDH enzyme activities is not a part of the routine care due to the technical difficulties [10]. there has been no study that has been successfully conducted on using IMPDH activity for MPA TDM [11].

1.2.3.1.1 Side effects of prescribing mycophenolic acid

Kitchin et al. [16] explained that the treatment therapy of MPA has some adverse outcomes including the effects on gastrointestinal tract (GIT), genitourinary, hematological, infections, carcinogenicity, and teratogenicity over extended usage. These effects are explained further below:

- GIT effects include the effect on the gut which can range from nausea, diarrhea, abdominal cramps to anorexia, vomiting, and anal tenderness. However, these effects also depend on the dose being given and the dosage form [16].
- Genitourinary effects include a general feeling of uneasiness, urgency, dysuria and burning sensation while urination [16].
- Hematologic effects affect the blood cells. MPA causes a decrease in the number of leukocytes, erythrocytes, and thrombocytes which further leads to a weakened health condition [16].
- Infections are highly prominent in patients who are being prescribed MPA. MPA works by non-selectively inhibiting the enzyme IMDPH which is responsible for the proliferation of T and B-lymphocytes. Since there is an overall decrease in these lymphocytes, the immune system becomes weaker which is ideal for accepting a new graft organ. However, this weakened immune system can lead to the body being more prone to infections. *Kitchin et al.* indicated that the number of viral and bacterial infections tend to increase when the patients are prescribed immunosuppressants such as MPA [16].
- Carcinogenicity and teratogenicity of MPA has not yet been proven, but the drug has the potential to be a carcinogen. There have been no studies done in pregnant women and so the teratogenic nature of the drug cannot be proven/explained [17].

1.2.3.2 *Pharmacokinetics of mycophenolic acid*

Pharmacokinetics is the study of the effects on the drug caused by the biological reactions in the body [18]. Pharmacokinetics of the drug or its metabolite(s) includes absorption,

distribution, metabolism, and excretion (or "ADME"). Immunosuppressants have been a topic of interest in the field of clinical pharmacology since they possess high pharmacokinetic variability and hence require therapeutic drug monitoring or dose optimization/individualization [8]. MPA is one of the immunosuppressants that is clinically used for kidney transplant patients and patients with lung or liver transplants. Pharmacokinetic evaluation of a drug can be done by characterizing the following parameters:

- ***C_{max}***: This is the maximum concentration that the drug or its metabolite can achieve in the blood or plasma via the systemic circulation [15]
- ***T_{max}***: This is the time that is required to achieve the maximum concentration of the drug or its metabolite in the systemic circulation [15]
- ***C_{min}***: This is the minimum observable concentration in the plasma after the drug is administered [15]
- ***AUC***: This is the area under the drug concentration-time curve [15]
- ***C_n***: Here, C refers to the concentration of the drug and/or its metabolite at any given 'n' time in the plasma. It can range from C_0 (concentration at the time 0 or at the start of drug administration, also known as the trough concentration) to C_1 (concentration after 1h of drug administration) and so on [15].

  The pharmacokinetics of MPA are as discussed below.

1.2.3.2.1 Absorption

MMF, when given through the oral route is extensively absorbed into the systemic circulation [11]. According to *Staatz et al.* [11], when MMF is administered to the patients, it

undergoes hydrolysis by esterases and gets converted to the active form MPA in the blood, tissues, stomach, and small intestine. Since MMF gets absorbed readily, it is not traceable in the plasma upon 10-30 minutes after an i.v. administration. Consistently, *Fulton et al.* [19] also indicated that MMF is rapidly absorbed and gets converted to MPA, hence the parent drug MMF is not measurable in the systemic circulation, whereas MPA can be measured for clinical purposes. The C_{max} of MPA is typically within 0.5-1 hour upon administration [11]. On the other hand, the absorption profile for EC-MPS is different than MMF, likely due to the enteric-coating, which releases MPA primarily in the small intestine [11], therefore, the T_{max} of MPA from EC-MPS is around 1.5 to 6 hours [11]. The C_{max} of MPA after given EC-MPS is approximately 10-18% lower compared to MMF [11]. It has also been reported that the AUC and the C_{max} of MPA in the stable renal transplant patients is 50% higher than in the patients who have had a recent renal transplantation [18]. In addition, bioavailability is defined as the fraction of the drug and/or its metabolite that reaches the systemic circulation after the drug has been administered.[20] The bioavailability of MPA is very high, that is 94% in healthy volunteers post MMF administration [11], whereas MPA bioavailability in kidney transplant patients is ~81% [11].

1.2.3.2.2 Distribution

Once the drug is absorbed in the system, it is then distributed in accordance with the extent of its binding to the serum albumin [11]. *Fulton et al.* mentioned that MPA binds to the serum albumin more at a lower drug concentration [19]. MPA and its glucuronide metabolite mycophenolic acid glucuronide (MPAG) have both shown to possess a high binding capacity of 97%-99% and 82%, respectively, to the serum albumin. The binding capacity of MPA also depends on the patient's time post-transplant, that is, a high binding capacity has been observed

in patients that have a longer time post-transplant as compared to the patients who just received a transplant [11]. MPA only binds to the serum albumin and not to the α1-1 acid glycoprotein [11]. However, this binding can also change depending on the health of the patient (e.g., hepatic diseases and renal dysfunction) [11]. When MPA reaches the systemic circulation (i.e., the whole blood), 99.99% gets distributed in the plasma compartment of the whole blood whereas only 0.01% of the drug goes to the remaining cellular compartments (e.g., erythrocytes, leukocytes, and thrombocytes) [21]. This is also one of the main reasons why the measurement of MPA and MPAG has more clinical relevance in the plasma. Of note, only the free form of MPA can undergo further metabolism and excretion, mediate the pharmacological effects by inhibiting IMPDH enzyme, and hence prevent the proliferations of T and B-lymphocytes [11].

1.2.3.2.3 Metabolism

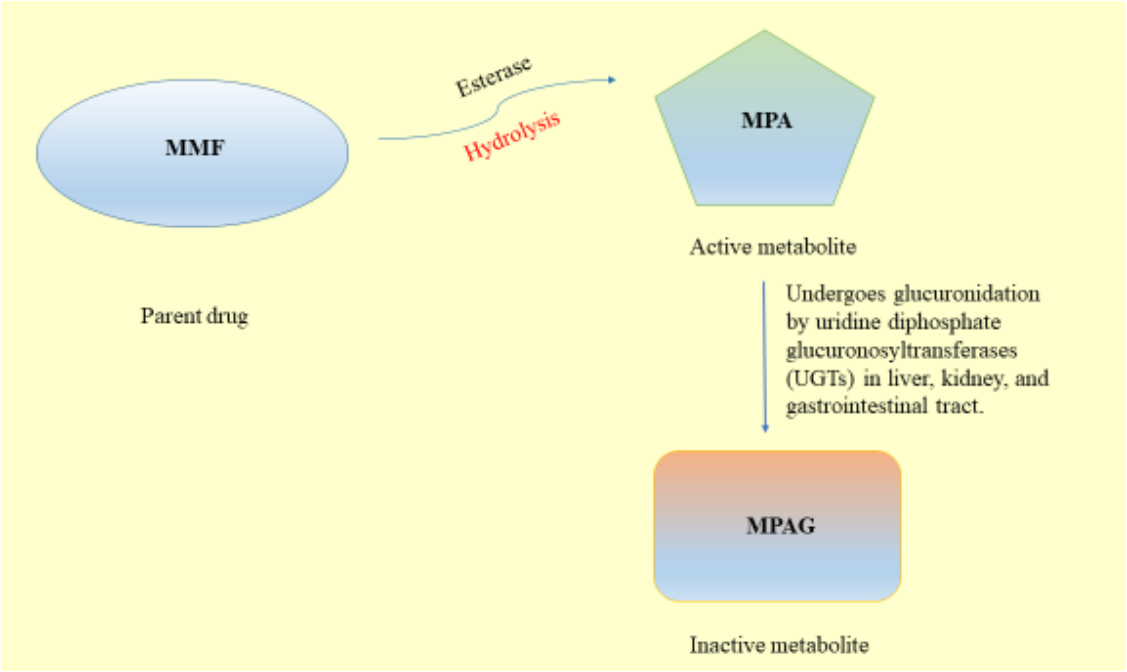

Figure 1.2 The metabolism pathway for mycophenolate mofetil as explained by Fulton et al. (Figure illustrated by Yashita Singh)

Fulton et al. [19] explained that when MMF is administered to the patient, it undergoes hydrolysis by the action of esterase and gets converted to the active metabolite, MPA. Since MPA is a hydrophobic compound, it needs to be further metabolized to increase its solubility. This is the process by which MPA is converted to the major, inactive metabolite MPAG by the action of uridine diphosphate glucuronosyltransferases (UGTs) enzymes in the liver, GIT, and kidneys (*as explained in the figure 1.2 above*). In addition, MPA is also metabolized to the minor, active metabolite mycophenolic acid acyl glucuronide (AcMPAG), and to the minor, oxidative metabolite, 6-O-desmethyl-mycophenolic acid (DM-MPA). The metabolism of MPA to MPAG is primarily mediated by UGT1A9 enzymes (which corresponded to 55%, 75%, and 50% of the metabolism in the liver, kidney, and intestines [22]) and through UGT1A7, UGT1A8, and UGT1A10 enzymes with less contributions [11]. On the contrary, the formations of AcMPAG and DM-MPA are mediated by UGT2B7 and cytochrome P450 (CYP)3A4/5 enzymes, respectively [11]. In the plasma, MPAG as the most abundant metabolite, is 20-100 times more prevalent as compared to MPA [11]. On the contrary, AcMPAG is only found at ~10% of the plasma concentration of MPA [11]. However, AcMPAG also inhibits IMPDH and helps prevent the proliferation of T and B-lymphocytes [23]. Moreover, AcMPAG can also generate side effects as it binds covalently to the DNA, proteins, and lipids in the body and thus cause tissue damage [11]. For patients who are administered MMF for a long term, AcMPAG can accumulate in the body and cause allergic reactions and drug toxicity [11]. *Staatz et al.* [11] also mentions that AcMPAG tends to initiate/promote the release of the cytokines as well as the process of cytokine mRNA expression in the blood cells.

1.2.3.2.4 Excretion

MPA is excreted primarily via urine, i.e., ~ 93% in the form of MPAG, and only 0.6% and 0.3% of the drug are in the form of MPA and AcMPAG; the rest of ~6% is excreted through feces [24]. This data was based on 4 healthy male volunteers taking radiolabeled MMF (i.e., mycophenolate-14C mofetil) in whom blood, urine, and fecal samples were collected [24]. Human renal organic anion transporter 3 (OAT3) and multidrug resistance associated protein 2 (MRP2) are considered to facilitate the excretion of MPAG into the urine [25-27]. Human OAT3 transporter is located on the basolateral membrane of renal proximal tubular cells and responsible for MPAG uptake from the systemic circulation into the cells [27]. Human MRP2 is located on the apical membrane and responsible for MPAG efflux from the renal proximal tubular cells into the urine tubules [25, 26]. In addition, *Staatz et al.* mentioned that MPA is subjected to undergo enterohepatic recirculation [11]. This is because the gastrointestinal bacteria produce glucuronidase enzyme which interacts with the MPAG in the system and converts it back to MPA via deconjugation process and hence causes the reabsorption of MPA into the colon [11]. This could be the reason why there is a second peak in the plasma concentration-time profiles observed for MPA at 6-12 hours post-drug administration [11]. This entero-hepatic recirculation process can explain ~40% of the total MPA exposure [11, 25]. Multiple transporters are involved in the enterohepatic recirculation process, e.g., organic anion transporting polypeptides 1B1/3 (OATP1B1/3), which are possibly responsible for the uptake of MPAG into the hepatocytes from the sinusoidal membrane [28-31]; and MRP2 [32-38] and/or breast cancer resistance protein (BCRP) transporters [30], which are responsible for excreting MPAG into the bile at the canalicular membrane [25-27]. MPA has an apparent half-life of 17.9

h with a clearance of 11.6 L/h when given through the oral route in patient populations with chronic renal insufficiency [18].

1.3 *p*-Cresol

1.3.1 Uremic toxins

In patients with chronic kidney disease, the renal capacity decreases significantly owing to several factors such as underlying health conditions (e.g., diabetes, hypertension, or a cardiovascular disease), smoking, family history of chronic kidney disease, or a congenital defect in the organ(s) [39]. This can lead to the body not being able to eliminate or excrete toxic metabolites and hence causing accumulation of a group of uremic retention solutes (or called uremic toxins) in the body [40]. According to *Cunha et al.* [41], most uremic toxins are the by-products from the metabolism of food and/or nutrients, which are accumulated in the body because of impaired renal function [40, 42]. Uremic toxin is a topic of interest recently, as it is associated with various toxicities in kidneys, heart, liver, blood vessels, and skins [40, 42]. According to *Cunha et al.* [41], uremic toxins can be divided based on their molecular weight and physiochemical characteristics: a) protein-bound uremic toxins (typically very low molecular weight less than 500 Daltons); b) middle molecules (with molecular weight greater than 500 Daltons); and c) small water-soluble compounds (molecular weights less than 500 Daltons). *Cunha et al.* [41] explained that the protein-bound uremic toxins are difficult to remove via dialysis alone since they have low molecular weights and are extensively bound to plasma proteins [42]. Protein-bound uremic toxins include indole acetic acid (IAA, Figure 1.3), indoxyl sulfate (IS, Figure 1.4), and *p*-cresol (*p*C, Figure 1.5).

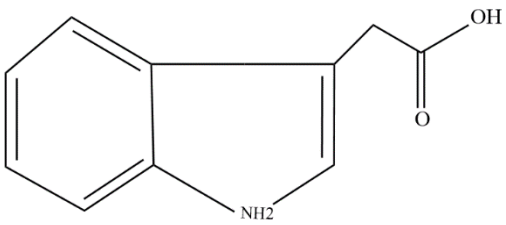

Figure 1.3 Chemical structure of indole acetic acid (IAA)

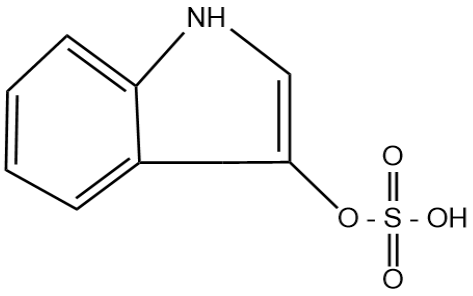

Figure 1.4 Chemical structure of indoxyl sulfate (IS)

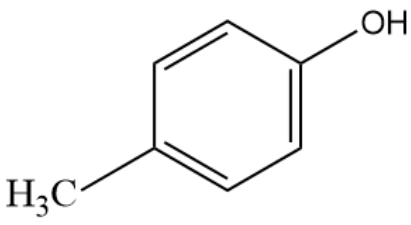

Figure 1.5 Chemical structure of p-cresol (pC)

The accumulation of large amounts of protein-bound uremic toxins may lead to severe consequences, for example, arterial stiffness, bone disease, diabetic nephropathy, cardiovascular disease, endothelial dysfunctions, inflammation, neurotoxicity, oxidative stress, renal tubule damage, and ultimately death [43, 44]. In addition to the above physiological consequences, protein-bound uremic toxins can potentially lead to alterations in the metabolism enzyme and transporter activities [40].

1.3.2 *p*-Cresol and its metabolites

*p*C is a prototypical protein bound uremic toxin that is derived from dietary amino acids (e.g., tyrosine and phenylalanine) metabolism by anaerobic bacteria in the large intestines [45, 46]. *Rong et al.* [47] explained that *p*C can be accumulated in the body when the renal functions are suppressed/insufficient. The failure to successfully remove these toxins from the body could be either because of a higher production by the intestinal bacteria or a reduced rate of elimination from the kidneys [47]. *p*C has a molecular weight of 108.1 Da and is a phenolic protein-bound uremic toxin. According to *Vanholder et al.* [46], *p*C possesses a very strong affinity to plasma proteins (about 100%) which makes it difficult to remove by dialysis [39]. *Gryp et al.* [45] explains that liver and colon are the main organs responsible for the detoxification of *p*C. *p*C primarily undergoes extensive first-pass metabolism in the formation of *p*-cresol sulfate (*p*CS, in a large amount [e.g., >90 [48]], through sulfonation pathway, Figure 1.6) and *p*-cresol glucuronide (*p*CG, in a small amount [e.g., <5% [48], Figure 1.7) [45].

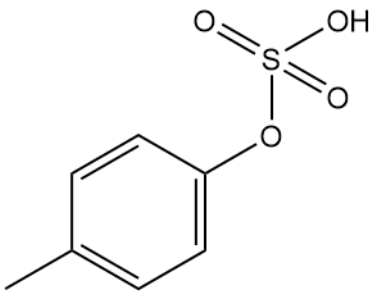

Figure 1.6 Chemical structure of p-cresol sulfate (pCS)

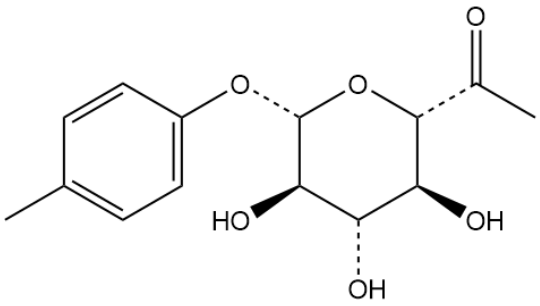

Figure 1.7 Chemical structure of p-cresol glucuronide (pCG)

As the major metabolite, *p*CS has a molecular weight of 188.2 Da and is ~95% bound to the plasma albumin proteins [45]. *Gryp et al.* [45] summarized that *p*CS could lead to the reduction of nicotinamide adenine dinucleotide phosphate (NADPH) oxidase and increase in the generation of reactive oxygen species (ROS) in cardiac muscle cells which ultimately leads to cardiomyopathy [49]. Hence, *p*CS have been reported to be among one of the causes of cardiovascular diseases in chronic kidney disease patients [45]. Apart from that, *Cunha et al.* [41] also mentioned that *p*CS cause a decline in the production of nitric oxide, which in turn increases the levels of ROS and leads to oxidative stress. *p*CS is also known to cause endothelial

dysfunction [41, 45] that progresses to endothelial structural damage and an increased release of the proinflammatory mediators. In addition, *p*CS also has been shown to hinder the natural glucose metabolism of the body, thereby leading to diabetes and improper glycolysis and glycogenesis [45]. On the other hand, *p*CG as the second major metabolite of *p*C, is mainly found as unbound form in the plasma, with protein binging of <10% [50]. *p*CG also exhibited negative biological effects in multiple in vitro/ex vivo models, e.g., damaging cellular structure of human kidney proximal tubular epithelial cells [51], inducing endothelial-to-mesenchymal transition in human kidney proximal tubular epithelial cells [52], reducing cell viability in HepaRG cells [53], and altering the mitochondrial membrane potential in primary cultures of human hepatocytes [54]. In addition, both *p*CS and *p*CG have been associated with increased cardiovascular and renal toxicities and overall mortality in the clinical studies, especially in chronic kidney disease patients [45].

1.3.3 Metabolism pathways of *p*-cresol

As *p*C is found in the forms of *p*CS and *p*CG in the human plasma, the responsible metabolism enzymes were characterized using human cytosols/microsomes and human recombinant sulfotransferases (SULT) or UGT enzymes [55, 56]. Based on *Rong et al.*, human SULT1A1 was identified the primary enzyme responsible for the formation of *p*CS, and human UGT1A6 showed the highest catalytic activities toward the generation of *p*CG [55, 56].

1.3.4 Detoxification of *p*-cresol and its metabolites

Since various toxic effects have been observed for *p*C and its metabolites, *Meyer et al*. [57] suggested that *p*C can be eliminated from the body by means of external agents (such as adsorbents, laxatives, and probiotics). These approaches are through reduction in the absorption of *p*C and its metabolites. On the other hand, another way to improve the elimination of uremic toxins such as *p*C is with the use of hemodialysis. Hemodialysis is an option for the elimination of water soluble uremic solutes, however, the efficiency of the elimination towards protein-bound uremic toxins such as *p*C and its metabolites is limited and depends on the nature of the solute [57]. According to *Meyer et al.*, the protein-bound uremic toxins can be removed via dialysis by means of increased dialysate flow and its size [57]. Additionally, employing a high-volume ultrafiltration with hemodialysis and using adsorbents like AST-120 can further lead to an enhanced elimination of uremic solutes without the need of repetitive hemodialysis sessions [57].

1.3.5 Uremic toxicity of *p*-cresol

*p*C is a lipid soluble protein bound uremic toxin that is difficult to remove via conventional method of dialysis and hence gets accumulated in the body [46]. Once this happens, this PBUT causes several adverse effects inside the body such as:

- An increase in the oxidative stress and inflammatory responses that ultimately lead to ageing and organ failure [58]. The mechanism behind this is that uremic toxins such as *p*C leads to the generation of reactive oxygen species (ROS) that is damaging to the tubular cell generation and hence affects the cell cycle in the G2 phase [58].

- *p*C and *p*CS get accumulated in the body and cause renal impairment and ultimately failure. This occurs when the expression of methyltransferases has increased in the DNA, which leads to the klotho gene hypermethylation thereby suppressing its expression.
- *Vanholder et al.* [59] mentioned that the in-vitro toxicity of aluminum in the liver and neuroblastoma cells has likely been due to the accumulation of *p*C and that the uremic toxins has been observed to increase this incidence of aluminum toxicity.
- Certain negative cardiovascular effects of *p*C include anemia, blood coagulation, immune dysfunction, hypertension, insulin resistance and other vascular diseases [60].
- The free *p*C exhibits a similar behavior as *p*CS and is therefore responsible for the cardiovascular ailments, increased occurrence of infectious diseases and ultimately senescence [60].

1.4 Interaction between mycophenolic acid and *p*-cresol

MPA is an immunosuppressant that is widely prescribed to kidney transplant patients, and *p*C is a phenol-based protein bound uremic toxin that is known to get accumulated in the body due to a higher generation and reduced elimination [11, 58]. MPA is primarily metabolized in humans via UGT1A9 glucuronidation pathways, and *p*C is known to be a potent inhibitor towards human UGT1A9 enzymes [47, 61]. The inhibitory effects of *p*C towards metabolism of MPA were characterized by *Rong et al.* using a translational approach [47, 61, 62]. The inhibitory effects of *p*C on the glucuronidation of MPA were determined in HepaRG cell line (i.e., a human hepatoma model), human liver microsomes, and cDNA-expressed human enzymes. The identified inhibitory concentrations of *p*C were physiologically attainable in adult

kidney transplant patients, suggesting that fluctuations in *p*C concentrations may be partially responsible for the large variabilities of MPA observed in the clinic. In addition, the interaction between MPA and *p*CS (the major metabolite of *p*C) was investigated in adult kidney transplant recipients within the first-year post-transplantation. Significant positive correlations were observed between the total MPA trough concentration and the plasma *p*CS concentration in a prospective, observational study [62]. These clinical findings confirmed a role of *p*C as a significant clinical variable affecting the pharmacokinetics of MPA in patients [62].

1.5 Therapeutic drug monitoring

As Paracelsus said, "*All things are poisons, for there is nothing without poisonous qualities. It is only the dose which makes a thing poison* [63]." Therapeutic drug monitoring (TDM), as the name suggests, is the monitoring of drugs that are being prescribed to the patients to achieve maximum therapeutic effect while keeping the drug levels within the safety window [64]. Dose individualization is an absolute necessity when the drug being prescribed to the patient needs to be monitored regularly and TDM is always employed for this purpose [64]. TDM plays an important role for various patient populations, such as those with a recent transplant, patients with chronic diseases (cancer, diabetes, etc.), pediatric population, and for the patients who have limited to no access to the healthcare facilities.

According to *Zwart et al.* [8], TDM is necessary in patients with transplant surgeries because of their wide pharmacokinetic variabilities. For the transplant patients, the main goal is to prevent graft rejection and to further keep the levels of the drug within its therapeutic window (therapeutic window is the range within which the drug levels are safe and effective with the

maximum therapeutic effect) [8]. For MPA, the TDM is generally based on the area under the concentration-time curve for understanding the pharmacokinetics of the drug [8].

Dose individualization is one parameter in TDM along with a few others, such as the age and sex of the patient, racial characteristics, biological functions of the drug user, time post-transplantation (in case of transplant recipients), and current drug regimen [8]. TDM has opened newer pathways to provide the best possible treatment plan for the patients to improve the quality of life for them.

1.5.1 The purpose of therapeutic drug monitoring

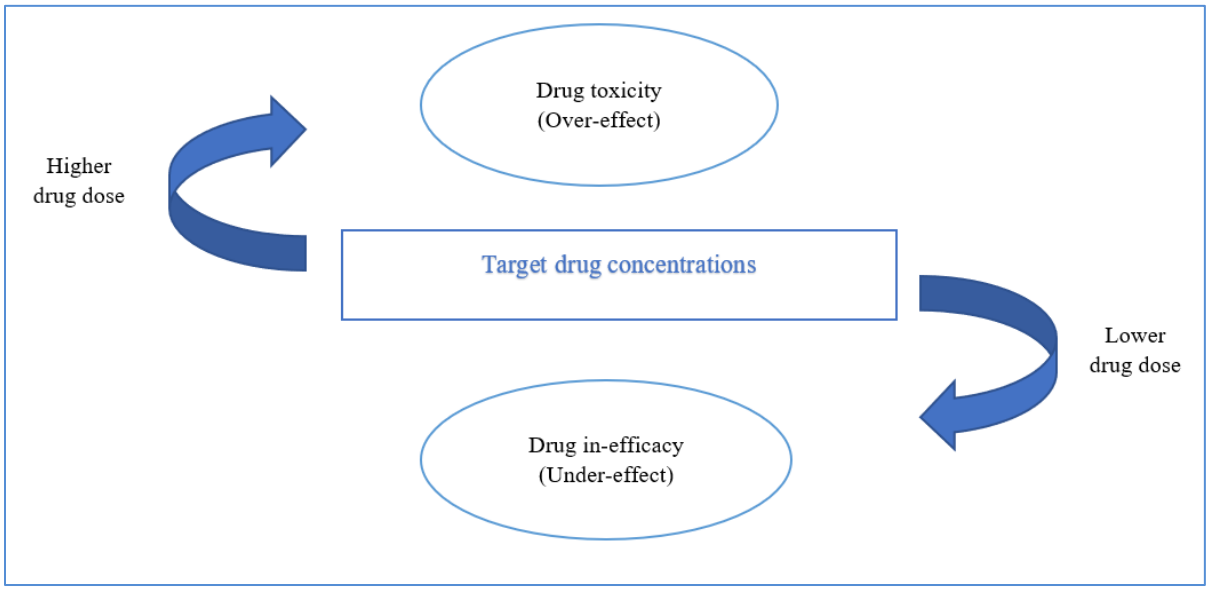

Figure 1.8 The flowchart above shows the effect of prescribing a drug under and over the therapeutic dose [64]. (Figure illustrated by Yashita Singh)

As discussed above, TDM is essential when it comes to monitoring of drugs in patient populations with large pharmacokinetic variabilities, for the drugs that have a narrow therapeutic window, and for the purpose of dose individualization [8]. *Kang et al.* [64] explains that TDM is a collaborative effort of all the people working in a clinical setting, to ensure that the patient receives the adequate treatment plan that is both safe and effective. The purpose of TDM can be explained as follows [64].

- To establish a standard treatment regimen for the patient, while keeping in mind various factors that can vary from one patient population to another (including patient demographics such as age, sex, race, bodily function(s), diet, pre-existing health conditions, and pre-existing drug regimen) [64].
- To achieve higher patient compliance. An adequate treatment plan might have better outcomes (in terms of prevention and cure) and thus will be better tolerated by the patient [64].
- Less chances of drug-drug interactions and toxicities. It may be possible that the patient is administered multiple drug regimens at the same time and has a higher chance of showing drug incompatibilities that could lead to under-effect or even no effect of the new drug. Hence, TDM is an excellent approach that can help clinicians to better understand the various drug regimens and prescribe them all at the same time in the best possible way [64].
- Discontinuing the drug therapy can often lead to unforeseen or adverse effects. In this case, TDM can help to monitor the unpredictable effects of discontinuation of the drug therapy and therefore make it possible for the clinicians to explore an alternative to it [64].

- Monitoring the plasma concentration has also been very useful for TDM. When the drug is administered to the patient, it gets absorbed into the systemic circulation and ultimately reaches the blood and plasma. This makes blood and plasma good matrices for monitoring the levels of the drug at any given time. Plasma drug concentration monitoring ensures that the patient is not being undertreated [64].
- TDM is also employed for monitoring the drugs with a narrow therapeutic window (such as digoxin and lithium) and therefore helps the clinicians to adjust the treatment therapy accordingly [64].

According to *Kang et al.* [64], plasma concentration monitoring is a tool by which the clinicians can adjust/modify the treatment regimen and the dose for the patients, to avoid any chances of drug toxicity or under-exposure. However, at times the toxicity does not need the plasma concentration measurement and can be assessed based on the symptoms that the patient exhibits.

1.5.2 Advantages and disadvantages of therapeutic drug monitoring

Zwart et al. [8] mentions that TDM as an approach to monitor the drugs in the body helps establish an individualized drug therapy catered to the patient's medical needs. This way, the clinicians can avoid any chances of toxicity or under-dosage in the treatment therapy. TDM is often based on the AUC that requires sampling from the patients over the entire dosing period, however, limited sampling strategy (LSS) can often reduce this need of sampling over a long time by decreasing the number of samples to be taken [65]. Similarly, TDM is also considered economically more effective since the use of this approach on patients will help prevent chances

of drug toxicity, under-dosage, predict the unforeseen adverse effects and monitor the body for other drug-drug interactions and therefore decrease the number of hospitalizations [65]. However, venous sampling, the most common TDM approach, is a very invasive method of sampling that needs highly trained professionals for sample collection and causes pain and unpleasantness to the patient. Other methods such as dried blood spotting (DBS) just requires a simple finger prick to collect the sample and can be done by the patient themselves. Venous sampling can also lead to iatrogenic infections and therefore decrease patient compliance [66].

TDM has always been a helpful means to optimize drug therapy in patients; however, it also has equal demerits as well. TDM is an excellent approach for the clinicians to study the behavior of a drug but may be inconvenient for the patients. This is because the patients may have to spend long hours at the clinics for the sampling to be done effectively and to minimize the diurnal errors [8]. To amend this and make the patient's experience better, various micro sampling approaches such as dried blood spots (DBS), volumetric absorptive micro sampling (VAMS) etc. can potentially minimize the drawbacks of conventional TDM, but more scientific evidence is required on these alternative approaches to be accepted and employed in the clinical setting [8]. Additionally, for the plasma drug concentration measurement, precautions need to be taken before, during and after the sample collection to eliminate any chances of errors [64]. The TDM for any drug requires the use of analytical assays that need to be accurate and precise (in accordance with regulatory associations such as the FDA) to be used clinically [64].

1.5.3 Current usage of therapeutic drug monitoring in the clinics

TDM is often based on AUC when it comes to immunosuppressants such as MPA [11]. This in fact requires the presence of patients at the clinics for long hours to facilitate proper sample collection and routine monitoring [67]. To make this feasible and convenient for the patients, newer sampling techniques such as DBS and VAMS have been introduced in clinics and hospitals, which help increase patient compliance [67].

These novel TDM approaches still need more scientific validation to be employed in the clinics and/or commercially. The conventional TDM approaches for monitoring drug concentrations are based primarily on, firstly, the analytical chromatographic assays, e.g., high performance liquid chromatography (HPLC) coupled with tandem mass spectrometry (LC-MS/MS); secondly, the IMPDH based enzyme inhibition assays (e.g., for MPA); thirdly, immunoassays such as cloned enzyme donor immunoassay (CEDIA) or particle-enhanced turbidimetric inhibition immunoassay (PETINIA) etc. [10]. The use of analytical, enzymatic, or immune assays and the respective detection methods depends on the biochemical nature of the drug [10].

Novel micro sampling techniques such as DBS and VAMS have the potential to be employed as point-of-care (POC) testing tools that may allow the patient to do the sampling by themselves, without the need of going to a clinic [8,67]. POC is an extremely useful approach in scenarios where the patients are not in a physically healthy condition to make it to the clinics, for the patients who have transportation issues (rural areas and smaller communities) and are unable to visit the clinics for regular monitoring, or in pediatric and geriatric patient populations who have limited blood/plasma volumes for sampling [67].

Overall, TDM is currently being employed in the clinics for the management of, as examples, immunosuppressants, lupus nephritis, inflammatory bowel disease, congenital disease screening in newborns, colitis, certain type of cancers, and specific drugs with narrow therapeutic window (such as digoxin and lithium etc.,) [8, 10, 64, 65, 67].

1.6 Literature review of alternative therapeutic drug monitoring approaches for mycophenolic acid

1.6.1 Therapeutic drug monitoring of mycophenolic acid

van Gelder et al. [68] explained that MPA exhibits a wide pharmacokinetic inter- and intra-variability, and this is where TDM can help in adjusting or altering the treatment regimen to improve outcomes. The chances of organ rejection after a solid organ transplant are highest in the first month post-transplantation [68]. *van Gelder et al.* also mentioned that MPA AUC estimation is a better TDM approach as compared to measurement of MPA trough concentrations but is not practically feasible nor convenient for the patients. A MPA AUC of 30 *mgh/L* – 60 *mgh/L* has been proposed as the target range in kidney transplant patients [68]. The estimation of the dose range or regimen using the AUC from the patient's data can be achieved by employing the Bayesian estimation methods, that have the following advantages over the conventional AUC and/or trough concentration measurement [68]:

- Irregular sampling times are not a limiting factor here for the Bayesian approach
- Accuracy is higher using Bayesian estimators as compared to models with multilinear regression equations.

- Bayesian estimation provides the data for complete AUC, therefore helps in identifying the appropriate treatment plan.

A TDM testing centre in France has employed the Bayesian estimator approach with several limited sampling strategies with suitable predictive performance as evident by bias of <10% [68]. For the TDM of MPA, it is recommended to start the sampling and monitoring at days 3-7 and then days 10 -14 post-transplantation (with a dosing of MMF 1.5 g twice a day) [68]. Additionally, TDM can be repeated at 3-4 weeks post-transplantation assuming the immune responses are normal, however, in case of a possible graft rejection (as observed by patient's vital functions), TDM needs to be repeated [68].

As discussed above, conventional sampling of MPA using plasma samples has several limitations. To find other matrices / approaches for MPA TDM that are less invasive, the literature was reviewed systematically, with reference to dried blood spots, saliva, and urine, which have been considered as possible alternatives for MPA.

1.6.2 Methodology to identify alternative approaches for mycophenolic acid therapeutic drug monitoring

An extensive search was conducted in PubMed and EMBASE, using the following keywords (and their combinations) - mycophenolic acid, dried blood spot(s), saliva, and urine. There was no time limit set for this review, however the articles were screened up until April 2022. A total of 73 articles were screened, out of which 14 were left after the final screening (Figure 1.9). The articles mentioned in the references of the chosen studies were also manually screened. Articles that were in any language apart from English were not included, and the same

applied to the articles that did not have human data. Other matrices such as interstitial fluid, peripheral blood mononuclear cells (PBMC), vitreous humour, tissue extract, and ultra-filtrate were screened but not included because they were considered invasive methods. Similarly, other reasons for exemption of the articles were non-paired studies, non-MPA studies, guidelines/recommendations, repetitions of the original articles, etc. These 14 peer-reviewed articles have been summarized in the tables (see Table 1.1 for more information). The various studies considered for this review can be classified as open label, prospective, and observational. Most of these studies comprehended the accuracy and precision which was in accordance with the FDA guidelines for bioanalytical method validation (less than ±15%).

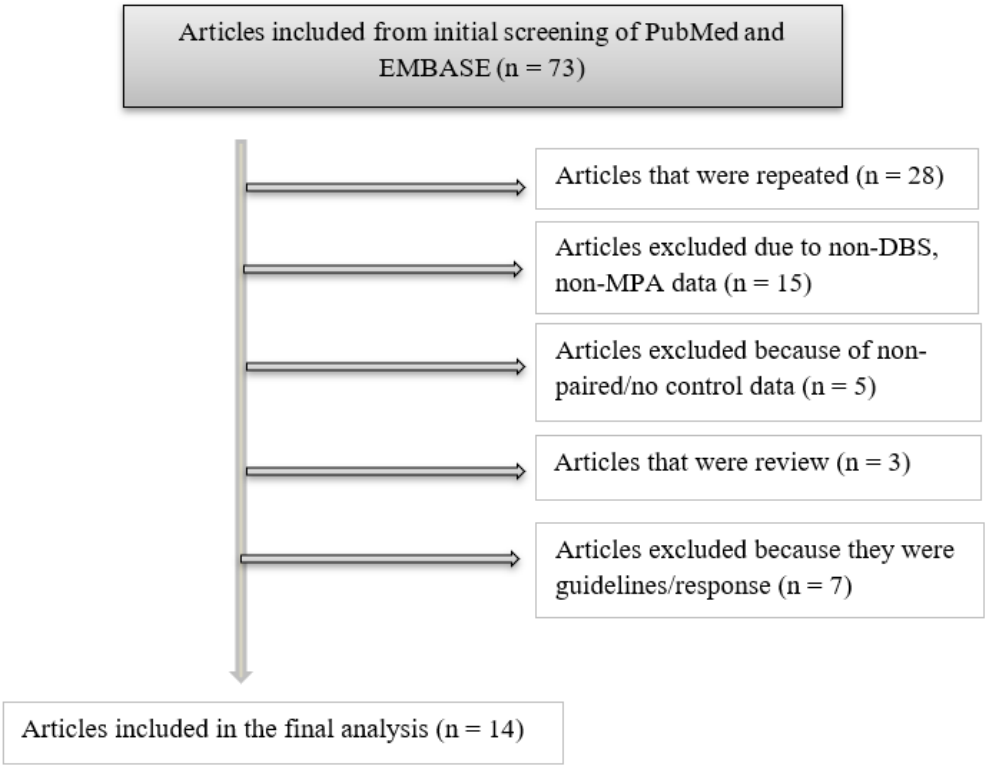

Figure 1.9: The flowchart explains the criteria for selection of the articles for our literature review

1.6.3 Alternative matrices for the therapeutic drug monitoring of mycophenolic acid

1.6.3.1 *Dried blood spot(s) studies*

The study by *Zwart et al.* [8] included a cohort of 65 patients, out of which 53 patients had undergone a renal transplantation and 12 patients had a pancreatic transplant. The patient population consisted of 21 females and 44 males, where 192 paired MPA samples were withdrawn from the groups altogether. The formulation of MPA prescribed/given to the patients was not specified, but the median dose was 1226 mg with the range of the dose being 500-2500

mg. Patient demographic data was collected, which specified the mean age (53.9 yrs.), time post-transplant (5.5 yrs.), glomerular filtration rate (55.3 mL/min.), and mean hematocrit (0.41%). As for the drug therapy, 52 patients were on tacrolimus and MPA and the remaining 13 patients were being given tacrolimus and prednisolone only. Upon the visit to the clinic, the patients were asked to give four DBS and whole blood (WB) samples each at the same time or with the time difference being no more than 5 minutes. To ease with the sampling, patients were assisted by the nurse(s) at the clinic for the first spot, which was later discarded, and the rest of the sampling was performed by patients themselves. This study by *Zwart et al.* demonstrated the use of a volumetric micro sampling device HemaXis® which consists of Whatman 903 protein saver card that helped with the collection of the DBS samples. These samples were processed and then analyzed using liquid chromatography with tandem mass spectrometry (LC-MS/MS). Their study made a direct comparison between DBS and WB samples and utilized Passing-Bablok regression, Bland-Altman plots, mean percentage prediction error and mean absolute prediction error for the statistical analysis of their data, with a correction factor of 0.68 (Table 1.1). Pharmacokinetic parameters such as mean concentration and the estimated AUC were also mentioned in their study. The mean percentage error (MPPE) was reported to be -2.48% with the Mean Absolute Percentage Error (MAPE) being 18.66%. Passing-Bablok analysis showed Y=0.90x+0.05 [95% confidence interval [CI] slope (0.86 to 0.94), intercept (-0.05 to 0.17)] and Y=0.96x-0.78 [95% CI slope (0.85 to 1.10), intercept (-5.10 to 3.77)] where Y represents the corrected DBS concentration and X represents the plasma concentration.

Arpini et al. [69] conducted a study in adult kidney transplant patients who received Mycophenolate mofetil MMF or EC-MPS as a prescription for their transplant. The cohort in their study had 19 patients in whom 77 paired samples were collected. Unlike Zwart (*Zwart et*

al., 2018 [8]), the patient demographics such as mean age, time post-transplant and glomerular filtration rate (GFR) were not specified. The DBS sampling was done using a commercial device Medlance® Plus Special lancets. The samples were then spotted onto the Whatman 903 protein saver card and dried at room temperature for 3 hours, followed by analysis using high performance liquid chromatography with diode array detector (HPLC-DAD). MMF sampling was conducted at 20 mins., 1h and 3h whereas EC-MPS sampling was conducted at 1h, 2h, 3h and 4h. The pharmacokinetic parameters mentioned here were the plasma and the DBS concentration along with an estimated plasma concentration from DBS (with individual and mean hematocrit) (Table 1.1). Mean plasma and DBS concentrations were 4.910 µg/mL and 3.137 µg/mL, respectively. The statistical analysis for this study by *Arpini et al.* [69] was done by Passing-Bablok regression and by means of standard deviation of the estimated plasma concentration (Table 1.1). MPE and root mean square error (RMSE) were not specified. The standard deviation (SD) of the estimated plasma concentration (EPC) from DBS and from the individual hematocrit (Hct) was reported as ± 10.23 and the EPC from DBS vs. EPC from the average Hct was specified as ± 11.60.

Iboshi et al. [70] reported a study of 12 patients who had undergone a lung transplant in the past two years. The patients were given mycophenolate mofetil, but the dose was not specified. From the 12 patients, 36 paired samples were withdrawn for the comparative study between DBS and whole blood. This study by *Iboshi et al.* is unique as it utilizes special non-cellulosic DBS cards for the collection of blood and employs a microwave-assisted drying technique to shorten the drying time and thus the sample processing time. The dried samples were processed using acetonitrile (ACN) and water and then analyzed in LC-MS/MS (using electrospray ionization mode). Patient demographics in this study by *Iboshi et al.* were only

restricted to the hematocrit range (29.3 % – 42.9 %). The pharmacokinetic parameters mentioned here were the mean MPA, MPAG and AcMPAG concentrations whereas the estimated AUC was not acknowledged. Here, the mean plasma and DBS MPA concentrations were reported as 1.86 ± 1.48 µg/mL and 1.89 ± 1.52 µg/mL respectively, for MPAG in plasma and DBS were 10.37 ± 8.24 µg/mL and 10.56 ± 8.90 µg/mL. The method of validation for this study covered all the necessary requirements such as accuracy, precision, recovery, specificity, selectivity, calibration curve, matrix effects, stability, and linearity in accordance with the different validation guidelines. Statistical analysis was done using Wilcoxon signed-rank test, Passing-Bablok regression analysis, and coefficient of variation (%CV). The Passing-Bablok analysis showed that Y=1.020x-0.016 [95% CI slope (0.964 to 1.061), intercept (-0.025 to 0.056)] where Y represents the corrected DBS concentration and X represents the plasma concentration for MPA and Y=1.039x-0.288 [95% CI slope (0.999 to 1.074), intercept (-0.590 to 0.011)] for MPAG. Even though the drying of samples was assisted by use of a microwave here, the accuracy and precision were within ±15% of the required criteria, which makes this approach clinically significant to studies by others.

Martial et al. [71] developed and validated an assay to measure the concentration of MPA and tacrolimus in DBS and WB using LC-MS/MS. This study was conducted in 28 pediatric kidney transplant patients in whom 32 paired samples were taken (trough, peak and mid range). The use of any MPA formulation was not specified and the dose given to the patients was 500 mg and ranging from 180-1000 mg. Patient demographics were specified. This study included a cohort of 28 patients where 22 patients were being given tacrolimus (13 patients out of these 22 being given MPA at the same time) and 6 being treated with MPA without tacrolimus. The method of sample collection for DBS was similar to the approach mentioned in

the study by *Zwart et al.* [8] that started from a finger-prick where each sample was taken at no more than 5 minutes apart. The samples taken on Whatman 903® cards were then dried at room temperature and stored until analysis in LC-MS/MS. Unlike the other three studies on DBS assay development and validation [8, 69, 70], pharmacokinetic parameters in DBS and plasma were not mentioned in this study. Bland-Altman plots, Passing-Bablok regression analysis, Mean Percentage Prediction Error and Root Mean Square Error were used for the statistical analysis of the data, where the value of the latter two was less than 15% (Table 1.1). The MPPE was reported as -3.5% (within ± 15%). Passing-Bablok regression analysis showed Y=1.0x-0.20 [95% CI slope (0.93 to 1.1), intercept (-0.39 to 0.18)] where Y represents the predicted MPA concentration in DBS and X represents the observed MPA concentration in plasma.

1.6.3.2 *Saliva as the matrix*

The study by Ferreira [72] described a simple LC-MS assay for the simultaneous determination of MPA and MPAG using limited sampling strategy (LSS) in renal transplant patients. Thirteen adult patients were chosen for this study which included 6 males and 7 females with the median age being 58 years. The oral fluid collection was done via a micro sampling device, Salivette®. The blood collection, as the study reported, was challenging because of the health complications that arise in a transplant patient. The oral fluid samples were collected at 0, 0.5, 1.0, 1.5, 2 and 12h. Unlike other studies summarized previously, this study did not specify the mean plasma and oral fluid concentration. The mean maximum concentration (C_{max}) for MPA in plasma and saliva was 10.22 µg/mL and 0.0361 µg/mL with T_{max} being at 1 h and 1.5 h, respectively. Mean C_{max} for MPAG in plasma and saliva were 82.03 µg/mL and 0.1147 µg/mL with T_{max} at 1.5 h and 1 h respectively. Correlation coefficient (r) was reported at 0.9646 for the

MPA concentration in saliva vs. plasma with the MPA AUC of saliva vs. plasma being at 0.9946. Similarly, the r value was reported at 0.9210 for the MPAG concentration in saliva vs. plasma with the MPAG AUC of saliva vs. plasma being at 0.9986. Their data showed a good correlation between the plasma and the saliva MPA and MPAG concentrations (within ± 15%).

The study by *Brooks et al.* [73] included a cohort of 20 adult renal transplant patients. The patients were given enteric-coated mycophenolate sodium along with tacrolimus and prednisolone. The study consisted of 11 females and 9 males with the mean age being 52.5 years. The other pharmacokinetic parameters have also been mentioned in this study (Table 1.1). The collection of the saliva samples was not stimulated, but rather a specialized collection device Salivette™ was used to collect 1-2 mL of saliva. The collection of plasma samples was conducted at the same time as the saliva samples for their paired comparison. This study is unique as it includes the total and the free saliva concentration unlike *Ferreira et al.* [72], which only considered the total plasma MPA concentration. MPA is present in the plasma both as the total and the free form, and it is the free form of the drug that is present in the saliva. *Brooks et al.* [73] made the comparison between the plasma (free/total) MPA and saliva MPA by means of correlation coefficient, accuracy by MPE and precision via RMSE. The MPE was reported at 210.54 mgh/L with the r^2 of total plasma vs. free plasma from 0.6-0.8, free plasma vs. saliva from 0.08-0.46, total plasma vs. saliva from 0.10-0.59. RMSE was specified as 424.26 mgh/L.

Alsmadi et al. [74] developed a population physiologically based pharmacokinetic model using the data present in the literature. Using this model, they prepared an assay for the quantification of MPA and MMF in pediatric kidney transplant patients which was analyzed in LC-MS/MS. A population of 26 pediatric kidney transplant patients was included in this study, which consisted of 15 males and 11 females. The patients were being given a mean dose of 500

mg MMF twice daily, along with tacrolimus and prednisolone. The samples from the patients were taken on the day of their visit to the clinic. The plasma and saliva samples were taken before giving the dose and an hour after giving the dose. The pharmacokinetic parameters in the saliva were not specified. One of the main purposes of this study was to prove that saliva is an alternative to plasma, which they were able to do by providing the correlation between plasma and saliva MPA & MMF. The population physiologically based pharmacokinetic model is a correction factor used in this study. The raw data does not possess a good correlation between plasma and saliva ($r = 0.31$-0.38), however when the model is used here to transform the data, the correlation is better ($r > 0.95$), which complies with that data reported in *Zwart et al.* [8].

Mendoza et al. [75] successfully developed and validated an assay for the quantification of MPA. The study population included 11 Caucasian males who were being given MMF twice daily. In addition, tacrolimus and prednisolone were also being given. Parallel samples of plasma and unstimulated saliva were collected over 12 hours with the time difference between them being less than 5 mins. Pharmacokinetic parameters in plasma were not specified. Total MPA concentration was calculated using HPLC-ultraviolet detector whereas the unbound fraction was analyzed using LC-MS/MS. The statistical comparison between the plasma and the saliva matrix was represented by the correlation coefficient. The MPPE and RMSE were not specified. On the contrary, for the saliva MPA, r^2-value was 0.909 for the total fraction and 0.910 for the unbound fraction. However, correlation alone does not give a good indication of the accuracy and precision. The study should have included the free plasma concentration on top of the mean concentrations.

The study by *Weisen et al.* [76] included the development and validation of an assay for measuring MPA and its glucuronide metabolite (MPAG) in plasma and saliva. The collection of

saliva samples was assisted here using a standardized collection device, Salivette® with a polyethylene swab. The clinical validation was done in a single pediatric kidney transplant patient aged 11 years who was being given a steady state dose of 500 mg MMF twice daily. The samples were collected before giving the drug, 30 minutes post-drug administration and 2 hours after drug administration. Saliva collection was done with the use of a swab that the patient was asked to chew on for a minute, whereas the plasma samples were collected by venous blood draw. Observed MPA concentrations at the time of drug administration (C_0), concentration at 0.5 h ($C_{0.5}$) and concentration at 2 hours post-drug administration (C_2) were reported. For MPA in plasma, C_0 = 3.25 µg/mL, $C_{0.5}$ = 15.89 µg/mL and C_2 = 8.69 µg/mL. For MPA in saliva, C_0 = 19.35 ng/mL, $C_{0.5}$ = 91.99 ng/mL and C_2 = 57.04 ng/mL. For MPAG in plasma, C_0 = 20.21 µg/mL, $C_{0.5}$ = 27.57 µg/mL and C_2 = 47.39 µg/mL. For MPAG in saliva, C_0 = 25.87 ng/mL, $C_{0.5}$ = 29.11 ng/mL and C_2 = 119.08 ng/mL. Elimination half-life was 25.4 h with the MPA area under the curve (AUC) being 78.6 µgh/mL. Their assay showed a good correlation and accuracy, whereas the data on its applicability on the test subject was not reported.

Shen et al. [77] developed and validated an assay for the determination of MPA in plasma and saliva using LC-/MS/MS. This study included a cohort of healthy volunteers as well as transplant patients, gender being male. The assay was developed for measuring the total, free and saliva MPA concentrations. The healthy volunteers were being given 1000 mg drug once a day whereas the kidney transplant patients were being given 750 mg twice daily, along with MMF, prednisolone and calcineurin inhibitors. Patient demographics have been summarized (Table 1.1). The pharmacokinetic parameters in the saliva were not specified. The collection of saliva and plasma (through venous draw) was done at the same time points, but the time points were different for healthy volunteers and the kidney transplant patients. Non-compartmental method

was chosen for the pharmacokinetic analysis where C_{max} and the T_{max} were directly extracted from the area under the concentration-time curve. Accuracy was determined by the correlation coefficient for total MPA (tMPA), free MPA (fMPA) and saliva concentration of MPA (sMPA). The r^2-value in the transplant patients for tMPA vs. fMPA was 0.992, tMPA vs. sMPA was 0.838, fMPA vs. sMPA was 0.816. However, no data was reported for the precision.

1.6.3.3 *Urine as the matrix*

The study by *Teshima et al.* [78] included a single patient for the drug monitoring, with no patient demographics reported. The blood sampling was conducted over the period of 12 hours, starting with the trough concentration, followed by sampling every hour. Urine sampling was done every 4 hours in the same time duration as the venous sampling. However, the serum samples were collected the day after the drugs were administered. The patient was being prescribed a combination of immunosuppressants, antiviral and antifungal agents. MPA was administered 1 g twice a day. Pharmacokinetic parameters in the urine were not specified (Table 1.1 A summary of the literature review featuring the various matrices that have been used to measure and monitor mycophenolic acid and its metabolites in kidney transplant recipients). The lack of bias and precision in this study could not rule out the possibility of poor correlation between the drug levels in plasma and urine. Overall, the study did not specify the challenges associated with urine as a matrix for MPA monitoring and failed to report the bias and precision data in the patient.

Benoit-Biancamano et al. [79] conducted their study in a cohort of 52 healthy volunteers that consisted of 31 males and 21 females. Volunteer demographics other than gender were not

specified. MPA was being given as a single dose of 1.5 g to the healthy volunteers. The use of drugs other than MPA was also not reported. Venous and urine sampling was done simultaneously over a period of 12 hours. Venous sampling took place at trough concentration, 20 mins post drug administration, 40 mins, 1h, 2h, 4h, 6h, 8h, 10h and 12 h post drug administration. The urine sampling was done in 2-time frames, which were 0-6h and 6-12h post drug administration. Pharmacokinetic analysis for the parameters was done using non-compartmental analysis. Although this study reported the accuracy and precision data for the assay, it failed to report the data for bias and precision of the approach for their assay application in the clinical setting. The plasma samples for their developed assay reported a slope of 0.053 with r^2 0.996 for total MPA, a slope of 0.129 with r^2 0.997 for MPAG, a slope of 0.185 with r^2 0.997 for AcMPAG and a slope of 0.004 with r^2 0.999 for free MPA. Similarly, the urine samples for their developed assay reported a slope of 0.038 with r^2 0.996 for MPA, a slope of 0.077 with r^2 0.992 for MPAG, a slope of 0.111 with r^2 0.995 for AcMPAG.

Jiao et al. [80] developed an assay to simultaneously quantify MPA and its metabolites in urine and plasma, using HPLC. Fluorescence detectors were used to detect MPA, whereas ultraviolet detector was used for the quantification of MPAG. This study included a group of 10 renal transplant patients, with no other demographics specified. Venous sampling was conducted at trough concentration, 30 mins, 1h, 1.5h, 2h, 3h, 4h, 6h, 8h, 10h and 12h after drug administration. The urine sampling was done in three time slots, 0-4h, 4-8h, 8-12h. The patients were being given cyclosporin A and prednisolone along with MPA. The pharmacokinetic parameters in plasma were not specified. The bias and precision for the clinical comparison in patients between plasma and saliva were also not specified.

Yau et al. [81] reported a study with an assay that quantifies MPA and MPAG simultaneously using ultraviolet detection in plasma and urine. The study was done in a Chinese renal transplant female, a 42-year-old patient who was being prescribed 500 mg of MMF twice a day for over 3 months. Venous sampling was done at trough concentration, 0.5h, 1h, 1.5h, 2h and 6h post drug administration. Urine samples were also collected after the two doses were given. Pharmacokinetic parameters in plasma and urine were both reported (Table 1.1). On the contrary, bias and precision for their method application in the patient was not reported.

1.6.4 Results

Table 1.1 A summary of the literature review featuring the various matrices that have been used to measure and monitor mycophenolic acid and its metabolites in kidney transplant recipients

MPA formulation or dose	**Study population**	**Concurrent drug therapy**	**Method of DBS collection**	**Bioanalytical assay**	**Pharmacokinetic parameters in plasma**	**Pharmacokinetic parameters in DBS**	**Bias**	**Precision**	**Reference**
DBS as a matrix									
Not specified Median dose: 1226 mg (500-2500 mg)	n=65 patients females 21 males 44 n=192 paired MPA samples drawn 53 from kidneys/ 12 from pancreatic transplants Mean Age: 53.9 (23.4-76.4, range) yrs. Mean time post-transplant: 5.5 (1.0-7.3) yrs.	52 patients given tacrolimus + MPA (± prednisolone) 13 patients given tacrolimus + Prednisolone (Without MPA)	Samples were assisted by the nurse initially, later on performed by the patient. Average time between the sample collection <5 min. Sampling done every hour for 3 hours (C0, C1, C2, C3) using HemaXis®.	LC-MS/MS	Mean concentration (from 192 paired samples): 5.47 *mg/L* 95% CI (4.74-6.20) *mg/L* Estimated AUC (from 43 paired samples): 42.8 *mgh/L* 95% CI (37.5-48.1) *mgh/L*	Mean concentration: 5.08(original 3.46 with correction factor of 0.68) *mg/L* 95% CI (4.40-5.76) *mg/L* Estimated AUC : 41.2 *mgh/L* 95% CI (35.9-46.6) *mgh/L*	Mean concentration: MPPE: -2.48% Passing-Bablok Y represents corrected DBS concentration and X represents plasma concentration: Y=0.90x+0.05 [95% CI slope	RMSE: Not specified MAPE: 18.66% Estimated AUC: (0-12h) 10.60%	Zwart 2018 [8]

	Mean GFR: 55.3 (27.0-84.0) *mL/min* Mean Hematocrit: 0.41(0.33-0.55) %						(0.86 to 0.94), intercept (-0.05 to 0.17)] Estimated AUC: (0-12h) -3.50% Passing-Bablok: Y=0.96x-0.78 [95% CI slope (0.85 to 1.10) intercept (-5.10 to 3.77)]		
Mycophenolate mofetil (MMF) and Mycophenolate sodium (EC-MPS) Median dose: Not specified Range: Not specified	n = 19 renal patients Gender not specified n = 77 paired samples Mean (Age, Time post-transplant, GFR): Not specified Mean Hct: 41	Mycophenolate mofetil (MMF) OR Mycophenolate sodium (EC-MPS)	Assembling of samples was done using Medlance® plus special lancets via finger prick, then applied onto Whatman 903® paper and left to dry at RT for 3 hours. MMF sampling was conducted at	HPLC-DAD	Mean concentration: 4.910 *µg/ml* AUC: Not specified	Mean concentration: 3.137 *µg/ml* EPC (from individual Hct): 5.247 *µg/ml* where correction factor was the equation EPC=DBS conc/[1-(Hematocrit/100)]	MPPE: Not specified Passing-Bablok: (Conc in plasma and DBS with average slope): Y=1.1036x -0.1633 Passing-Bablok: (EPC from	RMSE: Not specified S.D. ± 10.23 (EPC from DBS and EPC from individual Hct) S.D. ±	Arpini 2013 [69]

			20 min., 1h and 3h whereas EC-MPS sampling was implemented at 1h, 2h, 3h, and 4h. 6mm dia spots bored and extorted by a methanolic solution of MPA carboxybutoxy ether. Further recovered by 50:50 phosphate buffer & analyzed.			EPC (from mean Hct): 5.336 *µg/ml* AUC: Not specified	DBS and EPC from individual Hct, slope before correction): Y=0.6434x -0.0903 [(95% CI not specified; S.D. ± 10.23 between the average EPC and plasma concentration) (range 80.8-127.3%)] Passing-Bablok: (EPC from DBS and EPC from average Hct, slope after correction): Y=1.0563x -0.0739 [(S.D. ± 11.60) (range 76.5-127.2)]	11.60 (EPC from DBS and EPC from average Hct)	

Mycophenolate mofetil Median dose: Not specified Range: Not specified	n = 12 Gender not specified n = 36 paired samples from lung transplant patients. (time not specified) Mean (Age, Time post-transplant, GFR): Not specified Hct range: 29.3%-42.9%	Not specified	Blood was withdrawn and spotted on the non-cellulosic DMS card and dried in the microwave for 1 min at 460W. 3mm spots punched out, added to 50 µL water. Shaken in a microtube for 1 min (speed not mentioned) & and added to 200 µL ACN followed by centrifugation at 15,000 g for 5 mins. Supernatant was filtered and internal standard solution added, and subsequently analyzed.	LC/ESI-MS/MS	Mean concentration (MPA): 1.86 ± 1.48 *µg/mL* Mean concentration (MPAG): 10.37 ± 8.24 *µg/mL* Mean concentration (AcMPAG): Not specified Range: 0.1-30 *µg/mL* Estimated AUC: Not specified	Mean concentration (MPA): 1.89 ± 1.52 *µg/mL* using the equation Plasma concentration = DBS concentration/ (1-hematocrit value) as the correction factor. Mean concentration (MPAG): 10.56 ± 8.90 *µg/mL* Mean concentration (AcMPAG): Not specified Range: Not specified Estimated AUC: Not specified	MPPE: Not specified Passing-Bablok (Plasma conc and Hct corrected DBS conc for MPA): Y=1.020x-0.016 [95% CI slope (0.964 to 1.061), intercept (-0.025 to 0.056) where Y represents the corrected DBS concentration and X represents the plasma concentration Passing-Bablok (Plasma conc and	RMSE: Not specified %C.V.: Lower than 15% Precision tested at 4 levels (LLOQ, QCL, QCM, and QCH).	Iboshi 2017 [70]

							Hct corrected DBS conc for MPAG): Y=1.039x-0.288 [95% CI slope (0.999 to 1.074), intercept (-0.590 to 0.011)		
Not specified Median dose: 500 mg Range: 180-1000 mg	n = 19 renal transplant patients (pediatric) (Only 32 measured concentrations) Trough, Peak, Mid Conc n = 32 paired samples Females 13 Median Age: 13.5 (3-17) yrs. Median weight: 46 (13-93) kg Median height: 151	Total 28 pediatrics 22 patients given tacrolimus out of which 13 patients given tacrolimus + MPA and 6 patients given MPA w/o tacrolimus Conversion factor = 1.30	Finger was pricked, a sample was collected on Whatman 903® filter paper keeping <5 mins time difference between the sampling. Dried and stored at RT. Later, 7.5 mm disks were punched out and added to 250 µL of the ES. Shaken and 20 µL injected into the analyzer.	LC-MS/MS	Not specified	Not specified	MMPE: -3.5 % (Less than 15%) Passing-Bablok: Y=1.0x-0.20[95% CI slope (0.93 to 1.1), intercept (-0.39 to 0.18)] where Y represents the predicted MPA concentration in DBS and X	RMSE 12.8 % (Less than 15%)	Martial 2017 [71]

	(92-180) cm Mean time post-transplant: Not specified Median Hct: 0.36 (0.26-0.43) eGFR: 0-29 (7%) 30-59 (22%) 60-89 (52%) >90 (19%)						represents the observed MPA concentration in plasma. Bland-Altman plots: **Pred/Obs** (ULA = 1.5 Mean ratio = 0.99 LLA = 0.48) **Pred-Obs** (ULA = 2.6 Mean diff = -0.13 LLA = -2.9)		
Saliva as a matrix									
MPA formulation or dose	Study population	Concurrent drug therapy	Method of sample collection	Bioanalytical Assay	Pharmacokinetic parameters in plasma	Pharmacokinetic parameters in Saliva	Bias	Precision	Reference
Mycophenolate mofetil Dose given:	n = 13 kidney transplant patients	11 people being given corticosteroids 5 people having	Blood samples were collected using EDTA	LC-MS	**MPA** Mean C_{max} (µg/mL): 10.22	**MPA** Mean C_{max} (µg/mL): 0.0361	MMPE: Not specified	RMSE: Not specified	Ferreira 2018 [72]

750 mg twice a day (1.5 g/day)	6 Males & 7 Females Median age: 58 (39-75) years Median time post-transplant: 4 (0.5-11) years Median Body weight: 67 (49-90) kg Median Hct: Not specified	Cyclosporine 8 people with tacrolimus	tubes and saliva via Salivette®. Samples collected at 0, 0.5, 1, 1.5, 2 and 12 h. 150 µL saliva was pipetted and added to a 25 µL mix solution (containing MPA and MPAG) and vortexed. To this, internal standard (Ketoprofen), methanol and formic acid was added & finally centrifuged at 14,000 rpm at 4°C for 25 mins. Finally, supernatant was filtered through PVDF membrane and injected into LC-MS		(S.D. ± 18.54) Mean T_{max} (h): 1 (S.D. ± 12.34) Mean AUC_{0-12} (µgh/mL): 55.83 (S.D. ± 15.97) **MPAG** Mean C_{max} (µg/mL): 82.03 (S.D. ± 13.35) Mean T_{max} (h): 1.5 (S.D. ± 15.32) Mean AUC_{0-12} (µgh/mL): 472.13 (S.D. ± 11.65)	(S.D. ± 11.22) Mean T_{max} (h): 1.5 (S.D. ± 11.58) Mean AUC_{0-12} (µgh/mL): 0.331 (S.D. ± 13.12) **MPAG** Mean C_{max} (µg/mL): 0.1147 (S.D. ± 12.25) Mean T_{max} (h): 1 (S.D. ± 10.58) Mean AUC_{0-12} (µgh/mL): 0.7842 (S.D. ± 15.69)	Correlation coefficient (r) : MPA conc in saliva v/s plasma: 0.9646 MPA AUC of saliva v/s plasma: 0.9946 MPAG conc in saliva v/s plasma: 0.9210 MPAG AUC of saliva v/s plasma: 0.9986		
Mycophenolate mofetil Dose given:	n = 26 Pediatric stable kidney-	Patients were also being given tacrolimus (2 mg twice a	Not specified	LC-MS/MS	**5th-quantile predicted**: Frac absorbed: 1	Not specified	MPE: Not specified	RMSE: Not specified	Alsmadi 2019 [74]

500 (250-750) mg twice a day	transplant patients (SKTP) 15 Males and 11 Females Mean age: 11.63 (4-18) years Mean Body Wt.: 39.85 (17-87) kg GFR: Normal Serum creatinine: 0.3-1.14 mg/dL Mean time post-transplant: Not specified Mean Hct: **MPA** Saliva: -0.11 Plasma: -0.11 **MMF** Saliva: 0.76 Plasma: 0.34	day) and Prednisolone (10 mg once every other day)			F: 0.98 AUC 0-∞: 8.99 ng h/mL C_{max}: 0.58 ng/mL T_{max}: 1.9 h t1/2: 19.0 h **95th-quantile predicted**: AUC 0-∞: 4695367 n gh/mL C_{max}: 38270 ng/mL T_{max}: 0.25 h t1/2: 1015 h **5th-quantile predicted**: Frac absorbed: 1 F : 0.98 AUC 0-∞: 8.99 ng h/mL C_{max}: 0.58 ng/mL T_{max}: 1.9 h t1/2: 19.0 h **95th-quantile predicted**: AUC 0-∞: 4695367 ng h/mL		Pearson's correlation coeff. (r): 0.31-0.38		

					C_{max}: 38270 ng/mL T_{max}: 0.25 h t1/2: 1015 h				
Enteric-coated mycophenolate sodium (EC-MS) Dose given (mg): 720 twice daily in 19 patients & 540 twice daily in 1 patient	n = 20 adult renal transplant patients n = 19 Paired samples at different time points Mean Age: 52.5 (22-71) years 11 Females & 9 Males Mean Body Wt.: 78.8 (47.9-103) kg Mean Time post-transplant: 44 (30-63) days Serum creatinine: 120.5 (61-197) µmol/L eGFR: 71 (26-115) mL/min Mean Hct:	Patients given Enteric-coated mycophenolate sodium (Myfortic™) + tacrolimus (Prograf™ 7.5 mg) + Prednisolone (Panafcortelone ™ 17.5 mg)	Saliva samples (non-stimulated) were collected the same time as were plasma samples (from blood). Salivette™ used to collect 1-2 mL sample at each time point. 13 samples were collected pre-dose and others at 0.25, 0.5, 0.75, 1.0, 1.5, 2.0, 3.0, 4.0, 6.0, 9.0 and 12.0 h post-dose. Samples were centrifuged and stored at -80°C until further analysis. Samples were then	UPLC-MS/MS	**Total, Plasma MPA**: C_{max}: 12mg/L T_{max}: 3.5 h AUC: 54.2 (22.6-941.9) mgh/L Apparent Clearance: 31.8 (6.0-31.8) L/h **Free Plasma MPA**: C_{max}: 134 µg/L T_{max}: 4.0 h AUC: 515.6 (232.9-1510.6) µgh/L	**Saliva MPA**: Mean conc: 45.5 (1-819) µg/L C_{max}: 45 µg/L T_{max}: 2.0 h AUC: 216.2 (127.6-592.6) µgh/L	Median Prediction Error (MPE): 210.54 mgh/L Correlation coefficient (r2): **Total plasma vs free plasma** 0.6-0.8 **Free plasma vs saliva** 0.08-0.46 **Total, plasma vs saliva** 0.10-0.59 Bland-Altman plots: Mean = 309 (Saliva MPA is	RMSE: 424.26 mgh/L	Brooks 2019 [73]

	0.39 (0.28-0.47) g/L Serum albumin: 39.5 (33-47) µmol/L		deproteinated & 10 µL injected into UPLC reverse phase column.				under predicting) 95th percentile = 894 5th percentile = -276		
Mycophenolate mofetil Dose range: 500-1000 mg Twice a day	n = 11 patients n = 100 concentrations (11 trough + 89 other times) Gender: Males Race: Caucasian **Mean ± S.D.** Age: 55 ± 7 years Time post-transplant: 1.78 ± 1.74 years Mean GFR: Not specified Mean Hct: Not specified	All the patients were being given Mycophenolate Mofetil (Cellcept®) + tacrolimus + prednisolone	Parallel samples of blood & saliva (unstimulated) collected via passive drool with time difference of no more than 5 mins. Sampling took place early morning (7am) & patients were fasted for the initial 2 hours of the 12h sample collection and samples were stored at -80 ℃. Proteins were precipitated from the MPA saliva samples,	Total MPA concentration was determined by HPLC-ultraviolet detector & unbound fraction analyzed by LC-MS/MS	Mean concentration: Not specified	Mean ± S.D. saliva concentration: 31.4 ± 32.3 µg/L Range: 2.6-220.4 µg/L MPA trough conc: 79.8 ± 63.7 µg/L	MPE: Not specified Correlation coefficient (r): **Saliva MPA** Total r = 0.909 Unbound r = 0.910	RMSE: Not specified	Mendoza 2006 [75]

			followed by thawing and sonication and finally analyzing						
Mycophenolate mofetil Dose given: 500 mg steady state maintenance dose given twice a day	n = 1 pediatric renal transplant patient Age: 11 years Body Wt.: 34 kg Time post-transplant: Not specified Hematocrit: Not specified	Not specified	Samples were taken via standardized collection device. Patient was told to chew on the swab for a minute, meanwhile the blood samples were drawn too. Swab was then subjected to centrifugation, followed by drying and ultimately reconstitution with mobile phase and analyzed. Calibration std were prepared using pooled saliva samples from 6 healthy volunteers (4 males, 2	LC-MS/MS	Observed MPA concentrations: Co = 3.25 µg/mL C0.5 = 15.89 µg/mL C2 = 8.69 µg/mL Observed MPAG concentration: Co = 20.21 µg/mL C0.5 = 27.57 µg/mL C2 = 47.39 µg/mL	Observed MPA concentration: Co = 19.35 ng/mL C0.5 = 91.99 ng/mL C2 = 57.04 ng/mL Observed MPAG concentration: Co = 25.87 ng/mL C0.5 = 29.11 ng/mL C2 = 119.08 ng/mL Elimination half-life: 25.4 h MPA AUC (0-12h): 78.6 µgh/mL	MPE: Not specified	RMSE: Not specified	Wiesen 2012 [76]

			females).						
Mycophenolate Mofetil Dose given Healthy volunteers: 1000 mg single dose Renal transplant patients: 750 mg twice daily	Healthy volunteers n = 8 Renal transplant patients n = 9 Gender: Male Race: Chinese Age ± S.D. 23.4 ± 2.58 (20-25) years Body Wt.± S.D. 67.4 ± 4.10 (62-75) kgs Height ± S.D. 170 ± 2.86 (162-179) cm **Renal Transplant patients** n = 9 Gender: Male Age ± S.D. 32.5 ± 8.18 (18-48) years Height ±	Mycophenolate Mofetil + Calcineurin inhibitor + Prednisone	To analyze the MPA in saliva, the samples were subjected to protein precipitation by addition of ACN, followed by centrifugation. The supernatant obtained was then injected into the analytical column.	LC-MS/MS	**Healthy volunteers** AUC (0-t): 99.1 ± 26.6 mgh/L AUC (0-∞) : 104.3 ± 29.0 T ½: 11.6 ± 2.6 h T_{max}: 0.81 ± 0.51 h C_{max}: 41.0 ± 13.4 mg/L **Transplants patients** AUC (0-t) : 37.1 ± 11.5 mgh/L AUC (0-∞) : 40.1 ± 13.6 mgh/L T ½ : 3.0 ± 1.5 h T_{max}: 1.06 ± 0.53 h C_{max}: 17.7 ± 5.5 mg/L	Not Specified	MPE: Not specified Correlation coefficient (r) : **Healthy volunteers** tMPA vs fMPA: 0.980 tMPA vs sMPA: 0.914 fMPA vs sMPA: 0.849 **Transplants patients** tMPA vs fMPA: 0.992 tMPA vs sMPA: 0.838 fMPA vs sMPA: 0.816	RMSE: Not specified	Shen 2009 [77]

	S.D. 167 ± 5.65 (156-182) cm Body Weight ± S.D. 65.4 ± 9.60 (50-76) kgs Time post-transplant: 2-3 weeks								
Urine as a matrix									
MPA formulation or dose	Study population	Concurrent drug therapy	Method of DBS	Bioanalytical Assay	Pharmacokinetic parameters in plasma	Pharmacokinetic parameters in urine	Bias	Precision	Reference
Mycophenolate Mofetil Dose given: 1 g twice a day for 6 days	n = 1 renal transplant patient Gender: Not specified Age: Not specified Body Weight: Not specified Blood sampling	Mycophenolate mofetil + Tacrolimus + Cyclosporin A + Methylprednisolone + Acyclovir + Fluconazole	Patient's blood sampling was done before taking the drug (trough conc) and at 1 h interval for 12 hrs. Urine samples were obtained at 4 h intervals. Serum samples were prepared using SPE by treatment	HPLC	**Serum** **MPA** C_{max}: 6.9 µg/mL C_{min}: 0.7 µg/mL T_{max}: 1 h AUC (0-12h): 27.2 µg/mL/h **MPAG** C_{min}: 180.2 µg/mL C_{min}: 101.3 µg/mL	Not specified	Not specified	Not specified	Teshima 2003 [78]

	done at trough (0 h) and every hour till 12 h time point after administration of drug. Urine sample collection every 4 hrs. Serum samples collected on day 2 of drug regimen		with internal standard (methanol + benzoic acid for MPAG and n-butyl-p-hydroxybenzoate for MPA) and methanol. Urine samples were prepared after dilution with water (1:20).		T_{max}: 3 h AUC (0-12h): 1806.7 µg/mL/h				
Mycophenolate Mofetil Dose given: 1.5 mg as a single dose	n = 52 healthy volunteers Males 31 Females 21 Mean Age: Not specified Mean Body Wt.: Not specified	Not specified	Venous and urine samples were collected from 52 healthy donors. Blood sampling done at trough, 20 min, 40 min, 1h, 2h, 4h, 6h, 8h, 10h and 12h. Urine sampling done in 2 timeframes: 0-6 h and 6-12 h.	HPLC-MS/MS	AUC (0-12h) (mg h/L): Total MPA 60.70 ± 15.65 Unbound MPA 0.52 ± 0.17 Total MPAG 312.34 ± 92.57 Total AcMPAG 2.65 ± 1.34	Urinary excretion (0-12h): MPA 3.84 ± 3.69 mg MPAG 766.06 ± 218.65 mg AcMPAG 8.33 ± 3.91 mg	Not specified	Not specified	Benoit-Biancamano 2007 [79]

			Samples were subjected to centrifugation and acidification, while keeping them on ice and later were stored at -80°C until analysis.						
Mycophenolate mofetil Dose given: 750 mg twice daily	n = 10 renal transplant patients Gender: Not specified Age: Not specified Body Wt.: Not specified Venous sampling done at trough, 0.5, 1, 1.5, 2, 3, 4, 6, 8, 10 and 12 h after administration. Urine sampling	Mycophenolate mofetil + Cyclosporin A + Prednisolone	Urine samples (volume not specified) were collected over 12 h in three time slots (0-4h, 4-8h, 8-12h) and then vortexed for a minute. This was followed by five times dilution with blank urine and finally injected into the analyzer (20µL).	HPLC with post-column derivatization MPA detection by fluorescence & MPAG detection by ultraviolet detector	Not specified	Amount excreted in urine: MPA 6.75 mg MPAG 484.58 mg	% P.E.: Not specified	RMSE: Not specified	Jiao 2005 [80]

	done in three slots 0-4 h 4-8 h 8-12 h								
Mycophenolate mofetil Dose given: 500 mg twice daily for more than 3 months	n = 1 renal transplant patient Gender: Female Age: 42 years Race: Chinese Venous samples taken over 6 h (trough,0.5, 1, 1.5, 2, 6) Urine samples taken over 12 h (one at trough and the other at the next dose time)	Not specified	Samples (50mL) were collected and stored at -20°C until analysis. Once thawed, ACN was then added to the samples and vortexed (protein precipitation). After allowing the samples to settle, they were then centrifuged. The supernatants thus obtained, were injected into the analyzer	Reverse phase HPLC with ultraviolet detection	**MPA** C_{min}: 1.96 mg/L C_{max}: 16.2 mg/L T_{max}: 45 min. AUCss: 38.3 mg h/L **MPAG** C_{min}: 57.9 mg/L C_{max}: 111 mg/L T_{max}: 70 min. AUCss: 906.9 mg h/L	Concentration in urine: MPA 272 mg/L MPAG 9040 mg/L	Not specified	Not specified	Yau 2004 [81]

Abbreviation(s): AUC area under the concentration-time curve, ACN acetonitrile, b/w between, Conc concentration, C_{max} maximum concentration, C_{min} minimum concentration, T_{max} peak time, C_n concentration at time 'n', CI confidence interval, %C.V. coefficient of variation, DBS dried blood

spot, EC-MPS enteric coated mycophenolate sodium, ESI electrospray ionization, EDTA ethylene diamine tetra acetate, F bioavailability, fMPA free fraction of MPA, GFR glomerular filtration rate, HPLC-DAD high performance liquid chromatography with diode array detector, h hours, Hct hematocrit, HCL hydrochloric acid, HPLC high performance liquid chromatography, LC-MS/MS liquid chromatography tandem mass spectrometry, LC-MS liquid chromatography mass spectrometry, LC/ESI-MS/MS liquid chromatography electrospray ionization with tandem mass spectrometry, LLOQ lower limit of quantification, LLA lower limit of agreement, LSS limited sampling strategy, MPA mycophenolic acid, MPAG mycophenolic acid glucuronide, min minute, MPPE mean prediction percentage error, MMF mycophenolate mofetil, N number of people in the study, Obs observed concentration, Pred predicted concentration, PVDF polyvinylidene difluoride, RMSE root mean square value, %R.E. %R.E. [(found conc-theoretical conc)/theoretical conc * 100], RT room temperature, S.D. standard deviation, SPE solid phase extraction, sMPA MPA levels in saliva, tMPA total MPA, UPLC-MS/MS ultra-performance liquid chromatography tandem mass spectrometry, ULA upper limit of agreement, W watts, yrs. years, ∞ infinity

To conclude, our analysis indicated that DBS is a less-invasive matrix with acceptable precision and accuracy for monitoring MPA. DBS has the advantage of being more patient friendly, does not require the need of trained professionals, requires less volume of the sample, decreases the chance of getting iatrogenic infections and has been shown to give better bias and precision values [8, 69-71]. All these merits make DBS a better matrix in comparison to venous sampling, and therefore suitable for further development.

Saliva and urine are the non-invasive matrices that can be used supplementary to DBS but have not yet been proven to have good bias and precision when employed by themselves. In addition, saliva, and urine both have diurnal variation that can affect the levels of drug and therefore give inaccurate drug estimation. Saliva as a matrix has more contaminants (such as food particles, drug particles etc.) which may affect the drug levels in the system. Urine collection at multiple time points is also not very patient friendly [82].

In summary, the DBS matrix has greater advantages over saliva and urine for the therapeutic drug monitoring of MPA and therefore has been included in this thesis for further study and development.

1.7 Hypothesis

Kidney transplantation is the most common solid organ transplantation in humans, due to multiple causes such as acute kidney injury, renal failure, and chronic kidney diseases [1]. MPA is an immunosuppressant that is commonly prescribed (with tacrolimus and corticosteroids) to kidney transplant recipients [11]. MPA acts by inhibiting IMPDH enzyme, reducing the formation of T and B-lymphocytes [11]. *p*C is a protein bound uremic toxin that is accumulated

in patients with chronic kidney disease and has the potential to inhibit the metabolism of MPA. The therapeutic drug monitoring of MPA can optimize the precision dosing of this immunosuppressant. Understanding the relationship between pC and MPA concentrations can also help optimize the TDM of MPA. Based on our analysis, DBS appears to be a promising alternative approach (to plasma) for conducting MPA TDM.

The current thesis focuses on developing sensitive analytical assays for the quantification of MPA and *p*C and validating them in accordance with the Food and Drug Administration (FDA) guidelines using human plasma and DBS. In this Introduction chapter, we have provided the background on MPA and *p*C regarding their physiochemical properties and pharmacological effects. We have also summarized the pharmacokinetic studies done by other researchers in the past on MPA, *p*C, and their metabolites. It was also determined, based on our literature review, that DBS was the most promising approach for MPA TDM, other than the conventional plasma matrix. In chapter two of this thesis, I will provide the data on the development and validation of two high-throughput ultra-high performance liquid chromatography (UPLC) assays for the detection of MPA and *p*C (and associated metabolites). This is followed by a proof-of-concept study on measuring MPA and *p*C in DBS.

The **overall hypothesis** of my thesis is that it is feasible to conduct MPA and *p*C TDM using highly sensitive and high throughput UPLC analytical assays in plasma and DBS.

The objective of this thesis was 1) develop high-throughput ultra-high performance liquid chromatography assays for measuring MPA and *p*C in the plasma, 2) validate these assays in human plasma in accordance with the U.S. FDA guidance, and 3) to conduct a proof-of-concept feasibility study to assess the transferability of our assays to the DBS matrix. Overall, we have

developed highly sensitive analytical assays which can reliably measure MPA and *p*C in the human plasma, and our assay is transferable to DBS.

1.8 Summary of chapters

1. Chapter 1: General introduction, hypothesis, and objectives.
2. Chapter 2: Methods and Results sections on the development and validation of high-throughput ultra-high performance liquid chromatography assays for the detection of MPA and *p*C in plasma, and to test the applicability of our assays in DBS.
3. Chapter 3: Discussion, limitations, and conclusion.

Chapter 2

Development and validation of sensitive, high-throughput ultra-high performance liquid chromatography assays for the quantification of mycophenolic acid and *p*-cresol

2.1 Materials

Ammonium acetate (>97%) (Catalogue# 1220-1-70) was obtained from Caledon Laboratories Ltd. (Georgetown, ON, Canada) and passed through Millipore™ 0.45 μM filters from Fisher Scientific (Mississauga, ON, Canada). 2', 6'-dimethylphenol (DMP, Catalogue# D175005; Figure 2.1), formic acid (Catalogue# F057), mycophenolic acid (MPA, Catalogue# M5255, Figure 1.1), *p*-cresol (*p*C, Catalogue# C85751; Figure 1.5), sodium phosphate dibasic (Na2HPO4) (Catalogue# S7907), hydrochloric acid solution 12.0 M (Catalogue# H9892), and sodium hydroxide (>=98%) (Catalogue# S5881) were purchased from Sigma Aldrich Canada Co. (Oakville, ON, Canada). Mycophenolic acid carboxybutoxy ether (MPAC, Catalogue# M831555; Figure 2.2), mycophenolic acid β-D-glucuronide (MPAG, Catalogue# M831520; Figure 2.3), *p*-cresol sulfate (*p*CS, Catalogue# T536805; Figure 1.6), and *p*-cresol glucuronide (*p*CG, Catalogue# C782005; Figure 1.7) were purchased from Toronto Research Chemicals (North York, ON, Canada). The physiochemical properties of MPA, MPAG, MPAC, pC, pCS, pCG, and DMP were shown in Table 2.1. Human whole blood (Catalogue# IW1NAE) and human pooled plasma with EDTA (Catalogue# IPLA) were obtained from Innovative Research (Michigan, USA). HPLC grade methanol (Catalogue# 646377) and acetonitrile (ACN, Catalogue# 34998) was obtained from Sigma Aldrich (USA). 10 mL BD syringe (Catalogue# 309604) was obtained by Gibco® (USA). Whatman 903 Protein saver cards® was obtained from

Cytiva-Millipore Sigma™ (Massachusetts, USA). The ultra-high performance liquid chromatography (LC-2040C plus)-coupled with fluorescence detector (RF-20 AXS) instrument is obtained from the Shimadzu USA manufacturing Inc. (Figure 2.4). Agilent-Zorbax Eclipse XDB-C18, 5 µm, 4.6×250 mm (Catalogue# 990967-902; Figure 2.5) was obtained from Agilent® (California, USA).

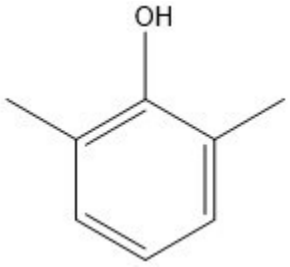

Figure 2.1 Chemical structure of 2', 6'-dimethylphenol (DMP)

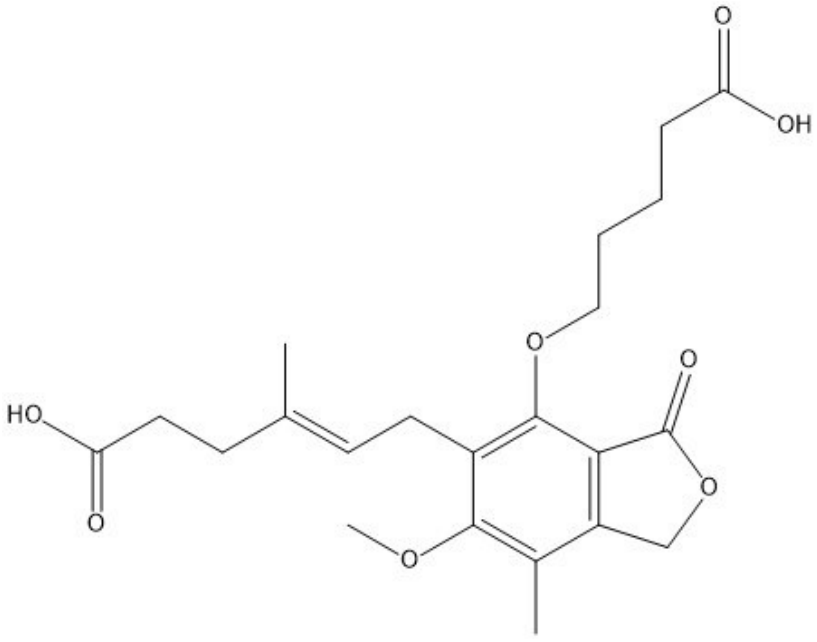

Figure 2.2 Chemical structure of mycophenolic acid carboxybutoxy ether (MPAC)

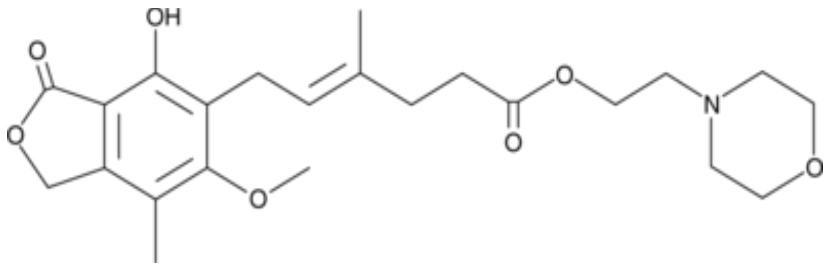

Figure 2.3 Chemical structure of mycophenolic acid glucuronide (MPAG)

The various physicochemical properties of the drug(s)/uremic toxin(s) and their metabolites that have been studied in this thesis are mentioned below, in Table 2.1.

Table 2.1 The physicochemical properties of the drugs and/or their metabolites included in our study

	MPA	**MPAG**	**MPAC**	***pC***	***p*CS**	***p*CG**	**DMP**
IUPAC names	(E)-6-(4-hydroxy-6-methoxy-7-methyl-3-oxo-1H-2-benzofuran-5-yl)-4-methylhex-4-enoic acid	(2S,3S,4S,5R,6S)-6-[[5-[(E)-5-carboxy-3-methylpent-2-enyl]-6-methoxy-7-methyl-3-oxo-1H-2-benzofuran-4-yl] oxy]-3,4,5-trihydroxyoxane-2-carboxylic acid	(E)-6-[4-(4-carboxybutoxy)-6-methoxy-7-methyl-3-oxo-1H-2-benzofuran-5-yl]-4-methylhex-4-enoic acid	4-methylphenol	(4-methylphenyl) hydrogen sulfate	(2S,3S,4S,5R,6S)-3,4,5-trihydroxy-6-(4-methylphenoxy) oxane-2-carboxylic acid	2,4-dimethylphenol
Molecular formula	$C_{17}H_{20}O_6$	$C_{23}H_{28}O_{12}$	$C_{22}H_{28}O_8$	C_7H_8O	$C_7H_8O_4S$	$C_{13}H_{16}O_7$	$C_8H_{10}O$
Molec	320.30	496.50	420.50	108.14	188.20	284.26	122.16

ular weight							
Physical nature	Solid [83]	Crystalline solid [84]	Solid [85]	Crystalline solid	Solid	Solid	Colourless crystals or amber coloured liquid
Log P	2.8 [83]	-	-	1.94	-	-	-
Solubility	Insoluble	Soluble in organic solvents (DMSO) [84]	Soluble in organic solvents [85]	Slightly soluble in water. Very soluble in organic solvents [86]	Soluble in organic solvents [87]	Soluble in organic solvents (ethanol) [88]	Very soluble in organic solvents (benzene, chloroform). Poorly soluble in water [89]
Protein binding	>98%	82% [90]	-	-	96.5% [91]	27.2% [91]	-

Abbreviation(s): DMP, di-methyl phenol; IUPAC, International Union of Pure and Applied Chemistry; Log P, logarithmic partition coefficient; MPA, mycophenolic acid; MPAG, mycophenolic acid glucuronide; MPAC, mycophenolic acid carboxybutoxy ether; *p*CS, *p*-cresol sulfate; *p*CG, *p*-cresol glucuronide.

Figure 2.4 The Shimadzu ultra-high performance liquid chromatography (UPLC) coupled with fluorescence detector instrument in our laboratory that has been employed for the development and validation of our analytical assays

Figure 2.5 The Agilent® Eclipse XDB-C18 reversed phase column (5 µm, 4.6×250 mm)

2.2 Methods for the mycophenolic acid assay

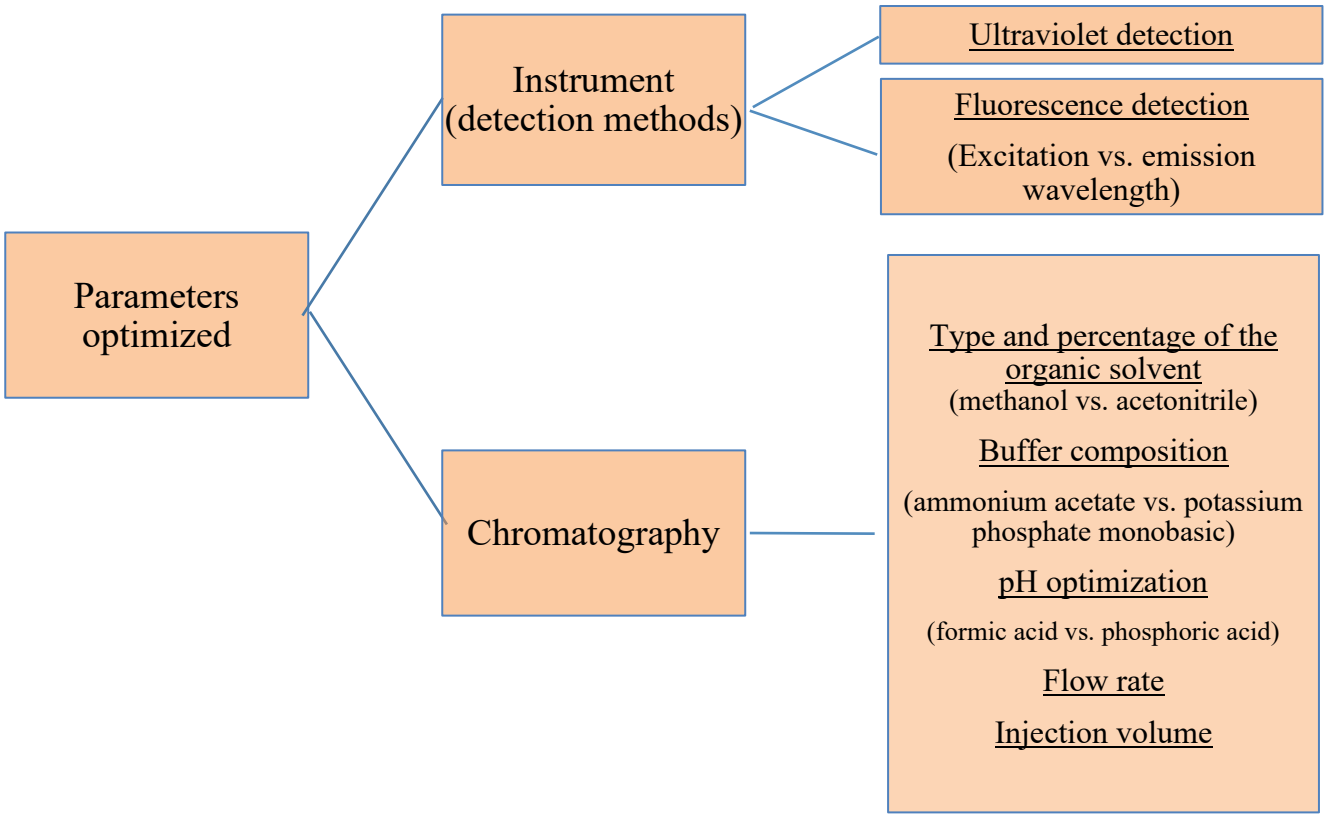

Figure 2.6 The flowchart representing the instrument and chromatographic parameters that have been optimized for our analytical assays

2.2.1 Spectral scan

2.2.1.1 *Spectral scanning of mycophenolic acid and its metabolites using ultraviolet-visible spectrophotometer*

As part of the initial development for the assay measuring MPA, parameters such as methods of detection and wavelengths of detection were first optimized (Figure 2.6). This was

done using the ultraviolet-visible spectrophotometer (Shimadzu® UV-2600i, Catalogue# 207-26000-58, Japan) and the fluorescence spectrophotometry (Shimadzu® RF-6000, Catalogue# 207-20400-58, Japan) using the following steps:

- **Step 1** Checking the solubility of the analytes and the internal standard in solvents (i.e., methanol and ACN). Using this solubility data, stock solution(s) with multiple concentration(s) were prepared.
- **Step 2** To determine the optimal testing concentration that was common to all analytes (MPA and its metabolites as well as internal standard MPAC) giving absorbance intensity in the range 0.2 to 0.8 on the ultraviolet spectrum based on intense (but non-saturated) colour intensities (red to orange).
- **Step 3** To check the effects of pH on the absorbance of analytes. This was done using three different pH levels (3, 4, and 7) adjusted using formic acid and ammonium acetate.
- **Step 4** To check the effects of using different solvents and solvent combinations on the absorbance. This was done by preparing the analyte working solutions in pure methanol, ACN, and a combination of solvents.

Working solutions of MPA, MPAG, and MPAC at a concentration of 30 µg/mL were prepared using 100% methanol at pH 3, pH 4 and pH 7. The pH was adjusted using formic acid and ammonium acetate. After the solutions were prepared, they were analyzed in the ultraviolet spectrophotometer (Table 2.2) to obtain the absorbance (within the range 0.2-0.8) that provided the highest (but non-saturating) intensity. The highest intensity associated wavelength is translated to highest sensitivity of the analytes, which will be useful for determining the sensitivity of detection on the UPLC instrument.

Table 2.2 Analytical conditions of the ultraviolet-visible spectrophotometer for detecting the MPA analytes

Instrument Name	**Ultraviolet-visible Spectrophotometer**
Model:	RF-6000 series
Excitation start wavelength:	200.0 nm
Excitation end wavelength:	600.0 nm
Data interval:	10.0 nm
Emission start wavelength:	200.0 nm
Emission end wavelength:	750.0 nm
Data interval:	10.0 nm
Scan speed:	High speed
Spectrum type:	Absorbance
Slit width:	2
Detector unit:	Direct receiving of light
Light source switch wavelength:	323
S/R switch:	Standard
Stair correction:	ON
Spectrum transformation:	OFF
Data processing table:	OFF

2.2.1.2 *Spectral scanning of mycophenolic acid and its metabolites using fluorescence spectrophotometry*

Similarly, the working solutions of MPA, MPAG, and MPAC (at 100 µg/mL) were also analyzed in the fluorimeter (using 100% ACN or 100% water at pH 3 and pH 7, Table 2.3) to obtain the wavelengths associated with high intensity colors on the spectral scans.

Table 2.3 Analytical conditions of the fluorescence spectrophotometry for the MPA analytes

Instrument Name	**Fluorescence Spectrophotometry**
Model:	RF-6000 Series
Spectrum type	3D
Excitation start wavelength:	200.0 nm
Excitation end wavelength:	600.0 nm
Data interval:	10.0 nm
Emission start wavelength:	200.0 nm
Emission end wavelength:	750.0 nm
Data interval:	10.0 nm
Scan speed:	6000 nm/min
Spectrum type:	Fluorescence

2.2.2 Chromatography optimization

A systematic approach was also followed to develop the chromatographic assay conditions (Figure 2.6), thereby yielding the final conditions associated with the assay.

2.2.2.1 *Solvent optimization – methanol*

After obtaining the optimal wavelengths from the ultraviolet spectrophotometer, the chromatography for MPA, MPAG, and MPAC was optimized first in methanol. The fluorescence wavelengths were not chosen after optimization, since MPA could not be detected with the fluorescence spectrophotometry (as explained in 3.1.1). The optimizations were done using the following instruments.

- Shimadzu® ultra-high performance liquid chromatography with ultraviolet-detection (UPLC-UV, model LC-2040C Plus) as shown in Figure 2.4
- The column used with the instrument was an Agilent® Eclipse XDB-C18 column (5 µm, 4.6×250 mm) as shown in Figure 2.5

Methanol concentration was the initial chromatographic parameter optimized (i.e., 50%, 60%, 70%, 80%, 90%, 100%) using a flow rate of 1 mL/min, a formic acid concentration of 0.1%, an ammonium acetate concentration of 2 mM, an injection volume of 10 µL, a run time of 17 mins, and ultraviolet wavelengths at 305 nm and 295 nm (discussed in results section). The criteria for selecting the chromatography conditions were i) high peak area counts (high sensitivity), ii) optimal peak shape (without peak distortion or fronting/tailing), and iii) short run time.

2.2.2.2 *Solvent optimization – acetonitrile*

Likewise, these chromatographic parameters were also optimized in ACN using the same approach as detailed above. This was done by preparing the analyte working solution (at a concentration of 10 µg/mL) and the instrument mobile phase in ACN. The concentrations of ACN were varied from 20% to 100% while ammonium acetate was kept at 2 mM, formic acid at 0.1%, flow rate 1 mL/min, injection volume 10 µL, run time 13 mins, ultraviolet wavelengths at 305 nm and 295 nm.

2.2.2.3 *Additive optimization – formic acid (in methanol)*

The pH of the mobile phase plays a significant role in chromatography (peak shapes, ideal run time, separation, etc.). To assess the effects of pH in our assays, MPA, MPAG, and MPAC were tested in a mixture to optimize the percentage of formic acid, ammonium acetate, and phosphoric acid in the mobile phase. Formic acid concentration was adjusted from 0.000% to 0.306% (i.e., 0.000%, 0.025%, 0.031%, 0.061%, 0.092%, 0.122%, 0.153%, 0.184%, 0.214%, 0.245%, 0.275%, 0.306%) at a methanol concentration of 60%, flow rate of 1 mL/min, ammonium acetate at 0.5 mM, injection volume of 10 µL, a run time of 13 mins, and ultraviolet wavelengths at 305 nm and 295 nm. The concentration of ammonium acetate in the mobile phase was kept at a fixed concentration (0.5 mM) while optimizing the formic acid.

2.2.2.4 *Additive optimization – formic acid (in acetonitrile)*

The concentration of formic acid was also varied from 0% to 0.1% (i.e., 0%, 0.01%, 0.02%, 0.03%, 0.04%, 0.05%, 0.06%, 0.07%, 0.08%, 0.09%, 0.10%) in 40% ACN, 2 mM ammonium acetate, 1 mL/min flow rate, 10 µL injection volume, 15 mins of run time, ultraviolet wavelengths at 305 nm and 295 nm. Formic acid optimization was followed by adjusting the concentration of ammonium acetate in the mobile phases to obtain the ideal pH conditions for optimal chromatographic conditions for MPA, MPAG, and MPAC (using a concentration of 10 µg/mL for each analyte).

2.2.2.5 *Additive optimization – ammonium acetate (in methanol)*

Similarly, while optimizing the ammonium acetate from 0 mM to 1.0 mM (i.e., 0, 0.1, 0.2, 0.3, 0.4, 0.5, 0.6, 0.7, 0.8, 0.9, 1.0 mM) in methanol, formic acid was kept at 0.306%, methanol concentration at 60%, flow rate of 1 mL/min, injection volume of 10 µL, a run time of 13 mins, and ultraviolet wavelengths at 305 nm and 295 nm.

2.2.2.6 *Additive optimization – ammonium acetate (in acetonitrile)*

The concentration for ammonium acetate was varied from 0 mM to 2 mM (i.e., 0, 0.2, 0.4, 0.6, 0.8, 1.0, 1.2, 1.4, 1.6, 1.8, 2.0 mM) while the formic acid concentration was fixed at 0.1%, ACN concentration in mobile phase at 40%, flow rate at 1 mL/min, injection volume 10 µL, run time of 15 mins, ultraviolet wavelengths at 305 nm and 295 nm.

2.2.2.7 *Additive optimization – phosphoric acid (in methanol)*

To test the effects of phosphate buffer on chromatography, phosphoric acid was varied from 0% to 0.66% (i.e., 0%, 0.07%, 0.13%, 0.20%, 0.26%, 0.33%, 0.39%, 0.46%, 0.53%, 0.59%, 0.66%), with methanol concentration fixed at 60%, potassium phosphate monobasic at 40 mM, flow rate of 1 mL/min, injection volume of 10 µL, a run time of 13 mins, and ultraviolet wavelengths at 305 nm and 295 nm.

2.2.2.8 *Additive optimization – phosphoric acid (in acetonitrile)*

Phosphoric acid concentrations were tested from 0% to 0.470% (i.e., 0%, 0.047%, 0.094%, 0.141%, 0.188%, 0.235%, 0.282%, 0.329%, 0.376%, 0.423%, 0.470%) in 40% ACN, 100 mM potassium phosphate monobasic, 1 mL/min flow rate, 10 µL injection volume, run time of 15 mins, ultraviolet wavelengths at 305 nm and 295 nm.

2.2.2.9 *Flow rate optimization (in methanol)*

The flow rate was adjusted using a mixture of MPA, MPAG, and MPAC (at 10 µg/mL) from 0.5 mL/min to 1.25 mL/min (i.e., 0.5, 0.75, 1.0, 1.25 mL/min) while the methanol concentration was kept at 60%, formic acid concentration 0.1% , ammonium acetate at 0.5 mM, injection volume of 10 µL, with ultraviolet wavelengths at 305 nm and 295 nm (run time was varied according to the flow rate). Only flow rates between 0.5 mL/min to 1.25 mL/min were used since the utilized UPLC column has a limited pressure range between 0.1 mL/min to 2 mL/min.

2.2.2.10 *Flow rate optimization (in acetonitrile)*

The flow rate was adjusted from 0.5 mL/min to 1.5 mL/min (i.e., 0.5, 1.0, 1.25, 1.5 mL/min) while the ACN concentration was fixed at 40%, ammonium acetate at 2 mM, formic acid at 0.1%, injection volume of 10 µL, run time at 15 mins, ultraviolet wavelengths at 305 nm and 295 nm.

2.2.2.11 *Injection volume optimization (in methanol)*

MPA, MPAG, and MPAC were prepared using pure methanol (at the concentration of 10 µg/mL) and injected into the UPLC at varying injection volumes (i.e., 10, 15, 20, 25, 30 µL) using a mobile phase consisting of 60% methanol, 0.1% formic acid, 0.5 mM ammonium acetate, flow rate of 1 mL/min, and ultraviolet wavelengths at 305 nm and 295 nm.

2.2.2.12 *Injection volume optimization (in acetonitrile)*

Injection volume was varied from 10 µL to 50 µL (i.e., 10, 15, 20, 25, 30, 35, 40, 45, 50 µL) with mobile phase ACN concentration fixed at 40%, ammonium acetate at 2 mM, formic acid at 0.1%, run time at 24 mins, ultraviolet wavelengths at 305 nm and 295 nm.

2.2.3 Sample preparation optimization

The various steps involved with the sample preparation/extraction process prior to injection into the UPLC instrument were also optimized in plasma to obtain optimal chromatography and assay sensitivity. ACN was utilized as the solvent for these subsequent assay developments (discussed below).

2.2.3.1 *Determination of lower limit of quantification using pure solvent*

The sample preparation/extraction protocol including MPA, MPAG, and MPAC was modified from a published manuscript from our lab group [61] which utilized LC-MS/MS in the measurement of MPA and MPAG [61, 62]. First, the limits of quantitation were tested, where the upper limit of quantitation (ULOQ) is the highest concentration in a standard calibration set that can successfully give a straight curve (without any peak area saturation) and the lower limit of quantitation (LLOQ) is the lowest concentration in the standard calibration set that can successfully quantify the analyte and gives acceptable chromatography (peak shape and separation) [92]. LLOQ is a measurement of the sensitivity of an assay [92]. Similarly, blank sample is devoid of any analytes that are to be tested or are currently being tested, while the zero calibrator is a sample with the same composition as the blank but also possesses the internal standard of the assay [92].

2.2.3.2 *Standard calibration curve in human plasma*

A standard calibration set was prepared using MPA, MPAG, and MPAC from 0.00003 µg/mL to 64 µg/mL in pure ACN using the final optimized chromatographic conditions (ACN concentration was 40%, ammonium acetate was kept at 2 mM, formic acid at 0.1%, injection volume of 10 µL, the run time at 24 mins, and ultraviolet wavelengths at 305 nm and 295 nm). However, there was no response observed below 0.125 µg/mL for MPA and 0.5 µg/mL for MPAG. Using the results from this standard curve prepared in pure ACN, the MPA and MPAG standard calibration ranges were further tested in human plasma. To accomplish this, pooled human plasma with EDTA was used to prepare several concentrations via serial dilutions. MPA and MPAG calibration concentrations were varied from 0.125 µg/mL to 64 µg/mL using human plasma while MPAC (the internal standard) was kept at a fixed concentration of 10 µg/mL. The samples for blank and zero calibrators were also prepared. The protein precipitation solution (PPS) for this assay was a combination of methanol and ACN (1: 1, at pH 5.70).

2.2.3.3 *Internal standard optimization for mycophenolic acid assay*

To obtain the ideal condition for the internal standard, the concentration of the internal standard (i.e., MPAC) was also optimized. A standard calibration set was prepared using MPAC only (devoid of MPA or MPAG) at varying concentrations ranging from 0.4 µg/mL to 121 µg/mL in human plasma to determine the concentration of MPAC providing robust instrument response without any peak area signal saturation on the UPLC.

2.2.3.4 *Concentrating and injection volume optimization*

To improve the sensitivity of the assay, sample drying (i.e., concentration) was tested as a part of the sample extraction process. This concentration process was achieved using the *SpeedVac* instrument (Thermo scientific® model# SPD1010-115, Massachusetts, USA) which utilizes the freeze-drying principle. MPA and MPAG were diluted in pooled human plasma and MPAC was later added to the samples (at a concentration of 30 µg/mL), followed by sample extraction. These samples were then centrifuged (Eppendorf® model# SN 5404HM131870, Germany) at 18600 g for 4 mins to remove the plasma protein, and the supernatant was extracted as per the assay protocol. The supernatant drying conditions were then tested using *SpeedVac* from 1 min to 20 mins (i.e., 1, 3, 5, 8, 10, and 20 mins) to check the volume of supernatant which remained. Similarly, the optimal sample injection volume for this assay was also optimized to increase the sensitivity of MPA. To check the effects of increasing injection volume, MPA (after sample processing) was injected from 10 µL to 50 µL (i.e., 10, 20, 30, 40, 50 µL) using the optimized UPLC conditions.

2.2.3.5 *Extraction solvent optimization*

After testing the calibration concentrations, further optimizations were done to increase the sensitivity of the analytes. The ratio of organic solvent to human plasma was optimized as a higher organic solvent to plasma ratio can possibly provide improved extraction and thus sensitivity. Multiple ratios of organic solvent (i.e., using ACN) to plasma sample extraction were tested (i.e., plasma: organic solvent 1:1, 1:2, 1:3), while fixing the volume of plasma sample.

2.2.4 Summary for sample preparation conditions

Once the various parameters of the assay extraction were optimized and the final conditions obtained, the assay was validated in accordance with the FDA guidelines for bioanalytical method validation [92]. The final assay protocol has been summarized in the flowchart below (Figure 2.7).

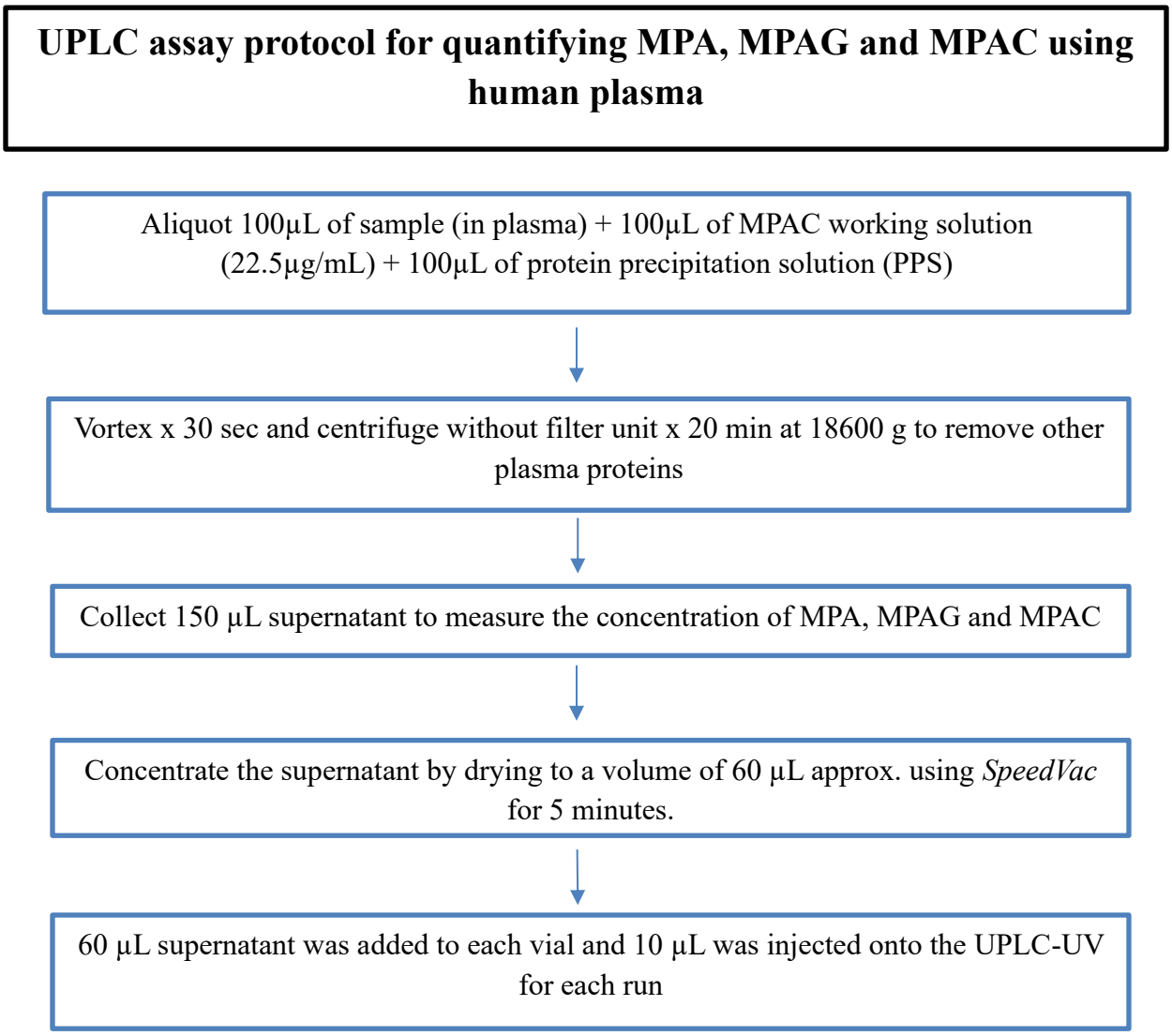

Figure 2.7 The final assay protocol with optimized assay preparation and instrument conditions for the MPA UPLC assay

2.2.5 Validation approach

Once the assay was developed, it needs to undergo a series of tests to determine its robustness, accuracy/precision, and stability [92].

2.2.5.1 *Mycophenolic acid assay validation accuracy and precision*

For the MPA assay, the validation guidelines by the FDA for bioanalytical method validation [92] were followed. Once the MPA assay calibration range was finalized, the accuracy and precision (A & P) of the assay was measured within the same day (intra-day A & P) and on 3 different days (inter-day A & P). For measuring the inter-day, A & P, 3 replicates of standard calibration curves (ranging from 0.3 to 10 µg/mL) were prepared with blanks and zero calibrators, followed by 5 replicates of the quality control samples (QC, i.e., 0.75, 2.25, 5, and 7.5 µg/mL). The criterion for passing the validation was to have an A & P within ±15% of the nominal concentration [92]. However, the A & P at the LLOQ could be within ±20%.

2.2.5.2 *Mycophenolic acid assay validation stability*

After testing the inter and intra-day variability of the assay, the next validation requirement was stability testing under various storage conditions as below.

- ***Benchtop*** - Benchtop stability samples were prepared and stored at room temperature (~24 °C) and were processed at a fixed time after storage (i.e., 3-6h) in order to determine the stability of the analyte(s) in the plasma. This stability condition was tested in high and low QC concentrations [92].

- ***Freeze-thaw -*** The plasma samples were stored in the freezer at -80°C without any further sample processing (no extraction, no drying). The samples were then thawed at room temperature after 24h (first freeze-thaw cycle). Similarly, the samples were stored in the freezer again and then thawed the next day until the third cycle is done. This stability condition was tested in high and low QC concentrations [92].
- ***Autosampler -*** The autosampler stability plasma samples were stored at ~4°C in the autosampler of the UPLC and later processed after 24h to determine the stability of the analyte(s). This stability condition was tested in high and low QC concentrations [92].
- ***Long-term -*** the plasma samples containing MPA, MPAG, and MPAC were stored at -80°C and later processed after 6 weeks of storage. This stability was tested in high and low QC concentrations [92].

2.2.5.3 *Mycophenolic acid assay extraction efficiency (in plasma)*

Assay recovery was determined using two sets of calibration standards where one set (with MPA, MPAG, and MPAC added before sample extraction) was subjected to the normal assay extraction procedures and the other set was only added the analyte standards (at equal molar concentrations) after matrix extraction. The extraction efficiency was calculated as follow.

$$Extraction\ efficiency\ \% = \frac{Peak\ area\ of\ analyte\ added\ after\ sample\ extraction}{Peak\ area\ of\ analyte\ added\ before\ sample\ extraction} \times 100\%$$

2.2.6 Dried blood spots

Dried blood spot (DBS) collection is a novel micro sampling technique by which the sample is collected using a finger or a heel prick [93]. DBS has the advantage of being less invasive, using lesser volume of blood, collection via a finger prick, and a better patient compliance in comparison to the conventional venipuncture [93, 94]. DBS is currently being used for the therapeutic drug monitoring of drugs, neonatal congenital disease screening, toxicokinetic-pharmacokinetic studies, and in forensic toxicology [93]. In this study, the applicability of DBS for the MPA assay was tested as a proof-of-concept to determine if the approach is generally feasible.

2.2.6.1 *Mycophenolic acid assay calibration set in dried blood spots*

Our initial test was to determine if the chromatographic conditions from the current MPA assay using plasma was suitable for the DBS approach. This was done by injecting a mixture of MPA and MPAC at a concentration of 10 µg/mL using the final assay conditions in the UPLC. Once the assay conditions were deemed appropriate (since a chromatography response was observed), a standard calibration curve of MPA was tested in DBS. The standard calibration set range was from 0.3 µg/mL to 10 µg/mL using whole blood (WB) spotted onto the Whatman 903 Protein Saver® cards. Since these standard calibration concentrations in plasma were not as sensitive in the DBS, adjustments were made, and the final calibration range of MPA ranged from 3.8 µg/mL to 28.57 µg/mL.

2.2.6.2 *Effects of adding the internal standard before vs. after sample extraction*

Once the standard calibration range was determined, additional parameters were also optimized to obtain higher peak areas and usable chromatography. First, the effects of adding the internal standard, MPAC, before or after sample extraction was tested. This was done by preparing replicates of the MPA calibrations sets where one replicate was subjected to the normal sample processing (MPAC added after spotting on DBS) and the experimental group where the analytes were subjected to the regular sample processing but with MPAC being added before spotting samples on the DBS.

2.2.6.3 *Extraction efficiency of mycophenolic acid in dried blood spots*

Extraction efficiency or recovery in DBS was done in the same process described for plasma (i.e., by preparing two sets of calibration standards where one set undergoes the normal assay extraction procedures, and the other set had the analytes added post-extraction).

2.3 Methods for the *p*-cresol assay

2.3.1 Spectral scan

2.3.1.1 *Spectral scanning of p-cresol and its metabolites using ultraviolet-visible spectrophotometer*

As part of the initial development for the assay measuring *p*C, parameters such as methods of detection and wavelengths of detection were first optimized. This was done using the

ultraviolet-visible spectrophotometer (Shimadzu® UV-2600i) and the fluorescence spectrophotometry (Shimadzu® RF-6000) using the following steps.

- **Step 1** – Checking the solubility of the analytes and the internal standard in solvents (i.e., water and ACN). Using this solubility data, stock solution(s) with multiple concentration(s) were prepared.
- **Step 2** – To determine the optimal testing concentration that was common to all analytes (*p*C and its metabolites, as well as internal standard DMP) giving absorbance intensity in the range 0.2 to 0.8 on the ultraviolet spectrum based on intense (but non-saturated) colour intensities (red to orange).
- **Step 3** – To check the effects of pH on the absorbance of analytes. This was done using two different pH levels (3 and 7) adjusted using formic acid and ammonium acetate.
- **Step 4** – To check the effects of using different solvents and solvent combinations on the absorbance. This was done by preparing the analyte working solutions in pure water, ACN, and a combination of solute solvents.

Working solutions of *p*C, *p*CS, *p*CG, and DMP at a concentration of 30 µg/mL were prepared using pure ACN and pure water at pH 3 and pH 7. The pH was adjusted using formic acid and ammonium acetate. After the solutions were prepared, they were analyzed in the ultraviolet spectrophotometer (Table 2.4) to obtain the absorbance (within the range 0.2-0.8) that provided the highest (but non-saturating) intensity. The highest intensity associated wavelength is translated to highest sensitivity of the analytes, which will be useful for determining the sensitivity of detection on the UPLC instrument.

Table 2.4 Analytical conditions of the ultraviolet-visible spectrophotometer for the pC analytes

Instrument Name	**Ultraviolet-visible Spectrophotometer**
Model:	RF-6000 series
Excitation start wavelength:	200.0 nm
Excitation end wavelength:	600.0 nm
Data interval:	10.0 nm
Emission start wavelength:	200.0 nm
Emission end wavelength:	750.0 nm
Data interval:	10.0 nm
Scan speed:	High speed
Spectrum type:	Absorbance
Slit width:	2
Detector unit:	Direct receiving of light
Light source switch wavelength:	323
S/R switch:	Standard
Stair correction:	ON
Spectrum transformation:	OFF
Data processing table:	OFF

2.3.1.2 *Spectral scanning of p-cresol and its metabolites using fluorescence spectrophotometry*

Similarly, the working solutions of *p*C, *p*CS, *p*CG, and DMP (at 30 µg/mL) were also analyzed in the fluorimeter (using 100% ACN or 100% water at pH 3 and pH 7, Table 2.5), to obtain the wavelengths associated with high intensity colors on the spectral scans.

Table 2.5 Analytical conditions of the fluorescence spectrophotometry for the pC analytes

Instrument name	**Fluorescence Spectrophotometry**
Model:	RF-6000 Series
Spectrum type	3D
Excitation start wavelength:	200.0 nm
Excitation end wavelength:	600.0 nm
Data interval:	10.0 nm
Emission start wavelength:	200.0 nm
Emission end wavelength:	750.0 nm
Data interval:	10.0 nm
Scan speed:	6000 nm/min
Spectrum type:	Fluorescence

2.3.2 Chromatography optimization

A systematic approach was also followed to develop the chromatographic assay conditions, thereby yielding the final conditions associated with the assay.

2.3.2.1 *Solvent optimization – methanol*

After obtaining the optimal wavelengths from the fluorescence spectrophotometry, the chromatography for *p*C, *p*CS, *p*CG, and DMP was optimized first in methanol to derive the ideal chromatography. The optimizations were done using the following instruments/parts.

- Shimadzu® ultra-high performance liquid chromatography with ultraviolet-detection (UPLC-UV) coupled with fluorescence detector: model LC-2040C Plus and model RF-20 AXS as shown in Figure 2.4
- The column used with the instrument was an Agilent® Eclipse XDB-C18 column (5 µm, 4.6×250 mm) as shown in Figure 2.5

Methanol concentration was the initial chromatographic parameter that was optimized (i.e., 71%, 72%, 73%, 74%, 75%, 76%, 77%, 78%, 79%, 80%) using a flow rate of 1 mL/min, a formic acid concentration of 0.02%, an ammonium acetate concentration of 0.4 mM, an injection volume of 10 µL, a run time of 15 mins, and fluorescence wavelengths at excitation 220 nm and emission 300 nm (discussed in results section). The criteria for selecting the chromatography conditions were i) high peak area counts (high sensitivity), ii) optimal peak shape (without peak distortion or fronting/tailing), and iii) short run time.

2.3.2.2 *Solvent optimization – acetonitrile*

Likewise, these chromatographic parameters were also optimized in ACN using the same approach as detailed above. This was done by preparing the analyte working solution (at a concentration of 10 µg/mL) and the instrument mobile phase in ACN. The concentrations of ACN were varied from 20% to 100% while ammonium acetate was kept at 0.4 mM, formic acid

at 0.02%, flow rate 1 mL/min, injection volume 10 µL, run time 13 mins, and fluorescence wavelengths at excitation 268 nm, emission 300 nm.

2.3.2.3 *Additive optimization – formic acid (in methanol)*

The pH of the mobile phase plays a significant role in chromatography (peak shapes, ideal run time, separation, etc.). To assess the effects of pH in our assays, *p*C, *p*CS, *p*CG, and DMP were tested in a mixture to optimize the percentage of formic acid, ammonium acetate, and phosphoric acid in the mobile phase. Formic acid concentration was adjusted from 0.000% to 0.505% (i.e., 0.000%, 0.051%, 0.101%, 0.152%, 0.157%, 0.202%, 0.253%, 0.303%, 0.353%, 0.404%, 0.454%, 0.505%) at a methanol concentration of 73%, flow rate of 1 mL/min, ammonium acetate at 0.4 mM, injection volume of 10 µL, a run time of 10 mins, and fluorescence wavelengths at excitation 220 nm, emission 300 nm. The concentration of ammonium acetate in the mobile phase was kept at a fixed concentration (0.4 mM) while optimizing the formic acid.

2.3.2.4 *Additive optimization – formic acid (in acetonitrile)*

The concentration of formic acid was also varied from 0% to 0.1% (i.e., 0%, 0.01%, 0.02%, 0.03%, 0.04%, 0.05%, 0.06%, 0.07%, 0.08%, 0.09%, 0.10%) in 40% ACN, 2 mM ammonium acetate, 1 mL/min flow rate, 10 µL injection volume, 13 mins of run time, and fluorescence wavelengths at excitation 268 nm and emission 300 nm. Formic acid optimization was followed by adjusting the concentration of ammonium acetate in the mobile phases to obtain

the ideal pH conditions for optimal chromatographic conditions for *p*C, *p*CS, *p*CG, and DMP (using a concentration of 10 µg/mL for each analyte).

2.3.2.5 *Additive optimization – ammonium acetate (in methanol)*

Similarly, while optimizing the ammonium acetate from 0 mM to 1.0 mM (i.e., 0, 0.1, 0.2, 0.3, 0.4, 0.5, 0.6, 0.7, 0.8, 0.9, 1.0 mM) in methanol, formic acid was kept at 0.1%, methanol concentration at 73%, flow rate of 1 mL/min, injection volume of 10 µL, a run time of 10 mins, and fluorescence wavelengths at excitation 220 nm, emission 300 nm.

2.3.2.6 *Additive optimization – ammonium acetate (in acetonitrile)*

The concentration for ammonium acetate was varied from 0 mM to 2 mM (i.e., 0, 0.2, 0.4, 0.6, 0.8, 1.0, 1.2, 1.4, 1.6, 1.8, 2.0 mM) while the formic acid concentration was fixed at 0.1%, ACN concentration in mobile phase at 40%, flow rate at 1 mL/min, injection volume 10 µL, run time of 13 mins, and fluorescence wavelengths at excitation 268 nm, emission 300 nm.

2.3.2.7 *Additive optimization – phosphoric acid (in methanol)*

To test the effects of phosphate buffer on chromatography, phosphoric acid was varied from 0% to 0.45% (i.e., 0%, 0.04%, 0.09%, 0.13%, 0.18%, 0.22%, 0.27%, 0.31%, 0.36%, 0.40%, 0.45%) with methanol concentration fixed at 73%, potassium phosphate monobasic at 10 mM, flow rate of 1 mL/min, injection volume of 10 µL, a run time of 10 mins, and fluorescence wavelengths at excitation 220 nm, emission 300 nm.

2.3.2.8 *Additive optimization – phosphoric acid (in acetonitrile)*

Phosphoric acid concentrations were tested from 0% to 0.470% (i.e., 0%, 0.047%, 0.094%, 0.141%, 0.188%, 0.235%, 0.282%, 0.329%, 0.376%, 0.423%, 0.470%) in 40% ACN, 100 mM potassium phosphate monobasic, 1 mL/min flow rate, 10 µL injection volume, run time of 13 mins, and fluorescence wavelengths at excitation 268 nm, emission 300 nm.

2.3.2.9 *Flow rate optimization (in methanol)*

The flow rate was adjusted using a mixture of *p*C, *p*CS, *p*CG, and DMP (at 10 µg/mL) from 0.25 mL/min to 1.25 mL/min (i.e., 0.25, 0.5, 0.75, 1.0, 1.25 mL/min) while the methanol concentration was kept at 73%, formic acid concentration of 0.1%, ammonium acetate at 0.1 mM, injection volume of 10 µL, with fluorescence wavelengths at excitation 220 nm, emission 300 nm (run time was varied according to the flow rate). Only flow rates between 0.25 mL/min to 1.25 mL/min were used since the utilized UPLC column has a limited pressure between 0.1 mL/min to 2 mL/min.

2.3.2.10 *Flow rate optimization (in acetonitrile)*

The flow rate was adjusted from 0.5 mL/min to 1.5 mL/min (i.e., 0.5, 1.0, 1.25, 1.5 mL/min) while the ACN concentration was fixed at 40%, ammonium acetate at 0.8 mM, formic acid at 0.1%, injection volume of 10 µL, run time at 13 mins, and fluorescence wavelengths at excitation 268 nm, emission 300 nm.

2.3.2.11 *Injection volume optimization (in methanol)*

*p*C, *p*CS *p*CG, and DMP were prepared using pure methanol (at the concentration of 10 µg/mL) and injected into the UPLC at varying injection volumes (i.e., 10, 15, 20, 25, 30, 35, 40, 45, 50 µL) using a mobile phase consisting of 73% methanol, 0.1% formic acid, 0.1 mM ammonium acetate, flow rate of 1 mL/min, and fluorescence wavelengths at excitation 220 nm, emission 300 nm.

2.3.2.12 *Injection volume optimization (in acetonitrile)*

Injection volume was varied from 10 µL to 50 µL (10, 15, 20, 25, 30, 35, 40, 45, 50 µL) with ACN concentration fixed at 40%, ammonium acetate at 0.8 mM, formic acid at 0.1%, run time at 24 mins, and fluorescence wavelengths at excitation 268 nm, emission 300 nm.

2.3.3 Sample preparation optimization

The various steps involved with the sample preparation/extraction process prior to injection into the UPLC instrument were also optimized in plasma to obtain optimal chromatography and assay sensitivity. ACN was utilized as the solvent for these subsequent assay developments (discussed below).

2.3.3.1 *Determination of lower limit of quantification using pure solvent*

The sample preparation/extraction protocol including *p*C, *p*CS, *p*CG, and DMP was modified from a published manuscript from our lab group [61] which utilized UPLC in the measurement of *p*C, and LC-MS/MS in the measurement of *p*CS and *p*CG [53, 55, 56, 62]. First, the limits of quantitation were tested, where the ULOQ is the highest concentration in a standard calibration set that can successfully give a straight curve (without any peak area saturation) and the LLOQ is the lowest concentration in the standard calibration set that can successfully quantify the analyte and gives acceptable chromatography (peak shape and separation) [92]. LLOQ is a measurement of the sensitivity of an assay [92]. Similarly, blank sample is a sample that is devoid of any analytes that are to be tested or are currently being tested, while the zero calibrator is a sample with the same composition as the blank but also possesses the internal standard of the assay [92].

2.3.3.2 *Standard calibration curve in human plasma*

A standard calibration set was prepared using *p*C, *p*CS, *p*CG, and DMP from 0.002 µg/mL to 250 µg/mL in pure ACN using the final optimized chromatographic conditions (ACN concentration in the buffer was 40%, ammonium acetate was kept at 2 mM, formic acid at 0.1%, injection volume of 10 µL, flow rate of 0.5 mL/min, the run time at 24 mins, and fluorescence wavelengths at excitation 268 nm, emission 300 nm). However, there was no response observed below 0.002 µg/mL for *p*C, 0.004 µg/mL for *p*CS, and 0.075 µg/mL for *p*CG. Using the results from this standard curve prepared in pure ACN, the *p*C, *p*CS, and *p*CG standard calibration ranges were further tested in human plasma. To accomplish this, pooled human plasma with

EDTA was used to prepare several concentrations via serial dilutions. *p*C, *p*CS, and *p*CG calibration concentrations were varied from 0.002 µg/mL to 50 µg/mL using human plasma while DMP (the internal standard) was kept at a fixed concentration of 10 µg/mL. The samples for blank and zero calibrators were also prepared. The PPS for this assay was pure methanol.

2.3.3.3 *Internal standard optimization for p-cresol assay*

To obtain the ideal condition for the internal standard, the concentration of the internal standard (i.e., DMP) was also optimized. A standard calibration set was prepared using DMP only (devoid of *p*C, *p*CS, or *p*CG) at varying concentrations ranging from 0.0025 µg/mL to 50 µg/mL in human plasma to determine the concentration of DMP providing robust instrument response without any peak area signal saturation on the UPLC.

2.3.3.4 *Extraction solvent optimization*

After testing the calibration concentrations, further optimizations were done to increase the sensitivity of the analytes. The ratio of organic solvent to human plasma was optimized as a higher organic solvent to plasma ratio can possibly provide improved extraction and thus sensitivity. Multiple ratios of organic solvent (i.e., in methanol) to plasma sample extraction were tested (i.e., plasma: organic solvent 1:1, 1:2, 1:3), while fixing the volume of plasma sample.

2.3.3.5 *Centrifuge parameter optimization*

To separate *p*CS and *p*CG peaks in the chromatogram, the centrifuge parameters including centrifuge speed (in g) and centrifuge time (min) were optimized. The mixture of *p*C, *p*CS, *p*CG, and DMP was prepared using methanol at a concentration of 25 µg/mL and the centrifuge speed was optimized from 4000 g to 20000 g (i.e., 4000, 8000, 12000, 16000, 20000 g) while keeping the centrifuge time at 10 mins. Similarly, the time of centrifugation was optimized from 10 mins to 20 mins (i.e., 10, 15, 20 mins) while keeping the centrifuge speed at 4000 g.

2.3.3.6 *Concentrating and injection volume optimization*

This was done by checking the effects of drying the sample supernatant on the peak separation and intensity. Two replicates of standard calibration curves with *p*C, *p*CS, and *p*CG were prepared using human plasma (from 0.0002 µg/mL to 50 µg/mL) with DMP at a fixed concentration of 25 µg/mL (in pure ACN). One group of the calibration curve was subjected to the normal sample processing (i.e., without drying), whereas the other calibration curve was subjected to an additional step of supernatant drying using the *SpeedVac* instrument (for 2 mins) after sample extraction. This was followed by injection volume testing, where the volume of the mixture for *p*C, *p*CS, *p*CG, and DMP was varied from 10 µL to 30 µL (i.e., 10, 20, 30 µL) using the final optimized chromatographic conditions (ACN concentration was 40%, ammonium acetate was kept at 2 mM, formic acid at 0.1%, injection volume of 10 µL, flow rate of 0.5 mL/min, the run time at 24 mins, and fluorescence wavelengths at excitation 268 nm, emission 300 nm).

After this optimization, the peaks for *p*CS and *p*CG still failed to separate, and hence these were not included in the assay protocol (please see discussions). Instead, the ideal chromatography conditions for using *p*C and DMP only were further optimized.

2.3.3.7 *De-conjugation testing and parameter optimization*

2.3.3.7.1 De-conjuration ratio testing

A de-conjugation procedure (to convert *p*CS and *p*CG to *p*C) was required in prior to sample analysis. *p*CS was prepared at concentrations 3 µg/mL and 10 µg/mL using human plasma, subsequently, the sample was subjected to heat and acid using a water bath at 90 °C and 6M hydrochloric acid, respectively, to facilitate the process of de-conjugation.

2.3.3.7.2 Heat and acid optimization

The parameters associated with the process of de-conjugation such as heating time and the concentration of the acid were optimized as follows: heating time was varied from no heat to 60 mins (i.e., 0, 15, 30, 45, 60 mins) while the acid concentration was fixed at 6 M. Similarly, the concentration of the acid was tested from no acid to 6M (i.e., 0, 3, 6 M) with the heat time maintained as the above-mentioned de-conjugation conditions.

2.3.4 Summary for sample preparation conditions

Once the various parameters of the assay extraction were optimized and the final conditions obtained, the assay was validated in accordance with the FDA guidelines for bioanalytical method validation [92]. The final assay protocol has been summarized in the flowchart below (Figure 2.8).

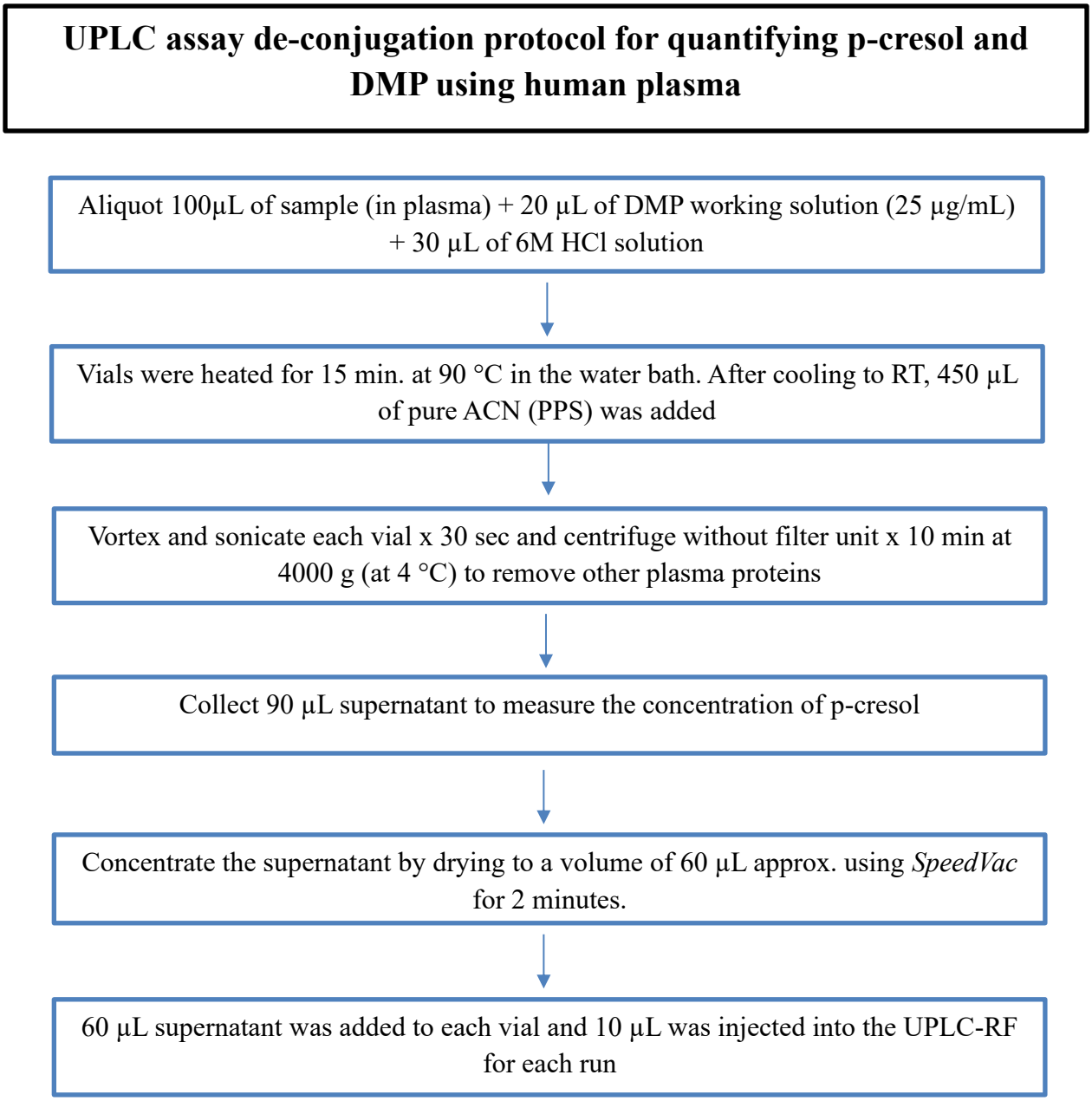

Figure 2.8 The final assay protocol with optimized assay preparation and instrument conditions for the pC UPLC assay

2.3.5 Validation approach

Once the assay was developed, it needs to undergo a series of tests to determine its robustness, accuracy/precision, and stability [92].

2.3.5.1 *p-Cresol assay validation accuracy and precision*

For the *p*C assay, the validation guidelines by the FDA [92] was also followed. Once the *p*C assay calibration range was finalized, the accuracy and precision (A & P) of the assay was measured within the same day (intra-day A & P) and on 3 different days (inter-day A & P). For measuring the inter-day, A & P, 3 replicates of standard calibration curves (ranging from 0.73 to 31.25 µg/mL) were prepared with blanks and zero calibrators, followed by 5 replicates of the quality control samples (QC, i.e., 1.0, 3.0, 12.5, and 25 µg/mL). The criterion for passing the validation was to have an A & P within ±15% of the nominal concentration [92]. However, the A & P at the LLOQ could be ±20%.

2.3.5.2 *p-Cresol assay validation stability*

After testing the inter and intra-day variability of the assay, the next validation requirement was stability testing under various storage conditions as below.

- ***Benchtop*** - Benchtop stability samples were prepared and stored at room temperature (~24 °C) and were processed at a fixed time after storage (i.e., 3-6h) in order to determine the stability of the analyte(s) in the plasma. This stability condition was tested in high and low QC concentrations [92].

- ***Freeze-thaw -*** The plasma samples after the dilutions were stored in the freezer at -80°C without any further sample processing (no extraction, no drying). The samples were then thawed at room temperature after 24h (first freeze-thaw cycle). Similarly, the samples were stored in the freezer again and then thawed the next day until the third cycle is completed. This stability condition was tested in high and low QC concentrations [92].
- ***Autosampler -*** The autosampler stability plasma samples were stored at ~4°C in the autosampler of the UPLC and later processed after 24h to determine the stability of the analyte(s). This stability condition was tested in high and low QC concentrations [92].
- ***Long-term -*** The plasma samples containing *p*C and DMP were stored at -80°C and later processed after 6 weeks of storage. This stability was tested in high and low QC concentrations [92].

2.3.5.3 *p-Cresol assay extraction efficiency (in plasma)*

Assay recovery was determined using two sets of calibration standards where one set (with *p*C and DMP added before sample extraction) was subjected to the normal assay extraction procedures and the other set was only added the analyte standards (at equal molar concentrations) after matrix extraction. The extraction efficiency was calculated as follow.

$$Extraction\ efficiency\ \% = \frac{Peak\ area\ of\ analyte\ added\ after\ sample\ extraction}{Peak\ area\ of\ analyte\ added\ before\ sample\ extraction} \times 100\%$$

2.3.6 Dried blood spot approach

In this study, the applicability of DBS for the *p*C assay was tested as a proof-of-concept to determine if the approach is generally feasible.

2.3.6.1 *p-Cresol assay calibration set in dried blood spots*

Our initial test was to determine if the chromatographic conditions from the current *p*C assay using plasma was suitable for the DBS approach. This was done by injecting a mixture of *p*C and DMP at a concentration of 31.25 µg/mL using the final assay conditions in the UPLC. Once the assay conditions were deemed appropriate (since a chromatography response was observed), a standard calibration curve of *p*C was tested in DBS. The standard calibration set range was from 0.73 µg/mL to 31.25 µg/mL (with DMP fixed at 25 µg/mL) using WB spotted onto the Whatman 903 Protein Saver® cards.

2.3.6.2 *Effects of adding the internal standards before vs. after sample extraction*

Once the standard calibration range was determined, additional parameters were also optimized to obtain higher peak areas and usable chromatography. First, the effects of adding the internal standard, DMP, before or after sample extraction was tested. This was done by preparing replicates of the *p*C calibrations sets where one replicate was subjected to the normal sample processing (DMP added after spotting on DBS) and the experimental group where the analytes were subjected to the regular sample processing but with DMP being added before spotting samples on the DBS.

2.3.6.3 *Extraction efficiency of p-cresol in dried blood spots*

Extraction efficiency or recovery in DBS was done in the same process described for plasma (i.e., by preparing two sets of calibration standards where one set undergoes the normal assay extraction procedures, and the other set had the analytes added post-extraction).

2.4 Results for mycophenolic acid assay

2.4.1 Spectral scan

2.4.1.1 *Spectral scanning of mycophenolic acid and its metabolites using ultraviolet-visible spectrophotometer*

MPA, MPAG, and MPAC working solutions were prepared in ACN at a concentration of 30 µg/mL at pH 3, pH 4 and pH 7 to determine the optimal wavelength using ultraviolet detection method. Figure 2.9 and Figure 2.10 represent the spectral scan from injecting blank ACN and methanol in the ultraviolet spectrophotometer, respectively, where the x-axis depicts the wavelength and y-axis depicts the associated absorbance. Using ultraviolet spectrophotometer, the absorbance intensity was recorded in the range from 0.2 to 0.8. As observed from the spectral scans using ACN below, MPA showed the maximum absorbance at 304.32 - 304.95 nm wavelength (Figure 2.11), MPAG at 294.68 - 295.04 nm wavelength (Figure 2.12), and MPAC at 294.80 - 294.90 nm wavelength (Figure 2.13). In addition, varying the pH (from pH 3 to pH 4 to pH 7) did not have any impact on the wavelength or absorbance (data not shown). Therefore, the final chosen wavelength for MPA, MPAG, and MPAC were 305 nm and 295 nm, which were used in the UPLC instrument.

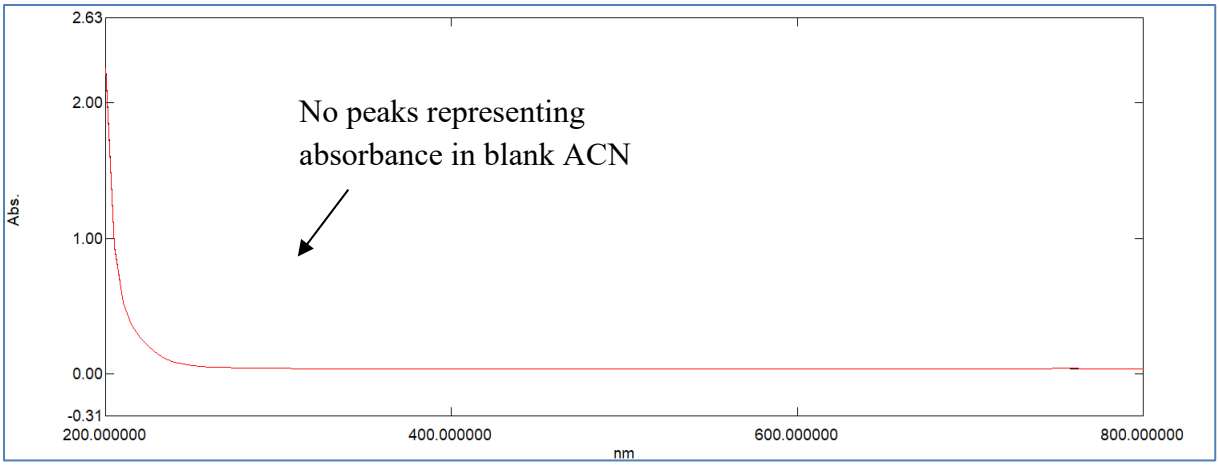

Figure 2.9 The spectral scan of pure ACN (blank, without any analyte, at pH 4.25) using the ultraviolet-visible spectrophotometer

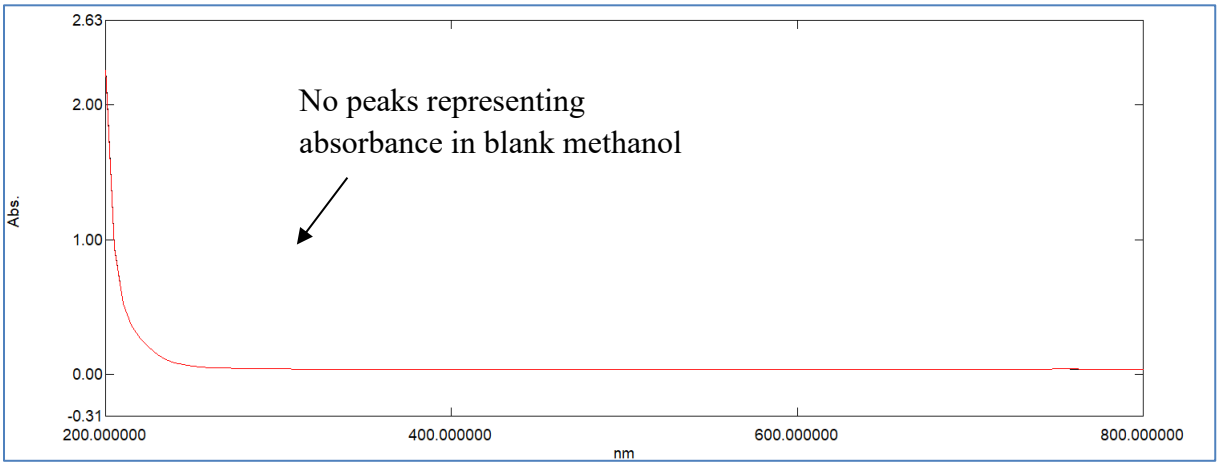

Figure 2.10 The spectral scan of pure methanol (blank, without any analyte, at pH 5.8) using the ultraviolet-visible spectrophotometer

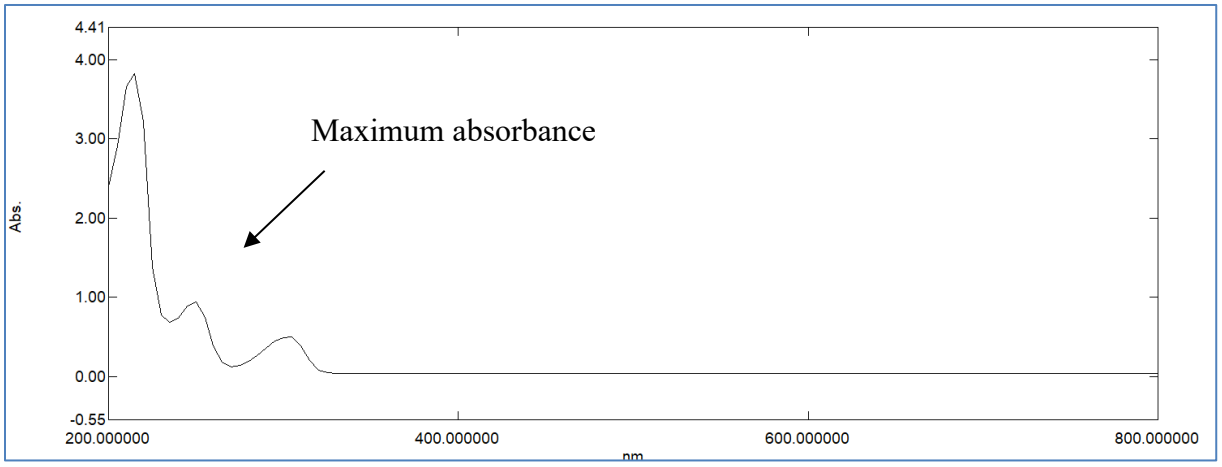

Figure 2.11: The spectral scan of MPA analyzed at pH 3 in pure acetonitrile using the ultraviolet-visible spectrophotometer

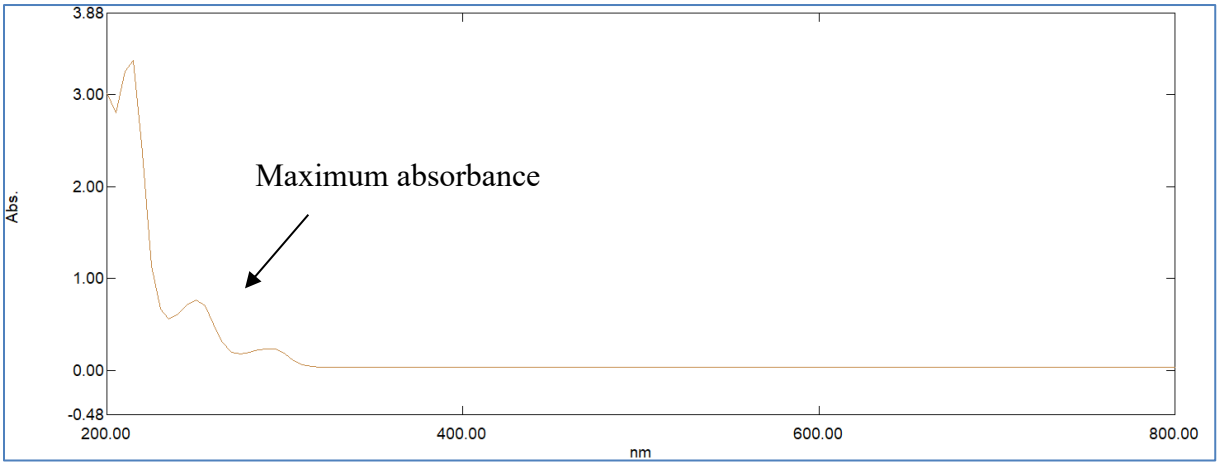

Figure 2.12 The spectral scan of MPAG analyzed at pH 3 in pure acetonitrile using the ultraviolet-visible spectrophotometer

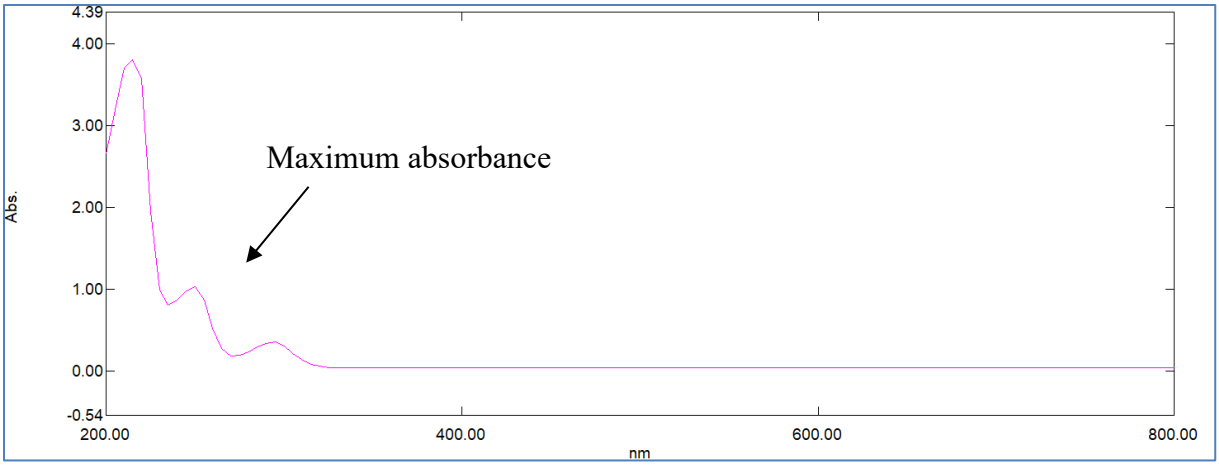

Figure 2.13 The spectral scan of MPAC analyzed at pH 3 in pure acetonitrile using the ultraviolet-visible spectrophotometer

2.4.1.2 *Spectral scanning of mycophenolic acid and its metabolites using fluorescence spectrophotometry*

As part of our assay development, MPA and its metabolites were also tested in the fluorescence spectrophotometer to determine the suitability of fluorescence detection. The testing in fluorescence spectrophotometry was done by preparing MPA, MPAG, and MPAC at a concentration of 30 µg/mL using 100% ACN at pH 3 and pH 7. In the fluorescence-spectra, a distinct 3D spectrum was observed with colors ranging from blue to orangish-red. The intensity of the color observed in the spectra is a representation of the associated wavelength. Higher wavelengths are confirmed by observing the green to orange color scheme, whereas low wavelengths are identified by the colors blue to yellow. In the figures below, the x-axis represents the emission wavelength, while the y-axis represents the excitation wavelength. For MPA, the fluorescence-spectra did not show areas of high intensity (because the spectra color

was blue) (Figure 2.14), however for MPAG (Figure 2.15) and MPAC (Figure 2.16), the 3D spectra showed bright orange to green responses. Varying the pH of analyte working solutions did not have a significant effect on the intensity of the color in the spectrum (data not shown). The wavelengths for MPAG and MPAC are shown below.

- MPAG: emission – 335 nm to 350 nm, excitation – 240 nm to 260 nm
- MPAC: emission – 335 nm to 365 nm, excitation – 240 nm to 260 nm

The fluorescence method of detection was acceptable for MPAG and MPAC, however, not applicable to our main analyte of interest, MPA. Hence, only the ultraviolet method of detection was further developed.

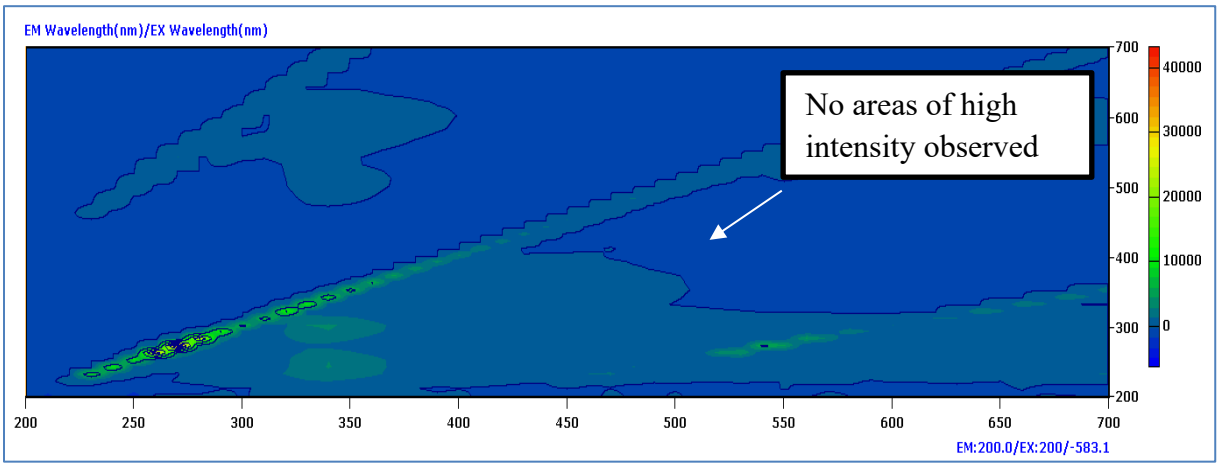

Figure 2.14 The spectral scan of MPA analyzed at pH 3 in pure acetonitrile using the fluorescence spectrophotometer

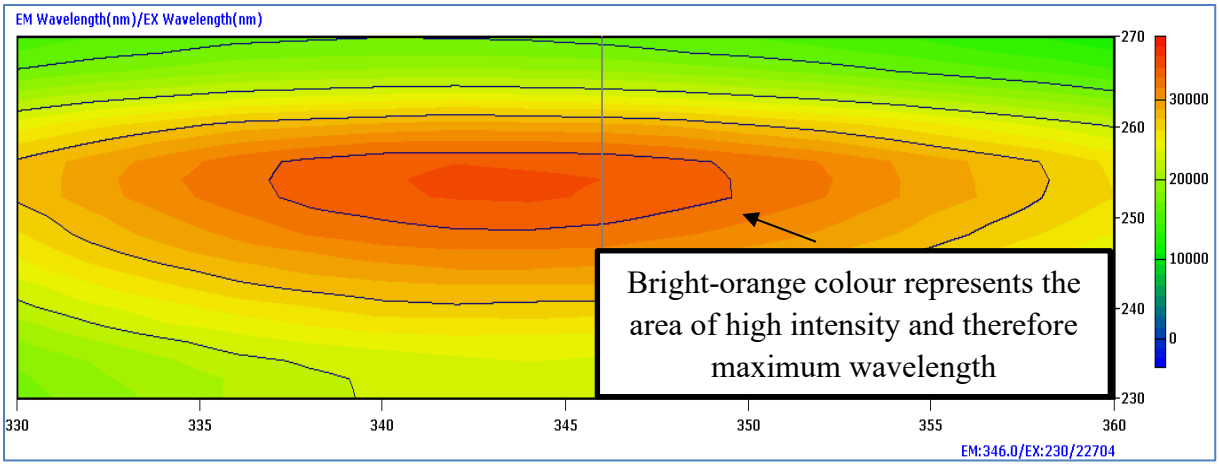

Figure 2.15 The spectral scan of MPAG analyzed at pH 3 in pure acetonitrile using the fluorescence spectrophotometer

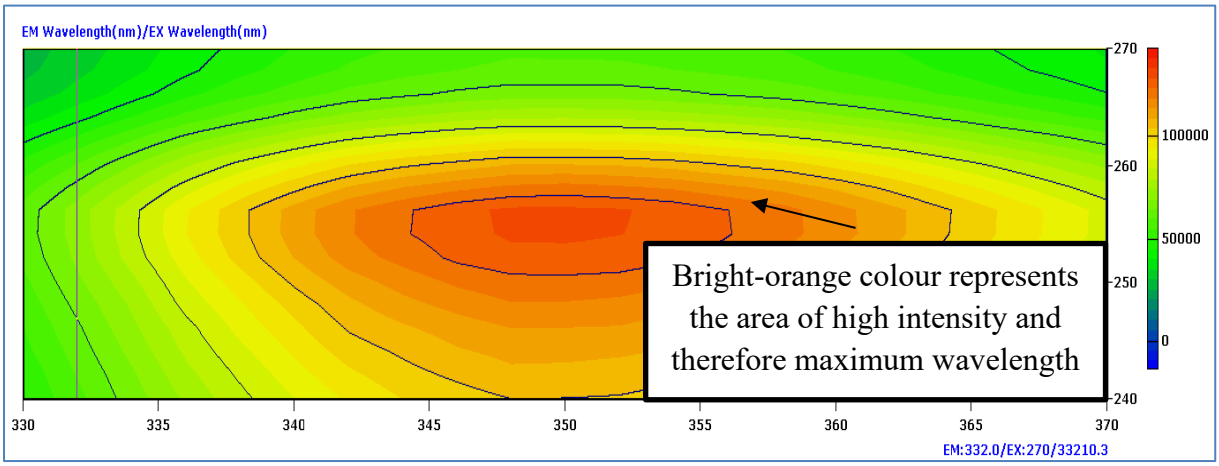

Figure 2.16 The spectral scan of MPAC analyzed at pH 3 in pure acetonitrile using the fluorescence spectrophotometer

2.4.2 Chromatography optimization

2.4.2.1 *Solvent optimization – methanol*

After obtaining the optimized wavelength from the ultraviolet-visible spectrophotometer, the concentration of methanol was optimized. In Figure 2.17, at 50% methanol, only MPAG (but not MPA) can be seen eluting. Hence, 50% methanol is not a workable condition for further chromatographic optimization. On the other hand, in Figure 2.18, it is clearly seen that the peaks for all the analytes (MPA and MPAG) are eluting very closely with 100% methanol. It was observed that the chromatography was affected by reducing methanol concentrations (i.e., at 60% methanol and 40% water, the resolution became better since the peaks eluted at distinct retention times (MPA – approximately 10.0 mins, MPAG – approximately 3.5 mins).

It is apparent that changing the concentration of the solvent affected the chromatography of the analytes by changing their elution times. Figure 2.19 illustrates the effects of 60% methanol where all the analytes can be eluted. At 60% methanol, the peaks also appear symmetrical, well-separated, and have relatively high peak area counts (as can be seen in Figure 2.19). The relationships between methanol concentration and MPA peak area can be seen in Figure 2.20.

In summary, it was observed that 60% methanol with 40% water provides better chromatography separation as compared to other conditions tested and hence was selected as the ideal methanol concentration.

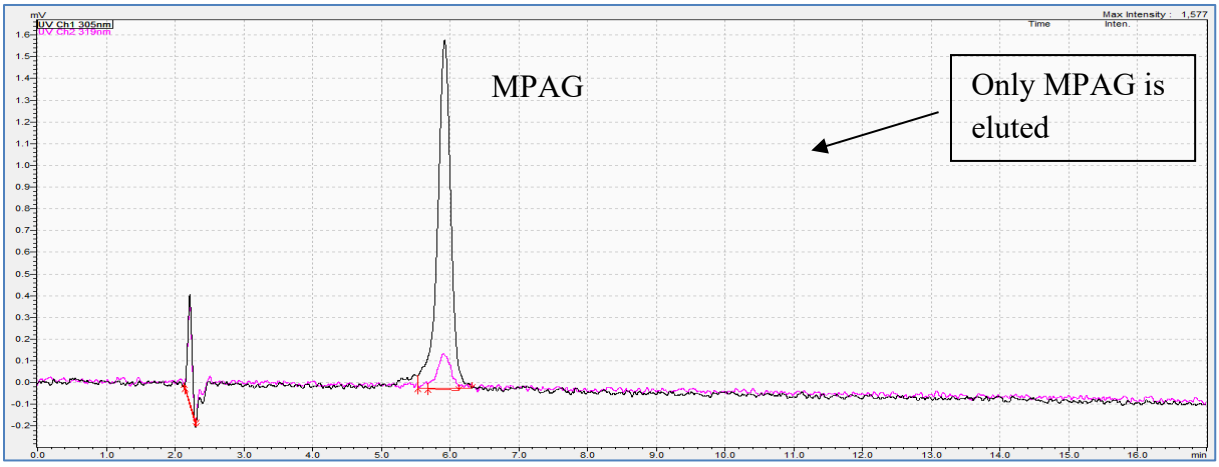

Figure 2.17 Methanol concentration optimization - the chromatogram of MPA and MPAG mixture using 50% methanol and 50% water in the mobile phase

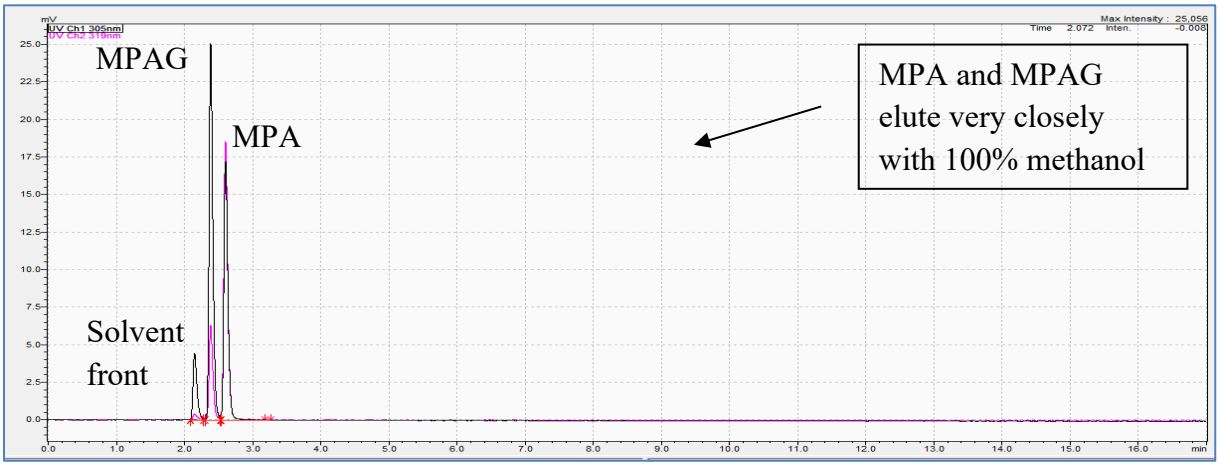

Figure 2.18 Methanol concentration optimization - the chromatogram of MPA and MPAG mixture using 100% methanol in the mobile phase

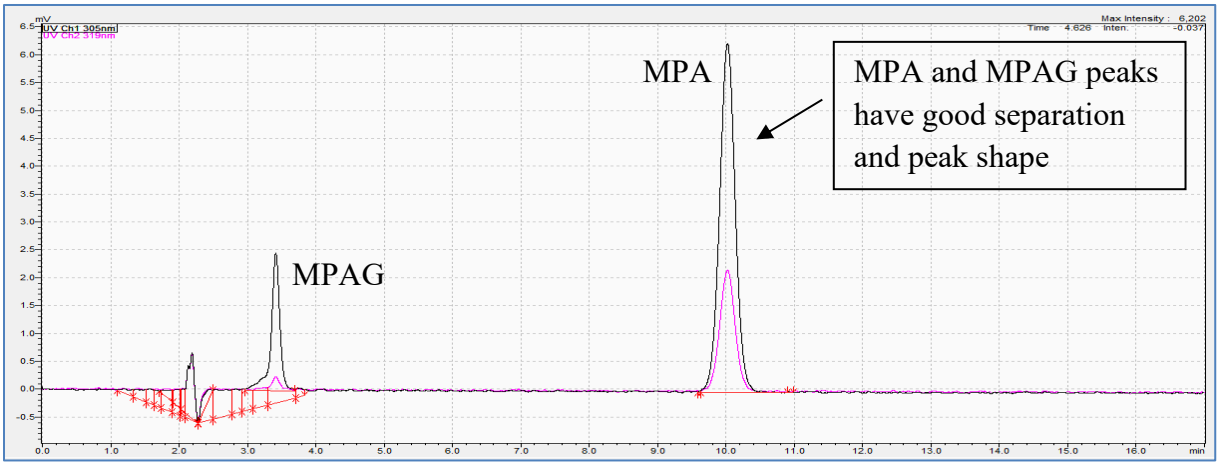

Figure 2.19 Methanol concentration optimization - the chromatogram of MPA and MPAG mixture using 60% methanol and 40% water in the mobile phase (optimized condition)

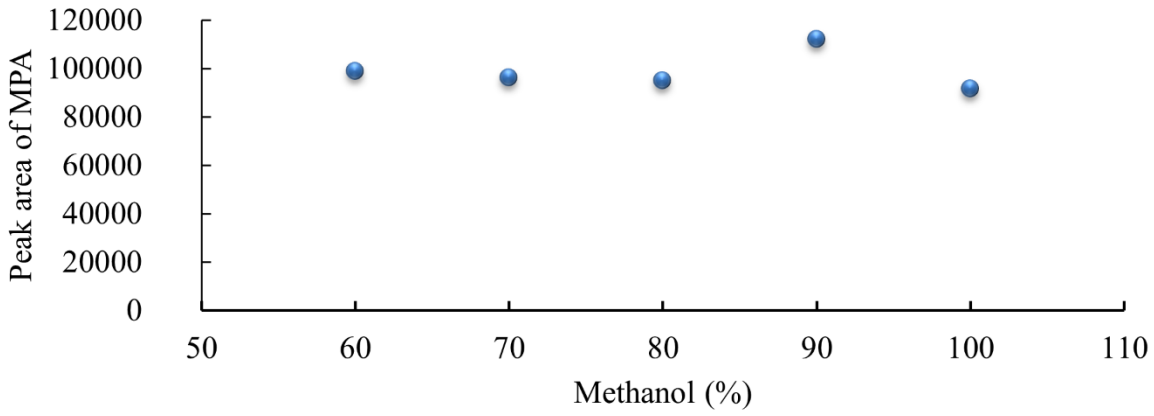

Figure 2.20 The correlation plot between methanol concentration in the mobile phase and the absolute peak area of MPA

2.4.2.2 *Solvent optimization – acetonitrile*

Once the optimized wavelength from the ultraviolet-visible spectrophotometer was obtained, the concentration of ACN was also optimized. In Figure 2.21, it is clearly seen that the

peaks for all the analytes (MPA, MPAG, and MPAC) are eluting very closely when using 100% ACN. Hence, 100% ACN is not a workable condition for further chromatographic optimizations. However, this trend changes as we move towards lower ACN concentrations i.e., at 40% ACN and 60% water (Figure 2.22) where the chromatography became better since the peaks elute at distinctive retention times (MPA – approximately 10.8 mins, MPAG – approximately 2.7 mins, MPAC –approximately 9.1) and have better peak separations. The peaks look symmetrical, well-separated, and have relatively high peak area counts (as can be seen in Figure 2.22). The relationships between ACN concentration and MPA peak area can be seen in Figure 2.23.

In summary, it was observed that 40% ACN with 60% water provides better chromatography separation as compared to other conditions tested and hence was selected as the ideal ACN concentration

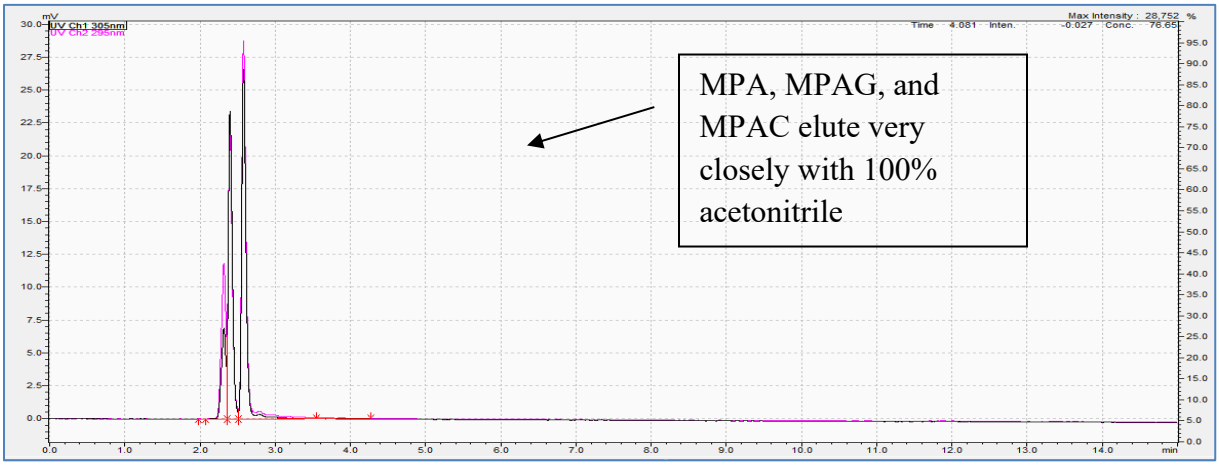

Figure 2.21 Acetonitrile concentration optimization - the chromatogram of MPA, MPAG, and MPAC mixture using 100% acetonitrile in the mobile phase

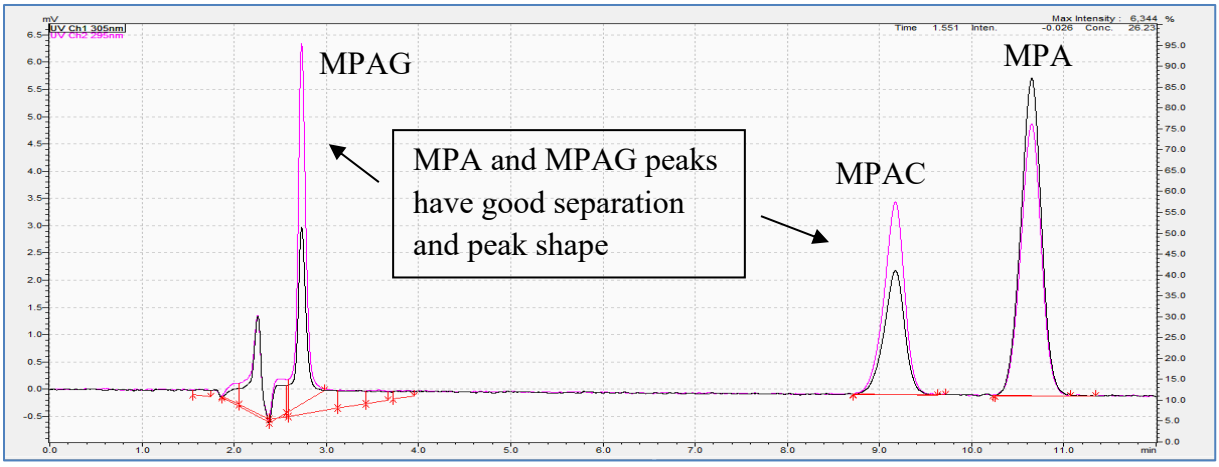

Figure 2.22 Acetonitrile concentration optimization - the chromatogram of MPA, MPAG, and MPAC mixture using 40% acetonitrile and 60% water in the mobile phase (optimized condition)

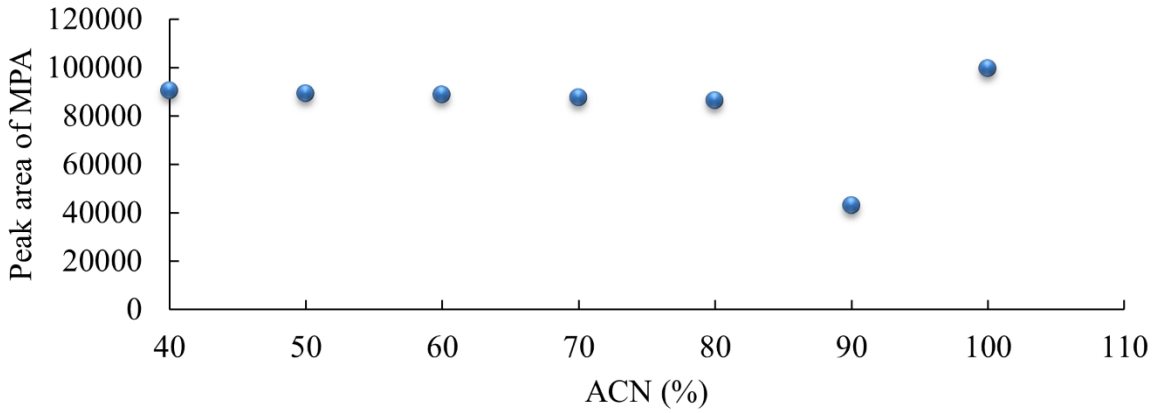

Figure 2.23 The correlation plot between acetonitrile concentration in the mobile phase and the absolute peak area of MPA

2.4.2.3 *Additive optimization – formic acid (in methanol)*

In Figure 2.24, the chromatography was obtained after injecting a mixture of MPA, MPAG, and MPAC (at a concentration of 10 µg/mL) using 0.306% formic acid and 0.5 mM ammonium acetate. It is evident that this concentration of formic acid results in symmetrical

peaks which are eluting at distinctive retention times (MPA – approximately 9.7 mins, MPAG – approximately 3.1 mins, MPAC – approximately 10.4 mins) with good peak separation. On the contrary, in Figure 2.25, there was no formic acid in the mobile phase with only ammonium acetate at 0.5 mM. When injecting the mixture sample (with MPA, MPAG and MPAC) at no formic acid in the mobile phase, the chromatography becomes not usable since the peaks are asymmetrical with apparent distortion/fronting. These data suggest that the lower the concentration of formic acid, the worse the chromatography can be observed (hence 0% formic acid was not a workable condition for further chromatographic optimizations). The relationships between formic acid concentration and MPA peak area can be seen in Figure 2.26.

In summary, the optimal concentration of formic acid in the mobile phase was determined to be 0.306% (with 0.5 mM ammonium acetate).

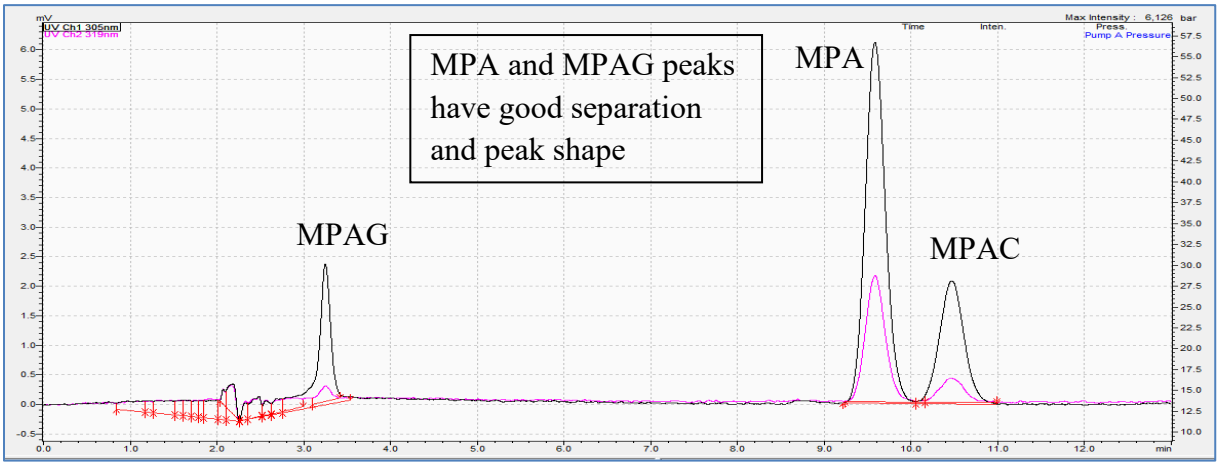

Figure 2.24 Formic acid concentration optimization (in methanol) - the chromatogram of MPA, MPAG, and MPAC mixture using 0.306% formic acid and 0.5 mM ammonium acetate in the mobile phase (optimized condition)

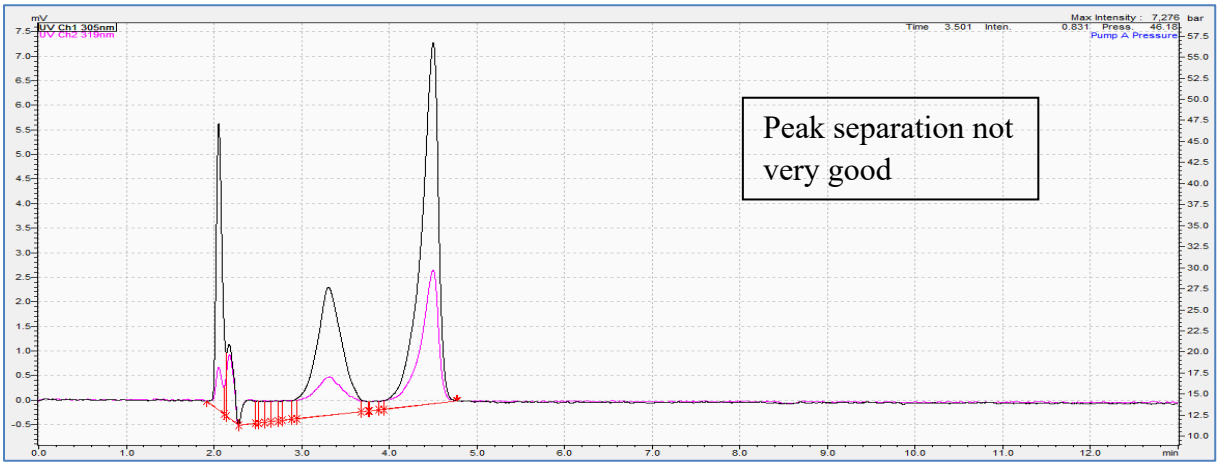

Figure 2.25 Formic acid concentration optimization (in methanol) - the chromatogram of MPA, MPAG, and MPAC mixture using 0% formic acid and 0.5 mM ammonium acetate in the mobile phase

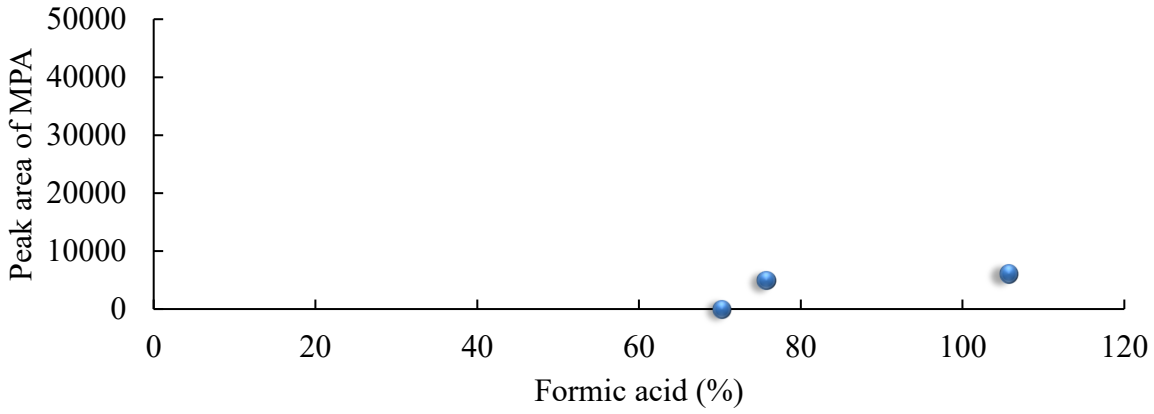

Figure 2.26 The correlation plot between formic acid concentration in methanol and the absolute peak area of MPA

2.4.2.4 *Additive optimization – formic acid (in acetonitrile)*

Using ACN, formic acid was also optimized while keeping ammonium acetate fixed at 2 mM. In Figure 2.27, the chromatography was obtained after injecting a mixture of MPA, MPAG, and MPAC (at a concentration of 10 µg/mL) using 0.1% formic acid and 2 mM ammonium acetate. It is evident that using this concentration of formic acid, the peak shapes for the analytes were symmetrical, and the peaks were eluting at distinctive retention times (MPA – approximately 10.1 mins, MPAG – approximately 2.8 mins, MPAC – approximately 8.7 mins.) with good separation. On the contrary, Figure 2.28 represents no formic acid in the mobile phase with only ammonium acetate (2 mM) being present, which resulted in relatively poor chromatography. The relationships between formic acid concentration and MPA peak area can be seen in Figure 2.29.

In summary, 0.1% formic acid with 2 mM ammonium acetate provides ideal chromatographic conditions in ACN.

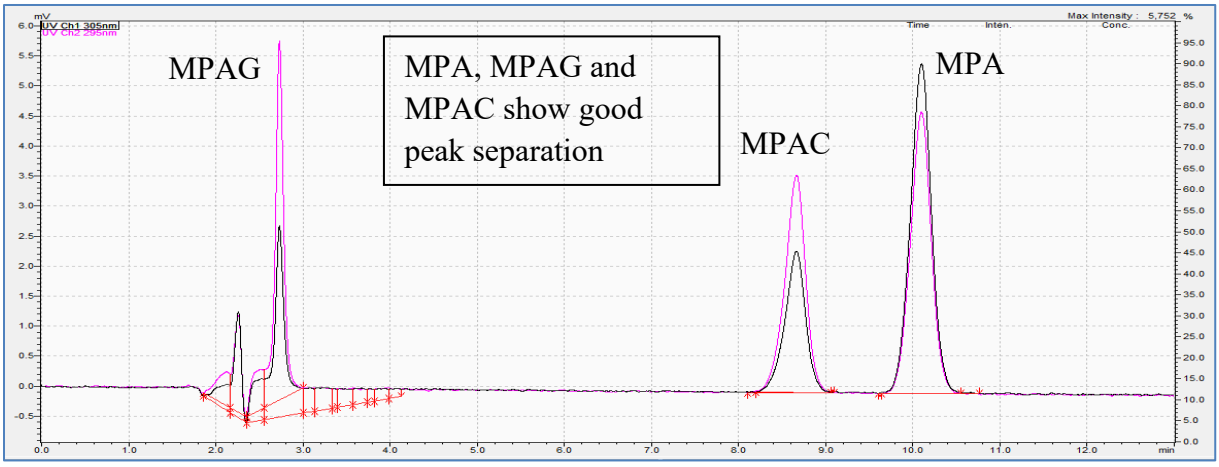

Figure 2.27 Formic acid concentration optimization (in acetonitrile) - the chromatogram of MPA, MPAG, and MPAC mixture using 0.1% formic acid and 2 mM ammonium acetate in the mobile phase (optimized condition)

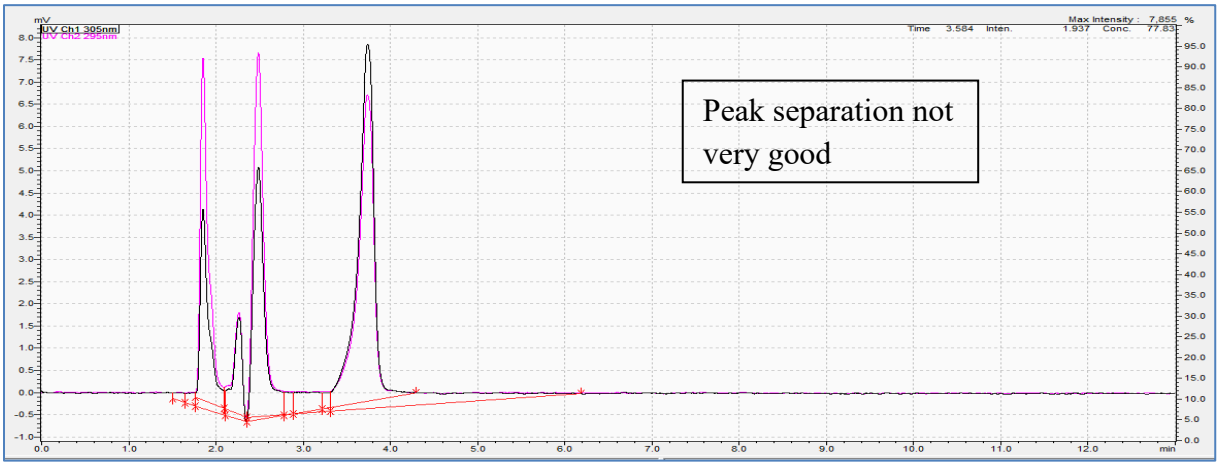

Figure 2.28 Formic acid concentration optimization (in acetonitrile) - the chromatogram of MPA, MPAG, and MPAC mixture using 0% formic acid and 2 mM ammonium acetate in the mobile phase

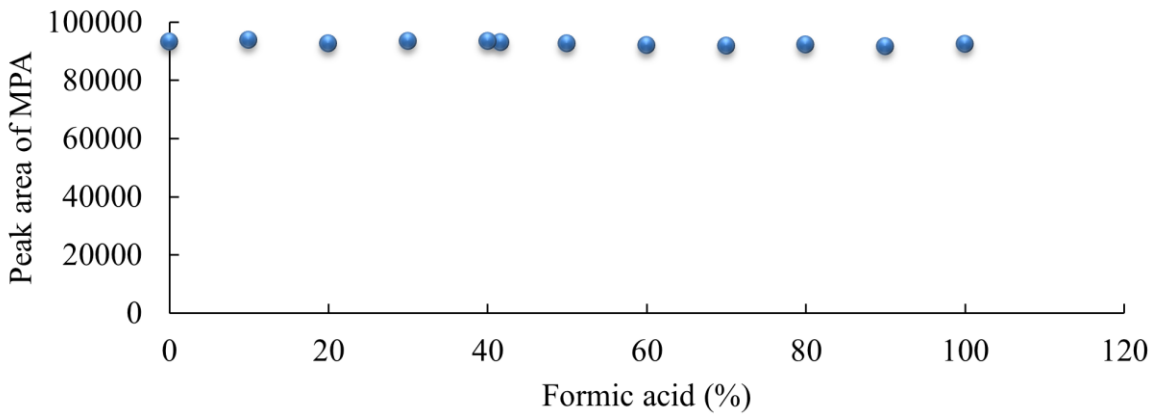

Figure 2.29 The correlation plot between formic acid concentration in acetonitrile and the absolute peak area of MPA

2.4.2.5 *Additive optimization – ammonium acetate (in methanol)*

Figure 2.30 represents the results when a mixture of MPA, MPAG, and MPAC was injected into the instrument (at a concentration of 10 µg/mL) using methanol, 1 mM ammonium acetate, and 0.306% formic acid. The peaks for the analytes have good symmetrical shapes, are well-separated (with elution times of MPA – approximately 9.7 mins, MPAG – approximately 3.2 mins, MPAC – approximately 10.3 mins), and have good separation from the solvent front. Overall, there were no interferences (between the peaks of analytes) that can be seen in the chromatogram. However, the opposite was observed when the mixture of MPA, MPAG, and MPAC was injected with no ammonium acetate and 0.3060% formic acid in the mobile phase (Figure 2.31). Figure 2.32 represents the relationships between the concentrations of ammonium acetate and the absolute peak area counts of MPA.

Hence, the final ammonium acetate concentration was chosen to be 1 mM with the formic acid at 0.306% for MPA, MPAG, and MPAC when using methanol in the mobile phase.

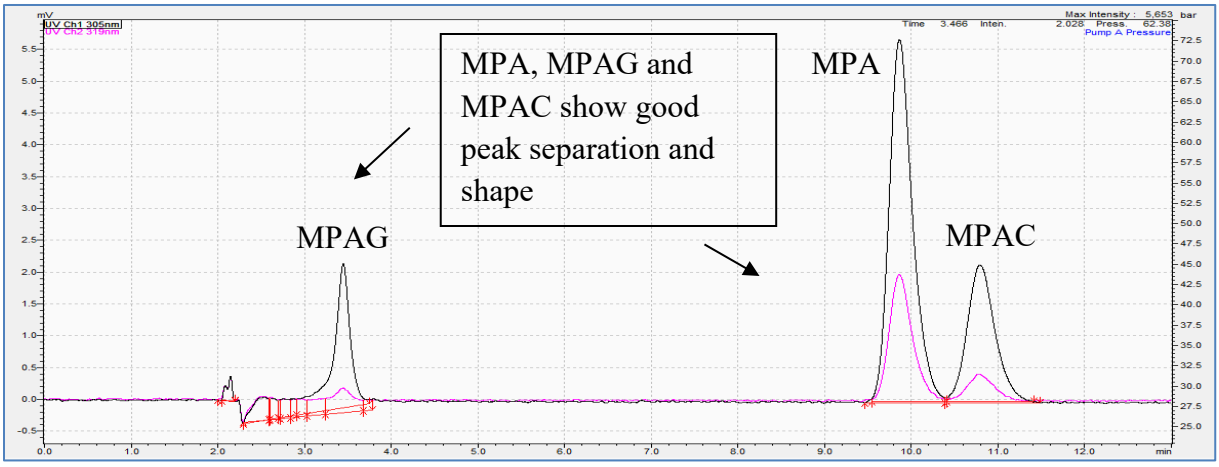

Figure 2.30 Ammonium acetate concentration optimization (in methanol) - the chromatogram of MPA, MPAG, and MPAC mixture using 1 mM ammonium acetate and 0.1% formic acid in the mobile phase (optimized condition)

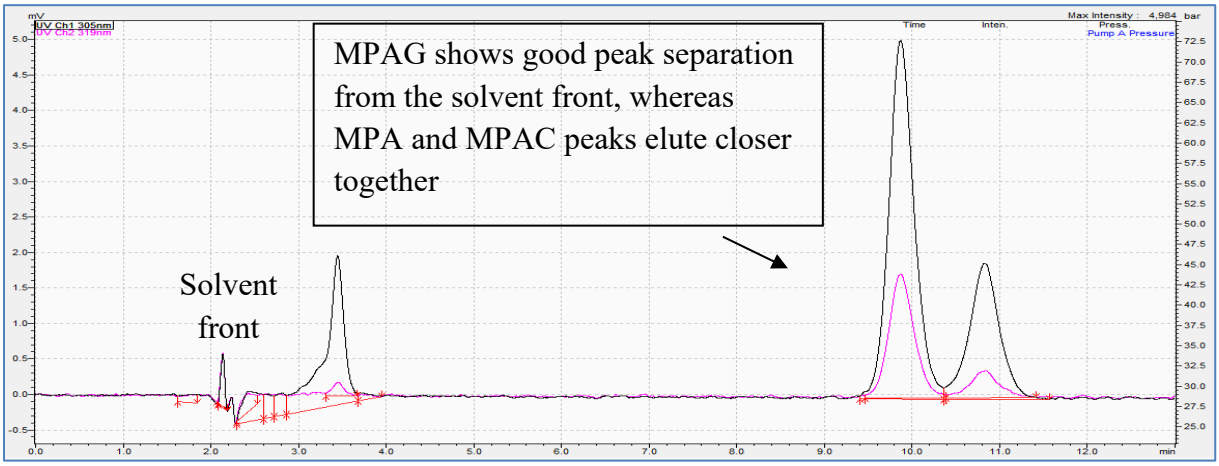

Figure 2.31 Ammonium acetate concentration optimization (in methanol) - the chromatogram of MPA, MPAG, and MPAC mixture using 0 mM ammonium acetate and 0.306% formic acid in the mobile phase

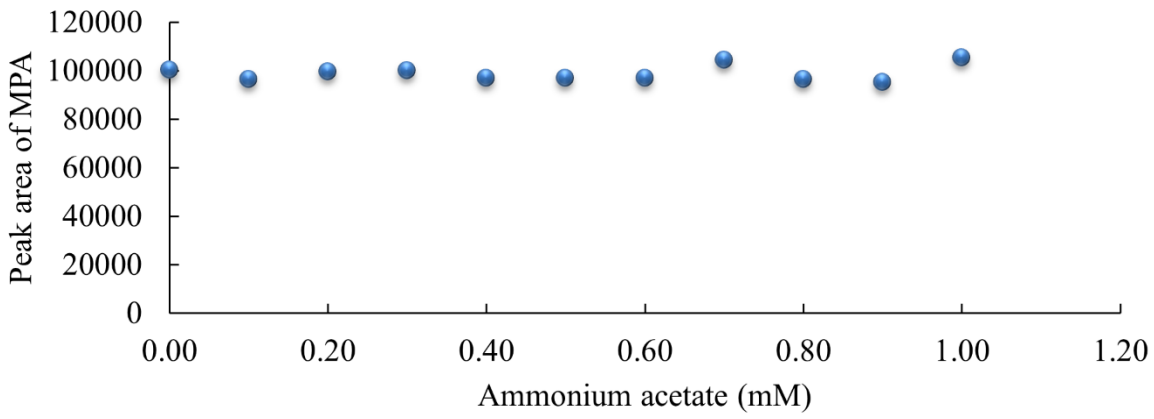

Figure 2.32 The correlation plot between ammonium acetate concentration in methanol and the absolute peak area of MPA

2.4.2.6 *Additive optimization – ammonium acetate (in acetonitrile)*

Figure 2.33 represents the results when a mixture of MPA, MPAG, and MPAC was injected into the instrument (at a concentration of 10 µg/mL) using ACN, 2 mM ammonium acetate, and 0.1% formic acid. The peaks for the analytes have good symmetrical shapes, are well-separated (with elution times at MPA – approximately 10.1 mins, MPAG – approximately 2.8 mins, MPAC – approximately 8.7 mins.), and have good separation from the solvent front. Overall, there were no interferences observed on the chromatogram. The same trend was observed when a mixture of MPA, MPAG, and MPAC was injected with no ammonium acetate and 0.1% formic acid in the mobile phase (Figure 2.34). Figure 2.35 represents relationships between the concentration of ammonium acetate and the absolute peak area counts of MPA.

The final ammonium acetate concentration was chosen to be 2 mM with the formic acid fixed at 0.1 % for MPA, MPAG, and MPAC when using ACN as the mobile phase.

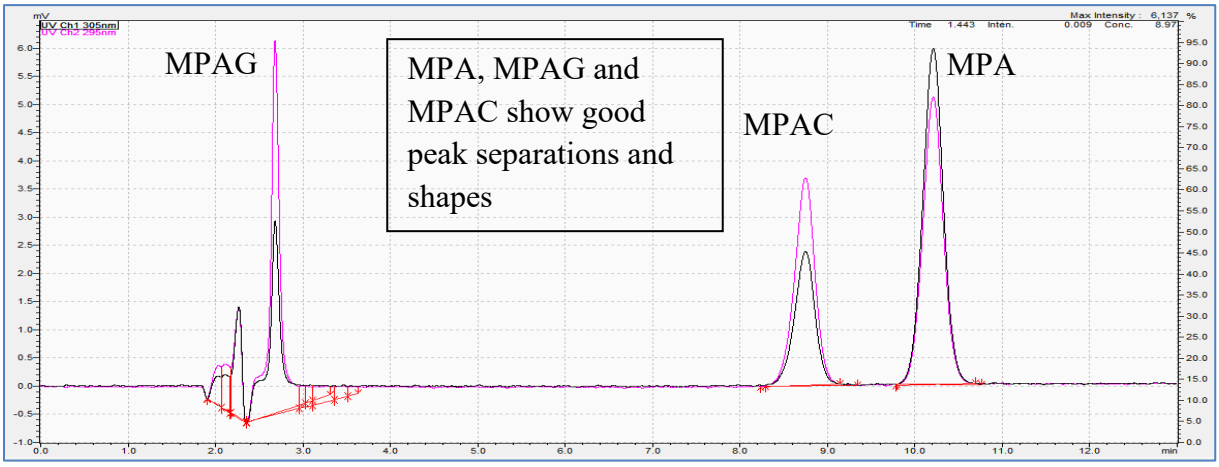

Figure 2.33 Ammonium acetate concentration optimization (in acetonitrile) - the chromatogram of MPA, MPAG, and MPAC mixture using 2 mM ammonium acetate and 0.1% formic acid in the mobile phase (optimized condition)

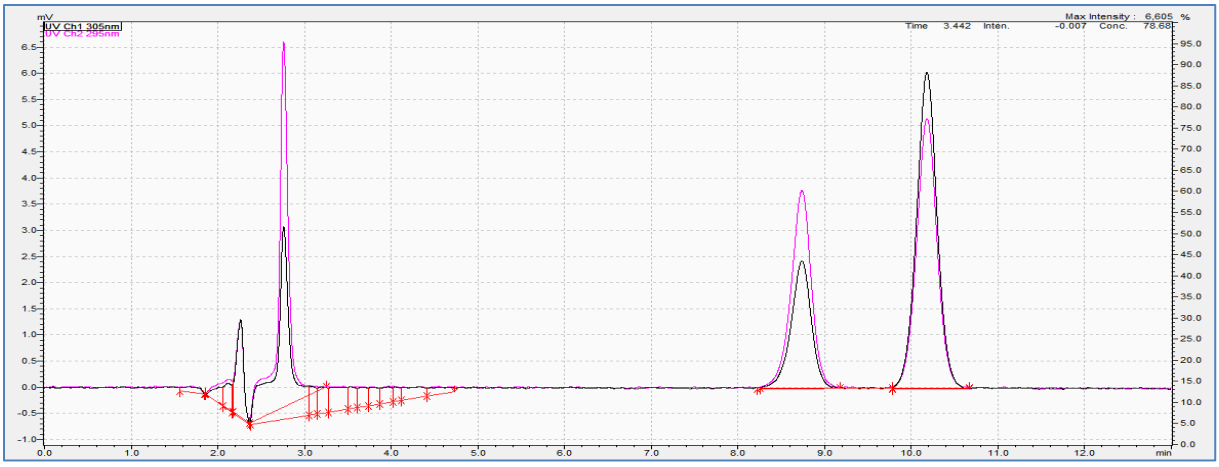

Figure 2.34 Ammonium acetate concentration optimization (in acetonitrile) - the chromatogram of MPA, MPAG, and MPAC mixture using 0 mM ammonium acetate and 0.1% formic acid in the mobile phase

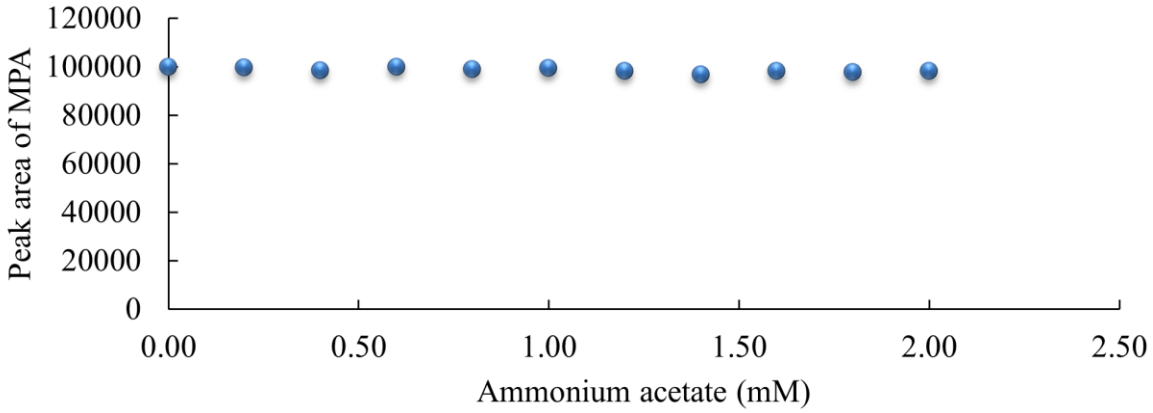

Figure 2.35 The correlation plot between ammonium acetate concentration in acetonitrile and the absolute peak area of MPA

2.4.2.7 *Additive optimization – phosphoric acid (in methanol)*

Phosphoric acid concentrations were varied in the mobile phase with the potassium phosphate monobasic fixed at 40 mM. As seen in Figure 2.36, the chromatogram represents the peaks of MPA, MPAG, and MPAC when injected at a concentration of 10 µg/mL, prepared in

methanol with 0.594% phosphoric acid and potassium phosphate monobasic at 40 mM. Although the peaks have relatively good shapes, the separation of MPA and MPAC was poor, with fronting of the MPAG peak. Additionally, a concentration of 0% phosphoric acid was also tested (as explained in Figure 2.37) but the pressure from the instrument was not stable. As the result, there was a lot of disturbances in the background of the chromatogram and no separate peaks were observed. Moreover, Figure 2.38 represents the relationships between the concentration of phosphoric acid in the mobile phase and the absolute peak areas of MPA. It is evident that at lower phosphoric acid concentrations (such as 0%, 0.066%, and 0.132%,), the analytes cannot be quantified.

In summary, phosphoric acid was not a suitable additive for the MPA assay since it generated un-usable chromatography.

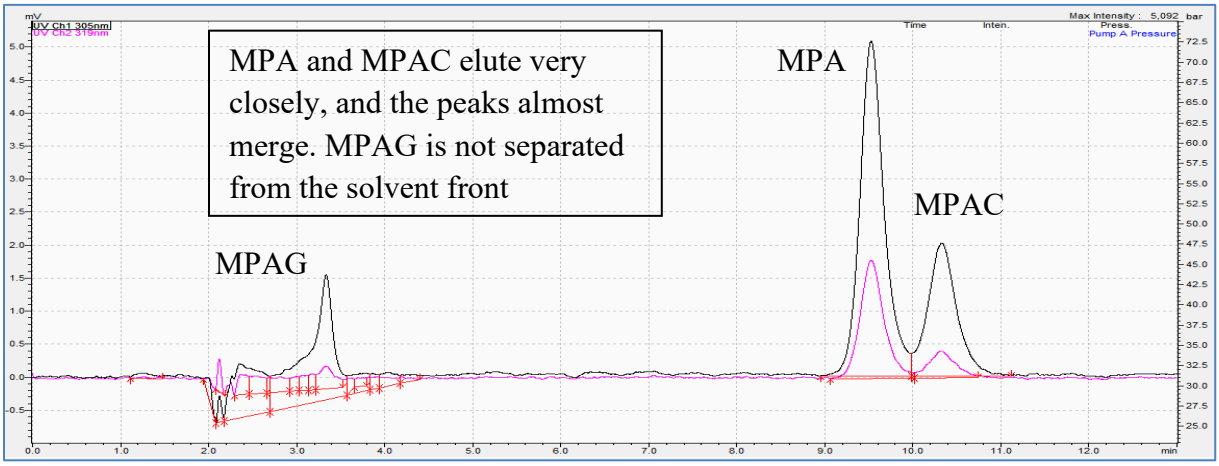

Figure 2.36 Phosphoric acid concentration optimization (in methanol) - the chromatogram of MPA, MPAG, and MPAC mixture using 0.594% phosphoric acid and 40 mM potassium phosphate monobasic in the mobile phase

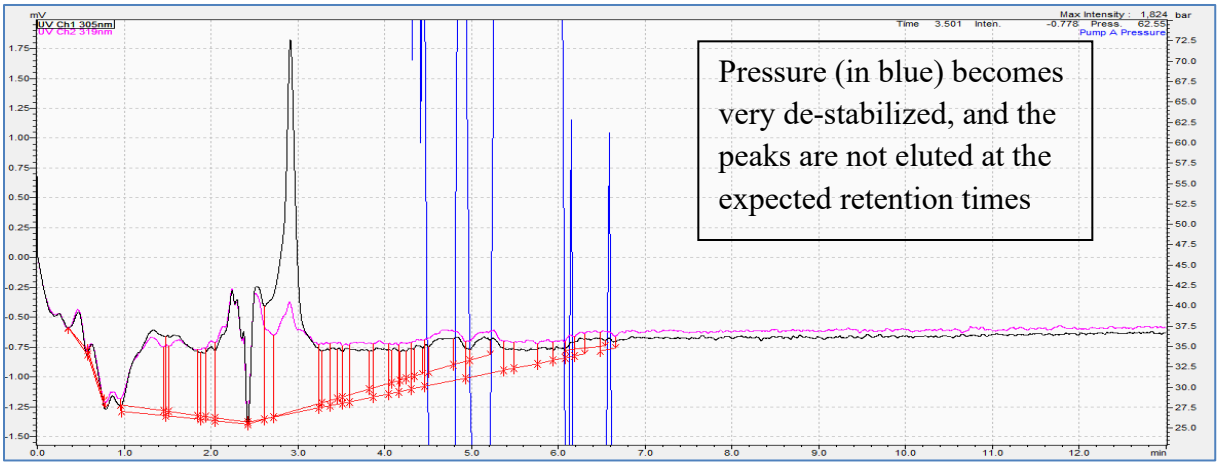

Figure 2.37 Phosphoric acid concentration optimization (in methanol) - the chromatogram of MPA, MPAG, and MPAC mixture using 0% phosphoric acid and 40 mM potassium phosphate monobasic in the mobile phase

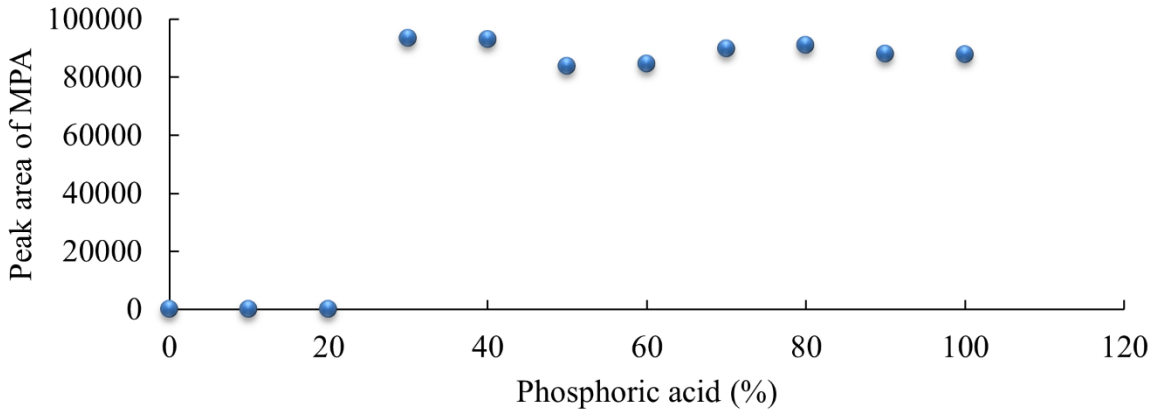

Figure 2.38 The correlation plot between phosphoric acid concentration in methanol and the absolute peak area of MPA

2.4.2.8 *Additive optimization – phosphoric acid (in acetonitrile)*

Phosphoric acid concentrations were varied in the mobile phase with the potassium phosphate monobasic fixed at 100 mM. As seen in Figure 2.39, the chromatogram represents the peaks of MPA, MPAG, and MPAC when injected at a concentration of 10 µg/mL, prepared in ACN with 0.47% phosphoric acid and potassium phosphate monobasic at 100 mM, however, the pressure in the instrument could not be maintained. Additionally, a concentration of 0.235% phosphoric acid was also tested (as explained in Figure 2.40) but the pressure from the instrument was not stable. As the result, there were a lot of disturbances in the background of the chromatogram and no separate peaks were observed.

In summary, phosphoric acid was not a suitable additive for the MPA assay since it generated un-usable chromatography.

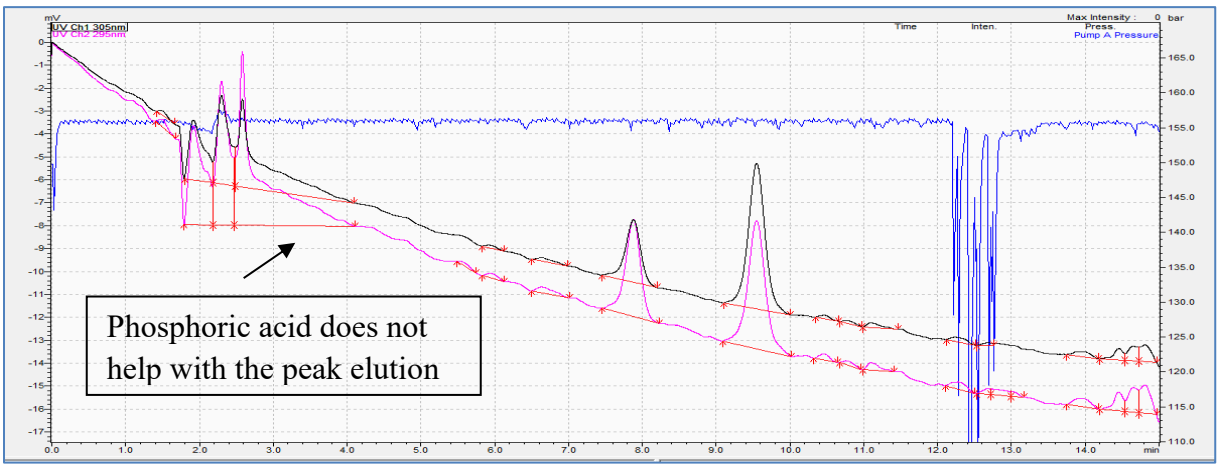

Figure 2.39 Phosphoric acid concentration optimization (in acetonitrile) - the chromatogram of MPA, MPAG, and MPAC mixture using 0.470% phosphoric acid and 100 mM potassium phosphate monobasic in the mobile phase

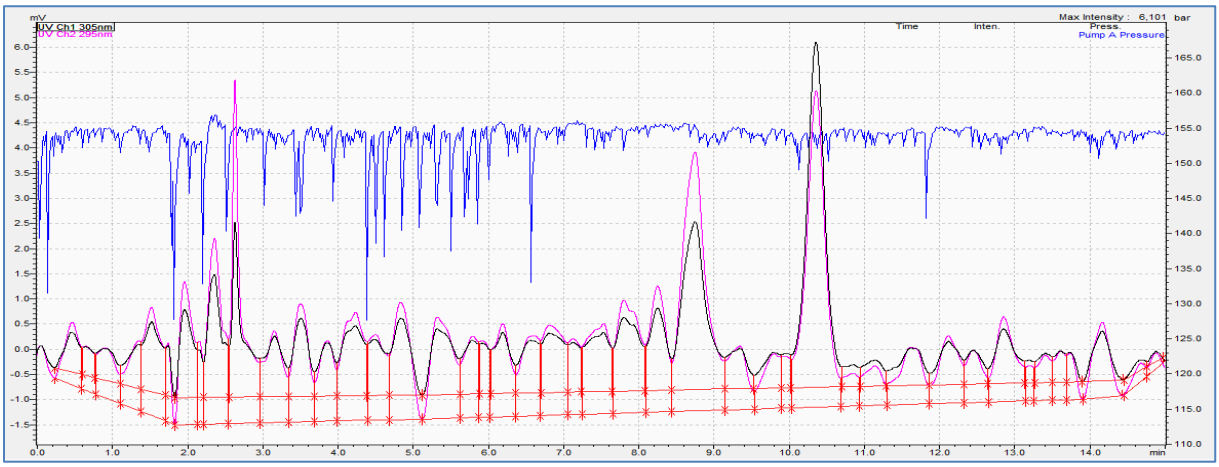

Figure 2.40 Phosphoric acid concentration optimization (in acetonitrile) - the chromatogram of MPA, MPAG, and MPAC mixture using 0.235% phosphoric acid and 100 mM potassium phosphate monobasic in the mobile phase

2.4.2.9 *Flow rate optimization (in methanol)*

The flow rate is the volume of the solvent (mobile phase) that flows through the column and the instrument per minute. The flow rate was optimized for MPA, MPAG, and MPAC using methanol as the solvent to check the effects on chromatographic peak separation and to improve the sensitivity of the assay. As observed in Figure 2.41, when the analytes MPA, MPAG, and MPAC are injected at a concentration of 10 µg/mL using 0.3060% formic acid and 1 mM ammonium acetate at a flow rate of 0.5 mL/min, the peak shape and separation for all the analytes appeared adequate (elution at MPA – approximately 9.7 mins, MPAG – approximately 3.2 mins, MPAC – approximately 10.3 mins.). Similarly, at 1.0 mL/min (in Figure 2.42), the peak shapes of all analytes were adequate; however, the peak separation between MPA and

MPAC was not ideal. Figure 2.43 represents the relationships between flow rate (variable) and the absolute peak area counts of MPA. The flow rate of 0.5 mL/min provides the highest peak area count, but the area count decreases when the flow rate is increased. The MPA sensitivity was observed to be decreased when going from 0.5 mL/min to 1.0 mL/min.

In summary, a flow rate of 0.5 mL/min was determined the optimal condition for the assay measuring MPA, MPAG, and MPAC when using methanol in the mobile phase.

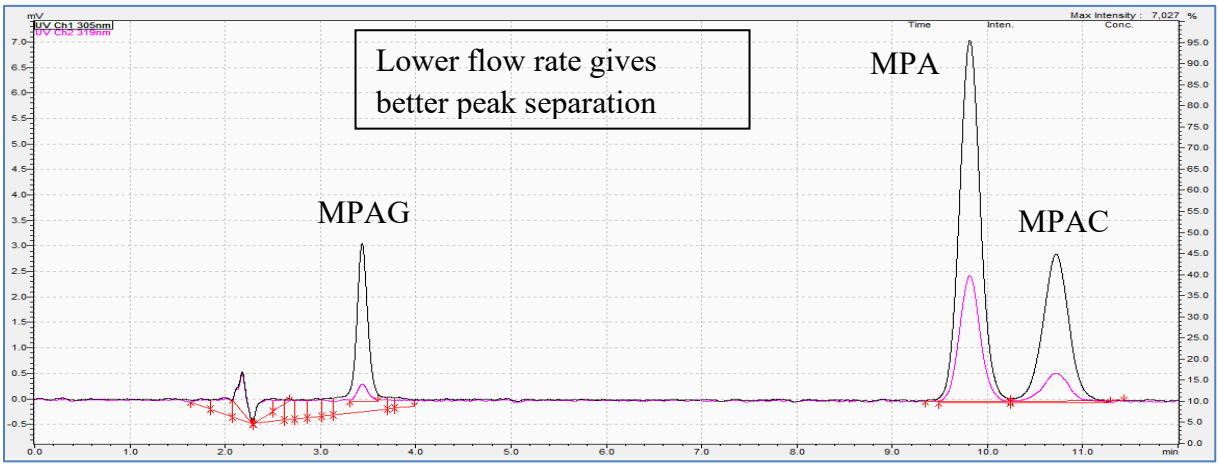

Figure 2.41 Flow rate optimization (in methanol) - the chromatogram of MPA, MPAG, and MPAC mixture using 0.5 mL/min flow rate (optimized condition)

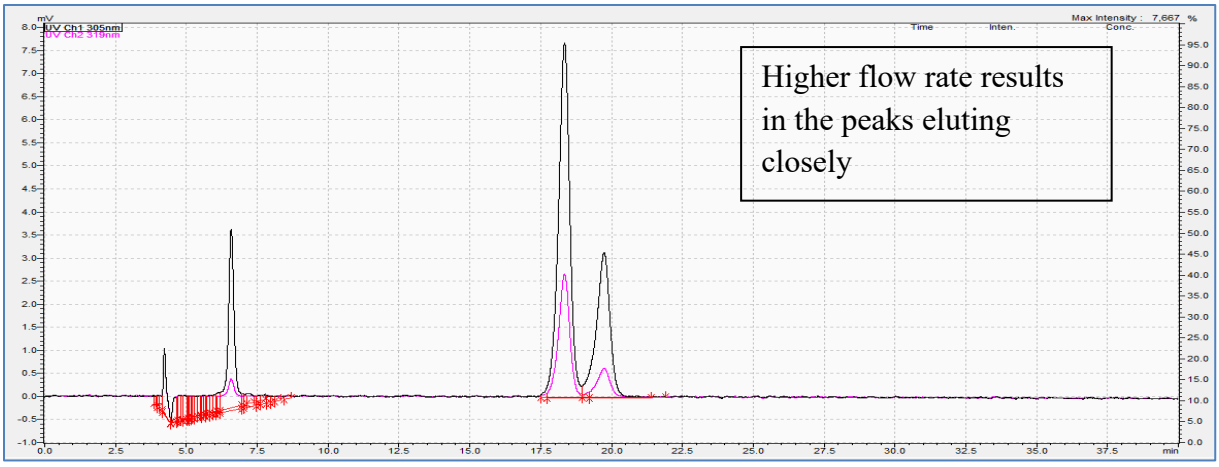

Figure 2.42 Flow rate optimization (in methanol) - the chromatogram of MPA, MPAG, and MPAC mixture using 1 mL/min flow rate

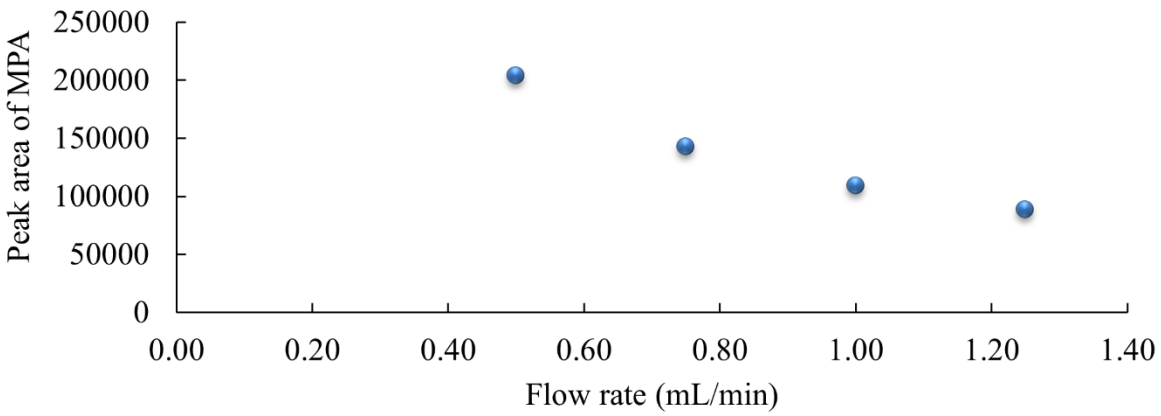

Figure 2.43 The correlation plot between flow rate using methanol and the absolute peak area of MPA

2.4.2.10 *Flow rate optimization (in acetonitrile)*

The flow rate was optimized for MPA, MPAG, and MPAC using ACN to check the effects on chromatographic peak separation and to improve the sensitivity of the assay. As observed in Figure 2.44, when the analytes MPA, MPAG, and MPAC were injected at a concentration of 10 µg/mL using 0.1% formic acid and 2 mM ammonium acetate at a flow rate of 0.5 mL/min, the peak shape and separation for all the analytes appeared adequate (elution at MPA – approximately 10.1 mins, MPAG – approximately 2.8 mins, MPAC –approximately 8.7 mins). Additionally, at 0.25 mL/min (in Figure 2.45), the peak shapes of all analytes were distorted and not ideal. Figure 2.46 represents the relationships between flow rate (variable) and the absolute peak area counts of MPA. The flow rate of 0.5 mL/min provides the highest peak area count, but the area count decreases as the flow rate is increased. The MPA sensitivity was observed to be decreased when going from 0.5 mL/min to 1.0 mL/min.

In summary, a flow rate of 0.5 mL/min was determined the optimal condition for the assay measuring MPA, MPAG, and MPAC when using ACN in the mobile phase.

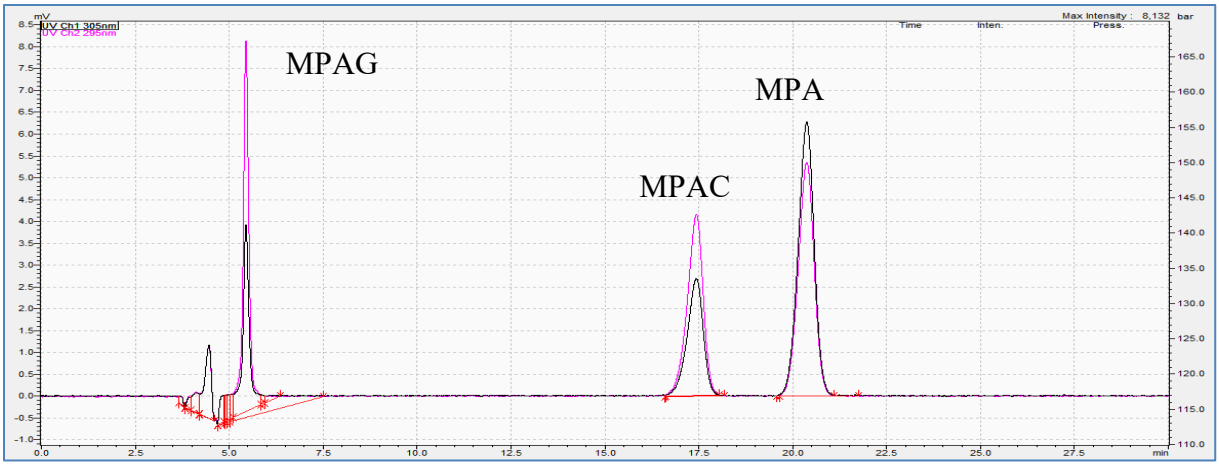

Figure 2.44 Flow rate optimization (in acetonitrile) - the chromatogram of MPA, MPAG, and MPAC mixture using 0.5 mL/min flow rate (optimized condition)

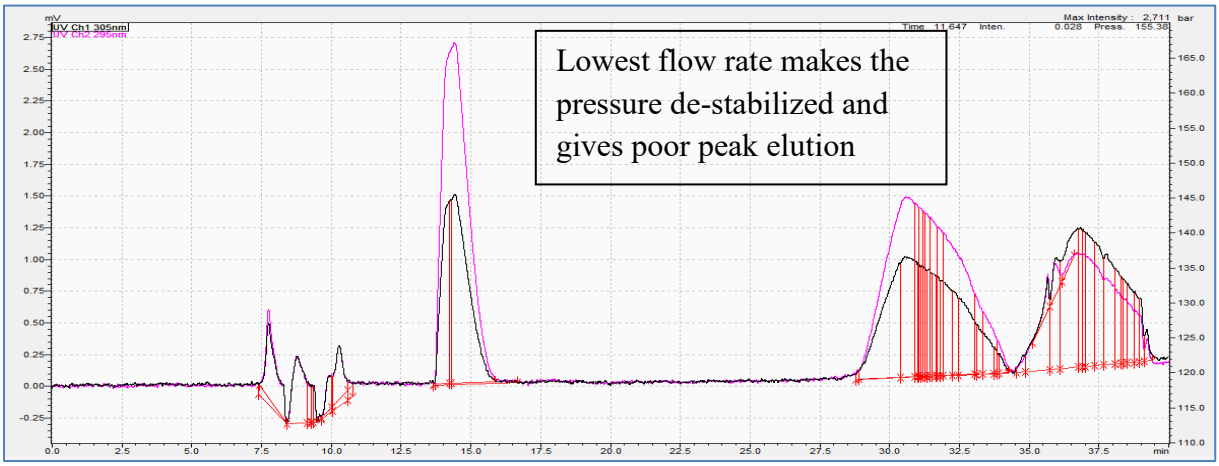

Figure 2.45 Flow rate optimization (in acetonitrile) - the chromatogram of MPA, MPAG, and MPAC mixture using 0.25 mL/min flow rate

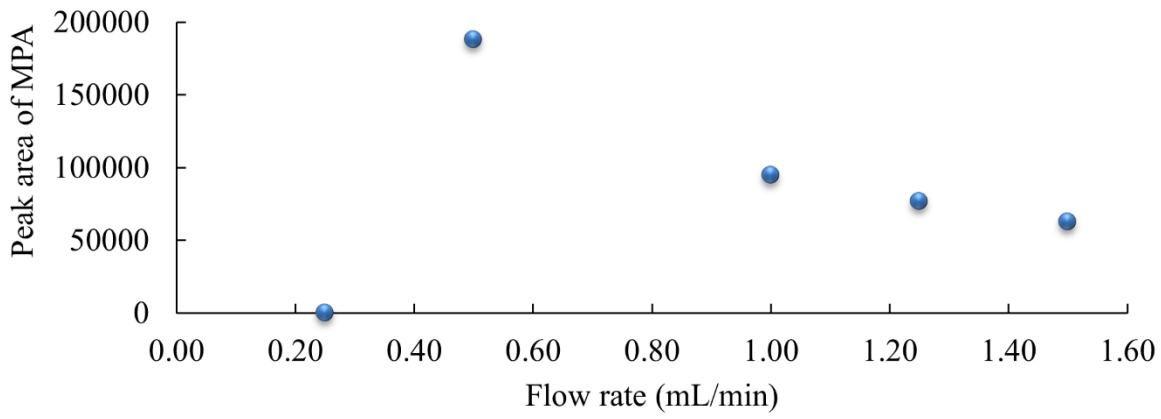

Figure 2.46 The correlation plot between flow rate using acetonitrile and the absolute peak area of MPA

2.4.2.11 *Injection volume optimization (in methanol)*

Injection volume is the volume of the sample that is injected into the UPLC for chromatographic analysis after the sample was prepared. This optimization was done using methanol at a concentration of 10 µg/mL. Figure 2.47 portrays the chromatography obtained after injecting a mixture of MPA, MPAG, and MPAC at an injection volume of 10 µL using the previously optimized chromatographic parameters. With this condition, all of the peaks were separated well, the peak shapes were symmetrical, there was good separation from the solvent front for MPAG, and there were no interferences observed with the other peaks. On the contrary, when the injection volume of the analyte mixture was increased to 25 µL (as seen in Figure 2.48), the peak shape became distorted and asymmetrical, all the analyte peaks exhibited fronting, and there were interferences between the peak for MPAG and the solvent front. MPA and MPAC were also seen to be merging at 25 µL injection volume. Figure 2.49 illustrates a

positive linear relationship between the injection volume and the MPA absolute peak areas; however, the peak shapes also become distorted with an increase in the injection volume.

In summary, 10 µL injection volume was found ideal to quantify MPA, MPAG, and MPAC using methanol.

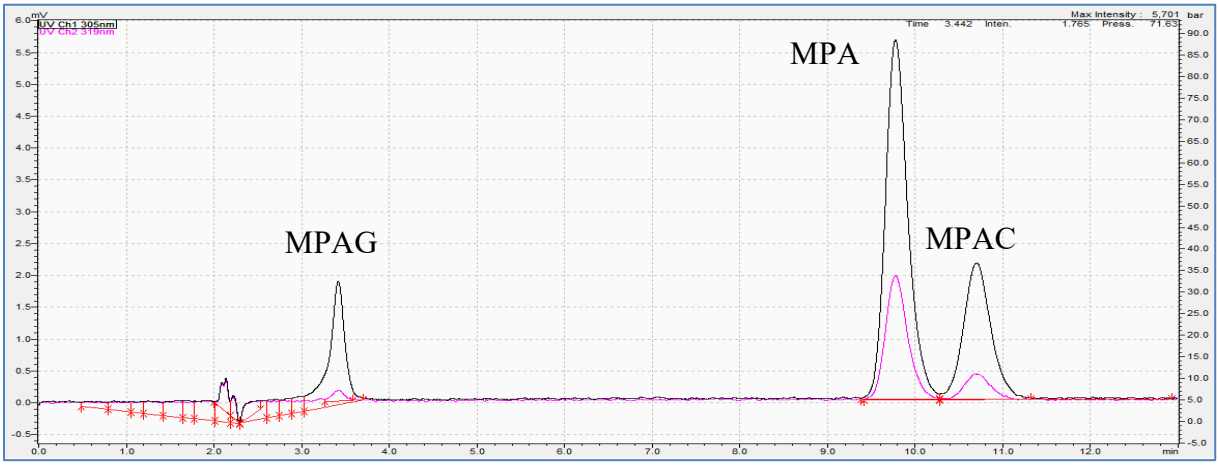

Figure 2.47 Injection volume optimization (in methanol) - the chromatogram of MPA, MPAG, and MPAC mixture using 10 µL injection volume (optimized condition)

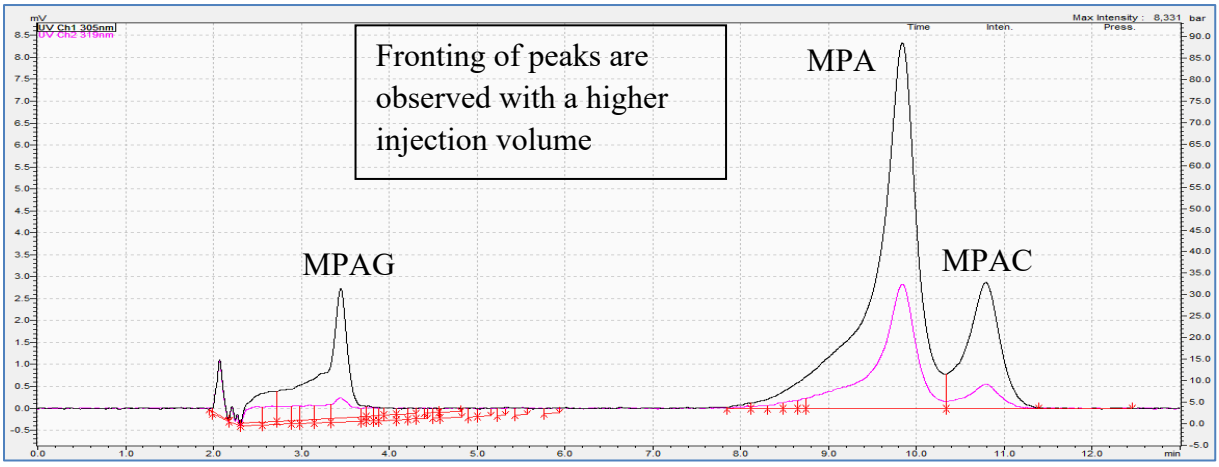

Figure 2.48 Injection volume optimization (in methanol) - the chromatogram of MPA, MPAG, and MPAC mixture using 25 µL injection volume

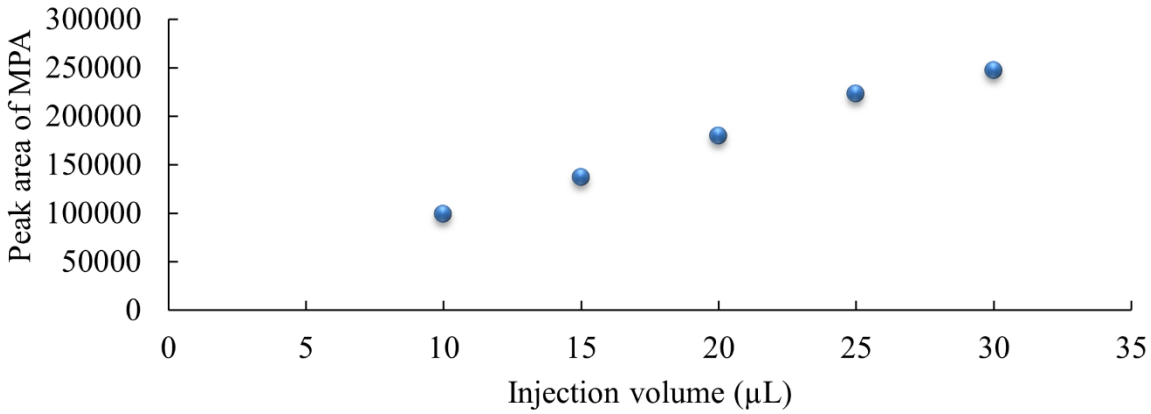

Figure 2.49 The correlation plot between injection volume using methanol and the absolute peak area of MPA

2.4.2.12 *Injection volume optimization (in acetonitrile)*

This optimization was done using methanol at a concentration of 10 µg/mL. Figure 2.50 portrays the chromatography obtained after injecting a mixture of MPA, MPAG, and MPAC at an injection volume of 10 µL using the previously optimized chromatographic parameters. With this condition, all of the peaks were separated well, the peak shapes were symmetrical, there was good separation from the solvent front MPAG, and there were no interferences observed with the other peaks. On the contrary, when the injection volume of the analyte mixture was increased to 25 µL (as seen in Figure 2.51), the peak shape became distorted and asymmetrical, all the analyte peaks exhibited fronting, and there were interferences between the peak for MPAG and the solvent front. MPA and MPAC were also seen to be merging at 25 µL injection volume. Figure 2.52 illustrates a positive linear relationship between the injection volume and the MPA absolute

peak areas; however, the peak shapes also become distorted with an increase in the injection volume.

In summary, 10 µL injection volume was found ideal to quantify MPA, MPAG, and MPAC using ACN.

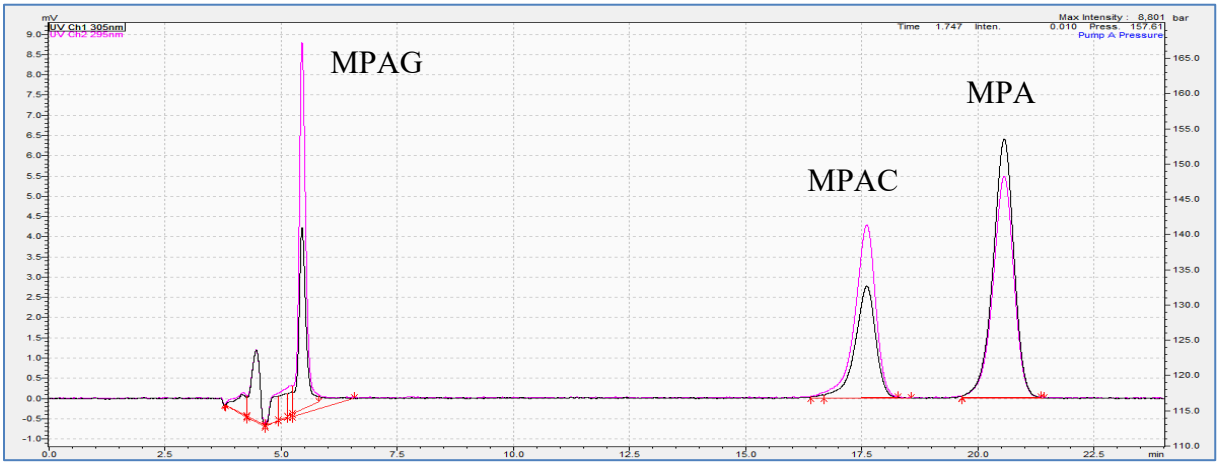

Figure 2.50 Injection volume optimization (in acetonitrile) - the chromatogram of MPA, MPAG, and MPAC mixture using 10 µL injection volume (optimized condition)

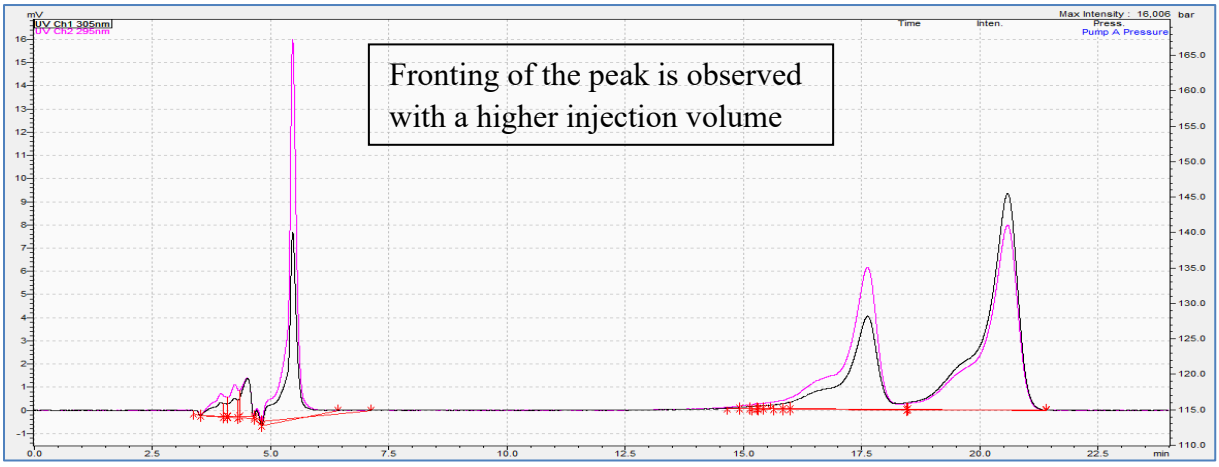

Figure 2.51 Injection volume optimization (in acetonitrile) - the chromatogram of MPA, MPAG, and MPAC mixture using 25 µL injection volume

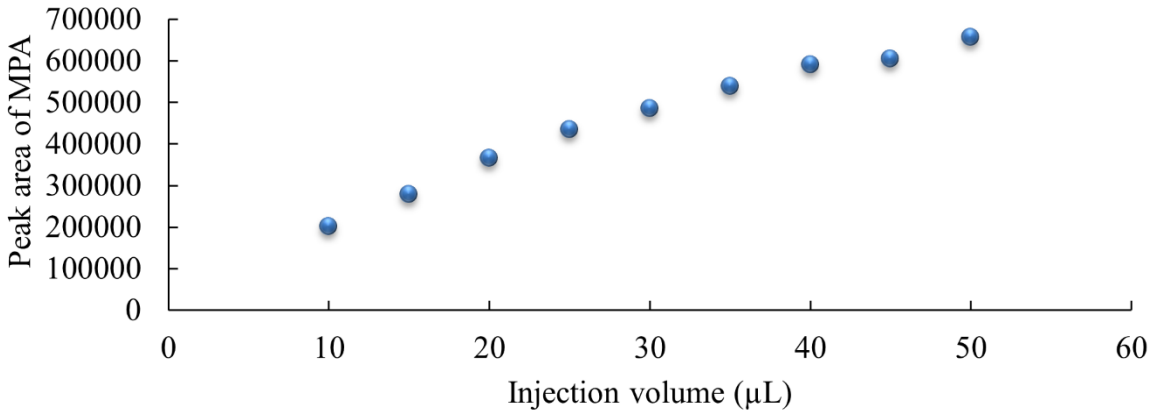

Figure 2.52 The correlation plot between injection volume using acetonitrile and the absolute peak area of MPA

2.4.3 Summary for chromatography conditions

Based on the comparisons of MPA absolute peak areas using optimized final conditions in acetonitrile and methanol at various injection volumes (Figure 2.53 and Figure 2.54 respectively), ACN is a better solvent in comparison to methanol for MPA assay. The final optimized chromatography conditions are shown in Figure 2.55 and Table 2.6.

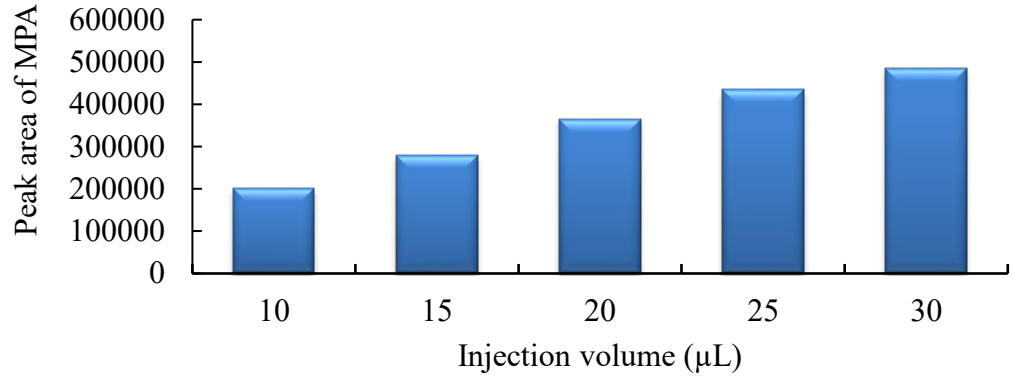

Figure 2.53 The comparisons of MPA absolute peak areas using optimized final conditions in acetonitrile at various injection volumes

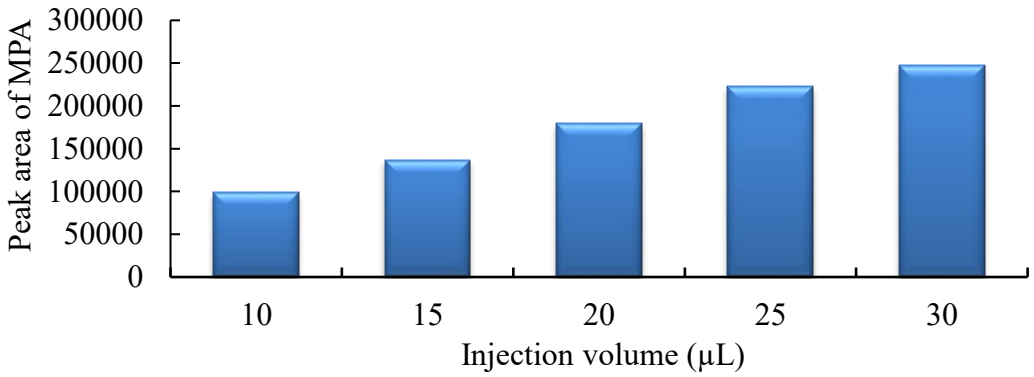

Figure 2.54 The comparisons of MPA absolute peak areas using optimized final conditions in methanol at various injection volumes

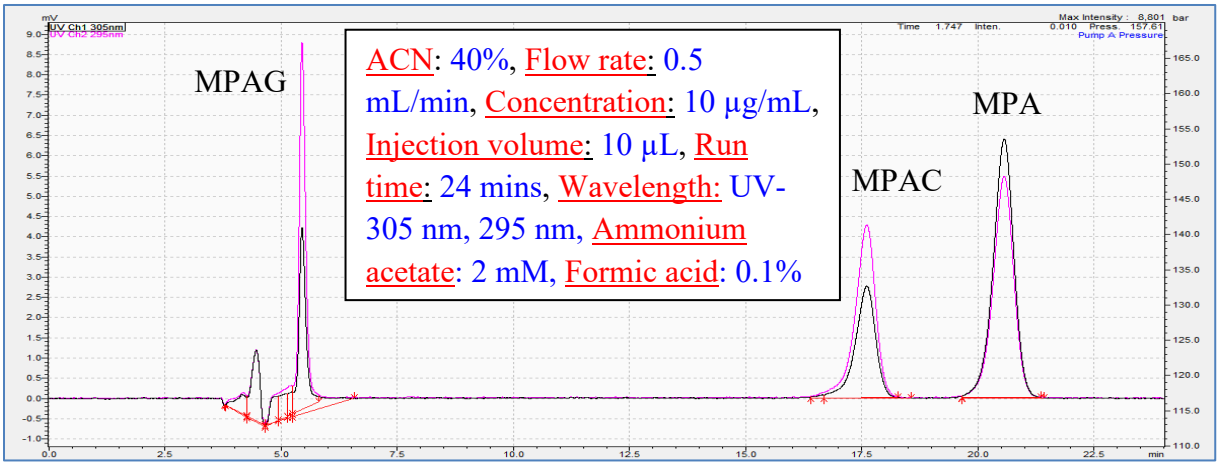

Figure 2.55 The final optimized chromatography conditions of MPA, MPAG, and MPAC using acetonitrile

Table 2.6 A summary of the final optimized parameters associated with the MPA, MPAG, and MPAC quantification in the UPLC

Final Optimized Chromatographic Parameters	
Acetonitrile concentration (%)	40
Formic acid (% v/v)	0.1
Ammonium acetate (mM)	2
Flow rate (mL/min)	0.5
Injection volume (µL)	10
Run time (mins.)	24
Detector used	Ultraviolet
Wavelength for quantification	305 nm & 295 nm

2.4.4 Mycophenolic acid sample preparation optimization

2.4.4.1 *Determination of lower limit of quantification using pure solvent*

For the LLOQ measurement in the MPA assay, a standard calibration set was prepared using MPA, MPAG, and MPAC from 0.00003 µg/mL to 64 µg/mL in ACN using the final optimized chromatographic conditions. The calibration curve of MPA showed a good linearity and a high correlation coefficient value (r^2) of 0.999. The lowest concentrations did not show any peaks in the chromatography and hence were not considered as the LLOQ. The LLOQ for MPA, MPAG and MPAC were found to be 0.125 µg/mL, 0.5 µg/mL, and 0.125 µg/mL, respectively. Figure 2.56 represents the calibration curve that was obtained by plotting the MPA absolute peak area vs. the concentrations in the calibration set. Figure 2.57 represents the chromatogram at the LLOQ for MPA (0.125 µg/mL) when the sample was injected using the final optimized chromatographic conditions. There was no peak interference observed for any of the analytes or the solvent front.

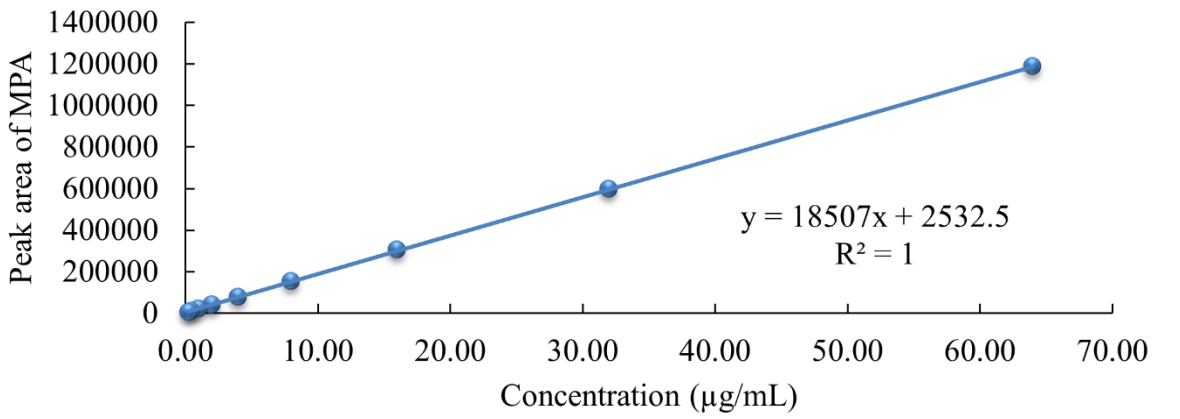

Figure 2.56 The calibration curve of MPA using final optimized conditions in pure acetonitrile (calibration curve ranged from 0.125 to 64 µg/mL)

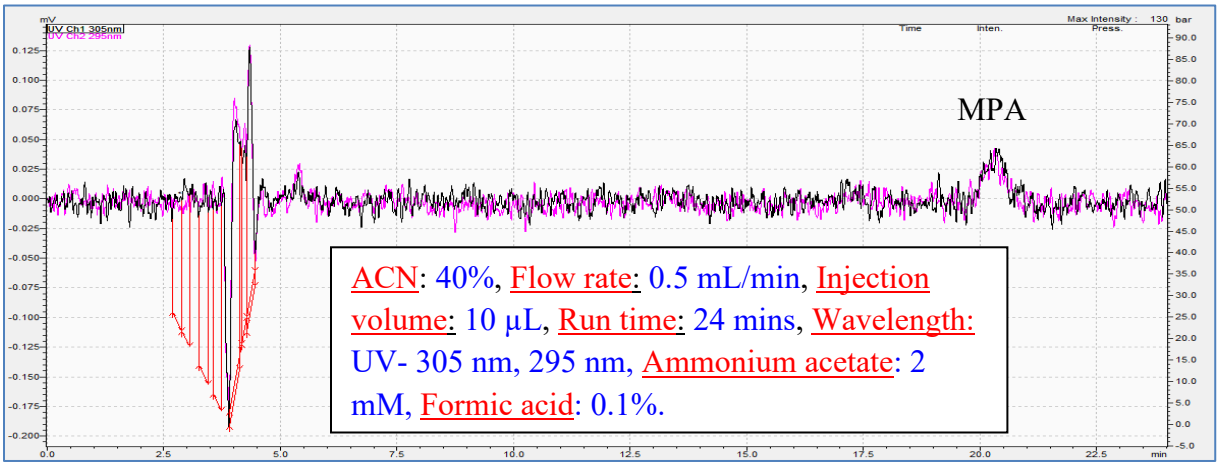

Figure 2.57 The chromatogram of MPA at the lower limit of quantification 0.125 µg/mL in pure acetonitrile

2.4.4.2 *Standard calibration set in human plasma*

The calibrators for MPA and MPAG (ranged from 0.125 to 64 µg/mL) were prepared using pooled human plasma as the matrix. Figure 2.58 represents the standard calibration curve of MPA that was prepared in pooled human plasma and analyzed using the final optimized conditions in the UPLC. The curve was observed to be linear (except for 32 µg/mL that was an outlier concentration) and the correlation coefficient for MPA had a high value (r^2 = 0.9943 as seen in Figure 2.58). The peaks for MPA, MPAG, and MPAC elute at their respective elution times, hence plasma as a matrix does not affect the retention times. Figure 2.59 shows the chromatography from the injection of the two analytes at the LLOQ (i.e., 0.125 µg/mL) and the internal standard MPAC (fixed at a concentration of 22.5 µg/mL).

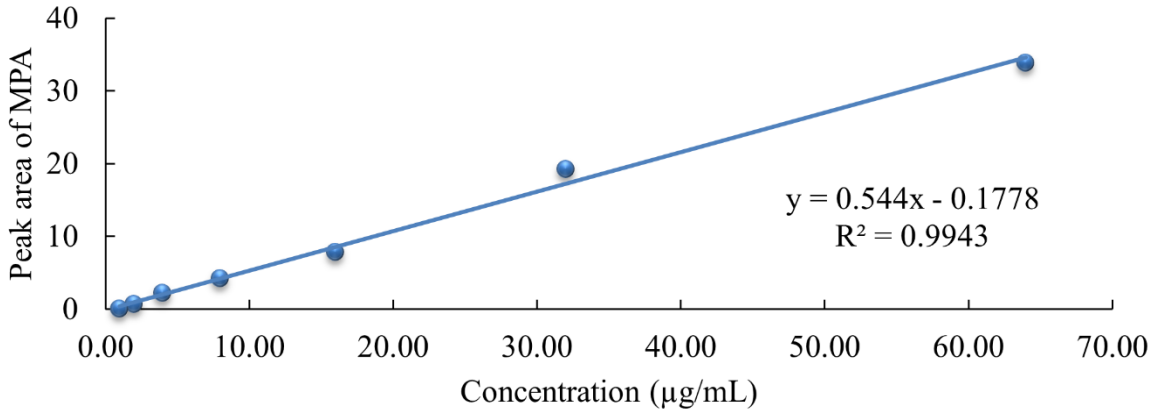

Figure 2.58 The calibration curve of MPA using final optimized conditions in human plasma (calibration curve ranged from 0.125 to 64 µg/mL)

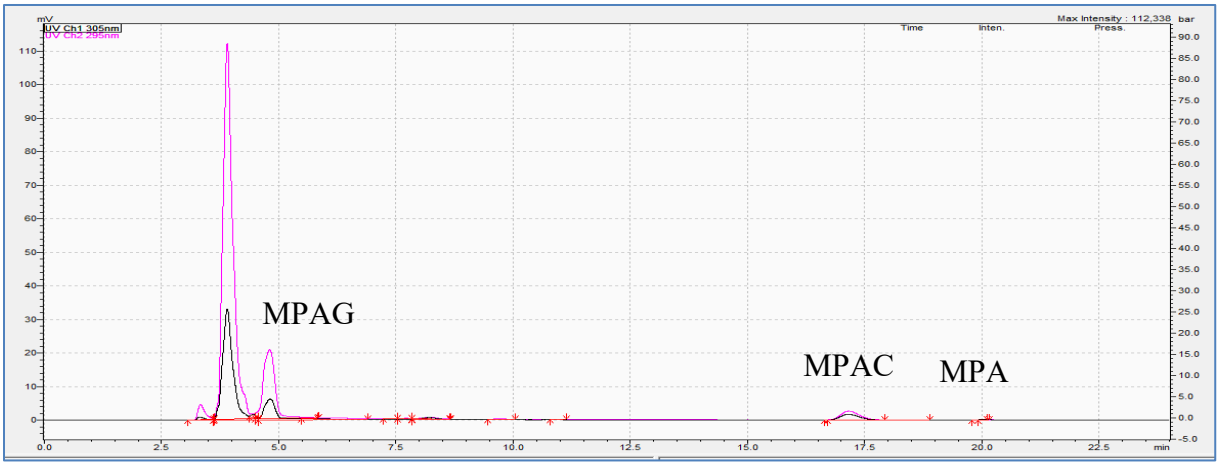

Figure 2.59 The chromatogram of MPA at the lower limit of quantification 0.25 µg/mL in human plasma

2.4.4.3 *Internal standard optimization for mycophenolic acid assay*

MPAC is the internal standard for the MPA assay and was optimized using the final optimized chromatographic assay conditions in the UPLC. This optimization was done by preparing a standard curve of MPAC (ranged from 0.4 µg/mL to 121.010 µg/mL) using pooled human plasma to ensure that the response of the final selected MPAC concentration was not saturated. MPAC peak areas were plotted against the various concentrations prepared as shown in Figure 2.60 The curve showed a good linearity with a high correlation coefficient value (r^2) of 0.9982. MPAC showed a linear response from 0.4 µg/mL to 121.010 µg/mL. The final MPAC concentration was selected to be 22.5 µg/mL, in which chromogram is shown in Figure 2.61.

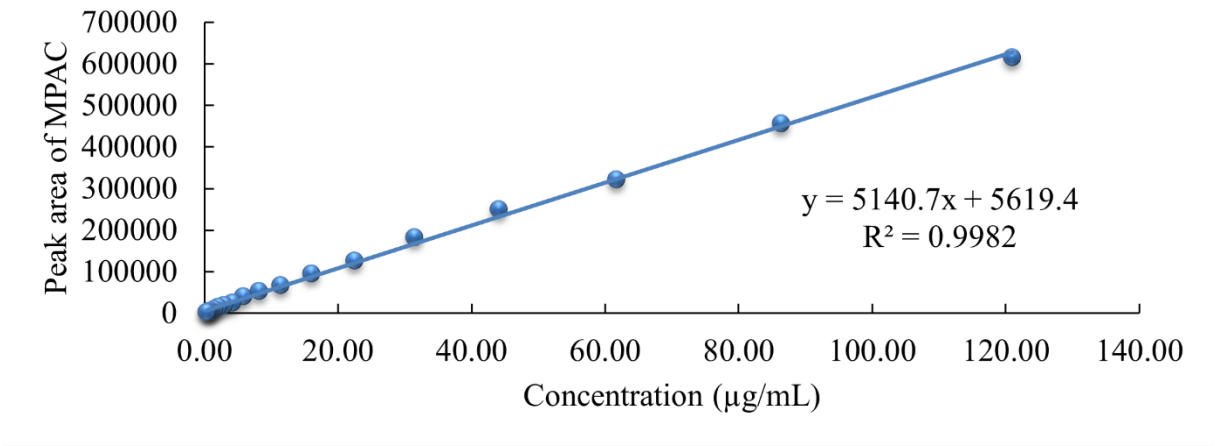

Figure 2.60 The calibration curve of MPAC using final optimized conditions in human plasma (calibration curve ranged from 0.40 to 121.01 µg/mL)

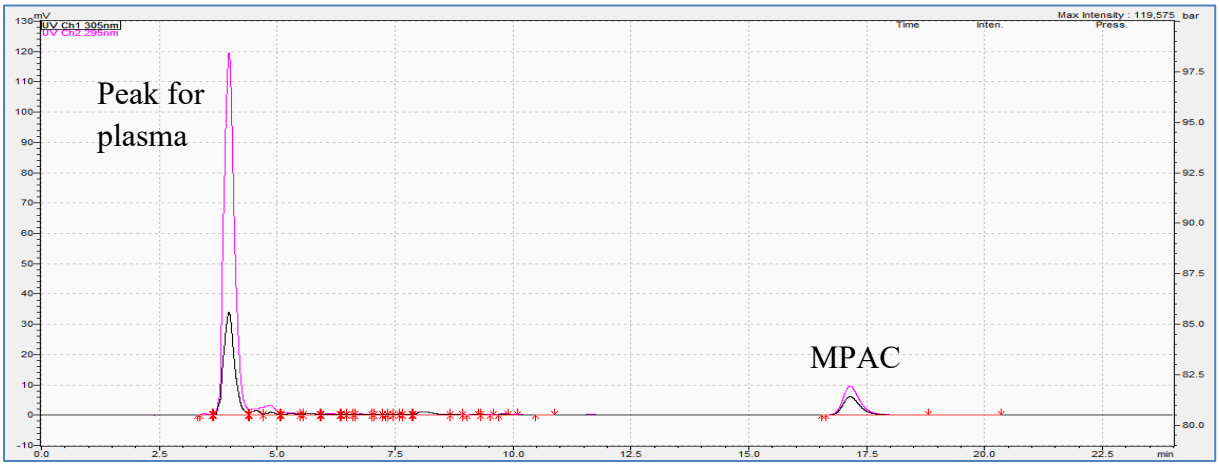

Figure 2.61 The chromatogram of MPAC at 22.5 µg/mL (i.e., the final optimized concentrations) in human plasma

2.4.4.4 *Drying optimization*

To increase the sensitivity of the MPA assay, the samples were subjected to drying in the *SpeedVac* instrument. Additionally, the injection volume was optimized as well. *SpeedVac* is an

instrument that helps in drying/concentrating the sample to increase its concentration by decreasing the total volume. In this assay, *SpeedVac* was used to dry the sample containing a mixture of MPA, MPAG, and MPAC. In this optimization, a set of standard calibrators was prepared for MPA, MPAG, and MPAC. The samples were concentrated using *SpeedVac* and at the same time, a higher injection volume was also tested to increase the sensitivity of this assay. The calibration curves were shown in Figure 2.62. Using human plasma as the matrix, the peaks showed relatively good shape and separation in higher concentrations, however towards the lower concentration (e.g., 0.0625 µg/mL), the peak for MPAG was not symmetrical (data not shown). The calibration curve plotted for MPA showed good linearity and the correlation coefficient (r^2 value) for MPA was observed to be high ($r^2 = 0.9982$, as seen in Figure 2.62).

Figure 2.63 summarizes the relationship between drying the MPA samples vs. not drying & its effect on the absolute peak areas. The blue bar represents the samples that have been dried in *SpeedVac* dryer, whereas the red bar represents the area counts of the samples that have not been dried. It is evident from the figure that the peak area counts of MPA are significantly improved after the sample was dried in the *SpeedVac*.

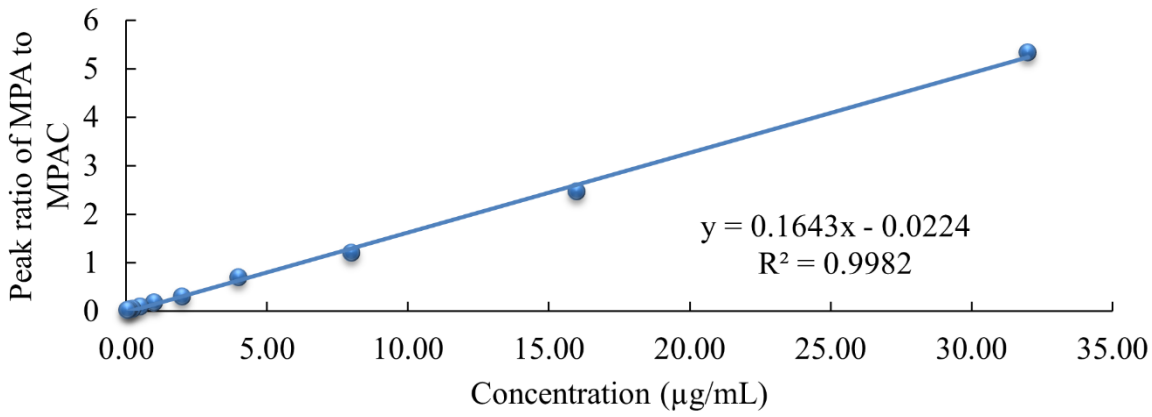

Figure 2.62 The calibration curve of MPA after the samples were dried in the SpeedVac for 5 minutes in human plasma (calibration curve ranged from 0.0625 to 32 µg/mL)

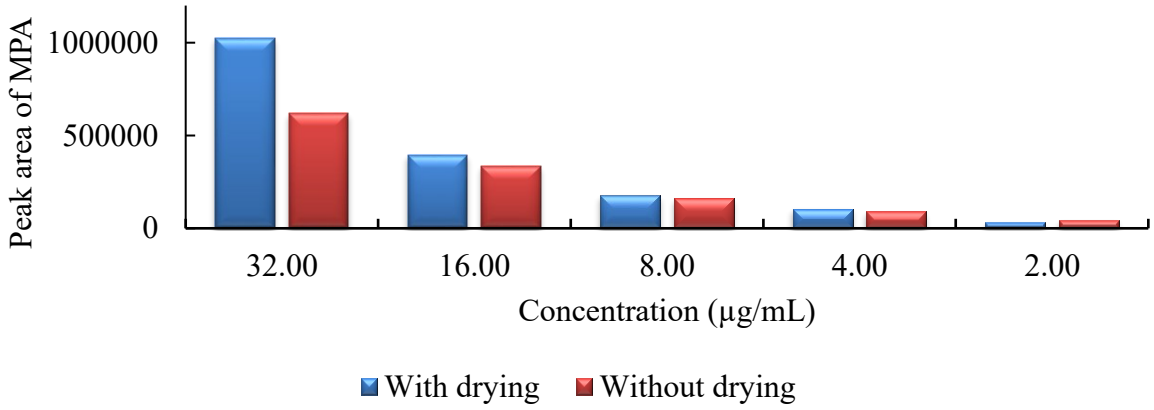

Figure 2.63 Comparisons of absolute MPA peak areas in samples with and without drying

The injection volume was also optimized for the MPA assay. This parameter was varied from 10 µL to 50 µL (i.e., 10, 20, 30, 40, 50 µL) using a mixture of MPA and MPAG at 4 different concentrations (i.e., 0.0625 µg/mL, 0.125 µg/mL, 16 µg/mL, and 32 µg/mL) while MPAC was fixed at 30 µg/mL. The elution times for MPA and MPAC were observed to be approximately 21.1 mins and approximately 17.6 mins, respectively. Figure 2.64 represents the

bar graph that shows the effects of changing the injection volume(s) on the MPA absolute peak area counts. The different colored bars represent different injection volumes tested at the concentrations mentioned above. Figure 2.65 shows a chromatogram obtained after injecting MPA, MPAG, and MPAC at 50 µL injection volume. As can be seen, the analyte peak shapes are distorted, and tailing of the peak is observed with a higher injection volume of 50 µL. On the other hand, Figure 2.66 represents the chromatogram obtained after injecting a sample mixture of MPA, MPAG, and MPAC where MPA was at a concentration of 32 µg/mL and is tested at an injection volume of 10 µL, which showed the ideal peak shape and separation without any peak interferences, distortion, or fronting.

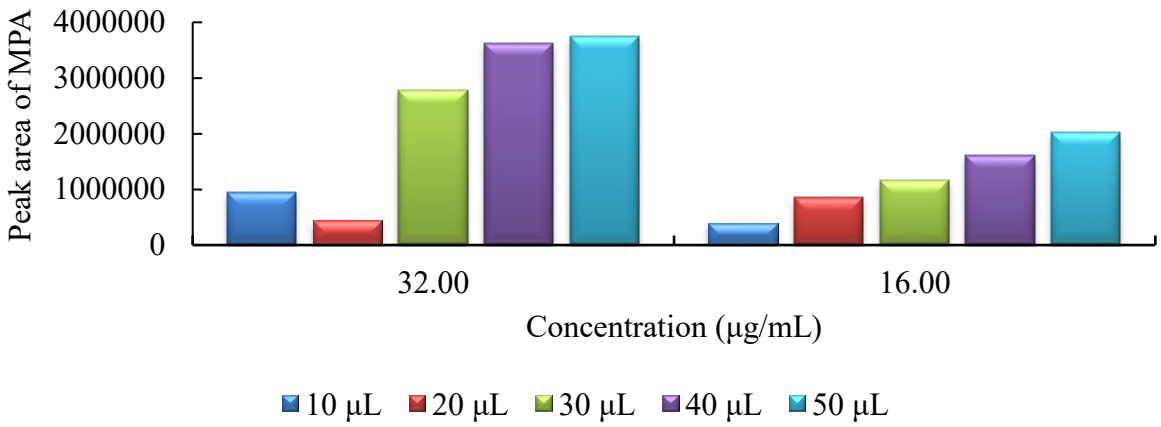

Figure 2.64: Comparisons of absolute MPA peak areas in samples with various injection volume

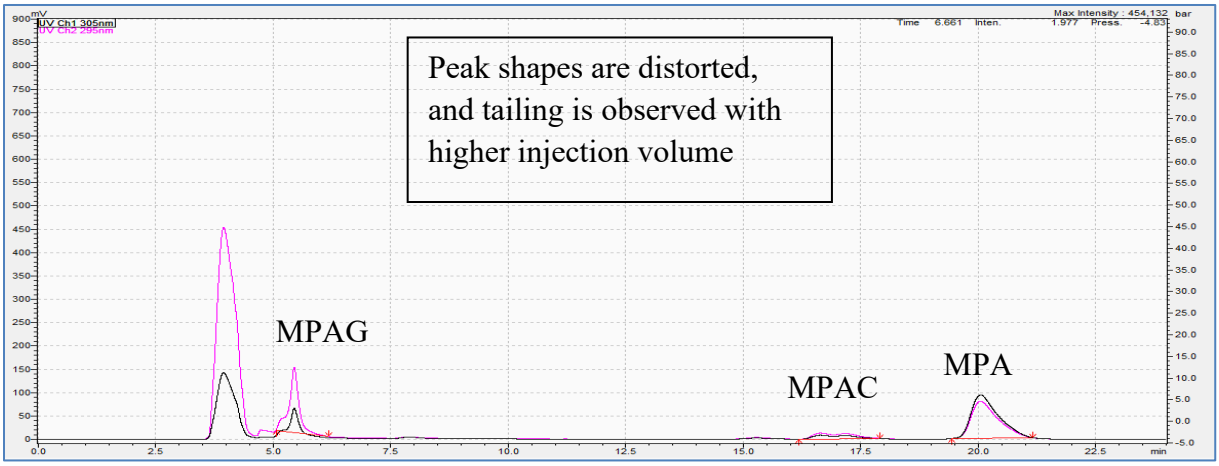

Figure 2.65 The chromatogram obtained after injecting a sample mixture of MPA, MPAG, and MPA, where MPA is at a concentration of 32 µg/mL and is tested at an injection volume of 50 µL

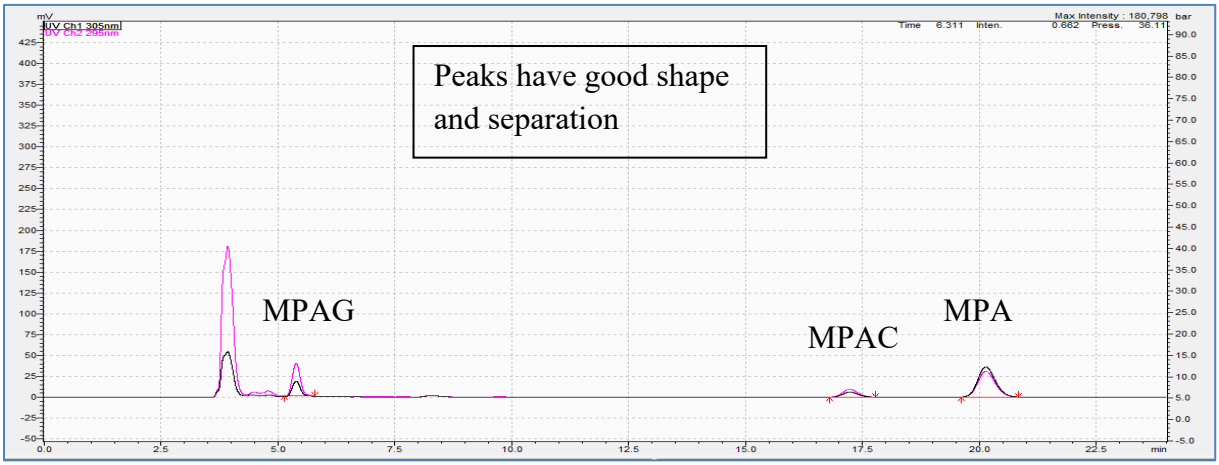

Figure 2.66 The chromatogram obtained after injecting a sample mixture of MPA, MPAG, and MPAC where MPA is at a concentration of 32 µg/mL and is tested at an injection volume of 10 µL (final optimized condition)

2.4.4.5 *Extraction solvent optimization*

Another way to increase the sensitivity is to have a higher solvent to plasma ratio in the sample extraction. Increasing the solvent volume in the sample preparation may improve extraction since there is more solvent for the analyte to be extracted to. This optimization was done by preparing a standard set of calibrators for MPA, MPAG, and MPAC where the organic solvent to the plasma/sample ratio was increased. The samples were concentrated using *SpeedVac* and an injection volume of 10 µL was utilized. Using the 10 µL injection volume, MPA was sensitive up to 0.1250 µg/mL. Figure 2.67 represents the effect of changing the volume of plasma to organic solvent from 1:1 to 1:2 on the MPA absolute area counts. The different colored bars represent different ratios tested at the concentrations mentioned above (red bar represents the 1:1 plasma to organic solvent ratio whereas the green bar represents 1:2 plasma to organic solvent ratio).

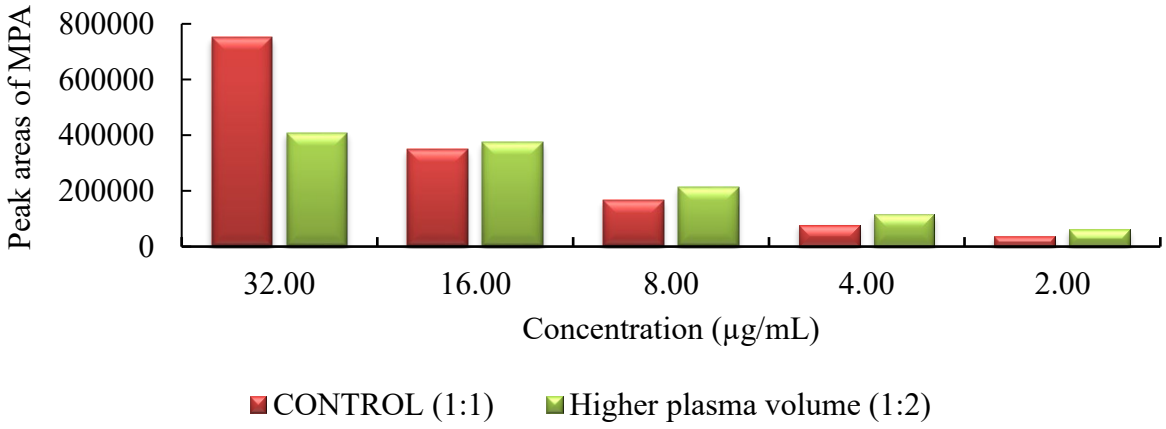

Figure 2.67 Comparisons of MPA absolute peak areas using different organic extraction solution volumes at various MPA concentrations

2.4.5 Validation approach

2.4.5.1 *Mycophenolic acid assay validation accuracy and precision data*

Using the final optimized chromatographic and assay parameters, the MPA assay was validated to calculate the accuracy and precision. The accuracy and precision testing were done in 3 batches on 3 different days (to account for the intra and inter-day accuracy and precision) as per the validation criteria. The QC samples showed acceptable accuracy & precision data for MPA since the A & P were within ±15% of the nominal concentration. Table 2.7 summarizes the accuracy and precision data for the quantification of MPA in human plasma.

Table 2.7 Accuracy and precision of MPA in human plasma

	Nominal concentration, µg/mL	Intra-day (1)		Intra-day (2)		Intra-day (3)	
MPA		Accuracy (%)	Precision (%)	Accuracy (%)	Precision (%)	Accuracy (%)	Precision (%)
	7.5	-6.672%	3.510%	-1.706%	7.281%	-0.382%	6.752%
	5.00	-4.175%	12.482%	-0.777%	7.614%	0.047%	5.948%
	2.25	-4.835%	7.607%	-2.635%	7.313%	2.447%	9.751%
	0.75	1.787%	7.693%	-11.668%	13.367%	-15.096%	13.742%

2.4.5.2 *Mycophenolic acid assay validation stability data*

Using the final optimized chromatographic and assay parameters, the MPA assay was validated to test the stability of the analytes under various storage conditions. Table 2.8

summarizes the stability data of MPA under various storage conditions in human plasma, which showed acceptable stability data for MPA since the accuracy were within ±15% of the nominal concentration.

Table 2.8 The stability data of MPA under various storage conditions in human plasma

	MPA	
	High QC	Low QC
Nominal concentration, µg/mL	7.5	2.25
Autosampler stability (%)	1.75%	-5.35%
Bench-top stability (%)	-7.34%	-13.06%
Freeze-thaw stability (%)	2.08%	-12.10%
Long-term stability (%)	-1.00%	-14.53%

2.4.5.3 *Mycophenolic acid assay extraction efficiency data (in plasma)*

Extraction efficiency is a measure of the overall effectiveness of the extraction process. Extraction efficiency also determines the percentage loss of the analyte after it undergoes the sample extraction procedures. It was observed that the MPA in the samples with extraction showed a recovery of 75.72%, 75.24%, 77.45%, and 80.79% at concentrations of 0.75 µg/mL

(LLOQ), 2.25 µg/mL (low QC), 5 µg/mL (mid QC), and 7.5 µg/mL (high QC), respectively. Similarly, the MPAC in the samples with extraction showed a recovery of 92.37%, 90.90%, 89.55%, and 93.99% at concentrations of 0.75 µg/mL, 2.25 µg/mL, 5 µg/mL, and 7.5 µg/mL, respectively (Table 2.9).

Table 2.9 The recovery/extraction efficiency data for the quantification of MPA and MPAC in human plasma

Recovery			
	Concentration, µg/mL	**MPA**	**MPAC**
1 (High QC)	7.5	80.79%	93.99%
2 (Med QC)	5	77.45%	89.55%
3 (Low QC)	2.25	75.24%	90.90%
4 (LLOQ)	0.75	75.72%	92.37%

2.4.6 Dried blood spot approach

2.4.6.1 *Spot volume optimization*

The first parameter to be optimized was the volume of blood to be spotted onto the DBS before sample processing. The volumes tested were 20 µL, 30 µL, 40 µL and 50 µL. The criteria for selection were that the spotted blood should be within the designated circular areas on the paper yet covering most of the circular disks. As observed in the Figure 2.68, the spot volume of 20 µL did not cover the entire spot area, the volume of 30 µL covered an area much more than

20 µL, and the volume of 40 µL blood covered majority of the spot area. However, the volume of 50 µL covered almost the entire spot area but also escaped the boundary of the circular spot. Hence, 40 µL was chosen as the ideal spot volume for further optimization.

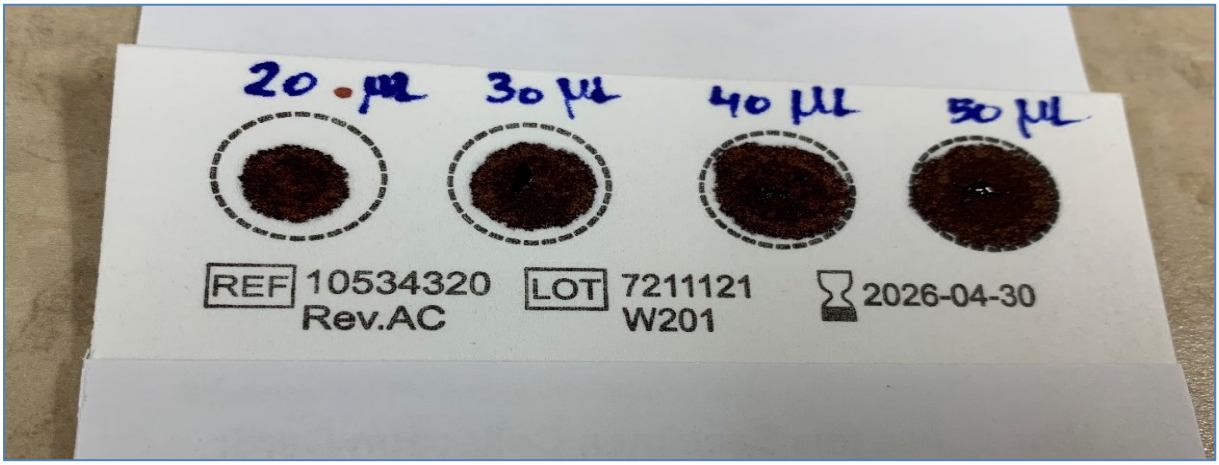

Figure 2.68 The effects of blood volume spotting on the Whatman 903 Protein Saver cards

2.4.6.2 *Mycophenolic acid assay calibration set in dried blood spots*

Figure 2.69 represents the standard calibration curve of MPA that was prepared in human whole blood, spotted onto the DBS cards, and analyzed using the final optimized conditions in the UPLC. The curve was observed to be linear, however, the correlation coefficient for MPA had a lower value (r^2 = 0.8725 as seen in Figure 2.69). To improve the calibration curve of MPA, the current calibration concentrations were increased and then plotted again (as seen in Figure 2.70). The new calibration range was plotted from 3.7946 µg/mL to 28.57 µg/mL. This was done to get a linear calibration curve with a high r^2 value of 0.9992.

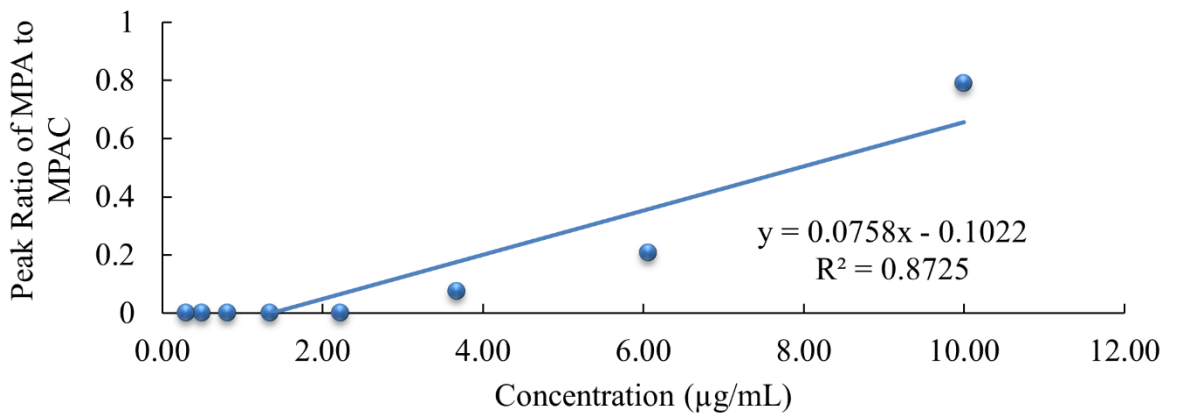

Figure 2.69 The calibration curve of MPA using dried blood spots (ranged from 0.3 to 10 µg/mL)

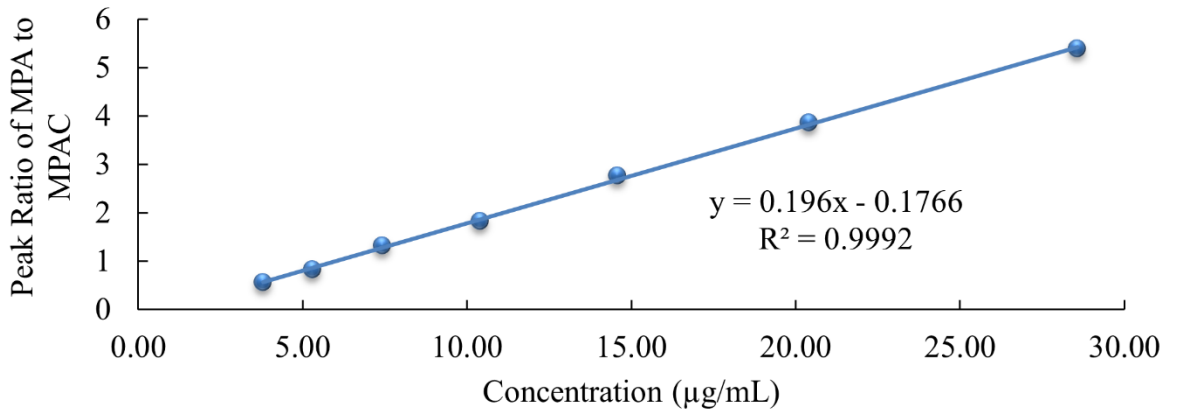

Figure 2.70 The calibration curve of MPA using dried blood spots (ranged from 3.7946 to 28.57 µg/mL)

2.4.6.3 *Effects of adding internal standards before vs. after sample extraction*

To optimize the final conditions for the MPA calibration curve, the internal standard (i.e., MPAC) was tested to be added at different stages of the sample preparation. As seen in Figure 2.71, the red color represents the peak areas of MPA when MPAC was added prior to or after the DBS preparation. The MPA peak areas were much higher when the internal standard was added after the blood spotting on DBS. In addition, the chromatographic peak for MPAC was also observed to be better in shape and symmetry when the analyte was added to the sample after (Figure 2.73) than before spotting blood on DBS (Figure 2.72). Finally, the calibration range was more linear when MPAC was added after DBS processing as well - Figure 2.75 (after DBS processing) vs. Figure 2.74 (before DBS processing)

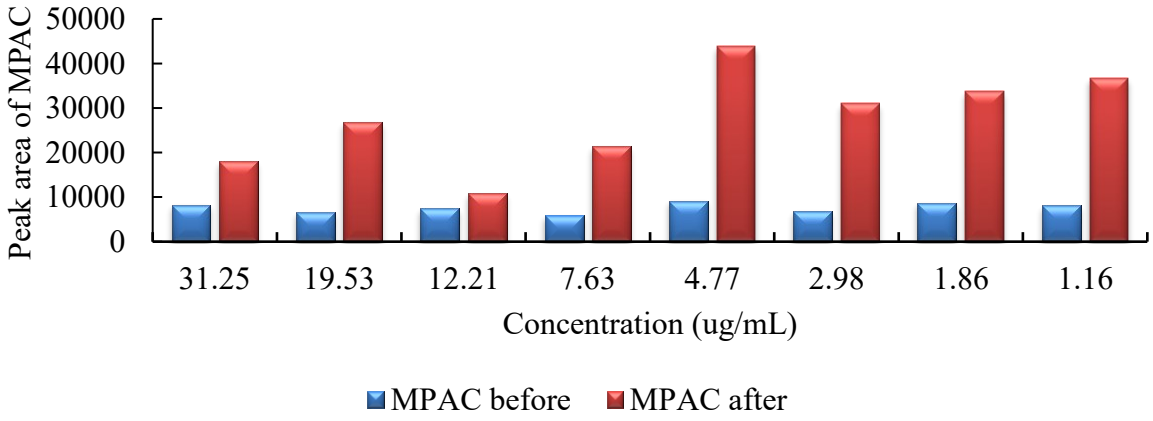

Figure 2.71 The comparisons of absolute MPAC peak areas when it is added before the DBS processing and after

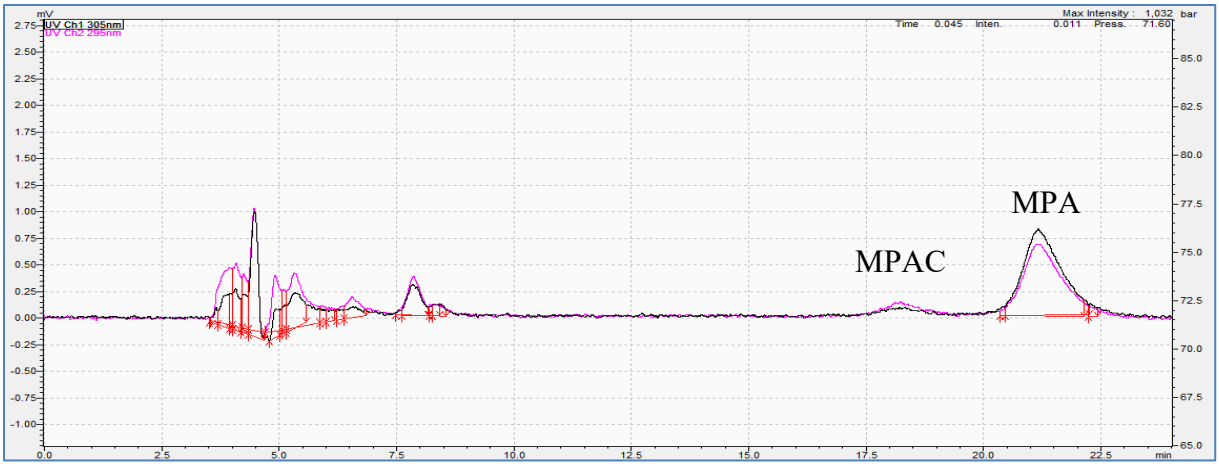

Figure 2.72 The chromatogram of a sample mixture of MPA and MPAC where MPAC is added before the DBS processing

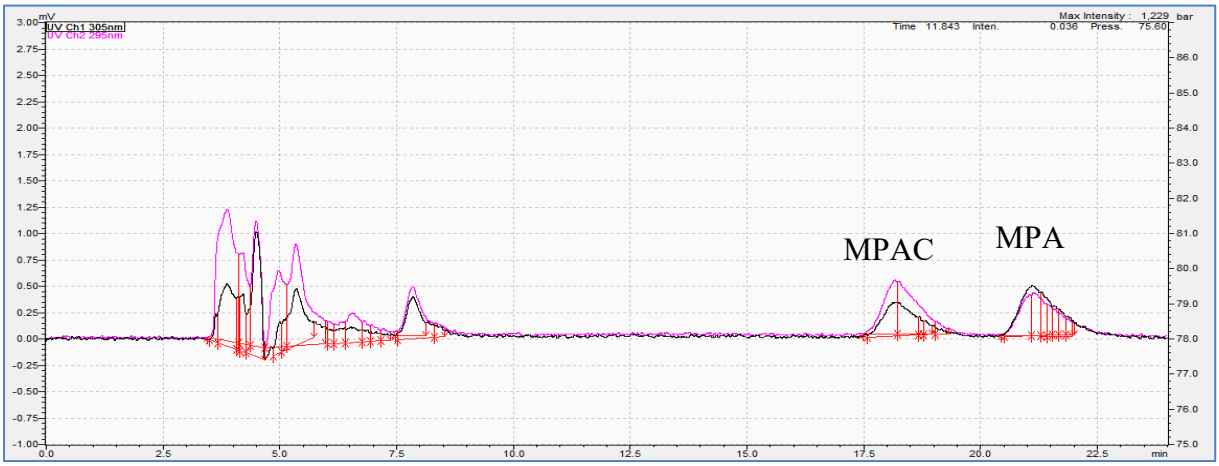

Figure 2.73 The chromatogram of a sample mixture of MPA and MPAC where MPAC is added after the DBS processing

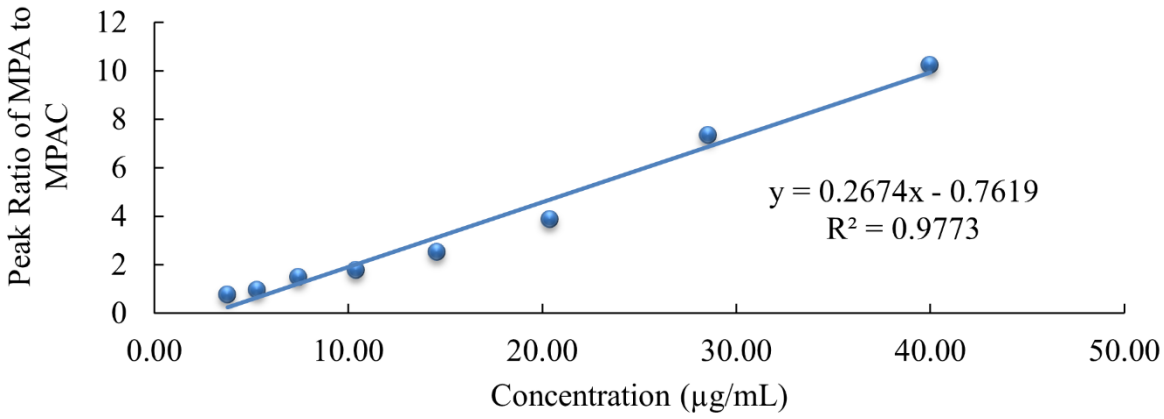

Figure 2.74 The calibration curve of MPA where MPAC is added before the DBS processing

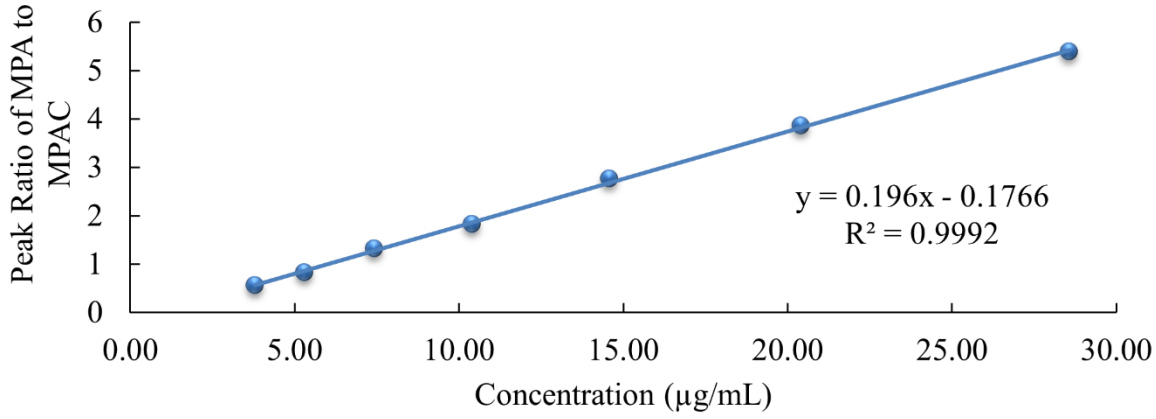

Figure 2.75 The calibration curve of MPA where MPAC is added after the DBS processing

2.4.6.4 *Extraction efficiency of mycophenolic acid in dried blood spots*

Another important parameter that needs to be optimized is the recovery/extraction efficiency of MPA in DBS. Figure 2.76 represents the comparison between the two test groups (one with MPA undergoing extraction and regular processing and the other with MPA added to

the final sample without any extraction). MPA showed higher peak areas when the analytes are added after the extraction. MPA recovery is highest for the Mid QC concentration and decreases with lower concentrations. MPA recovery ranges from 15% to 31% whereas MPAC recovery ranges from 42% to 88% (as seen in Table 2.10).

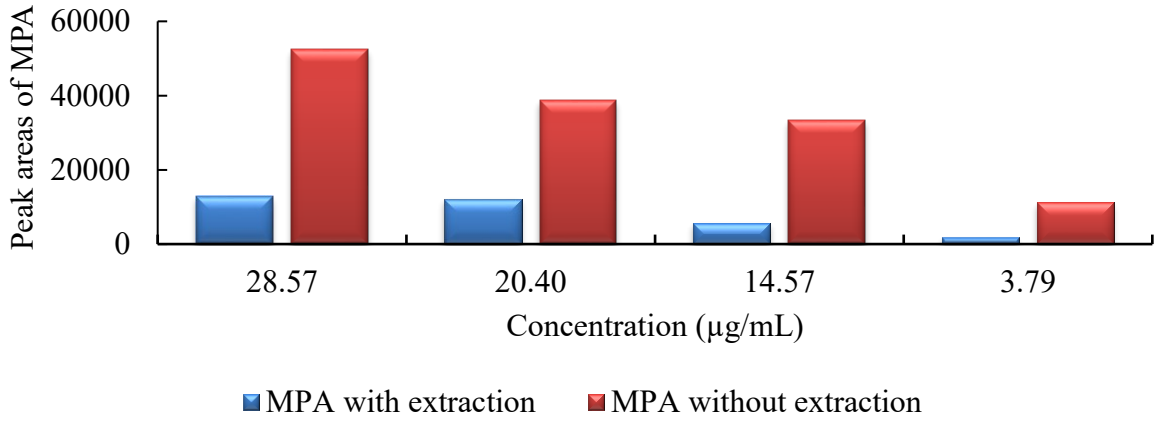

Figure 2.76 The comparison between the two groups (MPA with extraction in DBS, and MPA without extraction in DBS)

Table 2.10 The recovery/extraction efficiency data for the quantification of MPA and MPAC done in DBS

Recovery		
Concentration (µg/mL)	**MPA**	**MPAC**
28.57 ***(High QC)***	24.28%	60.26%

20.40 ***(Mid QC)***	31.58%	88.17%
14.57 ***(Low QC)***	16.92%	53.80%
3.794 ***(LLOQ)***	15.77%	42.32%

2.5 Results for *p*-cresol assay

2.5.1 Spectral scan

2.5.1.1 *Spectral scanning of p-cresol and its metabolites using ultraviolet-visible spectrophotometer*

*p*C, *p*CS, *p*CG, and DMP working solutions were prepared in water and ACN at a concentration of 30 µg/mL at pH 3 and pH 7 to determine the optimal wavelength using the ultraviolet detection method. Figure 2.77 and Figure 2.78 represent the spectral scan from injecting blank ACN and water in the ultraviolet spectrophotometer, respectively, where the x-axis depicts the wavelength and y-axis depicts the associated absorbance. Using ultraviolet spectrophotometer, the absorbance intensity was recorded in the range from 0.2 to 0.8. As observed from the spectral scan using ACN below, *p*C showed the maximum absorbance at 280.02 – 280.08 nm wavelength (Figure 2.79), and DMP at 270.12 – 270.65 nm wavelength (Figure 2.82). On the contrary, the absorbance response for *p*CS and *p*CG (Figure 2.80 and Figure 2.81, respectively) on the ultraviolet spectra while using pure ACN was too low to measure, which means that these detection conditions did not work for the two analytes. In

addition, varying the pH (from pH 3 to pH 7) did not have any impact on the wavelength or absorbance (data not shown).

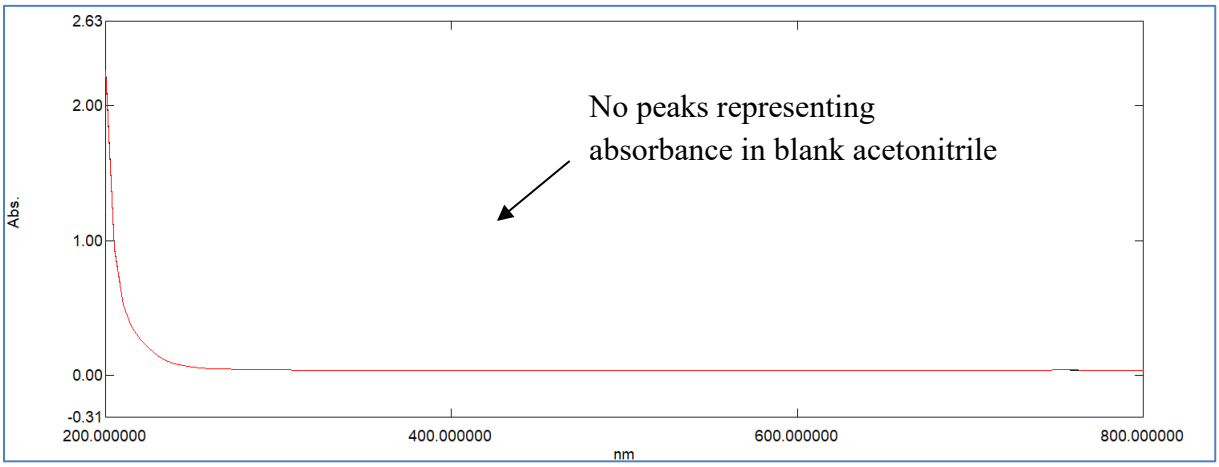

Figure 2.77 The spectral scan of pure ACN (blank, without any analyte, at 4.25 pH) using the ultraviolet-visible spectrophotometer

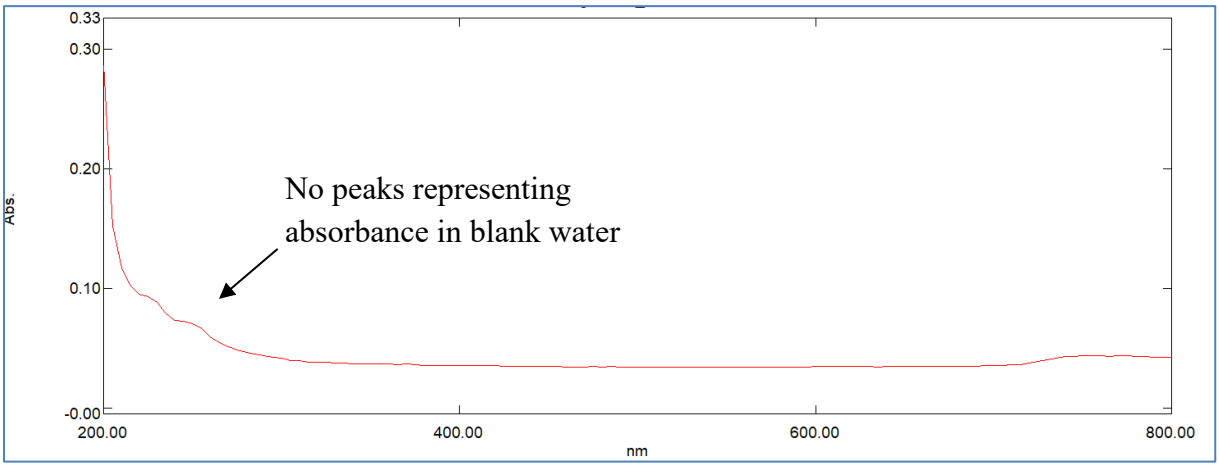

Figure 2.78 The spectral scan of pure water (blank, without any analyte, at 6.29 pH) using the ultraviolet-visible spectrophotometer

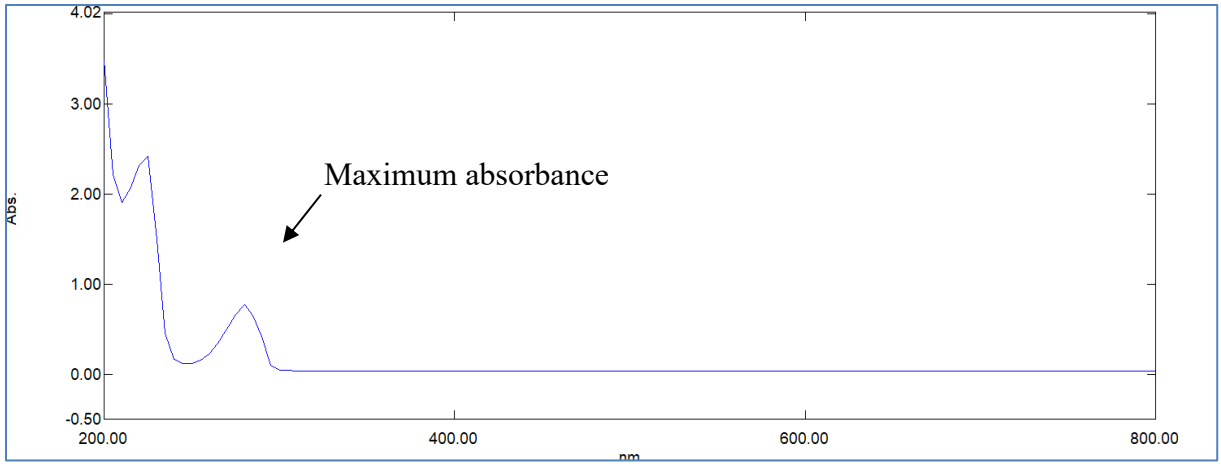

Figure 2.79 The spectral scan of pC analyzed at pH 3 in pure acetonitrile using the ultraviolet-visible spectrophotometer

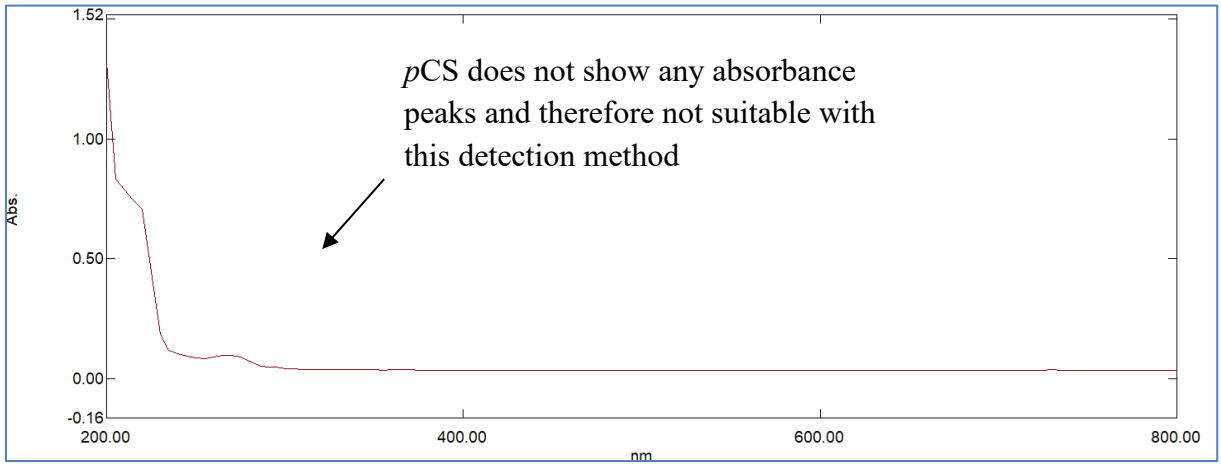

Figure 2.80 The spectral scan of pCS analyzed at pH 3 in pure acetonitrile using the ultraviolet-visible spectrophotometer

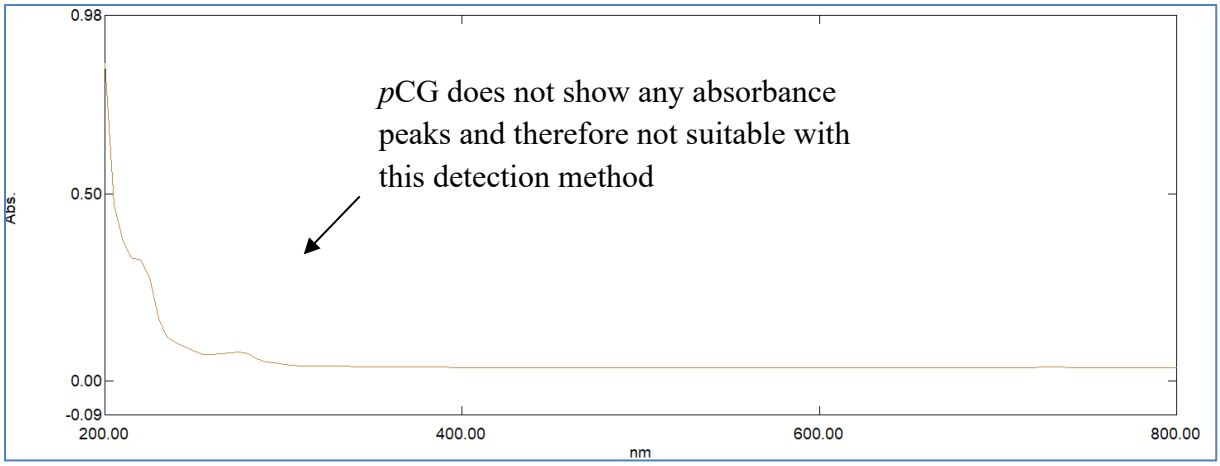

Figure 2.81 The spectral scan of pCG analyzed at pH 3 in pure acetonitrile using the ultraviolet-visible spectrophotometer

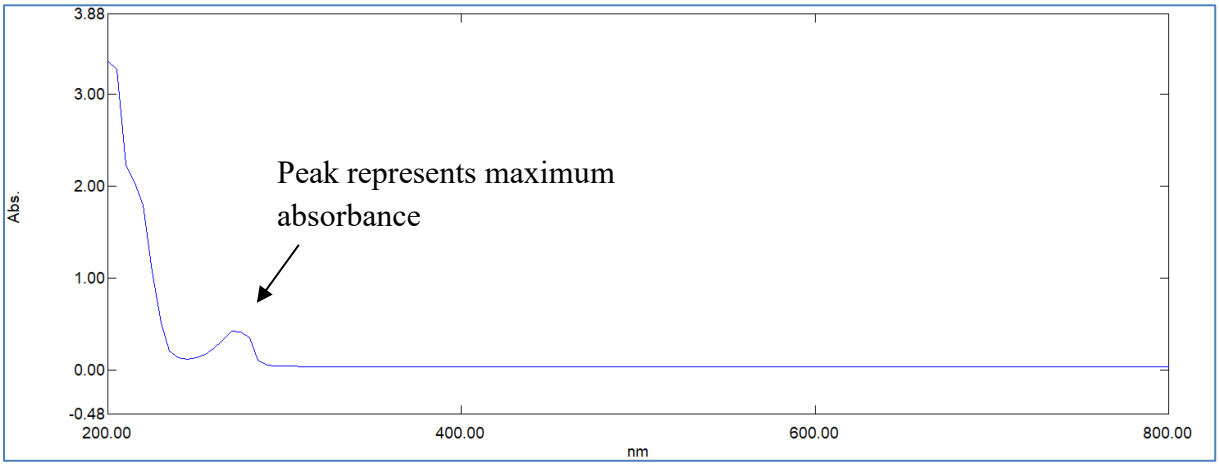

Figure 2.82 The spectral scan of DMP analyzed at pH 3 in pure acetonitrile using the ultraviolet-visible spectrophotometer

2.5.1.2 *Spectral scanning of p-cresol and its metabolites using fluorescence spectrophotometry*

As part of our assay development, *p*C and its metabolites were also tested in the fluorescence spectrophotometer to determine the suitability of fluorescence detection. The testing in fluorescence spectrophotometry was done by preparing *p*C, *p*CS, *p*CG, and DMP at a concentration of 30 µg/mL using 100% ACN at pH 3. For *p*C, the fluorescence-spectra showed areas of high intensity (since the 3D spectra color was bright orangish-green, as shown in Figure 2.83) and the same was observed for the other analytes *p*CS (Figure 2.84), *p*CG (Figure 2.85), and DMP (Figure 2.86). Varying the pH of analyte working solutions did not have a significant effect on the intensity of the color in the spectrum (data not shown). The optimal wavelength for *p*C, *p*CS, *p*CG, and DMP ranged from –

- *p*C: emission – 295 nm to 315 nm, excitation – 260 nm to 290 nm
- *p*CS: emission – 288 nm to 298 nm, excitation – 210 nm to 225 nm
- *p*CG: emission – 288 nm to 302 nm, excitation – 210 nm to 225 nm
- DMP: emission – 290 nm to 300 nm, excitation – 260 nm to 280 nm

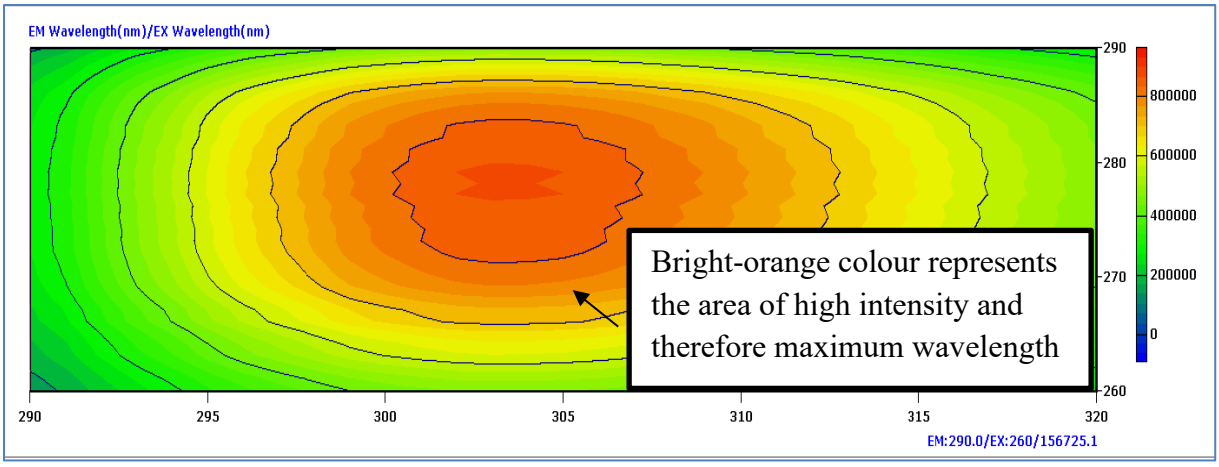

Figure 2.83 The spectral scan of pC analyzed at pH 3 in pure acetonitrile using the fluorescence spectrophotometer

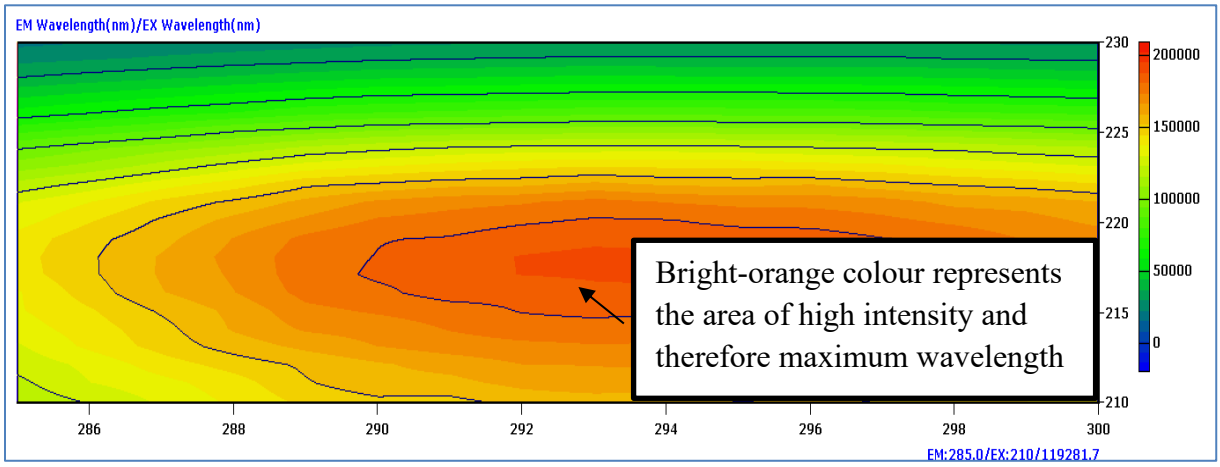

Figure 2.84 The spectral scan of pCS analyzed at pH 3 in pure acetonitrile using the fluorescence spectrophotometer

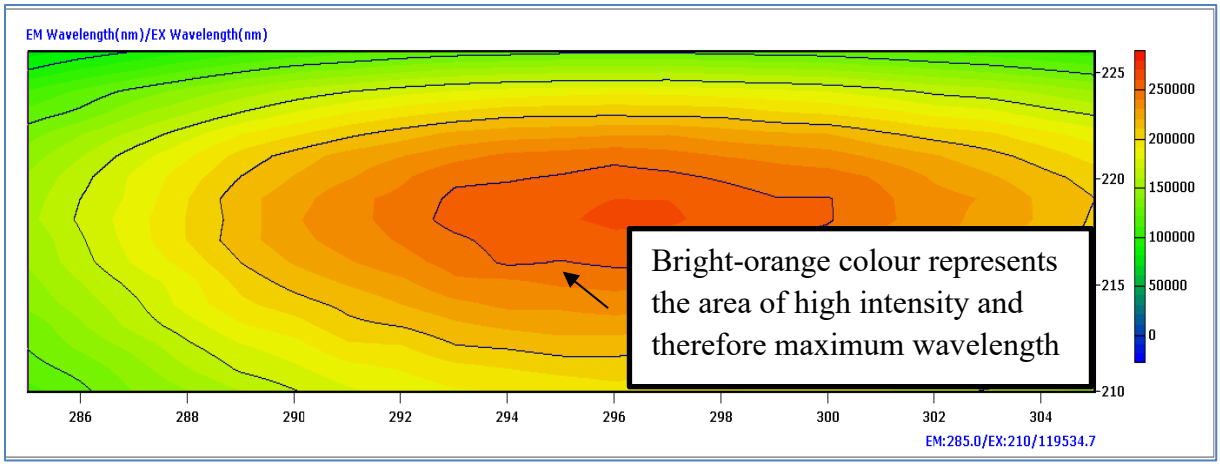

Figure 2.85 The spectral scan of pCG analyzed at pH 3 in pure acetonitrile using the fluorescence spectrophotometer

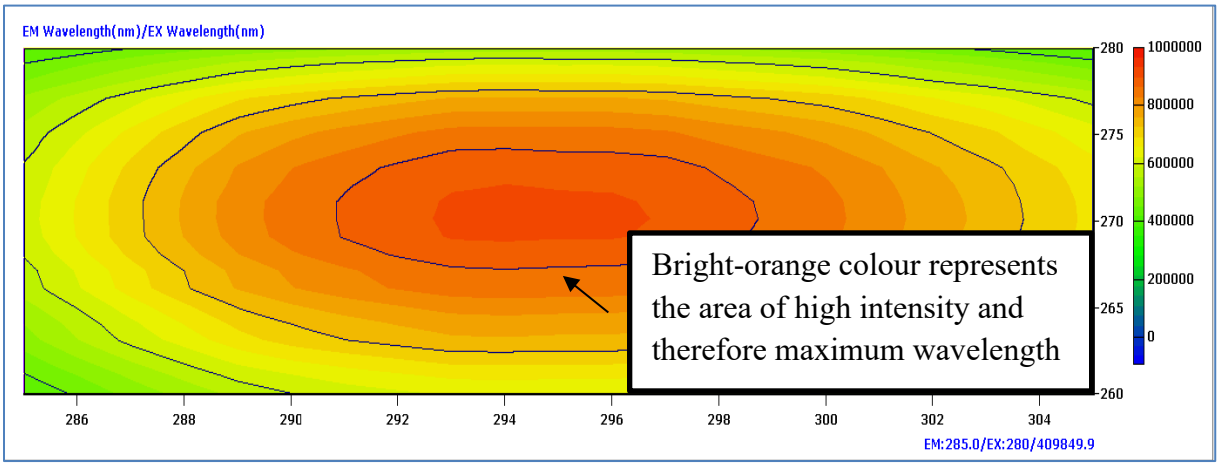

Figure 2.86 The spectral scan of DMP analyzed at pH 3 in pure acetonitrile using the fluorescence spectrophotometer

2.5.2 Chromatography optimization

2.5.2.1 *Solvent optimization – methanol*

After obtaining the optimized wavelength from the ultraviolet-visible spectrophotometer, the concentration of methanol was optimized next. In Figure 2.87, at 80% methanol, *p*C and DMP showed a good separation, whereas *p*CS and *p*CG can be seen eluting closely. Hence, 80% methanol is not a workable condition for further chromatographic optimization. However, this trend changes as we move towards lower methanol concentrations i.e., at 73% methanol and 27% water (Figure 2.88), the chromatography became better as the peaks can be eluted at separate retention times (*p*C – approximately 3.4 mins, *p*CS – approximately 3.0 mins, *p*CG – approximately 2.7 mins, DMP – approximately 4.1 mins). It is apparent that changing the concentration of the solvent affected the chromatography of the analytes by decreasing/increasing their elution times. The relationships between methanol concentration and *p*C peak area can be seen in Figure 2.89.

In summary, it was observed that 73% methanol with 27% water provides better chromatography as compared to other conditions tested and hence was selected as the ideal methanol concentration.

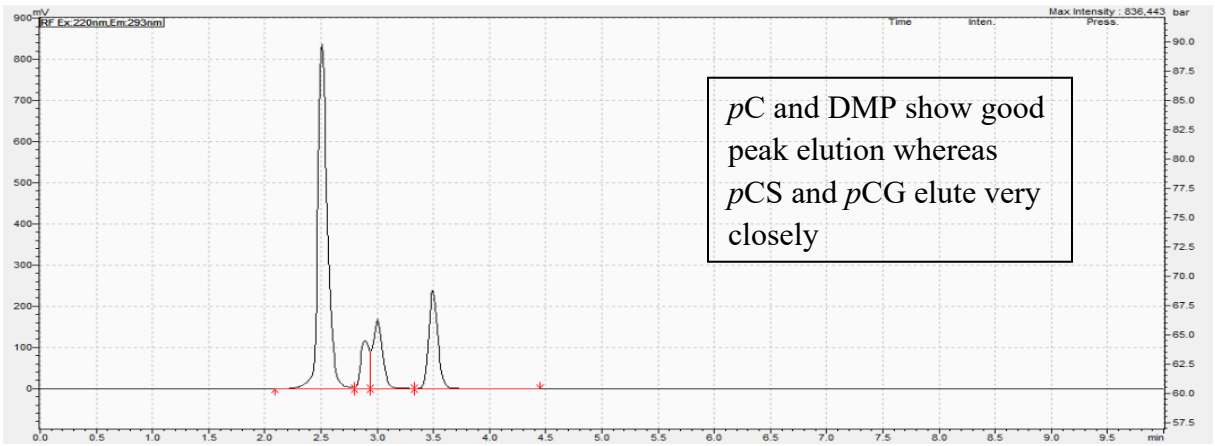

Figure 2.87 Methanol concentration optimization - the chromatogram of pC, pCS, pCG, and DMP mixture using 80% methanol and 20% water in the mobile phase

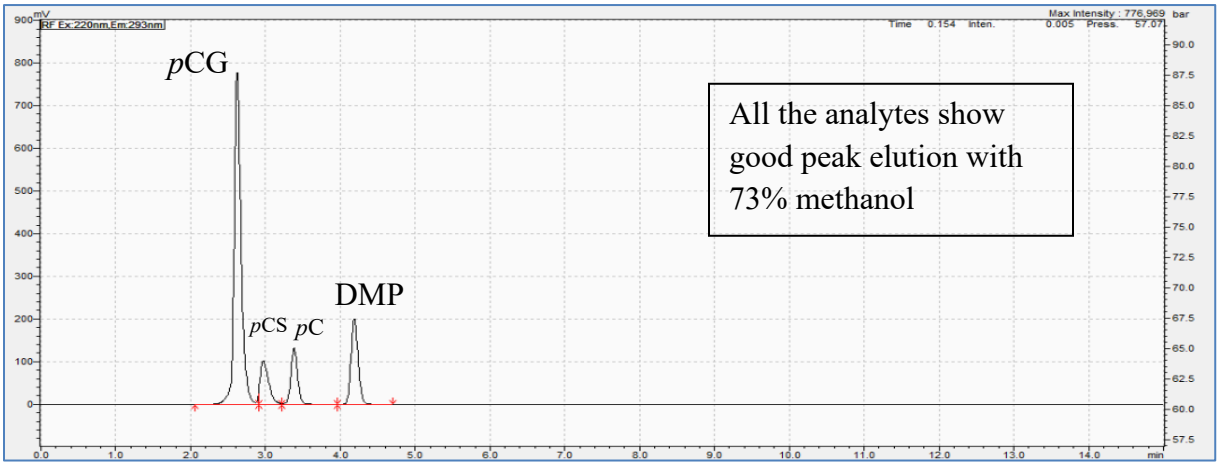

Figure 2.88 Methanol concentration optimization - the chromatogram of pC, pCS, pCG, and DMP mixture using 73% methanol and 27% water in the mobile phase (optimized condition)

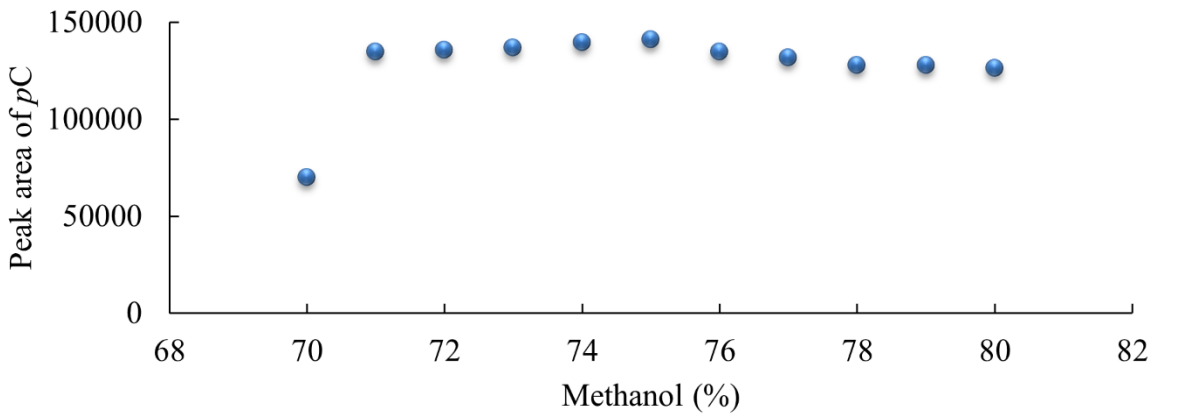

Figure 2.89 The correlation plot between methanol concentration in the mobile phase and the absolute peak area of pC

2.5.2.2 *Solvent optimization – acetonitrile*

Once the optimized wavelength from the fluorescence spectrophotometry was obtained, the concentration of ACN was also optimized. In Figure 2.90, the peaks for *p*C, *p*CS, *p*CG, and DMP can be seen having symmetrical peak shapes and well-separated using 40% ACN and 60% water. On the other hand, in Figure 2.91, using 90% ACN in the mobile phase, the analytes are eluting very closely. Hence, 90% ACN is not a workable condition for further chromatographic optimizations. The relationships between ACN concentration and *p*C peak area can be seen in Figure 2.92.

In summary, it was observed that 40% ACN with 60% water provides better chromatography separation as compared to other conditions tested and hence was selected as the ideal ACN concentration.

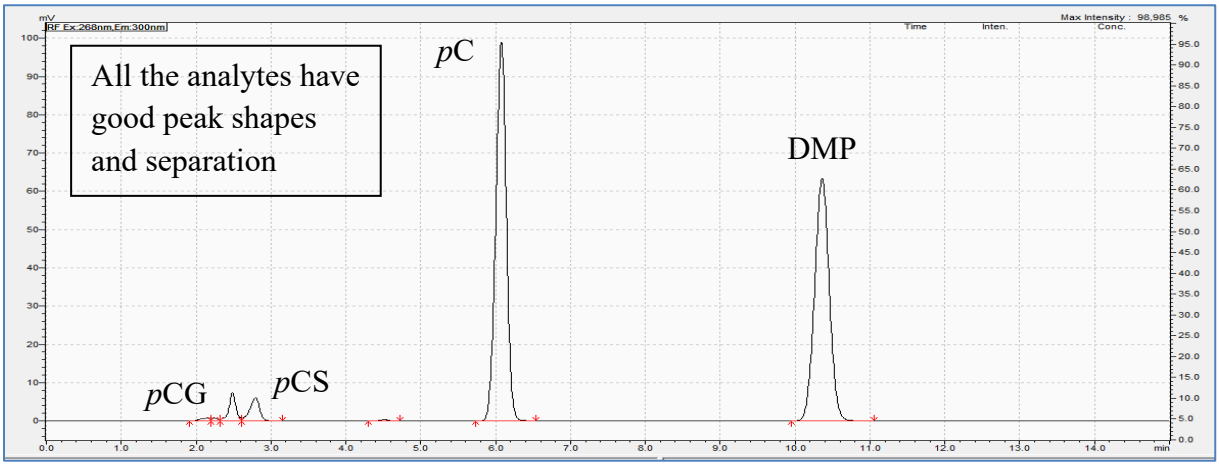

Figure 2.90 Acetonitrile concentration optimization - the chromatogram of pC, pCS, pCG, and DMP mixture using 40% acetonitrile and 60% water in the mobile phase (optimized condition)

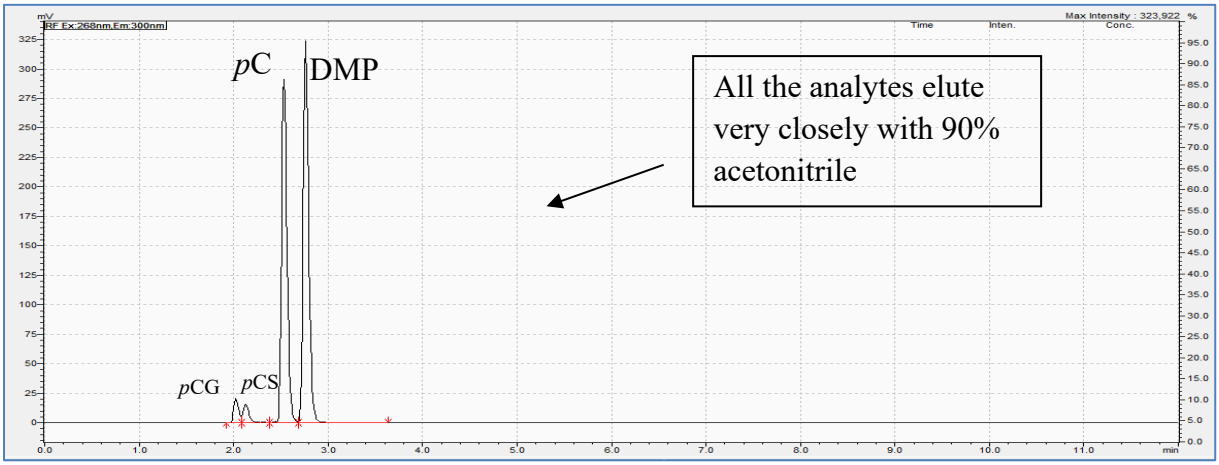

Figure 2.91 Acetonitrile concentration optimization - the chromatogram of pC, pCS, pCG, and DMP mixture using 90% acetonitrile and 10% water in the mobile phase (optimized condition)

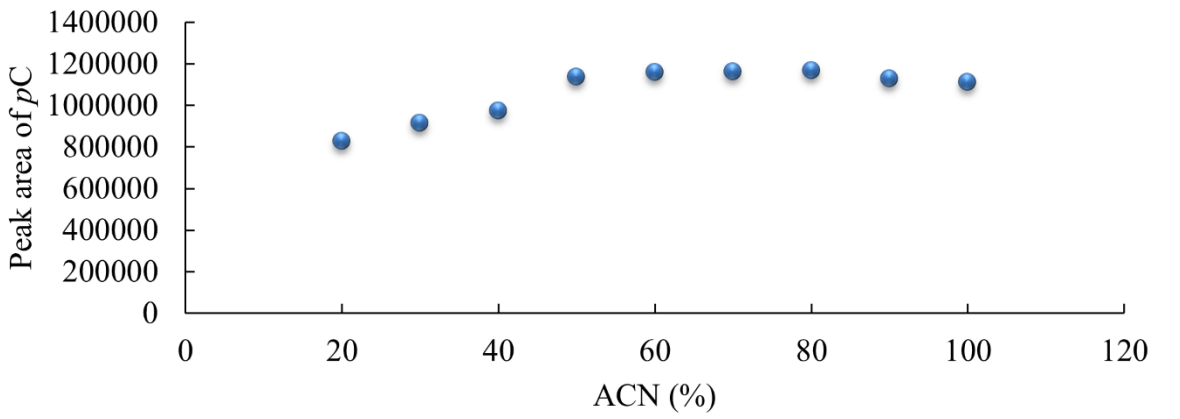

Figure 2.92 The correlation plot between acetonitrile concentration in the mobile phase and the absolute peak area of pC

2.5.2.3 *Additive optimization – formic acid (in methanol)*

In Figure 2.93, the chromatography was obtained after injecting a mixture of *p*C, *p*CS, *p*CG, and DMP (at a concentration of 10 µg/mL) using 0.505% formic acid and 0.4 mM ammonium acetate. It is evident that this concentration of formic acid results in symmetrical peaks which are eluting at distinctive retention times (*p*C – approximately 3.4 mins, *p*CS – approximately 3.0 mins, *p*CG – approximately 2.7 mins, DMP – approximately 4.1 mins) with good peak separation. On the contrary, in Figure 2.94, there was no formic acid in the mobile phase with only ammonium acetate at 0.4 mM. When injecting the mixture sample (with *p*C, *p*CS, *p*CG, and DMP) at no formic acid in the mobile phase, the chromatography becomes not usable since *p*CS and *p*CG did not elute with this condition. These data suggest that the lower the concentration of formic acid, the worse the chromatography can be observed (hence 0% formic acid was not a workable condition for the further chromatographic optimizations). The relationships between formic acid and *p*C peak area can be seen in Figure 2.95.

In summary, the optimal concentration of formic acid in the mobile phase was determined to be 0.505% (with 0.4 mM ammonium acetate).

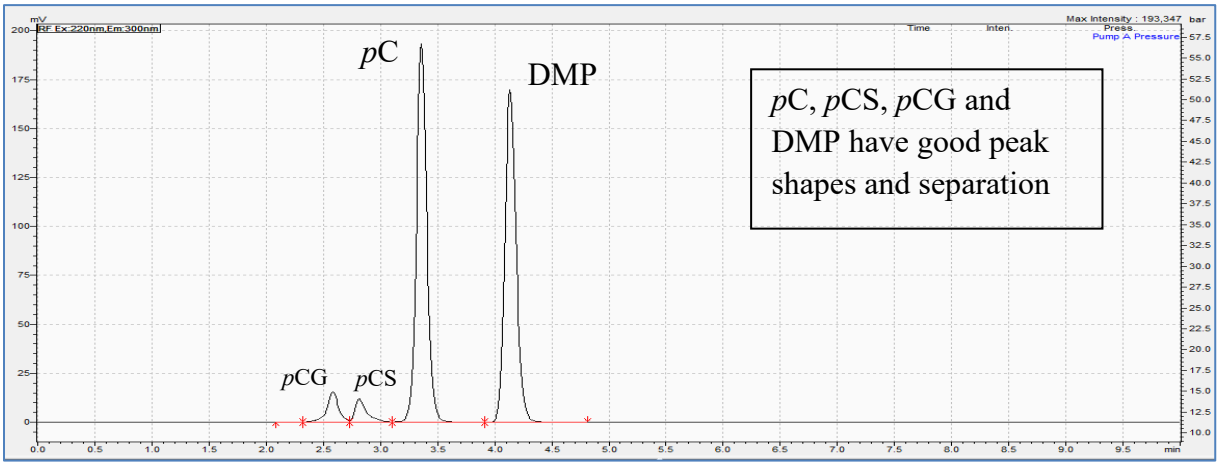

Figure 2.93 Formic acid concentration optimization (in methanol) - the chromatogram of pC, pCS, pCG, and DMP mixture using 0.505% formic acid and 0.4 mM ammonium acetate in the mobile phase (optimized condition)

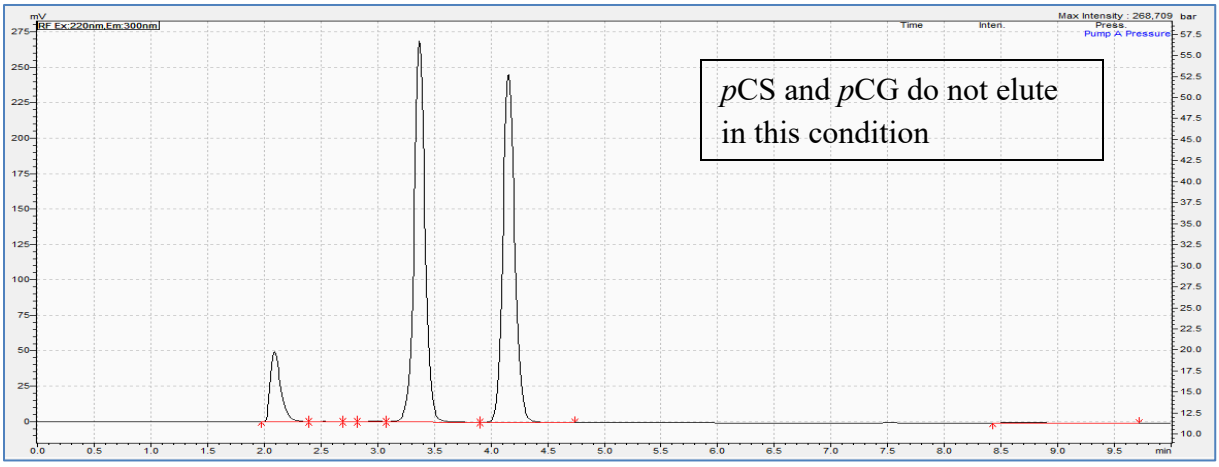

Figure 2.94 Formic acid concentration optimization (in methanol) – the chromatogram of pC, pCS, pCG, and DMP mixture using 0% formic acid and 0.4 mM ammonium acetate in the mobile phase

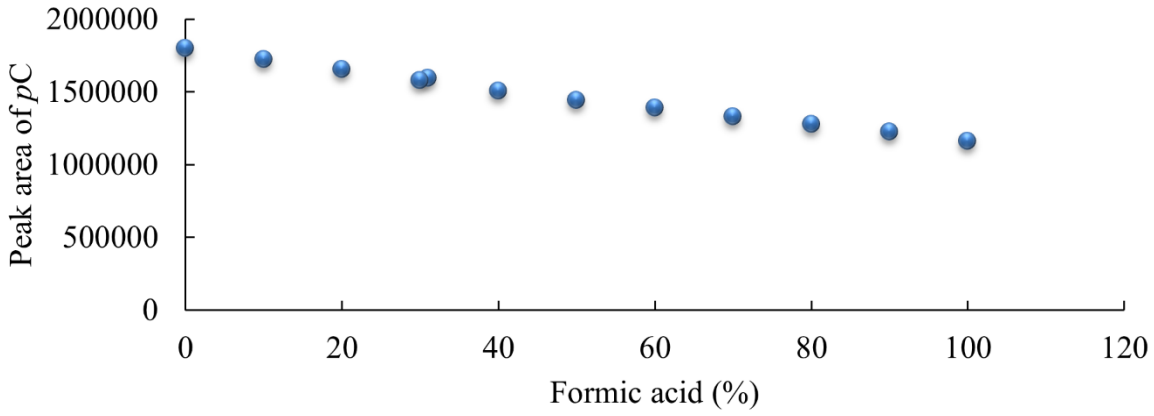

Figure 2.95 The correlation plot between formic acid concentration in methanol and the absolute peak area of pC

2.5.2.4 *Additive optimization – formic acid (in acetonitrile)*

Using ACN, formic acid was also optimized while keeping ammonium acetate fixed at 2 mM. In Figure 2.96, the chromatography was obtained after injecting a mixture of *p*C, *p*CS, *p*CG, and DMP (at a concentration of 10 µg/mL) using 0.1% formic acid and 2 mM ammonium acetate. It is evident that using this concentration of formic acid, the peak shapes for the analytes were symmetrical, and the peaks were eluting at distinctive retention times (*p*C – approximately 6.1 mins, *p*CS – approximately 2.9 mins, *p*CG – approximately 2.5 mins, DMP – approximately 10.3 mins) with good peak separation. On the contrary, Figure 2.97 represents no formic acid in the mobile phase with only ammonium acetate at 2 mM present. When injecting the mixture sample (*p*C, *p*CS, *p*CG, and DMP) at no formic acid in the mobile phase, which resulted in relatively poor chromatography. The relationships between formic acid concentration and *p*C peak area can be seen in Figure 2.98.

In summary, 0.1% formic acid with 2 mM ammonium acetate provides ideal chromatographic conditions in ACN.

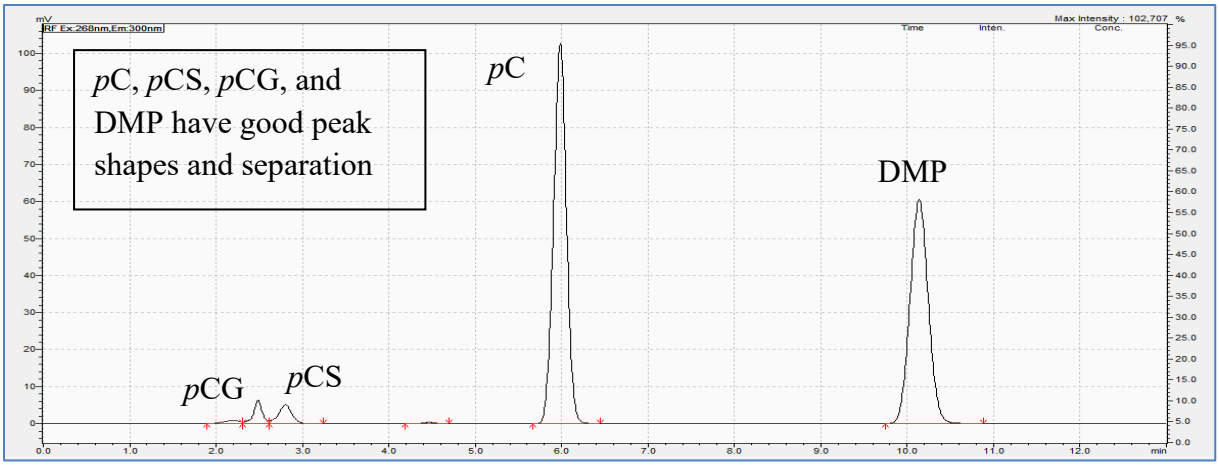

Figure 2.96 Formic acid concentration optimization (in acetonitrile) – the chromatogram of pC, pCS, pCG, and DMP mixture using 0.1% formic acid and 2 mM ammonium acetate in the mobile phase (optimized condition)

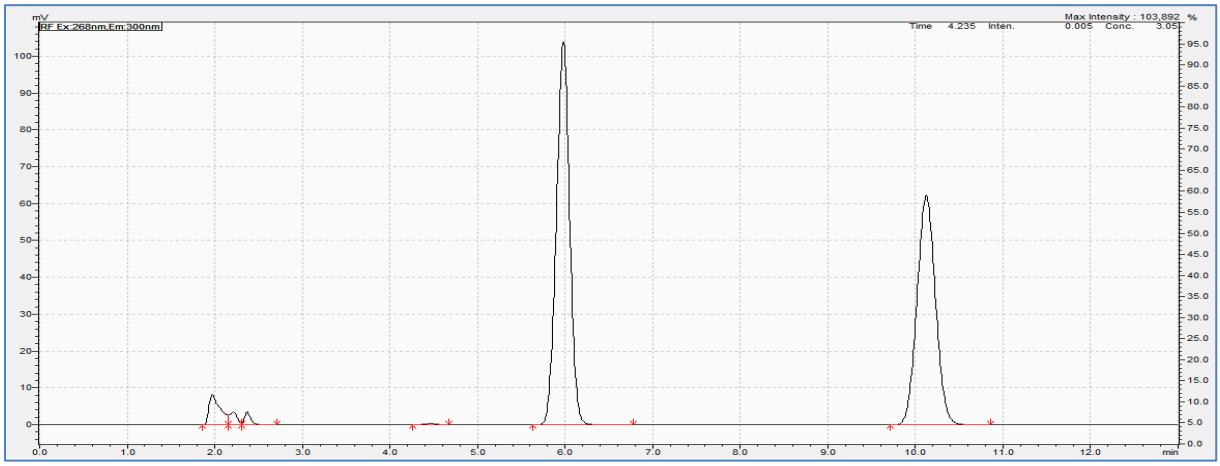

Figure 2.97 Formic acid concentration optimization (in acetonitrile) - the chromatogram of pC, pCS, pCG, and DMP mixture using 0% formic acid and 2 mM ammonium acetate in the mobile phase

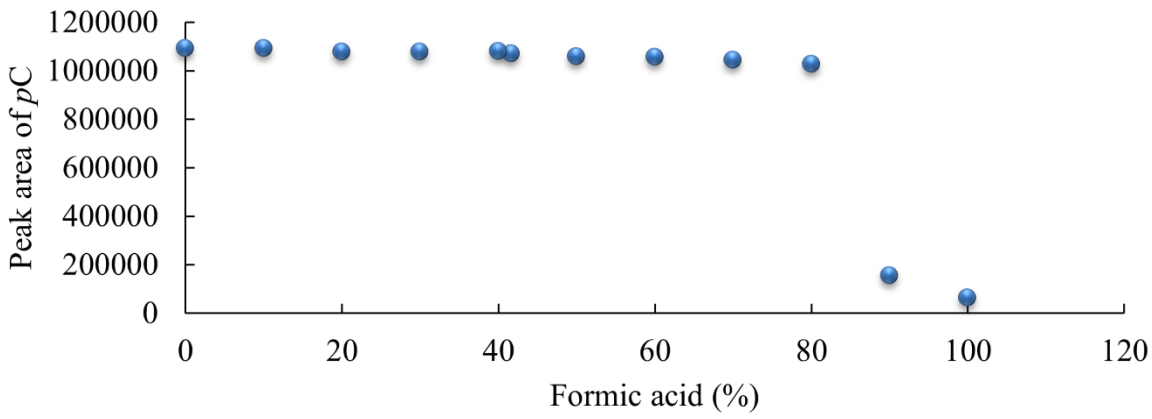

Figure 2.98 The correlation plot between formic acid concentration in acetonitrile and the absolute peak area of pC

2.5.2.5 *Additive optimization – ammonium acetate (in methanol)*

Figure 2.99 represents the results when a mixture of *p*C, *p*CS, *p*CG, and DMP was injected into the instrument (at a concentration of 10 µg/mL) using methanol, with 0.4 mM ammonium acetate and 0.02% formic acid. The peaks for the analytes have good symmetrical shapes, are well-separated (with elution times of *p*C – approximately 3.3 mins, *p*CS – approximately 2.9 mins, *p*CG – approximately 2.6 mins, DMP – approximately 4.3 mins), and have good separation from the solvent front. Overall, there were no interferences (between the peaks of analytes) that can be seen in the chromatogram. However, the opposite was observed when the mixture of *p*C, *p*CS, *p*CG, and DMP was injected with 1 mM ammonium acetate and 0.02% formic acid in the mobile phase (Figure 2.100). Figure 2.101 represents the relationships between the concentrations of ammonium acetate and absolute peak area counts of *p*C.

Hence, the final ammonium acetate concentration was chosen to be 0.4 mM with the formic acid at 0.02% for *p*C, *p*CS, *p*CG, and DMP when using methanol in the mobile phase.

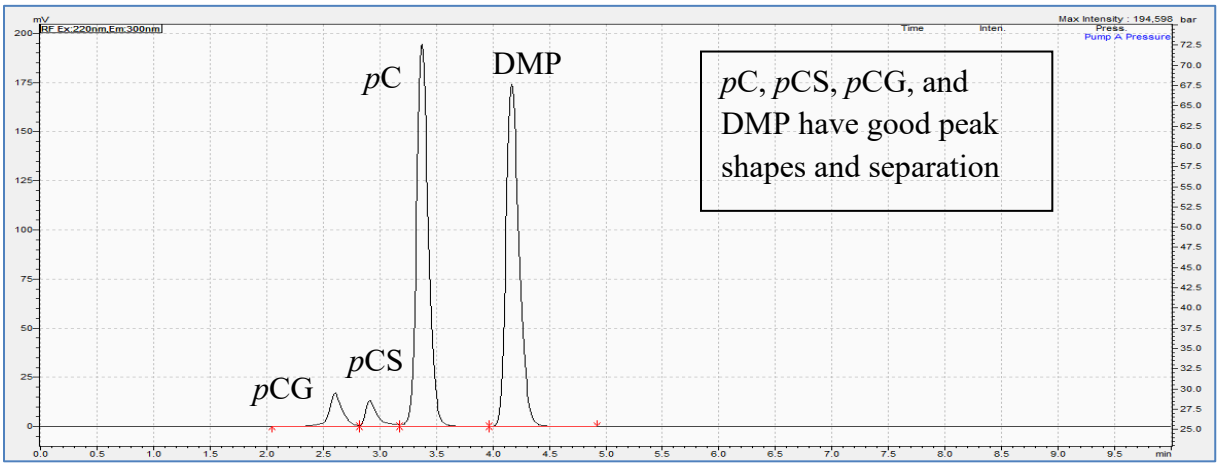

Figure 2.99 Ammonium acetate concentration optimization (in methanol) - the chromatogram of pC, pCS, pCG, and DMP mixture using 0.02% formic acid and 0.4 mM ammonium acetate in the mobile phase (optimized condition)

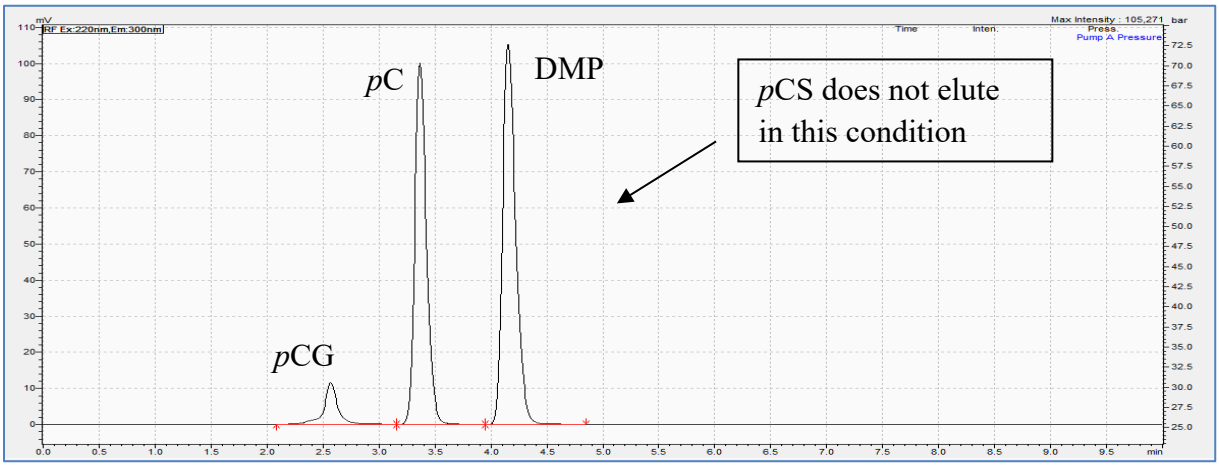

Figure 2.100 Ammonium acetate concentration optimization (in methanol) - the chromatogram of pC, pCS, pCG, and DMP mixture using 0.02% formic acid and 1 mM ammonium acetate in the mobile phase

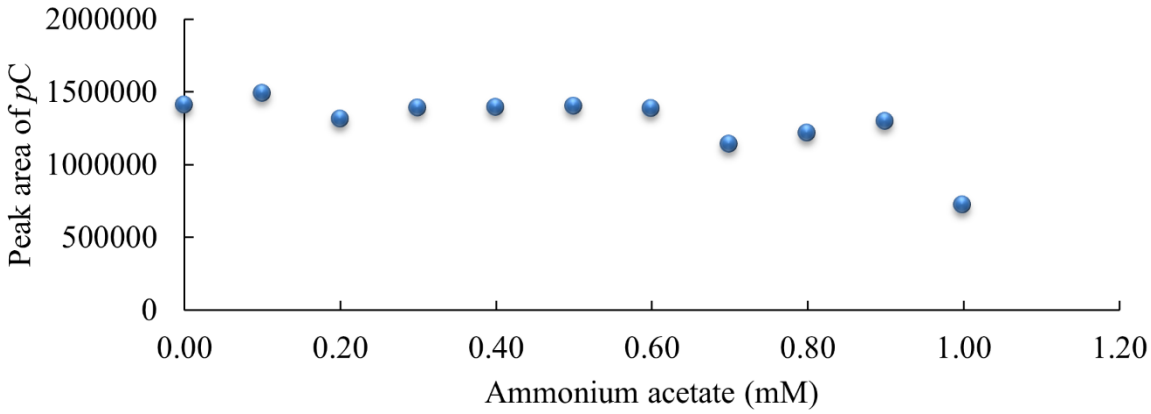

Figure 2.101 The correlation plot between ammonium acetate concentration in methanol and the absolute peak area of pC

2.5.2.6 *Additive optimization – ammonium acetate (in acetonitrile)*

Figure 2.102 represents the results when a mixture of *p*C, *p*CS, *p*CG, and DMP was injected into the instrument (at a concentration of 10 µg/mL) using ACN, 0.8 mM ammonium acetate, and 0.1% formic acid. The peaks for the analytes have good symmetrical shapes, are well-separated (with elution times of *p*C – approximately 6.0 mins, *p*CS – approximately 3.0 mins, *p*CG – approximately 2.5 mins, DMP – approximately 10.1 mins), and have good separation from the solvent front. Overall, there were no interferences observed on the chromatogram. The same trend was observed when a mixture of *p*C, *p*CS, *p*CG, and DMP was injected with 2 mM ammonium acetate and 0.1% formic acid in the mobile phase (Figure 2.103). Figure 2.104 represents relationships between the concentration of ammonium acetate and the absolute peak area counts of *p*C.

The final ammonium acetate concentration was chosen to be 0.8 mM with the formic acid fixed at 0.1 % for *p*C, *p*CS, *p*CG, and DMP when using ACN as the mobile phase.

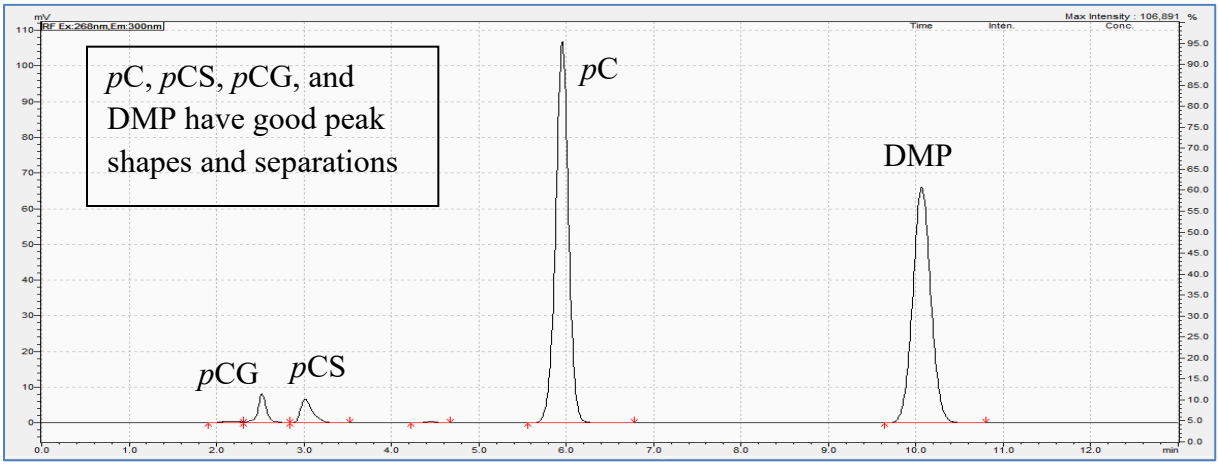

Figure 2.102 Ammonium acetate concentration optimization (in acetonitrile) - the chromatogram of pC, pCS, pCG, and DMP mixture using 0.1% formic acid and 0.8 mM ammonium acetate in the mobile phase (optimized condition)

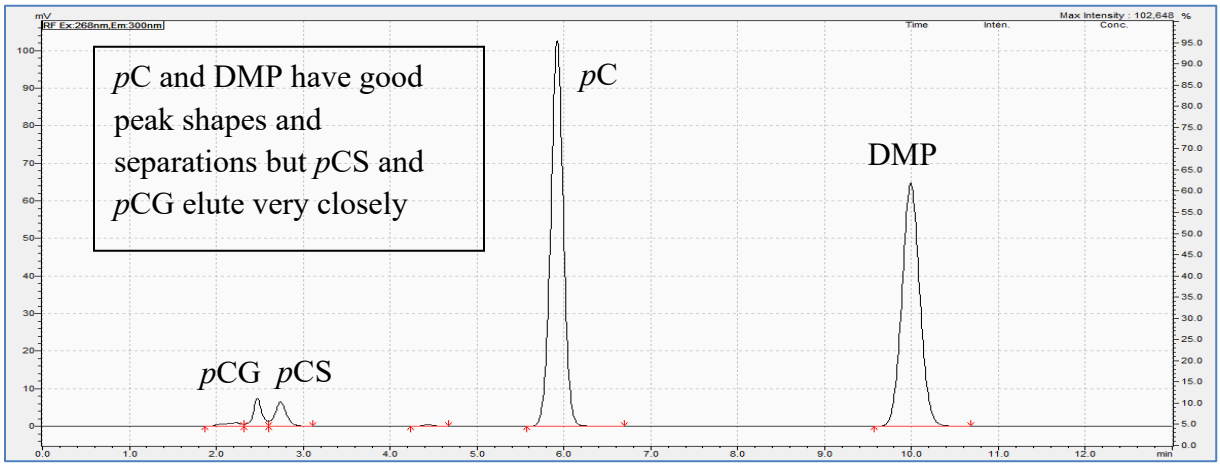

Figure 2.103 Ammonium acetate concentration optimization (in acetonitrile) - the chromatogram of pC, pCS, pCG, and DMP mixture using 0.1% formic acid and 2 mM ammonium acetate in the mobile phase

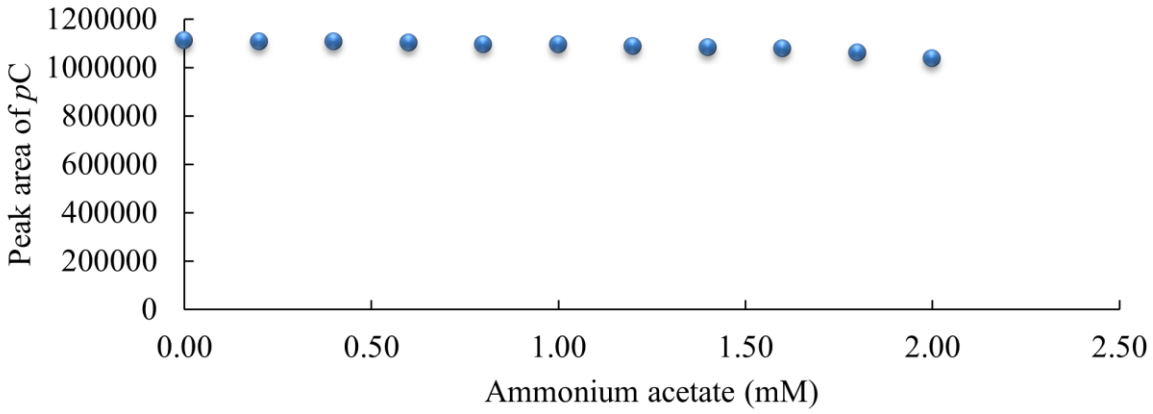

Figure 2.104 The correlation plot between ammonium acetate concentration in acetonitrile and the absolute peak area of pC

2.5.2.7 *Additive optimization – phosphoric acid (in methanol)*

Phosphoric acid concentrations were varied in the mobile phase with the potassium phosphate monobasic fixed at 10 mM. As seen in Figure 2.105, the chromatogram represents the peaks of *p*C, *p*CS, *p*CG, and DMP when injected at a concentration of 10 µg/mL, prepared in methanol with 0.359% phosphoric acid and potassium phosphate monobasic at 10 mM. Although the peaks for *p*C and DMP have relatively good shapes, the separation of *p*CS and *p*CG was poor, which were consistent when using other phosphoric acid concentrations. Moreover, Figure 2.106 represents the relationships between the concentration of phosphoric acid in the mobile phase and the absolute peak areas of *p*C.

In summary, phosphoric acid was not a suitable additive for the *p*C assay since it generated un-usable chromatography.

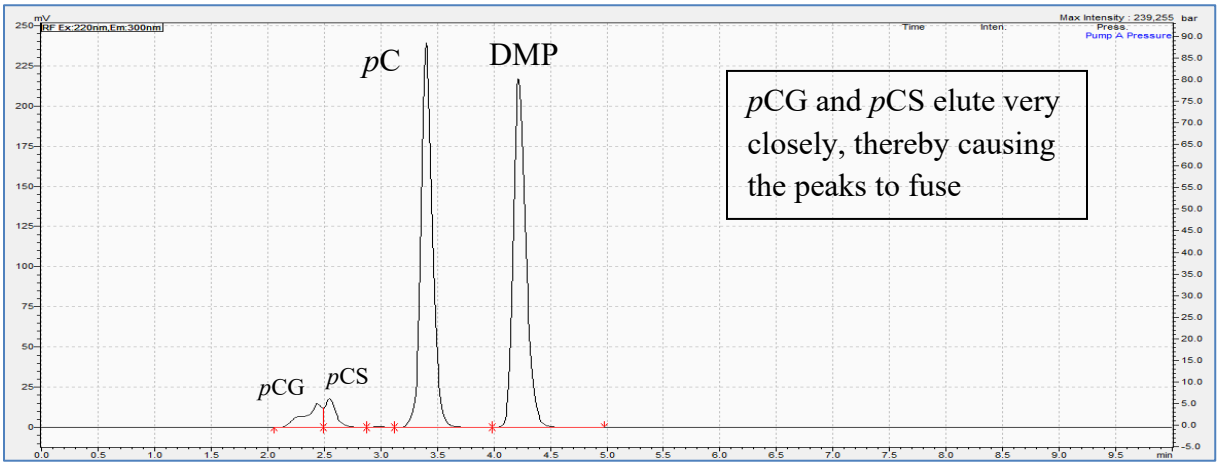

Figure 2.105 Phosphoric acid concentration optimization (in methanol) – the chromatogram of pC, pCS, pCG, and DMP mixture using 0.359% phosphoric acid and 10 mM potassium phosphate monobasic in the mobile phase

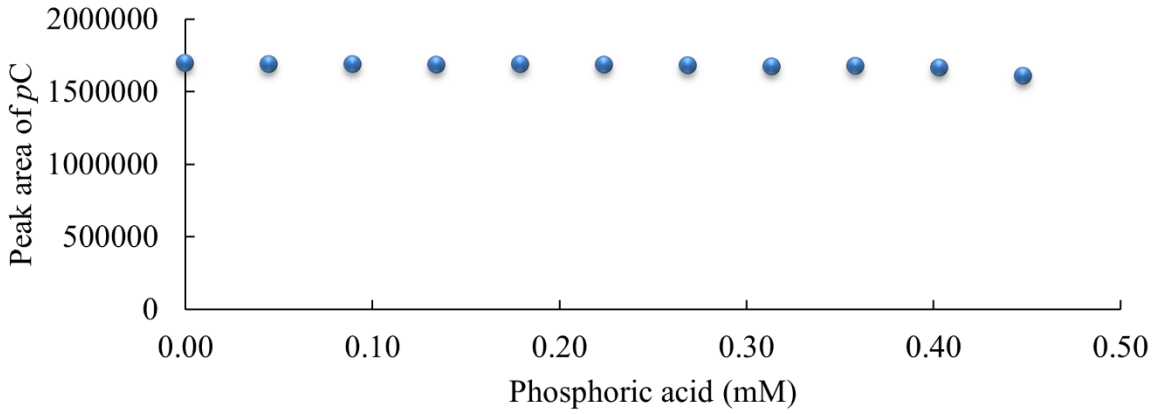

Figure 2.106 The correlation plot between phosphoric acid concentration in methanol and the absolute peak area of pC

2.5.2.8 *Additive optimization – phosphoric acid (in acetonitrile)*

Phosphoric acid concentrations were varied in the mobile phase with the potassium phosphate monobasic fixed at 100 mM. As seen in Figure 2.107, the chromatogram represents the peaks of *p*C, *p*CS, *p*CG, and DMP when injected at a concentration of 10 µg/mL, prepared in methanol with 0.1419% phosphoric acid and potassium phosphate monobasic at 100 mM. The pressure from the instrument was not stable. As the result, there was a lot of disturbances in the background of the chromatogram and no separate peaks were observed.

In summary, phosphoric acid was not a suitable additive for the *p*C assay since it generated un-usable chromatography.

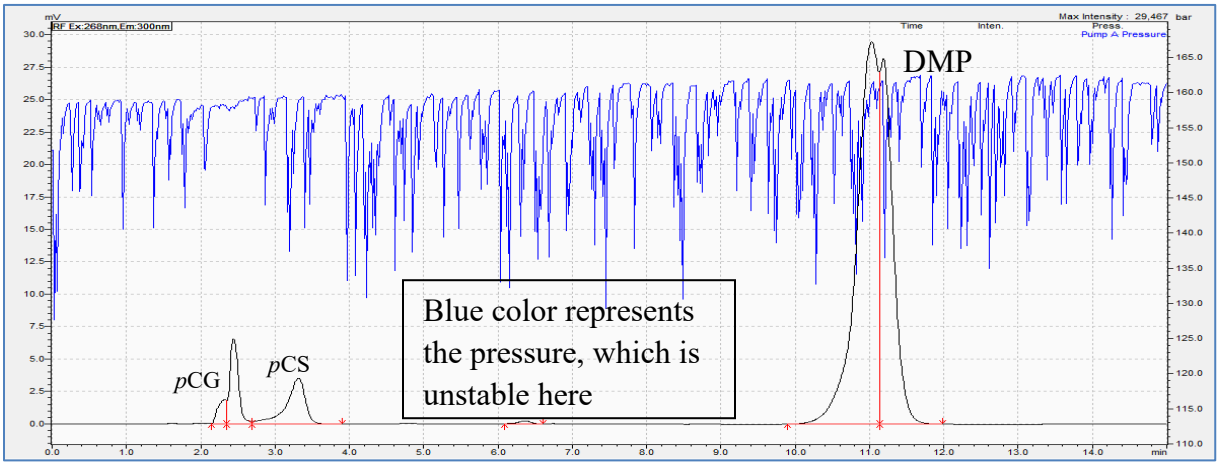

Figure 2.107 Phosphoric acid concentration optimization (in acetonitrile) - the chromatogram of pC, pCS, pCG, and DMP mixture using 0.1419% phosphoric acid and 100 mM potassium phosphate monobasic in the mobile phase

2.5.2.9 *Flow rate optimization (in methanol)*

The flow rate was optimized for *p*C, *p*CS, *p*CG, and DMP using methanol as the solvent to check the effects on chromatographic peak separation and to improve the sensitivity of the assay. As observed in Figure 2.108, when the analytes *p*C, *p*CS, *p*CG, and DMP are injected at a concentration of 10 µg/mL using 0.1% formic acid, 0.4 mM ammonium acetate, and a flow rate of 1 mL/min, the peak shape and separation for all the analytes appeared adequate (elution at *p*C – approximately 3.4 mins, *p*CS – approximately 3.0 mins, *p*CG – approximately 2.7 mins, DMP – approximately 4.1 mins). Similarly, at a flow rate of 1.5 mL/min (Figure 2.109), the peak shapes of all analytes were adequate; however, the peak separations between the analytes were not ideal. Figure 2.110 represents the relationships between flow rate (variable) and the absolute peak area counts of *p*C. The flow rate of 0.25 mL/min provides the highest peak area count, but the area count decreases as the flow rate is increased. The *p*C sensitivity was observed to be decreased when going from 0.25 mL/min to 1.5 mL/min. However, the lower flow rates were not selected for further optimization as the run times were too long for a single injection.

In summary, a flow rate of 1 mL/min was determined the optimal condition for the assay measuring *p*C, *p*CS, *p*CG, and DMP when using methanol in the mobile phase.

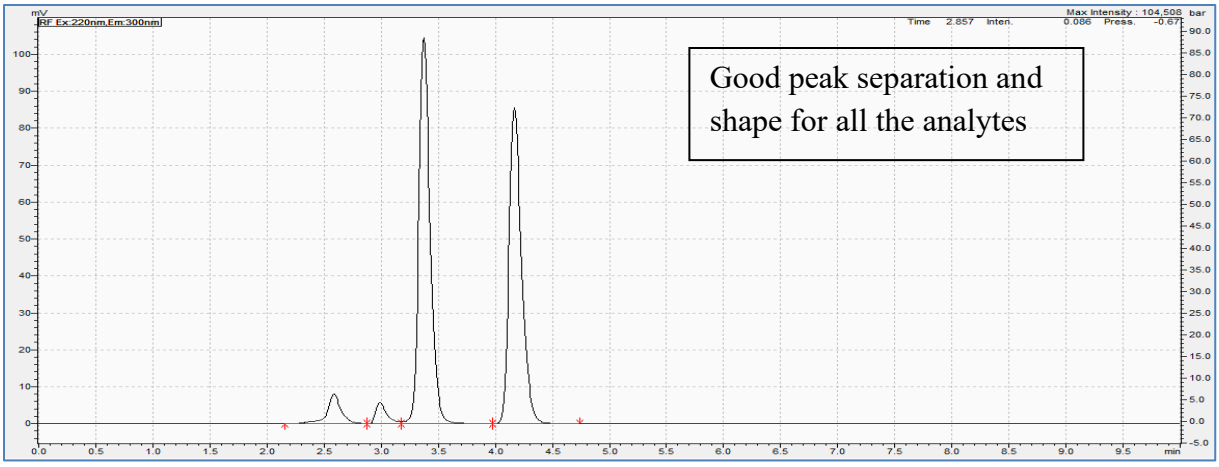

Figure 2.108 Flow rate optimization (in methanol) – the chromatogram of pC, pCS, pCG, and DMP mixture using 1 mL/min flow rate (optimized condition)

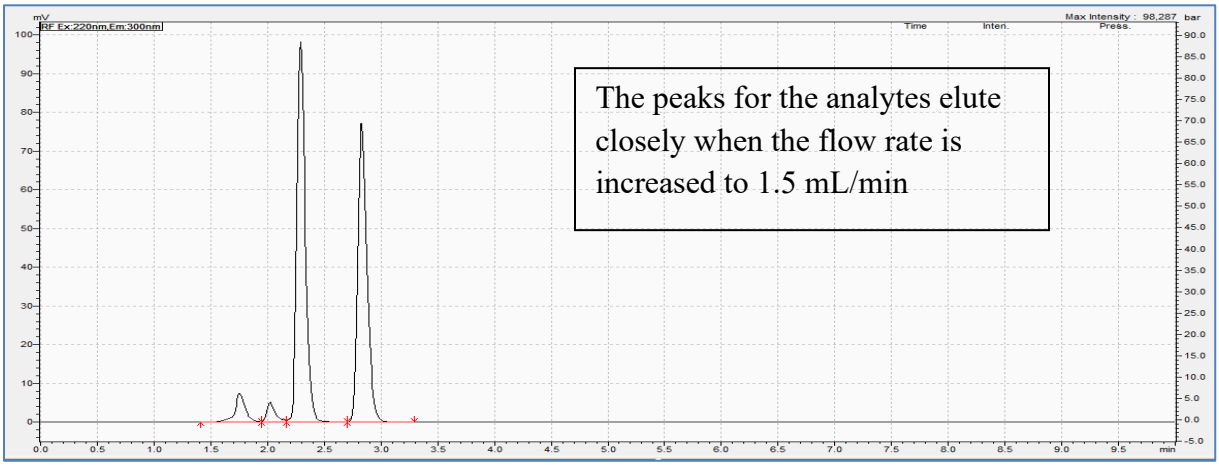

Figure 2.109 Flow rate optimization (in methanol) – the chromatogram of pC, pCS, pCG, and DMP mixture using 1.5 mL/min flow rate

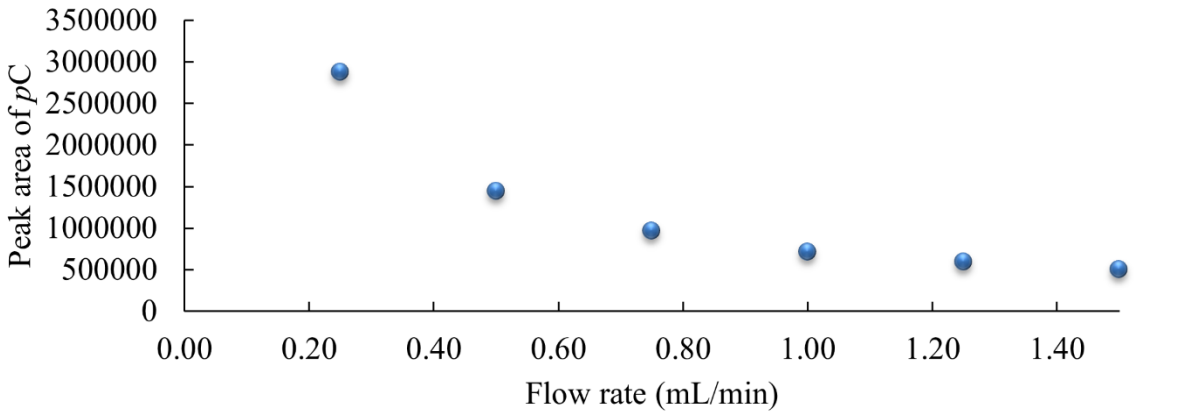

Figure 2.110 The correlation plot between flow rate using methanol and the absolute peak area of pC

2.5.2.10 *Flow rate optimization (in acetonitrile)*

The flow rate was optimized for *p*C, *p*CS, *p*CG, and DMP using methanol as the solvent to check the effects on chromatographic peak separation and to improve the sensitivity of the assay. As observed in Figure 2.111, when the analytes *p*C, *p*CS, *p*CG, and DMP are injected at a concentration of 10 µg/mL using 0.1% formic acid, 0.8 mM ammonium acetate, and a flow rate of 0.5 mL/min, the peak shape and separation for all the analytes appeared adequate (elution at *p*C – approximately 12.0 mins, *p*CS – approximately 5.9 mins, *p*CG – approximately 5.0 mins, DMP – approximately 20.0 mins). Similarly, at a flow rate of 0.25 mL/min (in Figure 2.112), the peak shapes of all the analytes were distorted. Figure 2.113 represents the relationships between flow rate (variable) and the absolute peak area counts of *p*C. The flow rate of 0.5 mL/min provides the highest peak area count with acceptable chromatography, but the area count decreases as the flow rate is increased. The *p*C sensitivity was observed to be decreased when

going from 0.25 mL/min to 1.5 mL/min. However, the lower flow rates were not selected for further optimization as the run times were too long for a single injection.

In summary, a flow rate of 0.5 mL/min was determined the optimal condition for the assay measuring *p*C, *p*CS, *p*CG, and DMP when using ACN in the mobile phase.

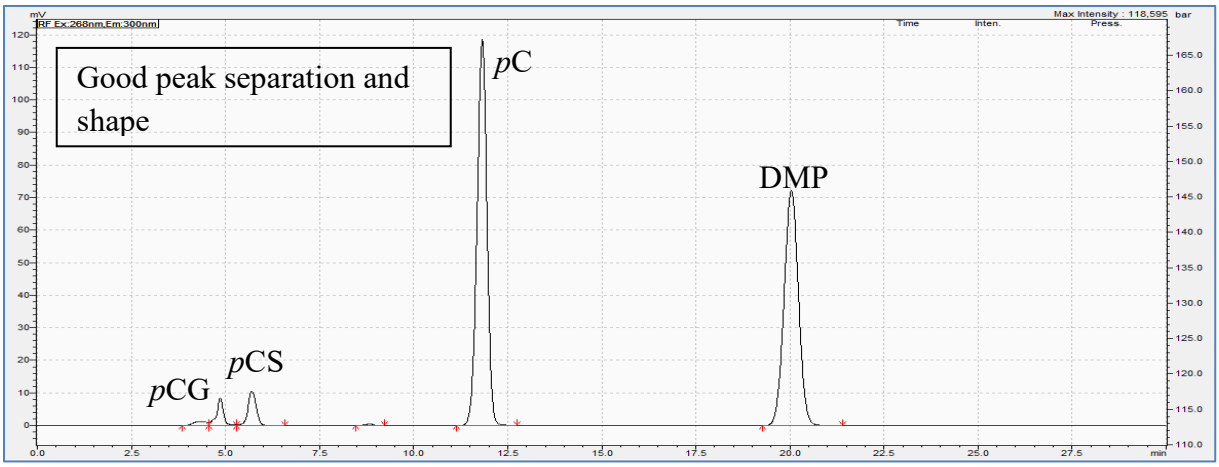

Figure 2.111 Flow rate optimization (in acetonitrile) - the chromatogram of pC, pCS, pCG, and DMP mixture using 0.5 mL/min flow rate (optimized condition)

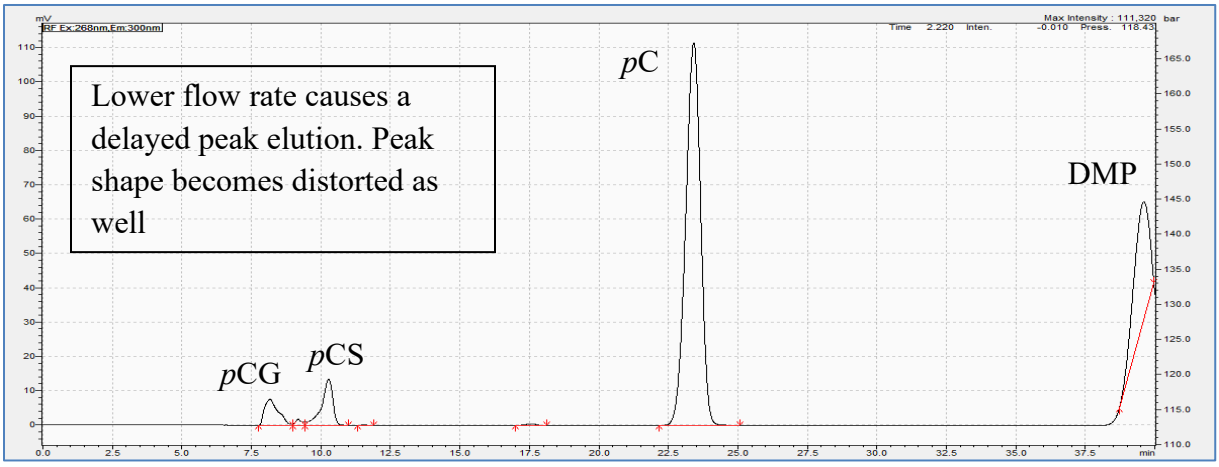

Figure 2.112 Flow rate optimization (in acetonitrile) - the chromatogram of pC, pCS, pCG, and DMP mixture using 0.25 mL/min flow rate

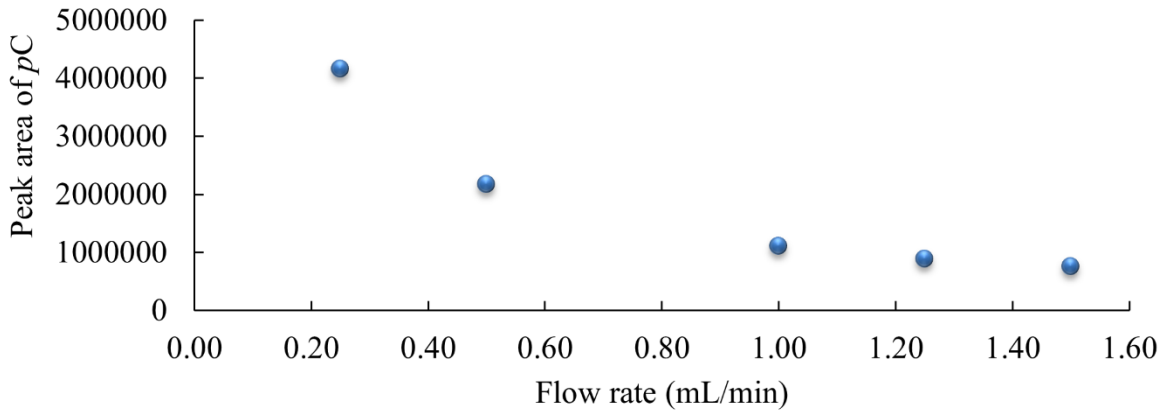

Figure 2.113 The correlation plot between flow rate using acetonitrile and the absolute peak area of pC

2.5.2.11 *Injection volume optimization (in methanol)*

This optimization was done using methanol at a concentration of 10 µg/mL. Figure 2.114 portrays the chromatography obtained after injecting a mixture of *p*C, *p*CS, *p*CG, and DMP at an injection volume of 10 µL using the previously optimized chromatographic parameters. With this condition, all of the peaks were separated well, the peak shapes were symmetrical, and there were no interferences observed between peaks. On the contrary, when the injection volume of the analyte mixture was increased to 30 µL (as seen in Figure 2.115), the peak shape became distorted and asymmetrical, all the analyte peaks exhibited fronting, and there were interferences between the peak for *p*CS and *p*CG. the peaks for *p*CS and *p*C were also overlapped at 30 µL injection volume. Figure 2.116 illustrates a positive linear relationship between the injection volume and the *p*C absolute peak areas; however, the peak shapes also become distorted with an increase in the injection volume.

In summary, 10 µL injection volume was found ideal to quantify *p*C, *p*CS, *p*CG, and DMP using methanol.

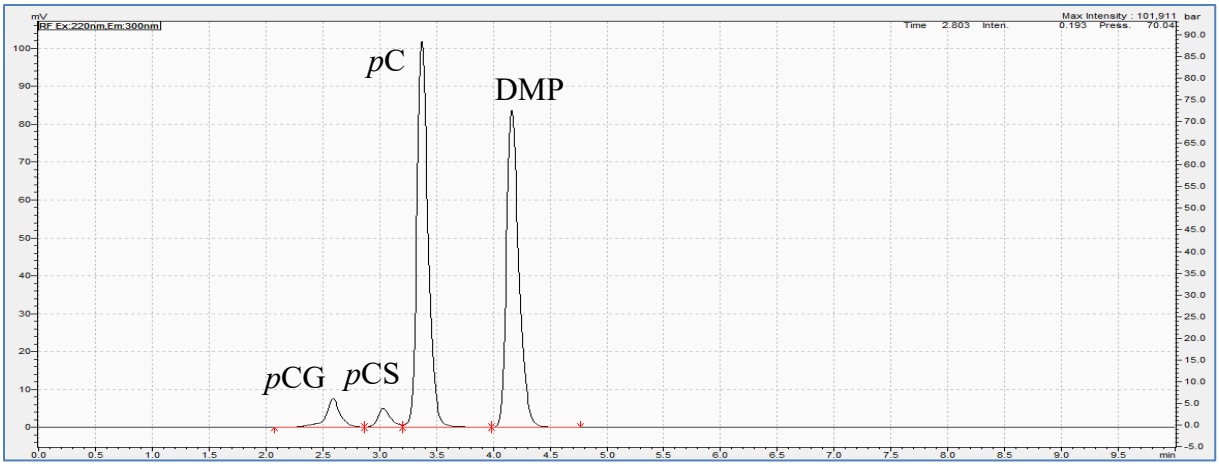

Figure 2.114 Injection volume optimization (in methanol) - the chromatogram of pC, pCS, pCG, and DMP mixture using 10 µL injection volume (optimized condition)

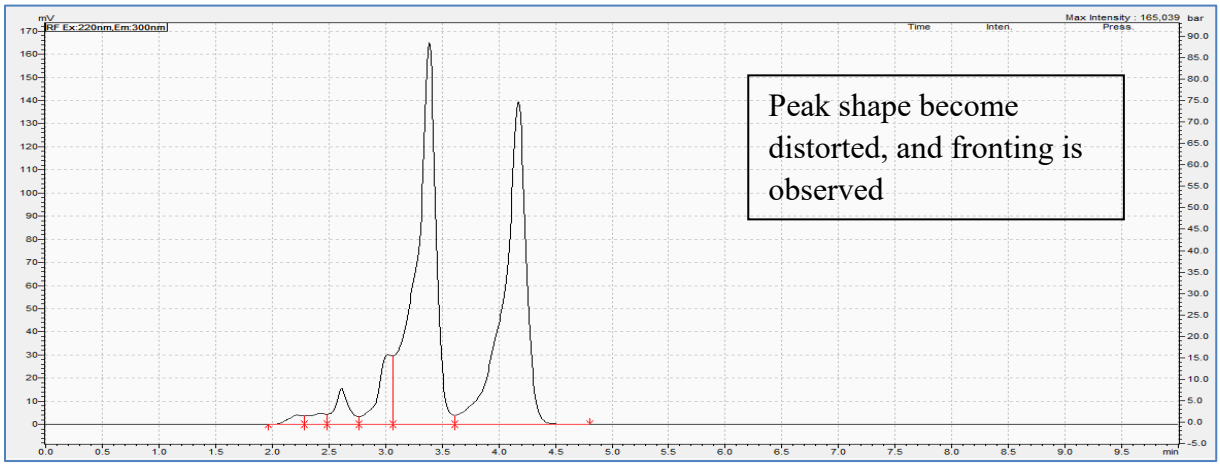

Figure 2.115 Injection volume optimization (in methanol) - the chromatogram of pC, pCS, pCG, and DMP mixture using 30 µL injection volume

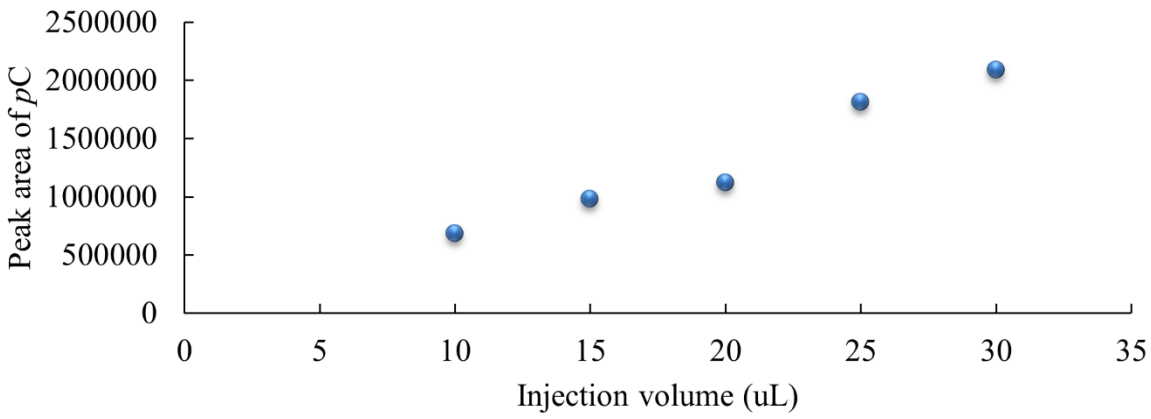

Figure 2.116 The correlation plot between injection volume using methanol and the absolute peak area of pC

2.5.2.12 *Injection volume optimization (in acetonitrile)*

This optimization was done using methanol at a concentration of 10 µg/mL. Figure 2.117 portrays the chromatography obtained after injecting a mixture of *p*C, *p*CS, *p*CG, and DMP at an injection volume of 10 µL using the previously optimized chromatographic parameters. With this condition, all of the peaks were separated well, the peak shapes were symmetrical, there was good separation from the solvent front, and there were no interferences observed between peaks. On the contrary, when the injection volume of the analyte mixture was increased to 30 µL (as seen in Figure 2.118), the peak shape became distorted and asymmetrical, all the analyte peaks exhibited fronting, and there were interferences between the peak for *p*CG and the solvent front, the peaks for *p*CS and *p*CG were also overlapped at 30 µL injection volume. Figure 2.119 illustrates a positive linear relationship between the injection volume and the *p*C absolute peak areas; however, the peak shapes also become distorted with an increase in the injection volume.

In summary, 10 µL injection volume was found ideal to quantify *p*C, *p*CS, *p*CG, and DMP using ACN.

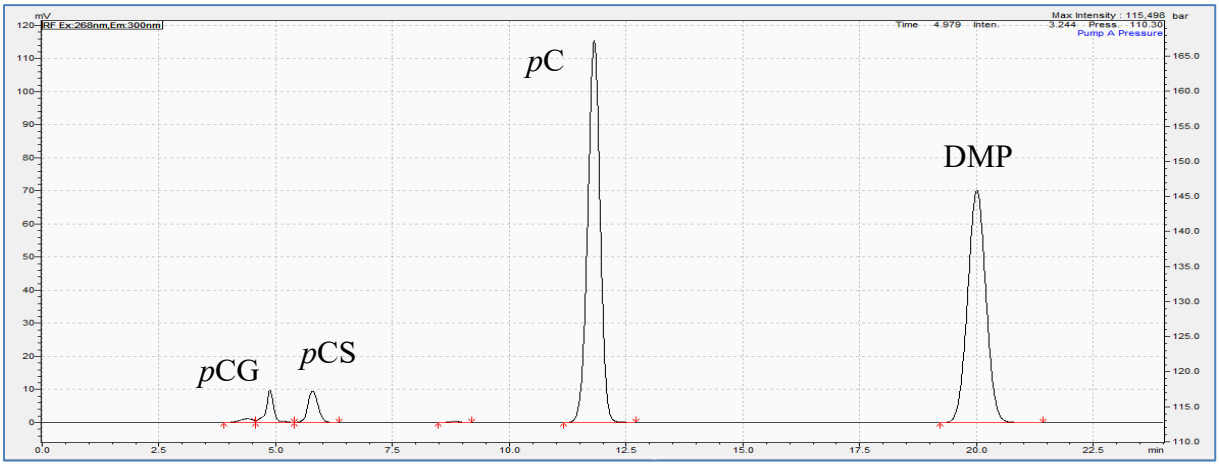

Figure 2.117 Injection volume optimization (in acetonitrile) – the chromatogram of pC, pCS, pCG, and DMP mixture using 10 µL injection volume (optimized condition)

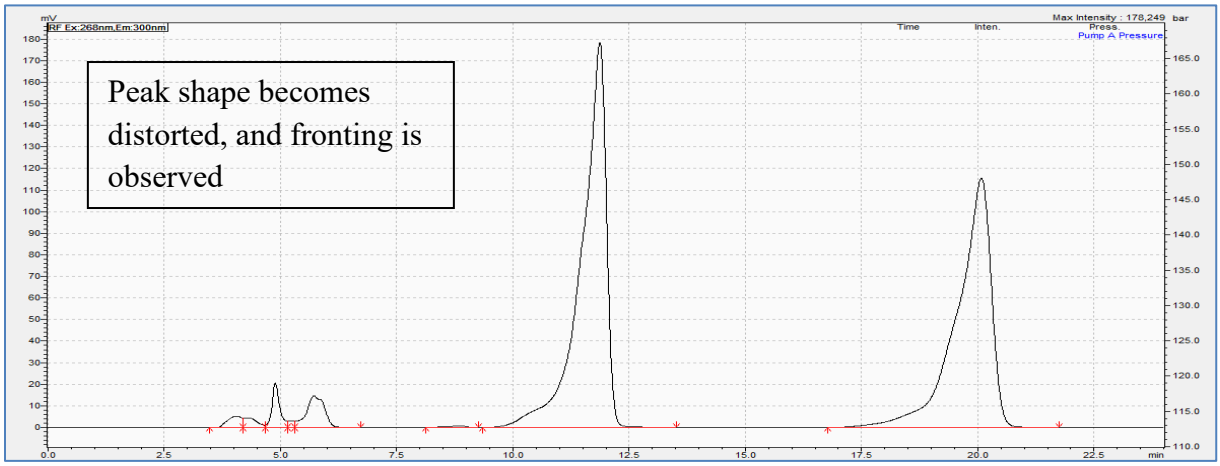

Figure 2.118 Injection volume optimization (in acetonitrile) – the chromatogram of pC, pCS, pCG, and DMP mixture using 30 µL injection volume

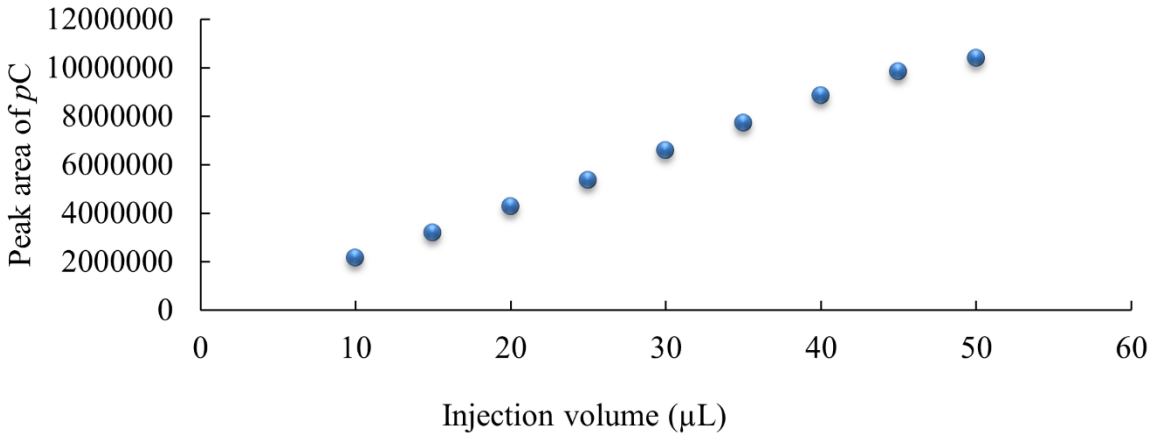

Figure 2.119 The correlation plot between injection volume using acetonitrile and the absolute peak area of pC

2.5.3 Summary for chromatography conditions

Based on the comparisons of *p*C absolute peak areas using optimized final conditions in acetonitrile and methanol at various injection volumes (Figure 2.120 and Figure 2.121), ACN is a better solvent in comparison to methanol for *p*C assay. The final optimized chromatography conditions are shown in Figure 2.122.

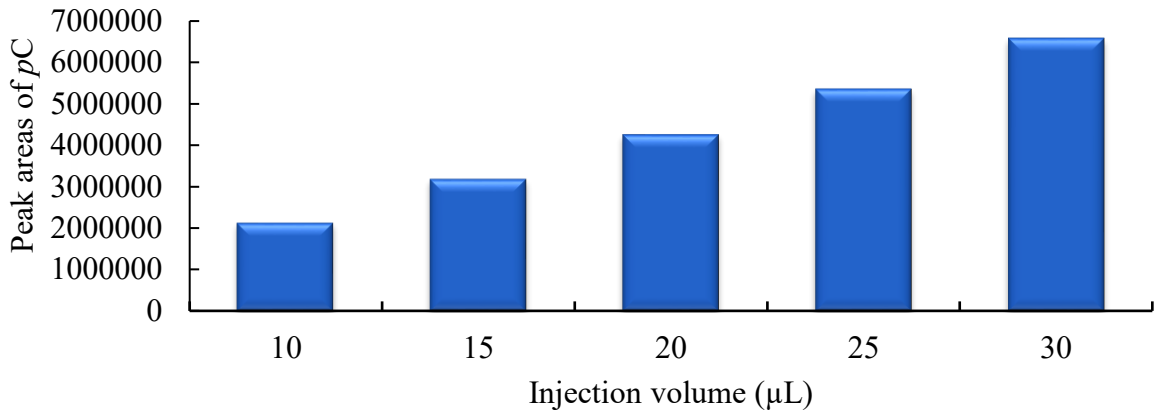

Figure 2.120 The comparisons of pC absolute peak areas using optimized final conditions in acetonitrile at various injection volumes

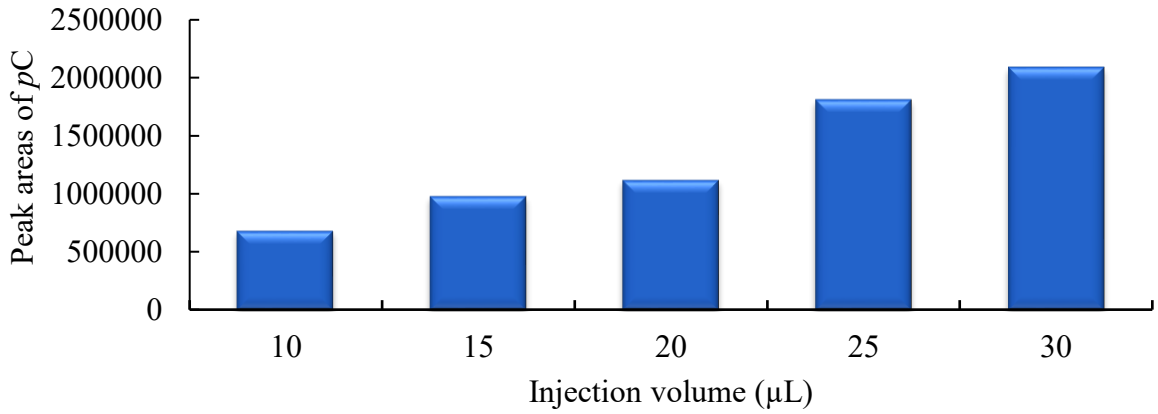

Figure 2.121 The comparisons of pC absolute peak areas using optimized final conditions in methanol at various injection volumes

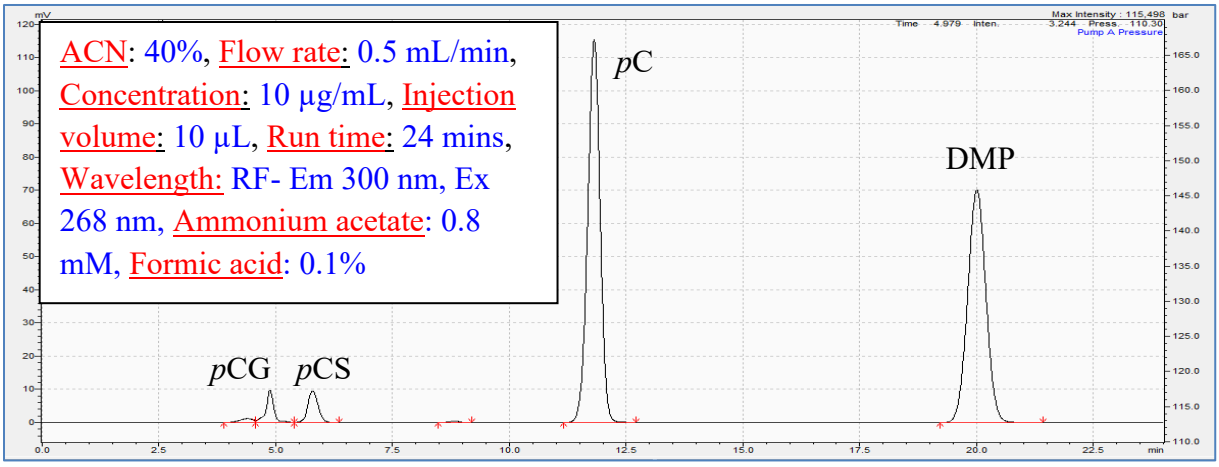

Figure 2.122 The final optimized chromatography conditions of pC, pCS, pCG, and DMP using acetonitrile

2.5.4 *p*-Cresol sample preparation optimization

2.5.4.1 *Determination of lower limit of quantification using pure solvent*

For the LLOQ measurement in the *p*C assay, a standard calibration set was prepared using *p*C, *p*CS, *p*CG, and DMP from 0.002 µg/mL to 250 µg/mL in methanol using the final optimized chromatographic conditions. The calibration curve of *p*C showed a good linearity and a high correlation coefficient value (r^2) of 0.9983. The peak for *p*C was still observable and quantifiable even at the lowest concentration in the chromatography. The LLOQ for *p*C, *p*CS, and *p*CG were found to be 0.112 µg/mL, 0.571 µg/mL, and 0.856 µg/mL, respectively. Figure 2.123 represents the standard curve that was obtained by plotting the *p*C absolute peak area vs. the concentrations in the calibration set (from the highest concentration to the LLOQ). Figure 2.124 represents the chromatogram at the LLOQ for *p*C (0.112 µg/mL) when the sample was

injected using the final optimized chromatographic conditions. There was no peak interference observed for any of the analytes or the solvent front.

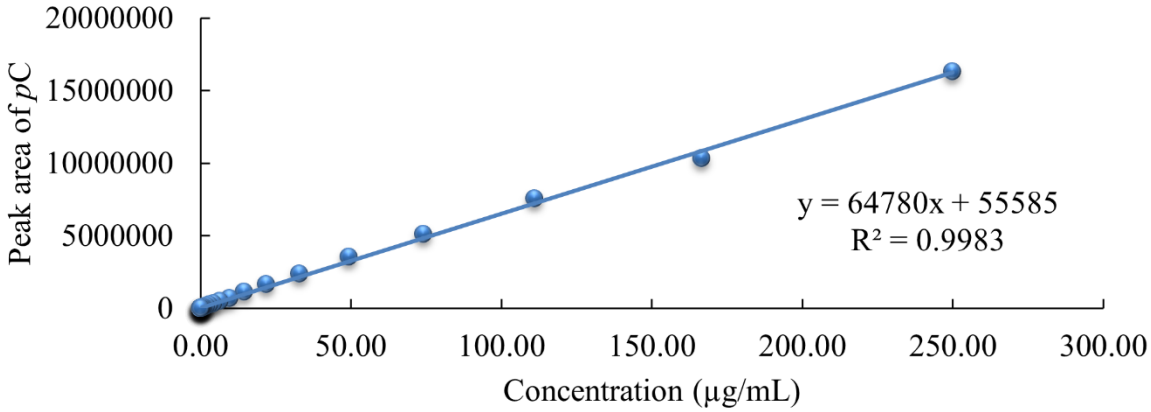

Figure 2.123 The calibration curve of pC using final optimized conditions in pure acetonitrile (calibration curve ranged from 0.002 to 250 µg/mL)

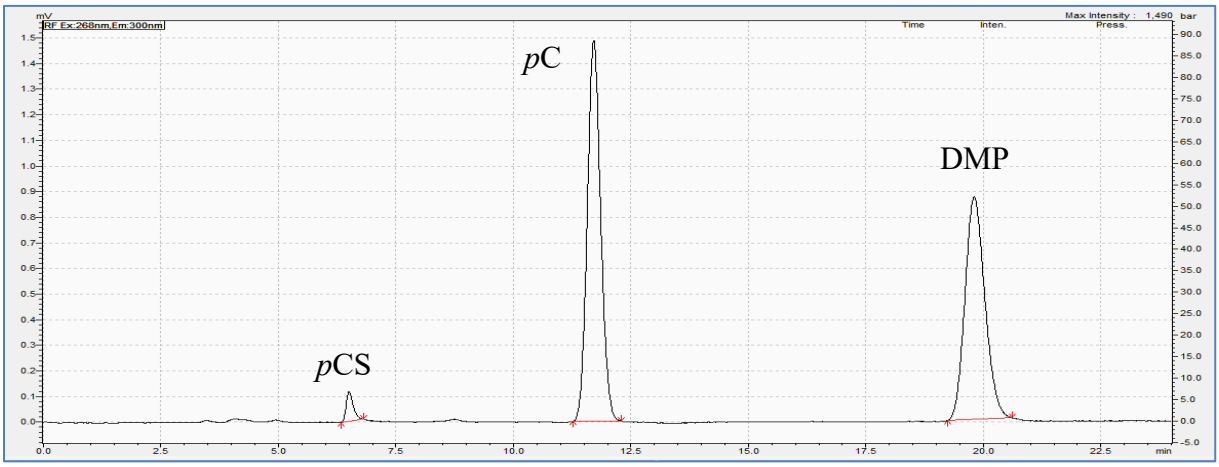

Figure 2.124 The chromatogram of pC at the lower limit of quantification 0.112 µg/mL in pure acetonitrile

2.5.4.2 *Standard calibration set in human plasma*

*p*C, *p*CS, *p*CG, and DMP (ranged from 0.002 µg/mL to 50 µg/mL) were prepared using human plasma as the matrix. Figure 2.125 represents the standard calibration curve of *p*C that was prepared in pooled human plasma and analyzed using the final optimized conditions in the UPLC. The curve was observed to be linear and the correlation coefficient for *p*C had a high value (r^2 = 0.9998 as seen in Figure 2.125). The peaks for *p*C and DMP elute at their respective elution times, hence plasma as a matrix does not affect the retention times. Figure 2.126 shows the chromatography from the injection of the two analytes at the highest concentration (i.e., 50 µg/mL) and the internal standard DMP (fixed at a concentration of 10 µg/mL).

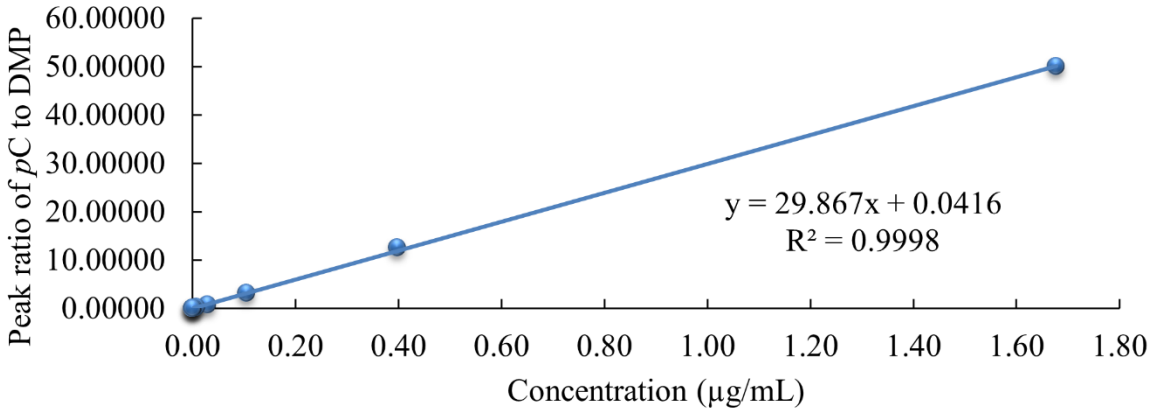

Figure 2.125 The calibration curve of pC using final optimized conditions in human plasma (calibration curve ranged from 0.002 to 50 µg/mL)

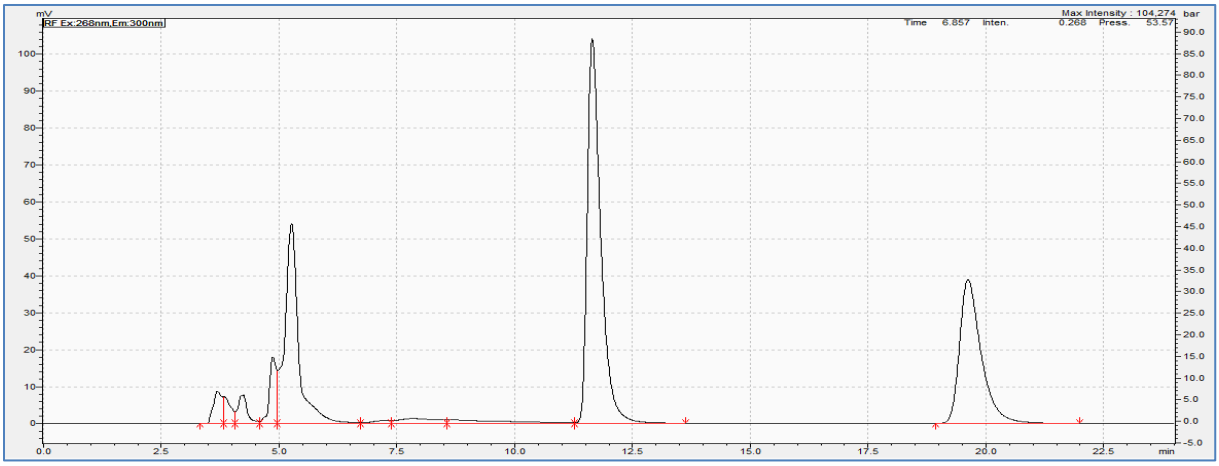

Figure 2.126 The chromatogram of pC at the highest concentration 50 µg/mL in human plasma

2.5.4.3 *Internal standard optimization for p-cresol assay*

For the optimization of the internal standard for the *p*C assay, a standard calibration set was prepared using DMP only (devoid of *p*C, *p*CS, or *p*CG) at varying concentrations ranging from 0.0025 µg/mL to 50 µg/mL in human plasma to determine the concentration of DMP that provided a robust instrument response without any peak area signal saturation on the UPLC. DMP peak areas were plotted against the various concentrations prepared as shown in Figure 2.127. The curve showed a good linearity with a high correlation coefficient value (r^2) of 0.9998. The final DMP concentration was selected to be 25 µg/mL.

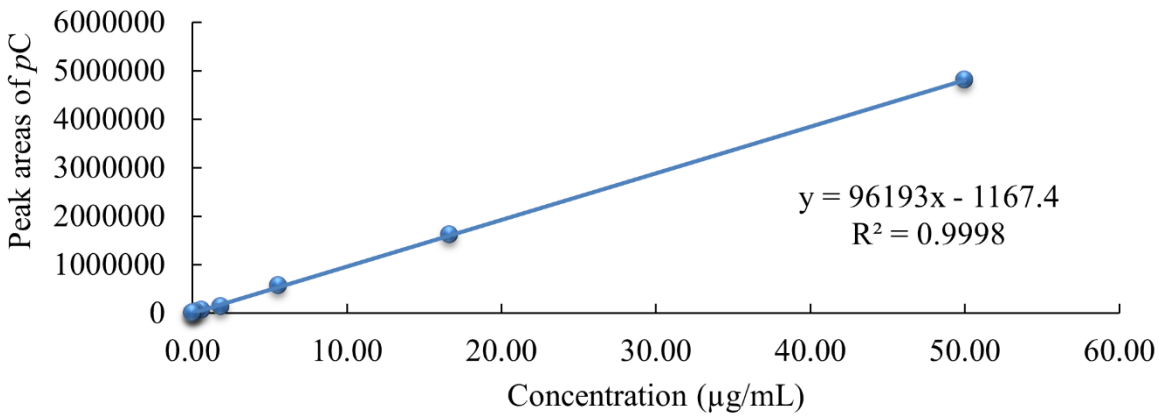

Figure 2.127 The calibration curve of DMP using final optimized conditions in human plasma (calibration curve ranged from 0.0025 to 50 µg/mL)

2.5.4.4 *Extraction solvent optimization*

This optimization was done by preparing a set of standards calibrators for *p*C, *p*CS, *p*CG, and DMP, where the organic solvent to the plasma/sample ratio was varied. Figure 2.128 represents the effect of changing the volume of plasma to organic solvent from 1:1 to 1:2 to 1:3 on the *p*C absolute area counts. The different colored bars represent different ratios tested at the calibration concentrations (blue bar represents the 1:1 plasma to organic solvent ratio, the red bar represents 1:2 plasma to organic solvent ratio and the green bar represents 1:3 plasma to organic solvent ratio). As observed, the ratio 1:2 at the highest concentration (50 µg/mL) showed the highest peak area count for *p*C as compared to 1:1 or 1:3 plasma to solvent ratio.

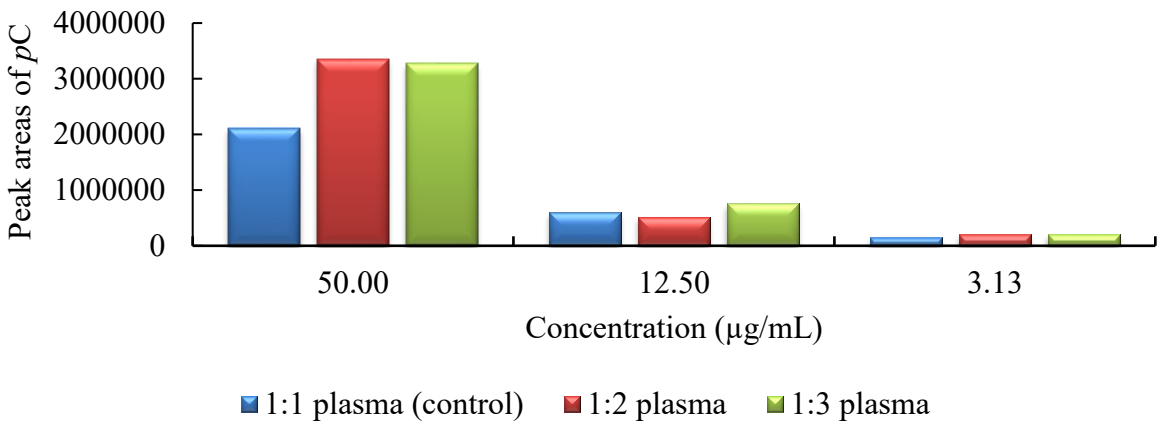

Figure 2.128 Comparisons of pC absolute peak areas using different organic extraction solution volume at various pC concentrations

2.5.4.5 *Centrifuge parameter optimization*

2.5.4.5.1 Centrifuge speed optimization

Centrifugation is one of the essential steps in the sample processing as it helps with the removal of the proteins from the biological matrix (plasma or DBS). The centrifuge speed was optimized from 4000 g to 20000 g (i.e., 4000, 8000, 12000, 16000, 20000 g) with the time of centrifugation fixed at 10 minutes. However, none of the parameters tested helped the separation of *p*CS and *p*CG. The highest centrifugation speed (20000 g) led to a more stable debris/sediment upon centrifugation but did not separate *p*CS and *p*CG. Figure 2.129 summarizes the various speeds tested to achieve the separation between *p*CS and *p*CG.

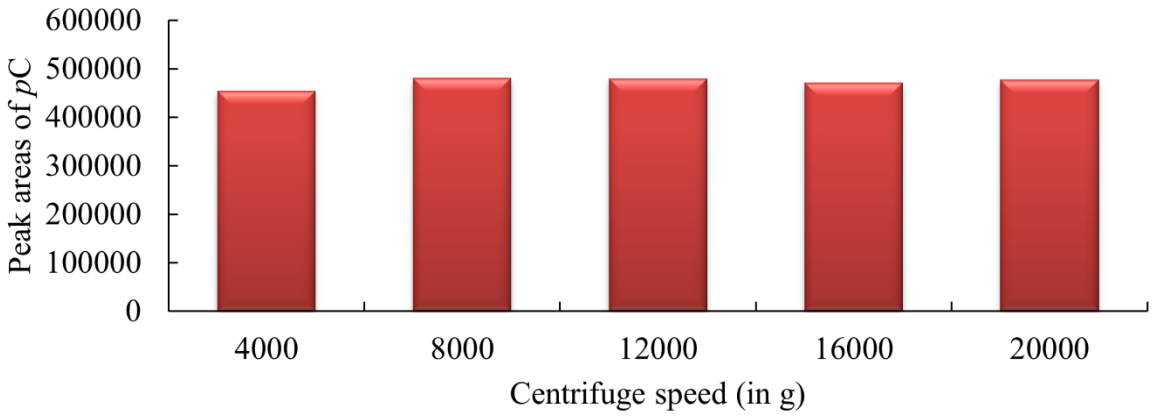

Figure 2.129 The effects of changing the centrifuge speed on the pC absolute area counts

2.5.4.5.2 Centrifuge time optimization

Similar to the centrifuge speed, the time required for sample centrifugation was also optimized. The mixture of *p*C, *p*CS, *p*CG, and DMP was prepared at a concentration of 10 µg/mL and was tested in the centrifuge at 4000 g (fixed centrifuge speed) for 10 mins, 15 mins and 20 mins. The various centrifuge times tested were plotted against the absolute peak areas of *p*C (as seen in Figure 2.130). However, longer centrifuge time(s) did not help with the peak separation of *p*CS and *p*CG.

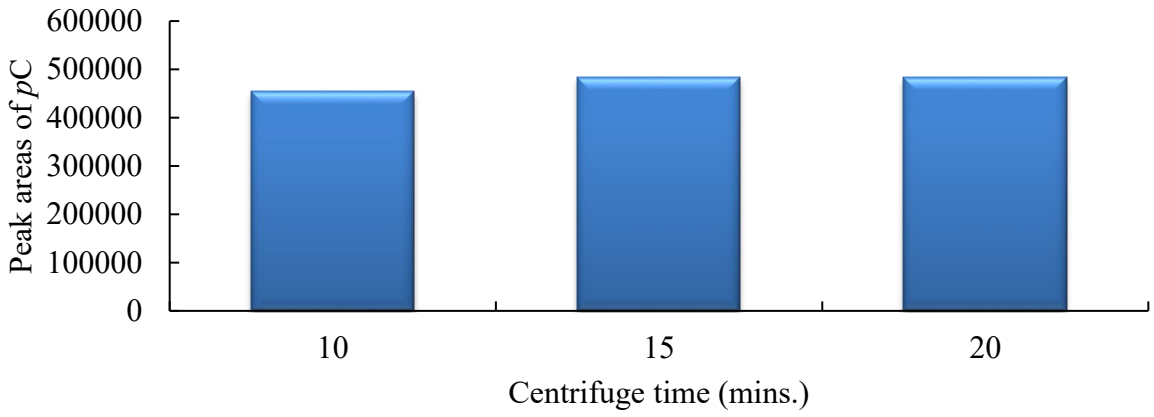

Figure 2.130 The effect of changing the centrifuge time on the pC absolute area counts

2.5.4.6 *Drying and concentrating optimization*

To increase the sensitivity of the *p*C assay, the samples were subjected to drying in the *SpeedVac* instrument. A standard set of calibrators was prepared for *p*C, *p*CS, *p*CG, and DMP from 0.0002 µg/mL to 50 µg/mL. The concentration of DMP was kept fixed at 25 µg/mL and the sample preparation was done using human plasma as the matrix. The samples were concentrated using *SpeedVac* to increase the sensitivity of this assay. With drying of the samples, the peaks for *p*CS and *p*CG showed higher peak areas as compared to the samples that were not dried as shown in Figure 2.131 (plots of *p*C peak areas vs. concentrations tested). However, drying the samples did not improve the separations between *p*CS and *p*CG. The peak area counts of *p*C are significantly improved after the sample was dried in the *SpeedVac*. The final drying time using *SpeedVac* for the sample containing *p*C, *p*CS, *p*CG, and DMP was chosen to be 2 mins.

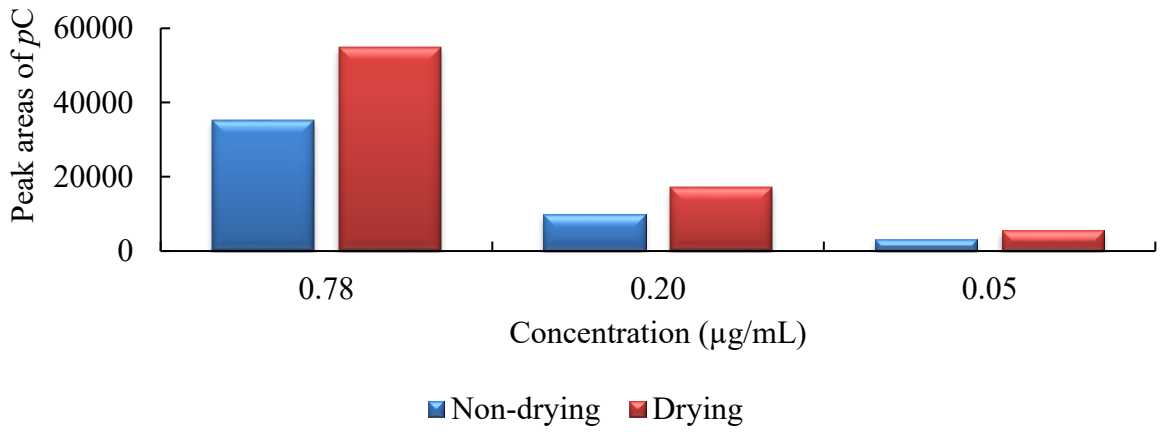

Figure 2.131 Comparisons of absolute pC peak areas in samples with and without drying

The injection volume used in the *p*C assay was also optimized. This parameter was varied from 10 µL to 30 µL (i.e., 10, 20, 30 µL) using a mixture of *p*C, *p*CS, *p*CG, and DMP at 5 different concentrations while DMP was fixed at 25 µg/mL. Figure 2.132 represents the bar graph that shows the effect of changing the injection volume(s) on the *p*C absolute peak area counts. The different colored bars represent different injection volumes tested at various concentrations. The effect of increasing the injection volumes also help in increasing the sensitivity.

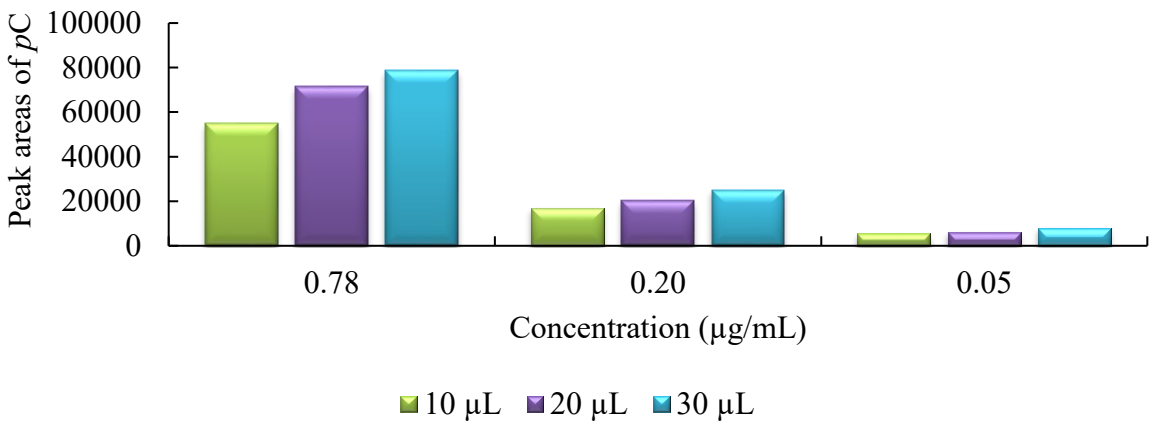

Figure 2.132 Comparisons of absolute pC peak areas in samples with various injection volume

2.5.4.7 *De-conjugation testing and parameter optimization*

2.5.4.7.1 Heat and acid optimization

After the final assay conditions for *p*C were determined, the parameters associated with the de-conjugation of *p*C were further tested and optimized. In this optimization, *p*C, and a mixture of *p*CS and *p*CG were prepared at a concentration of 50 µg/mL in human plasma with DMP fixed at 25 µg/mL. The mixture was de-conjugated using various combinations of heat and acid conditions. First, the heat given to the samples for de-conjugation was optimized from 15 minutes to 60 minutes (i.e., 15, 30, 45 and 60 minutes) while the HCl acid concentration was kept fixed at 6M. This de-conjugation heat time optimization was followed by the acid optimization from 3M to 12M (i.e., 3, 6, 9 and 12M) where the heat time was kept fixed at 15 minutes. A prolonged heat time and acid concentration led to a higher sample degradation. These conditions were labelled under various test groups (as shown in Figure 2.133) where different combinations of heat and acid were tested. The final conditions for the de-conjugation were

chosen to be a heating time of 15 mins and the HCl concentration of 6M since it provided the ideal peak shape, with minimal sample degradation and hence acceptable sensitivity for *p*C and DMP.

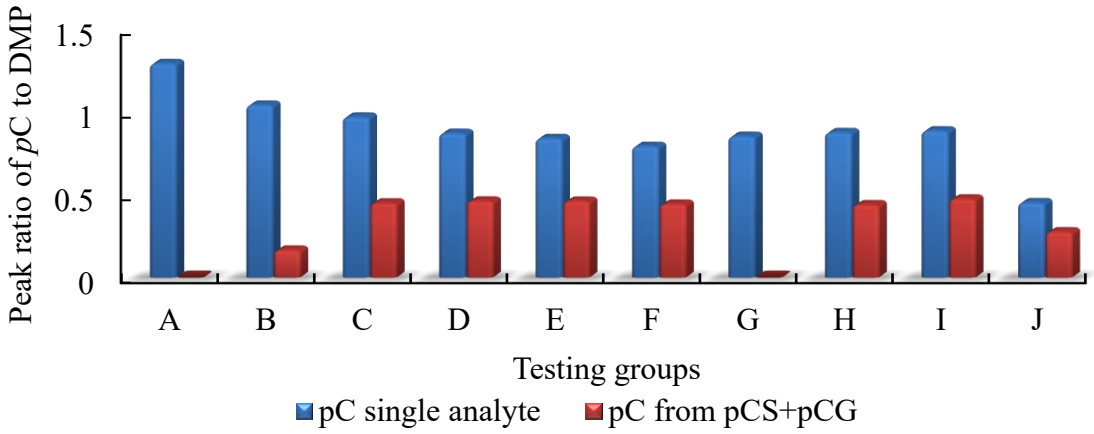

Figure 2.133 Comparison of various de-conjugation conditions on the pC peak ratios

A	No acid, No heat time (extraction only)
B	6M acid, No heat time
C	6M acid, 15 min. heat time
D	6M acid, 30 min. heat time
E	6M acid, 45 min. heat time
F	6M acid, 60 min. heat time
G	30 min. heat, No acid
H	30 min. heat, 3M acid
I	30 min. heat, 9M acid
J	30 min. heat, 12M acid

2.5.4.7.2 De-conjugation ratio testing

To estimate the fraction of *p*CS (as *p*CS is the major metabolites of *p*C) that has been converted to *p*C, de-conjugation ratio for this assay was calculated. This was done by preparing the working solutions of *p*CS (3 µg/mL and 10 µg/mL) using human plasma and a standard calibration set with *p*C only. These samples were then processed the same way as the *p*C sample preparation protocol (heat and acid, extraction, centrifugation and drying). The average *p*CS de-conjugation ratio was determined to be 79.79% at 3 µg/mL and 61.19% at 10 µg/mL (Table 2.11).

Table 2.11 The average de-conjugation ratio for the pC assay

Concentration (µg/mL)	**De-conjugation ratio**
10.00	61.19%
3.00	79.79%

2.5.5 Validation approach

2.5.5.1 *p-Cresol assay validation accuracy and precision data*

The *p*C assay was validated to determine accuracy and precision. The QC samples showed acceptable accuracy & precision data for *p*C since the A & P were within ±15% of the nominal concentration. Table 2.12 summarizes the accuracy and precision data for the quantification of *p*C.

Table 2.12 Accuracy and precision of pC in human plasma

	Nominal concentration, µg/mL	Intra-day (1)		Intra-day (2)		Intra-day (3)	
*p*C		Accuracy (%)	Precision (%)	Accuracy (%)	Precision (%)	Accuracy (%)	Precision (%)
	25	0.28%	4.87%	-1.71%	8.04%	-8.73%	4.88%
	12.5	3.34%	6.31%	1.98%	7.76%	-6.84%	4.24%
	3.00	-0.66%	6.33%	0.52%	13.29%	-0.59%	5.56%
	1.00	-10.90%	3.58%	-6.62%	13.40%	-12.16%	7.42%

2.5.5.2 *p-Cresol assay validation stability data*

The assay measuring *p*C passed the criteria for validation at various storage conditions (as the accuracy and precision were within ±15% of the nominal concentration). Hence, the assay that was developed to quantify *p*C with DMP as the internal standard was successfully validated using pooled human plasma (with the accuracy and precision within ±15% of the nominal concentration).

Table 2.13 The stability data of pC under various storage conditions in human plasma

	***p*C**	
	High QC	Low QC
Nominal concentration, µg/mL	25.00	3.00
Autosampler stability (%)	-2.83%	0.69%
Bench-top stability (%)	7.80%	5.05%
Freeze-thaw stability (%)	5.17%	1.62%
Long-term stability (%)	0.42%	-2.51%

2.5.5.3 *p-Cresol assay extraction efficiency data (in plasma)*

In this assay, there were two groups to be tested i.e., control group and the experimental group. The control group was in 3 replicates at 4 levels of QC concentrations that were prepared as part of the normal sample processing. It was observed that the *p*C in the samples with extraction showed a recovery of 44.31%, 33.12%, 28.16%, and 27.28% at concentrations of 1 µg/mL (LLOQ), 3 µg/mL (low QC), 12.5 µg/mL (mid QC), and 25 µg/mL (high QC),

respectively. Similarly, the internal standard, DMP, in the samples with extraction showed a recovery of 21.20%, 20.93%, 20.95%, and 21.44% at concentrations of 1 µg/mL, 3 µg/mL, 12.5 µg/mL, and 25 µg/mL, respectively. Table 2.14 summarizes the extraction efficiency data for the quantification of *p*C and DMP in pooled human plasma.

Table 2.14 The recovery/extraction efficiency data for the quantification of pC and DMP in human plasma

Recovery		
Concentration (µg/mL)	***p*C**	**DMP**
25.00 *(High QC)*	27.28%	21.44%
12.50 *(Mid QC)*	28.16%	20.95%
3.00 *(Low QC)*	33.12%	20.93%
1.00 *(LLOQ)*	44.31%	21.20%

2.5.6 Dried blood spot approach

In this study, the applicability of DBS in the assays (measuring the drugs in plasma) have been tested and later optimized to obtain the most favorable assay conditions in DBS. This was done to make a comparison in the assay protocols between the two matrices (plasma and DBS).

2.5.6.1 *p-Cresol assay calibration set in dried blood spots*

Once the spot volume was determined, the next DBS optimization was the preparation of a standard calibration set with *p*C and DMP using the same concentrations as in the plasma. *p*C calibration set was prepared from 0.7276 µg/mL to 31.25 µg/mL using human whole blood (WB) that was spotted onto the Whatman 903® protein saver cards. DMP was fixed at a concentration of 25 µg/mL. Figure 2.134 represents the standard calibration curve of *p*C that was prepared in human whole blood, spotted onto the DBS cards, and analyzed using the final optimized conditions in the UPLC. The curve was observed to be linear and the correlation coefficient for *p*C was high ($r^2 = 0.9692$ as seen in Figure 2.134).

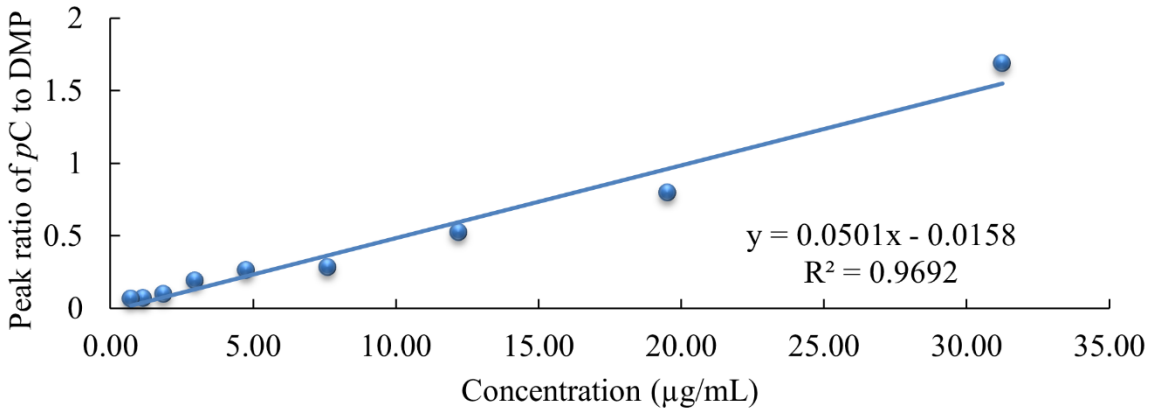

Figure 2.134 The calibration curve of pC using dried blood spots (ranged from 0.73 to 31.25 µg/mL

2.5.6.2 *Effects of adding internal standards before vs. after sample extraction*

To optimize the final conditions for the calibration curve with *p*C, the internal standard (i.e., DMP) was tested to be added at different stages of the sample preparation process. This was done by adding DMP before and after the spotting of blood onto the DBS card. As seen in Figure 2.135, the peak areas were much higher when the internal standard was added after the blood spotting on DBS. In addition, the chromatographic peak for DMP was also observed to be better in shape and symmetry when the analyte was added to the sample after (Figure 2.137) than before spotting (Figure 2.136). However, in contrast to the MPA DBS assay, we did not observe a difference in linearity for the pC calibration curve in either approach of DMP addition - Figure 2.138 (DMP added before DBS preparation) vs. Figure 2.139 (DMP added after DBS preparation).

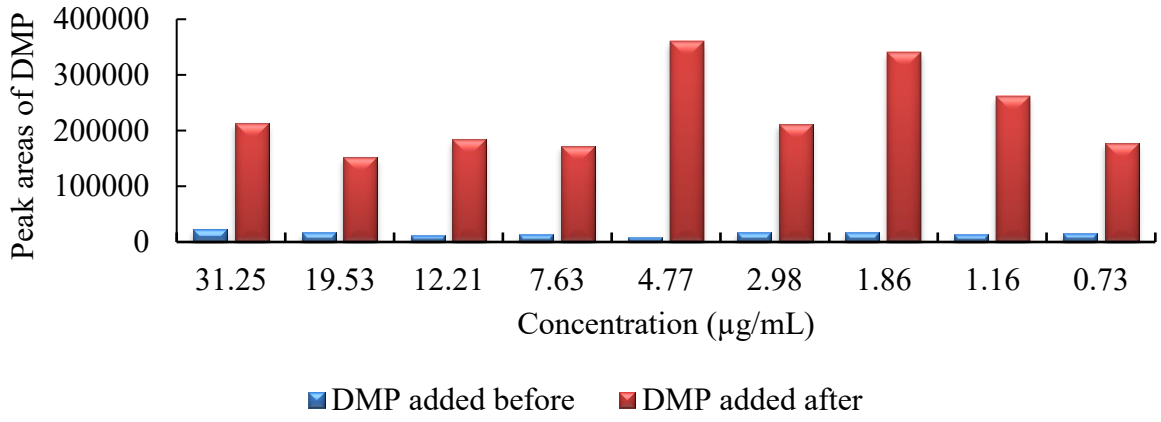

Figure 2.135 The comparisons of absolute DMP peak areas when it is added before the sample extraction and after

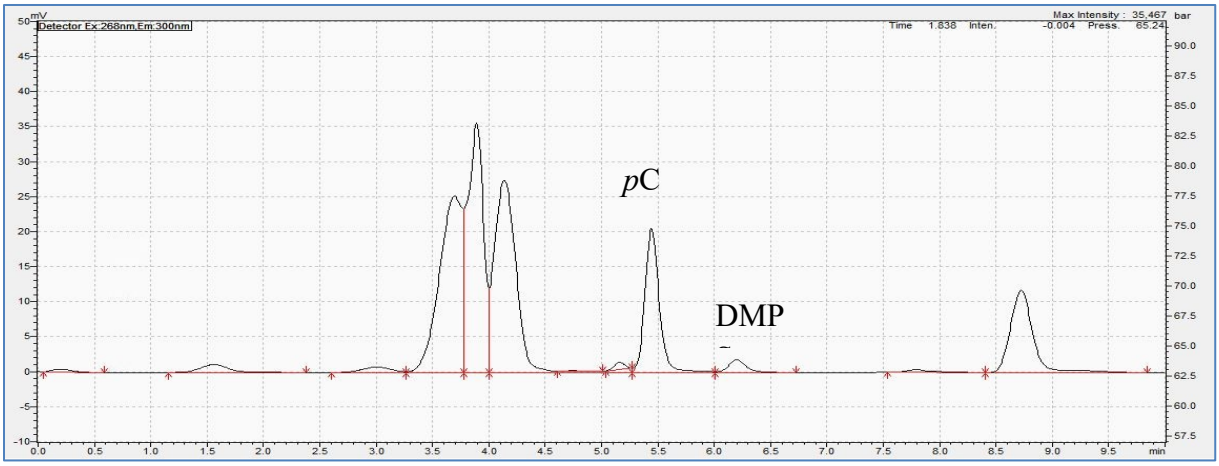

Figure 2.136 The chromatogram of a sample mixture of pC and DMP where DMP is added before the sample extraction

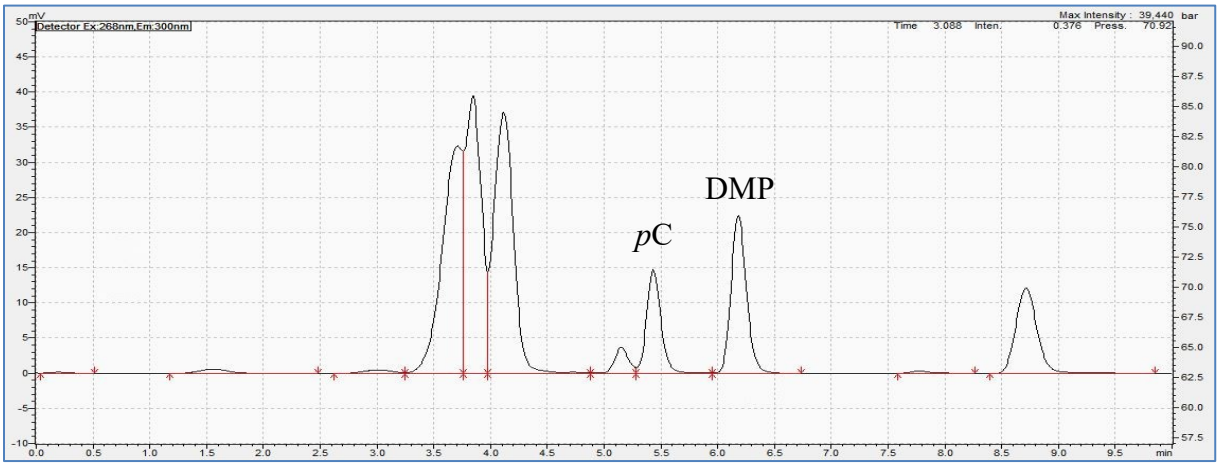

Figure 2.137 The chromatogram of a sample mixture of pC and DMP where DMP is added after the sample extraction

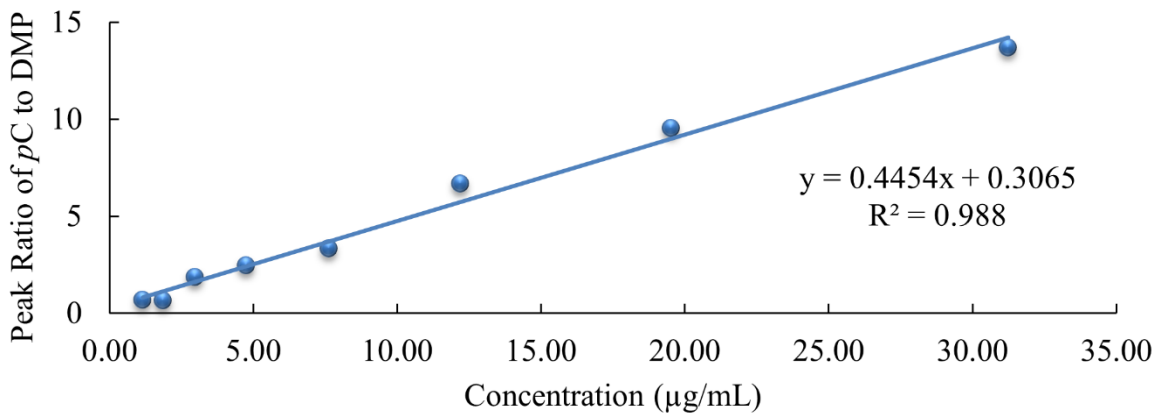

Figure 2.138 The calibration curve of pC where DMP is added before the DBS processing

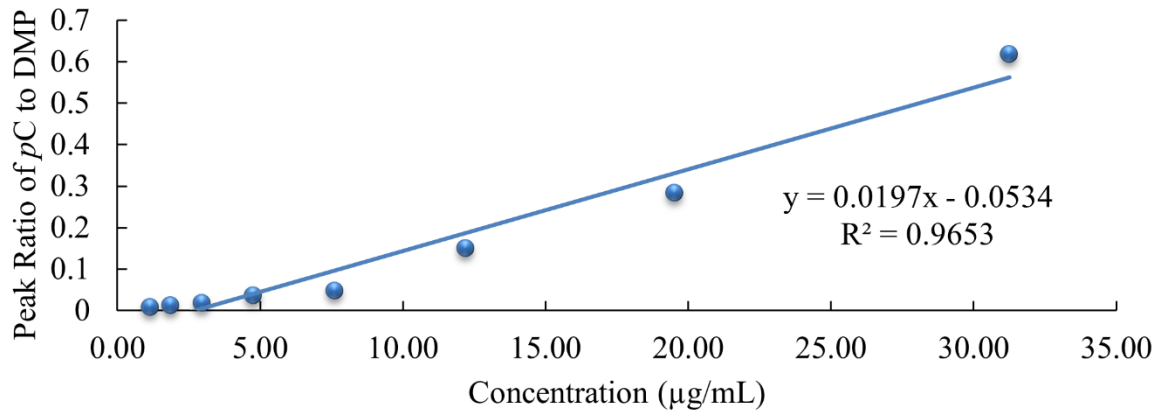

Figure 2.139 The calibration curve of pC where DMP is added after the DBS processing

2.5.6.3 *Extraction efficiency of p-cresol in dried blood spots*

Table 2.15 summarizes extraction efficiency of pC and DMP under two experimental conditions (where DMP was added either before or after the spotting of the DBS card).

Table 2.15 The recovery/extraction efficiency data for the quantification of pC and DMP conducted in DBS

	Recovery			
	DMP added before spotting		DMP added after spotting	
Concentration (µg/mL)	*p*C	DMP	*p*C	DMP
31.25	3.12%	8.32%	2.519%	92.17%
19.53	2.08%	5.70%	1.393%	58.34%
12.21	2.05%	5.11%	1.753%	84.10%
7.63	2.21%	5.38%	1.337%	62.84%
4.77	1.45%	2.50%	2.161%	95.55%
2.98	4.36%	6.77%	3.322%	103.07%
1.86	4.21%	5.31%	4.051%	93.41%
1.16	6.82%	5.47%	6.473%	114.01%
0.73	7.74%	4.25%	5.764%	59.30%

Chapter 3

Discussions

Kidneys are one of the most transplanted organs in patients with severe renal failure. When an organ is transplanted from a donor, the host's immune system can attack the organ, and immunosuppressants such as mycophenolic acid are utilized to prevent graft rejection. MPA is a commonly prescribed immunosuppressant in kidney transplant recipients (KTR). MPA works by selectively inhibiting the formation of the enzyme inosine monophosphate dehydrogenase (IMPDH), thereby causing a reduction in the proliferation of T- and B-lymphocytes. However, MPA usage can lead to a higher risk of infections since there is an overall decrease in the lymphocyte count. Furthermore, in KTR patients, the renal system may still be compromised which may lead to accumulation of drugs and/or toxic metabolites. *p*-Cresol (*p*C) is one of the phenol-based protein bound uremic toxins (PBUTs) that can get accumulated in the body due to either a reduced elimination (because of impaired renal function, such as in KTR patients) or increased generation (the major source of *p*-cresol is from the diet). MPA is primarily metabolized in humans via UGT1A9-mediated glucuronidation, and *p*C is known to be a potent inhibitor of this enzyme. This interaction between MPA and *p*-cresol is of clinical significance as first reported by our laboratory [47, 61, 62].

The overall hypothesis of this thesis was that it is feasible to conduct therapeutic drug monitoring of MPA and *p*C using highly sensitive and high throughput UPLC analytical assays in plasma and DBS. The objective of this thesis was to develop sensitive analytical assays for the quantification of MPA and *p*C and validating them in accordance with the U.S. Food and Drug

Administration (FDA) guidelines using human plasma and DBS. Initially, a literature review was conducted, and it was found that DBS was the most promising approach for the therapeutic drug monitoring (TDM) of MPA other than the conventional plasma matrix (please see **Chapter 1**). In **Chapter 2** of this thesis, the data on the development and validation of two high-throughput ultra-high performance liquid chromatography (UPLC) assays for the detection of MPA and *p*C (and associated metabolites) were presented. Our systematic assay development process included the optimizations of i) the method of detection, ii) chromatography (solvent concentration, additive concentration, flow rate, injection volume…etc.,), iii) sample preparation (i.e., determination of LLOQ and calibration ranges in human plasma, optimizing solvent volumes, and finding the ideal sequencing of adding the internal standards), and iv) assay validation in accordance with the FDA guidance. This was followed by a proof-of-concept study on measuring MPA and *p*C using dried blood spots (DBS).

3.1 Development of the UPLC-UV assay quantifying MPA:

3.1.1 Method of detection

The analytical assay measuring MPA was initially optimized to obtain the ideal wavelength that can be used in the UPLC to measure the analytes (MPA, MPAG and MPAC) with robust sensitivity. This was done by analyzing a mixture of analytes in the UV-visible spectrophotometer and RF-Spectro fluorophotometer, where different variables such as the type of solvent, solvent concentrations, and the effects of pH were characterized. The ideal absorbance range was between 0.2 to 0.8 (absolute units) representing relative intensity, as the range of the wavelength of the UV-spectrophotometer was fixed between 200 nm to 800 nm. In

the literature [95-97], various studies have employed UV as the method of detection for MPA; however, others [98-100] have also utilized fluorescence detection. These data indicated that both UV and fluorescence are both acceptable for the current set of analytes (i.e., MPA, MPAG and MPAC).

The initial parameter tested was the solvent composition (i.e., methanol, acetonitrile, and water) at various pH conditions (i.e., pH 3, pH 4 and pH 7). These pH values were selected to correspond to the likely pH ranges to be utilized in the mobile phases on our UPLC instrument. When MPA was injected into the UV spectrophotometer using pure methanol, the absorbance intensity recorded ranged between 0.43-0.47 at pH 3, pH 4 and pH 7 and the corresponding optimum wavelength was found to be ~304.79 nm. When MPA was tested using a combination of 30% methanol and 70% water, the absorbance recorded was between 0.71-0.90 at pH 3, pH 4 and pH 7 and the corresponding optimum wavelength was found to be ranging from 249-250 nm. The wavelengths that have been used in the literature to detect MPA using UV absorbance were reported at 250 nm [96], 215 nm [101], 214 [95] and 250 nm [69], which were consistent with our findings under our optimized conditions. Our data also indicated that the use of pure methanol or a combination of methanol and water (i.e., the final conditions for chromatographic separation) was acceptable since different conditions with varying methanol and water have yielded comparable wavelengths that correlated with the historical wavelengths used for MPA detection. Similarly, MPA was also prepared using pure acetonitrile, where the absorbance was recorded from 0.50 to 0.51 at pH 3 and pH 7, and the corresponding wavelength was found to be ranging from 304.30 to 304.62 nm. Moreover, the absorbance varied from 0.48 to 0.47 at pH 3 and pH 7 in pure water, and the corresponding wavelength was found to be ranging from 304.58 to 304.70 nm. Our data are consistent with that of *Sugioka et al.* [102] who reported using the

wavelengths 215 nm and 304 nm for the UV detection of MPA using acetonitrile-based phosphate buffer and *Wiwattanawongsa et al.* [103] who reported the use of methanol-based mobile phase for the detection of MPA and MPAG at 250 nm. The similarities observed in the absorbance wavelengths for MPA when using methanol, acetonitrile and water was further indication that either of these solvents could be used for detecting MPA and its metabolites. Additionally, it was apparent that changing the pH (from pH 3-7) did not drastically affect either absorbance or the wavelength of the tested analytes, and this could possibly be explained by the fact that MPA (and related analytes) are generally not extensively deprotonated (pKa of 5.6) [83] at the pH values that were tested in this thesis. In *Shen et al.* [98], MPA was tested and analyzed at pH of 9.2, where the optimal method of detection was determined to be fluorescence possibly because the phenolic portion of MPA undergoes deprotonation in this relatively more basic environment, making it more sensitive for this detection method [98]. This might also explain why the fluorescence approach did not work under our experimental conditions (with limited ionization), despite using relatively high analyte concentrations. One of the reasons why our MPA optimization was only done at pH 3 and pH 7 was due to limitations of our analytical column (Agilent-Zorbax Eclipse XDB-C18, 4.6X250mm), which could only be utilized within a limited pH range; therefore, it may be possible that fluorescence detection could also work in the future, but it would require other combinations of the mobile phase and column conditions. To summarize, MPA was tested using various solvents at different pH conditions via two methods of detection (UV and fluorescence). Using the UV-visible spectrophotometer, MPA showed acceptable absorbance with consistent wavelengths compared to the literature [95-97]. Similar solvent and pH conditions were also utilized by *Rong et al.* [61, 62] for measuring MPA, MPAG,

and AcMPAG with LC/MS-MS, indicating the general suitability of these conditions for quantifying MPA irrespective of the type of detector employed.

3.1.2 Chromatography optimization

The two solvents utilized for optimization were methanol and acetonitrile, which were consistent with that utilized in our detector optimization and commonly reported in the literature for MPA assays [98, 102-106]. The two solvents were further tested systematically (discussed below) independently, with the aim to obtain a final condition with a specific solvent representing the best assay sensitivity and chromatography. In general, the main criteria for assessing chromatography were peak shape, separation, high analyte sensitivity, and short sample run time (i.e., throughput) [10, 107, 108]. A combination of 60% methanol and 40% water was observed to have some peak separation and overall good shape, along with acceptable analyte sensitivity and a run time of 13 mins. Similarly, using ACN, the ideal solvent concentration observed was 40% ACN and 60% water with a run time of 15 mins, but with much improved peak separation between the analytes. In both scenarios, a higher fraction of the organic solvent resulted in poor peak resolution as evident by separation and distance to the solvent front. This maybe due to increased or more intense interactions between higher concentrations of the organic solvent and the analytes on the C18 column (a reverse phase coating favouring non-polar analytes) being used in our assay. Typically, in a reverse phase column, polar substances are eluted first (MPA metabolites), followed by non-polar entities (MPA) [61]. This might explain why the analytes (MPA, MPAG and MPAC) elute later when the fraction of water is increased in the mobile phase, and vice versa when the concentration of the organic solvent is higher (leading to poorer resolutions).

The pH of the mobile phase was adjusted using formic acid (HCOOH) and ammonium acetate ($C_2H_7NO_2$). Formic acid is a relatively weak acid and is mainly used to adjust the pH in the buffer system for our mobile phase, consistent with the literature [53, 109, 110]. The optimal formic acid concentration was first determined in methanol, where a concentration of 0.3% vol/vol was found better for chromatographic separation. Similarly, a concentration of 0.1% vol/vol formic acid was found ideal for acetonitrile in the mobile phase. Formic acid at different concentrations did not drastically affect the absolute peak area count (i.e., sensitivity) or the chromatography (as seen in Figure 2.29 and Figure 2.32). On the other hand, when formic acid was completely absent in the mobile phase, the peak shape was not ideal (Figure 2.28), and this may be due to the loss of buffer capacity especially in the sole presence of ammonium acetate in the mobile phase. In general, the combination of a weak acid, such as formic acid, and a weak base such as ammonium acetate can lead to a neutralization reaction which ends up forming a salt (ammonium formate) that maintains buffer capacity.

With the above parameters, the chromatographic peaks for MPA and MPAC were still eluting too close to each other; therefore, we also attempted to optimize the separation between the two analytes using other means. The subsequent optimization for ammonium acetate was done in methanol and acetonitrile which resulted in the final concentrations being 1 mM and 2 mM, respectively. Similar to formic acid, varying the ammonium acetate concentration did not affect the peak areas significantly. The resolutions of MPA and MPAG peaks were still poor in methanol, whereas when acetonitrile was used, the peaks exhibited much better separation (refer to Figure 2.33). The use of ammonium acetate and formic acid has previously been reported by *Rong et al.* [61, 62] in our lab using LC-MS/MS and other studies [2, 62, 96, 111-115], suggesting that this buffer system is generally suitable for MPA chromatography.

On the other hand, phosphoric acid (H_3PO_4) has also been commonly used in HPLC chromatography [69, 95, 101, 102, 104-106, 116, 117], but in different conditions as tested in our laboratory. In our hands, phosphoric acid was used in conjunction with potassium phosphate monobasic at 40 mM (in methanol) and 100 mM (using ACN). As seen in Figure 2.39, substituting formic acid with phosphoric acid resulted in very poor resolution of MPA and MPAC peaks. This may have been due to phosphoric acid being a weak triprotic acid potentially exhibiting more complex interactions with both the mobile phase and our analytical column. Phosphoric acid has typically been used at low pH values (i.e., 2.3) in the literature [69] which is in contrast with the condition utilized in our lab, where a higher pH of 4.3-5.1 was utilized. These findings further point to the need for the careful optimization of pH and buffer concentrations (as seen in Figure 2.40, Figure 2.42 and Figure 2.43). Moreover, phosphoric acid with potassium phosphate monobasic as a buffer system for MPA also generated more interference peaks in the background with apparent instability of the pressure readings in the UPLC instrument. These data suggested the incompatibility of phosphoric acid with our utilized reversed-phase column. Taken together, phosphoric acid was not further developed for this thesis.

Chromatography can also be affected by factors such as flow rate and injection volume [107, 108]. Flow rate is the volume of the solvent (mobile phase) flowing through the column and the instrument per unit time (i.e., minute). Flow rate is one of the parameters that can determine the overall chromatography quality, affecting the separation and the overall run time [10, 108]. The optimal flow rate conditions using methanol and acetonitrile were both found to be 0.5 mL/min (as seen in Figure 2.44 and Figure 2.47). It was observed that the peak area counts decreased as the flow rate was increased in methanol (**Error! Reference source not f**

ound.), possibly because a faster flow rate was associated with reduced interaction with the analytical column. As the same time, faster flow rates also led to the poor retentions of analytes on the column and hence this resulted in poor chromatographic separations. In general, slower movements of the mobile phase (i.e., low flow rate) increases the time of interaction between the stationary phase (column) and the mobile phase (with MPA), leading to a better analyte resolution at the expense of the total run time (for both solvents). On the contrary, when the flow rate was optimized for MPA using acetonitrile, the peak area count was the lowest at 0.25 mL/min, but maximum at 0.5 mL/min after which it started decreasing again. This flow rate condition of 0.5 mL/min was ideal and showed good peak shape(s) and separation overall. The difference observed on the effects of flow rate between ethanol and acetonitrile suggest different interactions between each organic solvent with the stationary phase and analytes, requiring a systematic approach in assay optimization.

A higher injection volume generally results in more analytes being available to interact with the column. An injection volume of 10 µL was found to be ideal for chromatographic peak separation and peak shape for MPA analytes in both methanol and acetonitrile. The optimal injection volume used in this assay has also been used in the analytical assay(s) developed by *Rong et al.* [61] using the same column, but with a different detector, suggesting that the volume parameter is likely tailored to the specific column. With a higher injection volume, peak tailing and asymmetry were observed, which may have been due to the over-saturation of the column exceeding the capacity of the already optimized mobile phase-stationary phase conditions (please see above). Notably, a few other studies have employed an injection volume of 10 µL in their MPA assays [61, 111, 115, 117, 118]. *Arpini et al.* [69], *Wilhelm et al.* [95], and *Zivanovic et al.* [101] utilized 25 µL injection volume in their HPLC assays to quantify MPA and its metabolites,

whereas others have used even higher injection volumes of 50-100 µL [79, 119]. These literature data highlight an advantage of our analytical assay of using a lower injection volume of 10 µL for the quantification of MPA, MPAG and MPAC. A lower analytical volume can translate to reduced assay complexity, reduced costs, lower number of samples required, and increased assay throughput.

3.1.3 Sample extraction optimization

Acetonitrile was chosen to be the optimal solvent (vs. methanol) to quantify MPA and its metabolites in our assay, primarily due to twice the peak area intensity and much improved chromatographic peak separation between MPA and MPAC compared to methanol (refer to Figure 2.56). However, a limitation of using acetonitrile was the extended eluting times, resulting in overall increased run time of 24 mins (i.e., sacrificing overall throughput). The final optimized conditions were - ACN at 40%, ammonium acetate at 2 mM, formic acid at 0.1% v/v, injection volume of 10 µL and the run time at 24 mins with UV wavelengths at 305 nm and 295 nm.

The calibration range is an important component of any given analytical assay since it provides a quantitative measure of assay sensitivity, linearity, and limits of detection [92, 120]. It also provides a qualitative assessment on the clinical relevance/utility of the assay [62]. The calibration range of an analyte has an upper limit of quantification (ULOQ) that represents the highest concentration up to which the analyte gives a linear response, and a lower limit of quantification (LLOQ) that represents the lowest concentration of the analyte that can be quantified reliably [92]. Initially, the LLOQ of MPA assay was tested using pure acetonitrile for

range/limit finding. The range was set from 0.00003 µg/mL to 64 µg/mL to capture the physiological concentrations of MPA (i.e., C_{max} of 36.8 µg/L and a C_{trough} of 0.7 µg/L have been observed in adult KTR [11]). Although the correlation coefficient had a high value of 0.999 on the calibration curve, the lowest concentration was not detectable and hence was not considered as the LLOQ in our assay. With these preliminary data, further assay optimizations were conducted in human plasma to obtain a linear response of MPA and MPAG with a high correlation coefficient value (with the calibration range being set between 0.125 µg/mL to 64 µg/mL, i.e., still within the normal physiological range). MPAC was fixed at 30 µg/mL, but this concentration of the internal standard was also further optimized to obtain the ideal sensitivity in the plasma matrix (please see below). As the human plasma has large quantities of proteins [121], the extraction protocols also had to be optimized for sample clean up. Our approach was adapted from another method in our lab by *Rong et al.* [61] who used a single step extraction protocol for detecting MPA in the human plasma [61, 62]. Various other assays for MPA had used more complex extraction methods with multi-step processes [76, 79, 96, 97, 122, 123], thus our sample work up method reduces the overall complexity and increases the overall throughput of the assay. In human plasma on our UPLC assay, the LLOQ was later optimized along with the other parameters to be 0.3003 µg/mL, indicating our analytical assay was able to detect physiologically relevant concentrations of MPA as stated above. In general, our assay has comparable sensitivity compared to the literature: *Kunicki et al.* [120] developed the assay with a simple protein precipitation extraction to quantify MPA from 0.1 – 40 µg/mL. *Shen et al.* [98] measured the free MPA from 5 to 1000 µg/mL, whereas *Hosotsubo* [99] measured MPA from 0.2 to 20 µg/mL. Likewise, *Kagaya et al.* [104] quantified MPA from 0.05 to 50 µg/mL, *Liu*

[109] validated their assay for MPA within the range of 0.1 – 50 µg/mL, and *Wiwattanawongsa et al.* [103] quantified MPA from 0.2 to 50 µg/mL.

MPAC, the internal standard employed for this assay, has previously been used in the literature for the quantification of MPA due to the similarities in the chemical structures of the two compounds [69, 95, 96, 117]. Our data indicated a potential interference between high concentrations of MPAC and the chromatography or the sensitivity of MPA; therefore, MPAC was further optimized in human plasma to avoid saturating the UPLC column or the detector. To do so, MPAC was optimized from 0.4 µg/mL to 121.01 µg/mL (please refer to section 2.4.4.3), and the final MPAC concentration used was 22.5 µg/mL which provided sufficient intensity without interference or saturation at the detector.

Sample concentration using *SpeedVac*, higher injection volume (please refer to section 2.4.4.4) and a higher solvent extraction volume (refer to section 2.4.4.5) were also systematically optimized. Further concentration of samples using *SpeedVac* improved the sensitivity (as explained in section 2.4.4.4) by increasing the peak area counts for MPA by 2-3 folds, which was expected based on the reduced absolute volume while maintaining the same quantity of analytes. Similarly, injection volume was increased from 10 µL to 50 µL (as explained in section 2.4.4.4) but was ultimately kept at 10 µL for the plasma matrix since increasing the injection volume also caused peak distortion and tailing, similar to our optimization results in pure organic solvent (discussed above). Moreover, using the higher PPS-to-plasma ratio also resulted in an increase in the sensitivity of MPA, which was most likely due to increased contact surface area between the analyte and the organic solvent during the liquid extraction process.

3.1.3.1 *Matrix effects of plasma (on MPAG)*

There were apparent matrix interferences observed with MPAG in plasma samples, which were not observed in pure organic solvents (Figure 2.55). This is likely due to the proteins and macromolecules known to be present in the plasma [121] likely having eluted at the same retention times as MPAG due to similar hydrophilicity. In this assay, using the best optimized conditions, the elution of MPA was at approximately 20.2 mins, MPAG at approximately 5.4 mins, MPAC at approximately 17.5 mins, and the solvent front at approximately 4.5 mins. The peak for MPAG was eluting very closely to the solvent front and this interference was not preventable unless further extensive changes in mobile phase or column conditions were made. For example, this interference can be potentially minimized by using a gradient condition, using a higher purity of blank plasma, or decreasing the volume of plasma in the sample preparation (which would require further improvements in assay sensitivity). Alternatively, the LC-MS/MS could also circumvent this interference issue [61], but this would require the utilization of very costly mass spectrometry detectors which may not be readily available in all academic settings. As the result, further testing, or quantification of MPAG was not considered in plasma or in DBS. However, this ultimately does not affect our overall hypothesis testing, since MPA is the primary analyte measured for the purpose of TDM clinically [124-127]. Although it is ideal to quantify MPA and MPAG within the same assay, it is not yet done routinely in the clinic.

3.1.4 Assay validation

Our assay was fully validated in human plasma in accordance with the guidelines put forward by the United States Food and Drug Association (U.S.F.D.A) for bioanalytical method validation [92]. The FDA has several criteria for validation: standard calibration range

determination (with high r^2 values), accuracy and precision calculation using quality control samples (QCs), sensitivity quantification, selectivity, recovery, and stability of the analyte(s) [92]. The main purpose for validating an assay is to ensure the assay is accurate and precise in the measurement of the analytes in any given matrix, is reproducible, and is robust under various storage conditions [92]. Our validation criteria were tailored to the clinical usage of this assay. For example, our storage condition and freeze-thaw conditions were designed based on typical conditions observed in tertiary Canadian teaching hospitals where transplant clinics are situated. The purpose of recovery testing was to estimate the fraction of the analyte that was being extracted or the fraction that was lost during the sample preparation process [92]. The recovery for MPA (refer to table 2.9) was estimated to be between 76% to 95% using human plasma, which is generally considered optimal and consistent with the literature. *Ferreira et al.* [72] presented a recovery of 85±5%, whereas *Resendiz-Galvan et al.* [128] developed and validated an assay with the MPA recovery ranging from 90.96% to 105.13%. The assay developed by *Kunicki et al.* [120] showed a recovery of 86.04% and the recovery of MPA, as reported by *Liu et al.* [109], ranged from 89.1% to 92.0%. The fraction of MPA that was lost (~5%) may have been due to several factors such as impurities in the plasma that may have interfered with the extraction of MPA, inadequate organic solvent contact time/volume, inadequate centrifugation…etc. Therefore, the extraction efficiency may be further improved by the use of different solvent systems (methanol instead of ACN or a mixture of methanol and ACN), longer centrifugation time, higher centrifugation speed, longer vortex time, and higher solvent concentrations or volumes. The current assay calibration range was from 0.3003 µg/mL to 10 µg/mL, which adequately covered the normal physiological range of MPA measured in the clinics for KTR [95, 111, 119]. As discussed above, the LLOQ of this assay was generally

comparable to that reported in the literature for MPA, and lower than a few existing assays – *Elbarby et al.* [116] reported an LLOQ of 1 µg/mL, *Indjova et al.* [117] reported an LLOQ of 1 µg/mL and, *Tszyrsznic et al.* [114] used the LLOQ of 1 µg/mL for their assay. Collectively, not only has this assay been fully validated for use in the clinics for the quantification of MPA, but it also performs relatively better than many already published methods.

3.1.5 MPA measurement using dried blood spots

Dried blood spot (DBS) collection is a novel micro sampling technique by which the sample is collected using a finger or a heel prick [93]. The conventional whole blood sampling via venipuncture is still considered the 'gold standard' as compared to DBS collection [93]. However, venipuncture has some drawbacks, such as the need of a skilled or trained professional for sample collection which adds to the costs of care; highly invasive nature with potential for iatrogenic infection; low patience compliance; and poorly accepted in pediatric patients (fear of needles) or geriatrics (complications in finding the circulatory veins) [93]. DBS, on the other hand, has the advantage of being a minimally invasive sample collection via a needle prick; suitable for patient self collection; requiring significantly reduced blood volume; and potentially improving patient compliance especially in pediatrics and geriatrics [93, 94]. Furthermore, the DBS method is useful for patients residing in rural areas who may not have access to laboratory services, requires less complex analytical assays (as demonstrated in our proof-of-concept analyses), and has much improved sample stability compared to whole blood (i.e., can be mailed via Canada Post) [93].

For proof-of-concept, our validated MPA assay was applied to the DBS method to determine if this approach was feasible in our laboratory. Ultimately, the goal was to be able to replace venous plasma sampling of MPA for the purpose of TDM. The adaptation of our validated UPLC-UV assay in DBS involved generating a standard calibration curve to test the overall linearity, sensitivity, and reproducibility (i.e., proof-of-concept). Our findings indicated that the assay response in plasma was relatively higher than DBS, which may be explained by reduced extraction efficacy (Table 2.10) with DBS papers. As the result, the standard calibration range for MPA in DBS was further calibrated from 3.7946 μg/mL to 28.57 μg/mL (as shown in Figure 2.71). Overall, our collective findings indicated that our plasma MPA assay can be easily translated to the DBS, and the only change needed was to increase the ULOQ and LLOQ of MPA. Furthermore, for potential clinical use, the internal standard can be either added at the point of care (i.e., by the patient) or by laboratory people processing the received DBS card. To further optimize our DBS assay, the effects of adding the internal standard, MPAC, before or after DBS spotting was also tested (section 2.4.6.3), as it was suspected that the extraction process may have affected the reproducibility of the assay. Our results indicated that adding MPAC after DBS spotting resulted in reduced variability compared to adding the internal standard during sample spotting. Our data can potentially streamline the design of the DBS collection process once our findings are translated to the clinic.

To further extend our positive, proof-of-concept findings, the sensitivity, and the precision of our MPA DBS assay can be improved. Here are a few approaches that can possibly help in increasing the sensitivity of detecting MPA in DBS:

- Use of different solvent conditions (isocratic vs. gradient or methanol instead of acetonitrile)

- Optimization of the solvent compositions and/or volume
- Increasing the time of extraction
- Decreasing the drying time for the DBS cards
- Optimizing the centrifuge parameters
- Increasing the injection volume (without saturating the response at the column)

To further improve the extraction efficiency (ranging from 24% to 35% in DBS) and reproducibility, other types of DBS cards may be utilized. The current DBS card is the Whatman 903® Protein saver card, and other studies have also reported using non-cellulosic DMS cards [70], Whatman FTA DMPK-C sampling papers [129, 130], Whatman no. 10 535 097 [131], 097 Whatman paper [132, 133], and the Whatman FTA DMPK-A paper [134]. The different materials of each unique DBS platform may provide additional means to optimize the assay. In addition, the volume of the blood spotted can also be increased, depending on the absorbance area of the spot on the DBS card(s). The spot volume for this assay has already been optimized and finalized at 40 μL, where this volume of blood did not escape the boundary areas on the DBS while covering most of the spot area (please refer to section 2.4.6.1).

Once the sensitivity and precision of the DBS assay has been optimized, we will proceed to validate the DBS approach according to the FDA guidelines (please see section 2.2.5.1, 2.2.5.2, 2.2.5.3). Once validated successfully in the laboratory setting, the assay will also need to be validated in the clinical setting where capillary blood and plasma are to be collected simultaneously from the same patients to allow us to conduct direct concentration comparisons of MPA in both matrices. Prediction-error analysis including the use of specific mathematical tools such as correction factors, Bland-Altman plots, Passing-Bablok regression analysis of both

$AUC_{0\text{-}24h}$ and C_{trough} samples will be conducted [8, 69-71]. Once validated, the performance of our assay can also be systematically compared to the limited number of MPA DBS assays already reported in the literature (refer to **Chapter 1**, Table 1.1).

3.2 Development of the UPLC-RF assay quantifying *p*-cresol

3.2.1 Method of detection

Many studies in the literature have employed fluorescence [135-137] for the detection of *p*C and its metabolites. Other studies have also used UV detection for *p*C and associated analytes (e.g. [53]). Fluorescence works on the principle of exciting a proton to a higher energy level that causes a release of energy as it returns to the ground state [138]. *p*-Cresol has a hydroxyl group in its chemical structure (Figure 1.3) which can get deprotonated at low pH and potentially release the excited hydrogen atom which emits fluorescence. This may be the reason why fluorescence detection proved to be more sensitive in our laboratory for *p*C compared to UV absorbance. Additionally, using the fluorescence detection method, distinct 3D spectra for *p*C and metabolites were observed (Figure 2.79-Figure 2.82). The fluorescence wavelength that was obtained after injecting *p*C in pure acetonitrile showed an excitation and emission wavelengths of 270-290 nm and 295-315 nm respectively (regardless of the pH). Similarly, the fluorescence wavelength that was obtained after injecting *p*C in pure water showed an excitation and emission wavelengths of 220-290 nm and 295-315 nm respectively (regardless of the pH). Based on these data, changing the pH or the solvent did not affect the optimal wavelength or the detection of *p*C, indicating our conditions for *p*C detection to be relatively robust and consistent with the literature [135].

3.2.2 Chromatography optimization

Using methanol, a combination of 73% methanol and 27% water was observed to have the ideal peak separation and peak shape, along with good analyte sensitivity with a run time of 15 mins. Similarly, using ACN, the ideal solvent concentration observed was 40% ACN and 60% water with a similar run time of 15 mins. Using methanol, the peaks for *p*C, *p*CS, *p*CG and DMP were observed to be eluting very close to each other, and in close proximity to the solvent front especially at higher solvent concentrations. This maybe due to strong organic phase interactions with these analytes, pulling them away from the reverse phase C18 column being used for the chromatography (Agilent®-Zorbax Eclipse XDB-C18 with 4.6X250mm). This may also explain why these analytes (*p*C, *p*CS, *p*CG and DMP) elute later in the chromatography when the fraction of water is increased in the mobile phase. Once the composition of the solvent(s) was optimized, the next parameter to be optimized was the pH of the mobile phase, adjusted using formic acid (HCOOH) and ammonium acetate ($C_2H_7NO_2$). The formic acid was first optimized using methanol, where a concentration of 0.505% vol/vol was found ideal chromatography. Similarly, a concentration of 0.100% vol/vol formic acid was found ideal for the chromatography in acetonitrile. The effects of formic acid on the *p*C assay were generally similar to that described for MPA (provided above), acting in the capacity of a buffering reagent. Moreover, the optimization for ammonium acetate was conducted using methanol and acetonitrile that resulted with the final concentrations being 0.4 mM and 0.8 mM, respectively. Similar to the MPA assay, the peaks showed better separation with acetonitrile than methanol, and these initial findings suggested that acetonitrile was the likely better solvent for *p*C, as it was

for MPA (discussed above). Likewise, the use of phosphoric acid (H_3PO_4) in conjunction with potassium phosphate resulted in very poor resolution of *p*CS and *p*CG peaks.

The optimal flow rate conditions using methanol and acetonitrile were found to be 1.0 mL/min and 0.5 mL/min respectively (as seen in Figure 2.107 and Figure 2.110). The peak area counts when flow rate was optimized using methanol were inversely correlated to the flow rate (Figure 2.109), as discussed for the MPA assay. Similarly, an injection volume of 10 µL was also found to be ideal condition to obtain the best chromatographic peak separation and peak shape for the *p*-cresol assay in both methanol and acetonitrile. The injection volume used in this assay (10 µL) has also been used in the analytical assay(s) developed by *Korytowska et al. [139]* and *Rong et al.* [61] using LC/MS-MS. As discussed for the MPA assay, a higher injection volume resulted in tailing and asymmetrical peaks due to likely saturating effects. Compared to the literature, *Smet et al.* used a high injection volume of 50 µL for their analytical assay [140] whereas *Zhu et al.* [53] utilized a very small volume of 5 µL in their HPLC assay to quantify *p*-cresol and its metabolites; therefore, a 10 µL volume provided a relatively improved performance compared to the other analytical assays [140] mentioned in the literature.

3.2.3 Sample preparation optimization

The peaks for *p*C, *p*CS, *p*CG and DMP using methanol were eluting at approximately 3.4 mins, 3.0 mins, 2.6 mins, and 4.2 mins respectively, with an overall run time of 10 mins. As evident from the elution times, the peaks for *p*CS and *p*CG were resolving very close to each other, which was not ideal for this assay. On the contrary, when using acetonitrile, the peaks for the solvent front, *p*C, *p*CS, *p*CG and DMP were eluting at approximately 4.0 mins, 12.0 mins,

6.0 mins, 5.0 mins and, 20.0 mins respectively, with an overall run time of 24 mins. As evident from the elution times, the separation between *p*CS and *p*CG was ideal with the sensitivity much improved with this particular solvent. Furthermore, the LLOQ of the *p*C assay was tested using pure methanol where the calibration range was set between 0.002 µg/mL to 250 µg/mL, which corresponded with the physiological concentrations of *p*-cresol reported in the literature (*Smet et al.* (0.432 – 1.373 µg/mL in healthy volunteers) and (5.78 – 16.004 µg/mL in outpatients); *Vandholder et al.* [141], (2.199 – 44.797 µg/mL total *p*C concentration) using human plasma and (0.539 – 27.745 µg/mL free *p*C concentration). However, although the correlation coefficient had a high value of 0.9983 for the *p*C calibration curve, the lowest tested concentration did not show peaks in the chromatography and hence was not considered as the LLOQ. As the result, the calibration range was set from 0.250 µg/mL to 64 µg/mL in human plasma, and the internal standard DMP was fixed at a concentration of 25 µg/mL. Our overall approach was adopted from another method by our lab [53] which used a relatively simple single step extraction protocol for the detection of *p*CS and *p*CG in HepaRG cell culture. Ultimately, it was evident that *p*C, *p*CS, *p*CG were all detectable at a low concentration of 0.002 µg/mL, and the LLOQ was found to be 0.7276 µg/mL, which is still physiologically relevant given the *p*C concentration range reported above.

DMP has previously been used in the literature as the internal standard for the quantification of *p*C, *p*CS and *p*CG because of the similarity in the chemical structures between these compounds (i.e., the presence of phenolic functional group [48, 53, 140]). Using the same approach as stated for the MPA assay (discussed above), the optimal concentration of DMP was also optimized in plasma, where a concentration of 25 µg/mL did not saturate the column or the detector, with acceptable chromatography. After the concentration of the internal standard was

optimized, there were a few more parameters that were tested for improving the sensitivity of pC and to achieve the peak separation between *p*CS and *p*CG, using the same approach discussed for the MPA assay. Overall, the sensitivity (peak area counts) of *p*C was observed to be higher and the overall separation better between *p*C and DMP when using acetonitrile as compared to methanol, which is why the former was chosen as the solvent for our further characterization. Unfortunately, in regardless of our optimization efforts, *p*CG and *p*CS peaks were observed to be merging with the solvent front peak, possibly due to matric interference which was also observed and discussed for the MPA assay. Hence, the two metabolites of the analytes were not included in our subsequent development or validation.

p-Cresol is a protein-bound uremic toxin that gets accumulated in the biological fluids and is metabolized to *p*CS (major metabolite) and *p*CG (minor metabolite) [48]. Although the ideal assay should be able to measure *p*C, *p*CS, and *p*CG simultaneously, this was not achieved in our assay development efforts. Alternatively, one could measure "total" *p*-cresol content, which is the sum of *p*C, *p*CS, and *p*CG concentrations in the plasma, an approach that widely accepted in the literature (e.g., *Rong et al.* [55]). In order to measure total *p*C, we needed to subject our samples to de-conjugation using heat and acid conditions. The two components of a de-conjugation process, heat, and acid (similar to the de-conjugation of *p*C in the living system after metabolism), were optimized in our *p*C assay based on protocols adapted from [48, 135, 142]. First, the optimal heating time was tested from 15 to 60 minutes (please refer to section 2.5.4.7.1) with the acid concentration fixed at 6M, and it was found that heating time longer than 15 minutes caused sample degradation. Similarly, the concentration of HCl was optimized from 3M to 12M, where the heating time was fixed at 15 mins. The ideal HCl acid concentration was found to be 6M based on *p*C peak area counts. Moreover, as the deconjugation process was not

complete, a deconjugation ratio was calculated (refer to section 2.5.4.7.2) as a correction factor to accurately estimate the total *p*C concentrations. To estimate the fraction of *p*CS that has been converted to *p*C, de-conjugation ratio for this assay was found to be between 79.79% at 3.00 µg/mL and 61.19% at 10.00 µg/mL (as mentioned in table 2.11), which are considered workable under physiological concentrations of *p*C. Alternatively, one could utilize LC-MS/MS assays to quantify *p*C and *p*CG individually as evident by our published assay [62], but access to this instrument may be restrictive in some academic settings. Based on these limitations, only total *p*C concentrations using our optimized deconjugation method was used for the subsequent assay validation.

3.2.4 Assay validation

Our total *p*C assay in plasma was fully validated in accordance with the guidelines put forward by the United States Food and Drug Association (U.S.F.D.A) for bioanalytical method validation [92]. However, the recovery for the *p*C assay in plasma (refer to table 2.14) was estimated to be between 30% to 45%, a value significantly lower than that reported for our MPA assay. As discussed for MPA, this extraction efficiency may be further improved by using alternative solvent conditions (methanol instead of ACN or a mixture of methanol and ACN), longer centrifugation time, higher centrifuge speed, longer vortex time, higher solvent concentration or volume, and further optimization of de-conjugation conditions. The assay calibration range for *p*C in our assay was from 0.7276 µg/mL to 31.25 µg/mL, which is consistent with the reported physiological range of *p*-cresol measured in the clinics in KTR [48, 136, 140, 141]. The current LLOQ of this assay is 0.7276 µg/mL, which is also lower than that reported by a few others, such as, *Korytowska et al.* [139] LLOQ is 0.85 µg/mL], indicating that

we have further improved the assay performance for *p*C and contributed positively to the literature body.

3.2.5 p-Cresol measurement using dried blood spots (DBS)

Similar to the MPA assay, we were also able to successfully translate our plasma *p*C assay to the DBS matrix as a proof-of-concept, although the assay response in DBS was significantly reduced possibly due to the significantly reduced extraction efficiency (please refer to table 2.15). The standard calibration curve for *p*C in DBS was from 0.7276 µg/mL to 31.25 µg/mL, which is considered physiologically relevant. In contrast to the MPA assay, the effects of adding the internal standard, DMP, before and after the DBS spotting was comparable, with no clear advantage with either approach; therefore, further testing is required to elucidate this particular assay condition. In regard to future work to expand on our positive data, the sensitivity and precision/extraction of *p*C DBS assay can be further improved using criteria already discussed for the MPA DBS assay (please see above). A similar clinical validation paradigm for *p*C using DBS as described for MPA can be conducted simultaneously, as a means to further validate the drug interaction between these agents already documented in our recent clinical report [62]. Our *p*C assay in DBS is also the first reported in literature to our knowledge.

3.3 Limitations

In addition to the limitations that have already been discussed in this chapter:

- In our study, only the UV-visible spectrophotometer and RF-Spectro photo fluorimeter were used to detect MPA and *p*-cresol. Therefore, the use of other

detectors such as diode array detector (DAD) or the LC-MS/MS could also be considered in the future to further improve sensitivity and selectivity.

- Our assay only systematically tested methanol and acetonitrile as the organic solvents. Therefore, additional mobile phase compositions using isopropanol, ethanol, butanol, carbon tetrachloride, propanone, or ethyl acetate with different chemical interactions with the analytes and the column can potentially further improve chromatography and sensitivity (i.e., for MPAG, *p*CG, or *p*CS).
- The current column used in our study was a reversed phase (RP) Agilent-Zorbax Eclipse XDB-C18, 5 µm, 4.6×250 mm column, but we could have tested other HPLC columns such as biphenyl RP columns, C4 RP columns, C8 RP columns, polar embedded RP columns, porous graphitic carbon RP column, or phenyl-hexyl RP column, etc. that may also be suitable for resolving MPA and *p*C.
- We had developed separate assays for both MPA and *p*C in plasma and DBS. Ideally, further developments should consider combining the two analytical assays to improve the overall efficiency and minimize the number / volume of blood samples required from patients.

3.4 Conclusions

In conclusion, we have successfully developed and validated two analytical assays for the quantification of MPA and *p*C in human plasma. In addition, we were able to successfully translate, as a proof-of-concept, these assays to the DBS matrix. Our assays have generally improved performances compared to published assays in the literature. This is also the first instance where *p*C has been analyzed from a DBS card. We anticipate our assays to be utilized in

the transplant population to efficiently detect the MPA-*p*C interaction in a minimally invasive manner. Ultimately, our assay can potentially improve the precision dosing and TDM of MPA, resulting in improved patient care in this already fragile population.

References

1. Favi, E. and R. Cacciola, *Clinical and Surgical Challenges in Kidney Transplantation: Toward a Personalized Approach?* Medicina (Kaunas), 2022. **58**(5).
2. *Kidney Foundation of Canada. Facing the facts*. 2020 cited June 29, 2022]; Available from: https://kidney.ca/KFOC/media/images/PDFs/Facing-the-Facts-2020.pdf.
3. Information, C.I.f.H., *Summary Statistics on Organ Transplants, Wait-Lists and Donors* 2021, Canadian Institute for Health Information: Ottawa, Ontario, Canada.
4. Baker, R.J., et al., *Renal association clinical practice guideline in post-operative care in the kidney transplant recipient.* BMC Nephrol, 2017. **18**(1): p. 174.
5. Lai, X., et al., *Tackling Chronic Kidney Transplant Rejection: Challenges and Promises.* Front Immunol, 2021. **12**: p. 661643.
6. Moudgil, A., *Renal transplantation.* Indian J Pediatr, 2003. **70**(3): p. 257-64.
7. Buchwald, A., K. Winkler, and T. Epting, *Validation of an LC-MS/MS method to determine five immunosuppressants with deuterated internal standards including MPA.* BMC Clin Pharmacol, 2012. **12**: p. 2.
8. Zwart, T.C., et al., *Therapeutic drug monitoring of tacrolimus and mycophenolic acid in outpatient renal transplant recipients using a volumetric dried blood spot sampling device.* Br J Clin Pharmacol, 2018. **84**(12): p. 2889-2902.
9. Di Maira, T., E.C. Little, and M. Berenguer, *Immunosuppression in liver transplant.* Best Pract Res Clin Gastroenterol, 2020. **46-47**: p. 101681.
10. Bergan, S., et al., *Personalized Therapy for Mycophenolate: Consensus Report by the International Association of Therapeutic Drug Monitoring and Clinical Toxicology.* Ther Drug Monit, 2021. **43**(2): p. 150-200.
11. Staatz, C.E. and S.E. Tett, *Clinical pharmacokinetics and pharmacodynamics of mycophenolate in solid organ transplant recipients.* Clin Pharmacokinet, 2007. **46**(1): p. 13-58.
12. Ltd., H.-L.R., *Product Monograph Including Patient Medication Information (CellCept® mycophenolate mofetil)*, H.-L.R. Ltd., Editor. 2022: Mississauga, Ontario, Canada.
13. Jayne, D., *Non-transplant uses of mycophenolate mofetil.* Curr Opin Nephrol Hypertens, 1999. **8**(5): p. 563-7.
14. Allison, A.C., *Mechanisms of action of mycophenolate mofetil.* Lupus, 2005. **14 Suppl 1**: p. s2-8.
15. Currie, G.M., *Pharmacology, Part 1: Introduction to Pharmacology and Pharmacodynamics.* J Nucl Med Technol, 2018. **46**(2): p. 81-86.
16. Kitchin, J.E., et al., *Rediscovering mycophenolic acid: a review of its mechanism, side effects, and potential uses.* J Am Acad Dermatol, 1997. **37**(3 Pt 1): p. 445-9.
17. Wong, G. and J.R. Chapman, *Cancers after renal transplantation.* Transplant Rev (Orlando), 2008. **22**(2): p. 141-9.
18. Meier-Kriesche, H.U., et al., *Pharmacokinetics of mycophenolic acid in renal insufficiency.* Ther Drug Monit, 2000. **22**(1): p. 27-30.
19. Fulton, B. and A. Markham, *Mycophenolate mofetil. A review of its pharmacodynamic and pharmacokinetic properties and clinical efficacy in renal transplantation.* Drugs, 1996. **51**(2): p. 278-98.

20. Toutain, P.L. and A. Bousquet-Melou, *Bioavailability and its assessment.* J Vet Pharmacol Ther, 2004. **27**(6): p. 455-66.
21. Cossart, A.R., et al., *Characterizing the pharmacokinetics and pharmacodynamics of immunosuppressant medicines and patient outcomes in elderly renal transplant patients.* Transl Androl Urol, 2019. **8**(Suppl 2): p. S198-S213.
22. Picard, N., et al., *Identification of the UDP-glucuronosyltransferase isoforms involved in mycophenolic acid phase II metabolism.* Drug Metab Dispos, 2005. **33**(1): p. 139-46.
23. Staatz, C.E. and S.E. Tett, *Pharmacology and toxicology of mycophenolate in organ transplant recipients: an update.* Arch Toxicol, 2014. **88**(7): p. 1351-89.
24. Bullingham, R.E., A.J. Nicholls, and B.R. Kamm, *Clinical pharmacokinetics of mycophenolate mofetil.* Clin Pharmacokinet, 1998. **34**(6): p. 429-55.
25. Sherwin, C.M., et al., *The evolution of population pharmacokinetic models to describe the enterohepatic recycling of mycophenolic acid in solid organ transplantation and autoimmune disease.* Clin Pharmacokinet, 2011. **50**(1): p. 1-24.
26. Benjanuwattra, J., D. Pruksakorn, and N. Koonrungsesomboon, *Mycophenolic Acid and Its Pharmacokinetic Drug-Drug Interactions in Humans: Review of the Evidence and Clinical Implications.* J Clin Pharmacol, 2020. **60**(3): p. 295-311.
27. Uwai, Y., et al., *Interaction and transport characteristics of mycophenolic acid and its glucuronide via human organic anion transporters hOAT1 and hOAT3.* Biochem Pharmacol, 2007. **74**(1): p. 161-8.
28. Geng, F., et al., *The association of the UGT1A8, SLCO1B3 and ABCC2/ABCG2 genetic polymorphisms with the pharmacokinetics of mycophenolic acid and its phenolic glucuronide metabolite in Chinese individuals.* Clin Chim Acta, 2012. **413**(7-8): p. 683-90.
29. Inoue, K., et al., *Influence of UGT1A7 and UGT1A9 intronic I399 genetic polymorphisms on mycophenolic acid pharmacokinetics in Japanese renal transplant recipients.* Ther Drug Monit, 2007. **29**(3): p. 299-304.
30. Miura, M., et al., *Limited sampling strategy for simultaneous estimation of the area under the concentration-time curve of tacrolimus and mycophenolic acid in adult renal transplant recipients.* Ther Drug Monit, 2008. **30**(1): p. 52-9.
31. Picard, N., et al., *The role of organic anion-transporting polypeptides and their common genetic variants in mycophenolic acid pharmacokinetics.* Clin Pharmacol Ther, 2010. **87**(1): p. 100-8.
32. Miura, M., et al., *Influence of SLCO1B1, 1B3, 2B1 and ABCC2 genetic polymorphisms on mycophenolic acid pharmacokinetics in Japanese renal transplant recipients.* Eur J Clin Pharmacol, 2007. **63**(12): p. 1161-9.
33. Fukuda, T., et al., *UGT1A9, UGT2B7, and MRP2 genotypes can predict mycophenolic acid pharmacokinetic variability in pediatric kidney transplant recipients.* Ther Drug Monit, 2012. **34**(6): p. 671-9.
34. Hesselink, D.A., et al., *Cyclosporine interacts with mycophenolic acid by inhibiting the multidrug resistance-associated protein 2.* Am J Transplant, 2005. **5**(5): p. 987-94.
35. Kobayashi, M., et al., *Cyclosporin A, but not tacrolimus, inhibits the biliary excretion of mycophenolic acid glucuronide possibly mediated by multidrug resistance-associated protein 2 in rats.* J Pharmacol Exp Ther, 2004. **309**(3): p. 1029-35.

36. Naesens, M., et al., *Multidrug resistance protein 2 genetic polymorphisms influence mycophenolic acid exposure in renal allograft recipients.* Transplantation, 2006. **82**(8): p. 1074-84.
37. van Gelder, T., et al., *Comparison of the effects of tacrolimus and cyclosporine on the pharmacokinetics of mycophenolic acid.* Ther Drug Monit, 2001. **23**(2): p. 119-28.
38. Westley, I.S., et al., *Role of Mrp2 in the hepatic disposition of mycophenolic acid and its glucuronide metabolites: effect of cyclosporine.* Drug Metab Dispos, 2006. **34**(2): p. 261-6.
39. Cigarran Guldris, S., E. Gonzalez Parra, and A. Cases Amenos, *Gut microbiota in chronic kidney disease.* Nefrologia, 2017. **37**(1): p. 9-19.
40. Prokopienko, A.J., et al., *Development and validation of a UHPLC-MS/MS method for measurement of a gut-derived uremic toxin panel in human serum: An application in patients with kidney disease.* J Pharm Biomed Anal, 2019. **174**: p. 618-624.
41. Cunha, R.S.D., et al., *How do Uremic Toxins Affect the Endothelium?* Toxins (Basel), 2020. **12**(6).
42. Chinnappa, S., et al., *Association between Protein-Bound Uremic Toxins and Asymptomatic Cardiac Dysfunction in Patients with Chronic Kidney Disease.* Toxins (Basel), 2018. **10**(12).
43. Graboski, A.L. and M.R. Redinbo, *Gut-Derived Protein-Bound Uremic Toxins.* Toxins (Basel), 2020. **12**(9).
44. Liabeuf, S., C. Villain, and Z.A. Massy, *Protein-bound toxins: has the Cinderella of uraemic toxins turned into a princess?* Clin Sci (Lond), 2016. **130**(23): p. 2209-2216.
45. Gryp, T., et al., *p-Cresyl Sulfate.* Toxins (Basel), 2017. **9**(2).
46. Vanholder, R., R. De Smet, and G. Lesaffer, *p-cresol: a toxin revealing many neglected but relevant aspects of uraemic toxicity.* Nephrol Dial Transplant, 1999. **14**(12): p. 2813-5.
47. Rong, Y. and T.K.L. Kiang, *Mechanisms of Metabolism Interaction Between p-Cresol and Mycophenolic Acid.* Toxicol Sci, 2020. **173**(2): p. 267-279.
48. de Loor, H., et al., *Gas chromatographic-mass spectrometric analysis for measurement of p-cresol and its conjugated metabolites in uremic and normal serum.* Clin Chem, 2005. **51**(8): p. 1535-8.
49. Han, H., et al., *p-Cresyl sulfate aggravates cardiac dysfunction associated with chronic kidney disease by enhancing apoptosis of cardiomyocytes.* J Am Heart Assoc, 2015. **4**(6): p. e001852.
50. Liabeuf, S., et al., *Does p-cresylglucuronide have the same impact on mortality as other protein-bound uremic toxins?* PLoS One, 2013. **8**(6): p. e67168.
51. Mutsaers, H.A., et al., *Proximal tubular efflux transporters involved in renal excretion of p-cresyl sulfate and p-cresyl glucuronide: Implications for chronic kidney disease pathophysiology.* Toxicol In Vitro, 2015. **29**(7): p. 1868-77.
52. Mutsaers, H.A., et al., *Uremic toxins inhibit renal metabolic capacity through interference with glucuronidation and mitochondrial respiration.* Biochim Biophys Acta, 2013. **1832**(1): p. 142-50.
53. Zhu, S., Y. Rong, and T.K.L. Kiang, *Effects of p-Cresol on Oxidative Stress, Glutathione Depletion, and Necrosis in HepaRG Cells: Comparisons to Other Uremic Toxins and the Role of p-Cresol Glucuronide Formation.* Pharmaceutics, 2021. **13**(6).

54. Weigand, K.M., et al., *Uremic solutes modulate hepatic bile acid handling and induce mitochondrial toxicity.* Toxicol In Vitro, 2019. **56**: p. 52-61.
55. Rong, Y. and T.K.L. Kiang, *Characterizations of Human UDP-Glucuronosyltransferase Enzymes in the Conjugation of p-Cresol.* Toxicol Sci, 2020. **176**(2): p. 285-296.
56. Rong, Y. and T.K.L. Kiang, *Characterization of human sulfotransferases catalyzing the formation of p-cresol sulfate and identification of mefenamic acid as a potent metabolism inhibitor and potential therapeutic agent for detoxification.* Toxicol Appl Pharmacol, 2021. **425**: p. 115553.
57. Meyer, T.W. and T.H. Hostetter, *Uremic solutes from colon microbes.* Kidney Int, 2012. **81**(10): p. 949-954.
58. Chen, J.H. and C.K. Chiang, *Uremic Toxins and Protein-Bound Therapeutics in AKI and CKD: Up-to-Date Evidence.* Toxins (Basel), 2021. **14**(1).
59. Vanholder, R., R. De Smet, and N. Lameire, *Protein-bound uremic solutes: the forgotten toxins.* Kidney Int Suppl, 2001. **78**: p. S266-70.
60. Neirynck, N., et al., *An update on uremic toxins.* Int Urol Nephrol, 2013. **45**(1): p. 139-50.
61. Rong, Y. and T.K.L. Kiang, *Development and validation of a sensitive liquid-chromatography tandem mass spectrometry assay for mycophenolic acid and metabolites in HepaRG cell culture: Characterization of metabolism interactions between p-cresol and mycophenolic acid.* Biomed Chromatogr, 2019. **33**(8): p. e4549.
62. Rong, Y., et al., *Significant Correlations between p-Cresol Sulfate and Mycophenolic Acid Plasma Concentrations in Adult Kidney Transplant Recipients.* Clin Drug Investig, 2022. **42**(3): p. 207-219.
63. Magoon, R., N. Makhija, and J. Jose, *Oxygen therapy in the critically ill: Less is the new more?* J Anaesthesiol Clin Pharmacol, 2020. **36**(4): p. 433-434.
64. Kang, J.S. and M.H. Lee, *Overview of therapeutic drug monitoring.* Korean J Intern Med, 2009. **24**(1): p. 1-10.
65. Oellerich, M., P. Kanzow, and P.D. Walson, *Therapeutic drug monitoring - Key to personalized pharmacotherapy.* Clin Biochem, 2017. **50**(7-8): p. 375-379.
66. Bhatti, P., et al., *Blood spots as an alternative to whole blood collection and the effect of a small monetary incentive to increase participation in genetic association studies.* BMC Med Res Methodol, 2009. **9**: p. 76.
67. Vermeire, S., et al., *How, When, and for Whom Should We Perform Therapeutic Drug Monitoring?* Clin Gastroenterol Hepatol, 2020. **18**(6): p. 1291-1299.
68. van Gelder, T., et al., *Therapeutic drug monitoring of mycophenolate mofetil in transplantation.* Ther Drug Monit, 2006. **28**(2): p. 145-54.
69. Arpini, J., et al., *Clinical evaluation of a dried blood spot method for determination of mycophenolic acid in renal transplant patients.* Clin Biochem, 2013. **46**(18): p. 1905-8.
70. Iboshi, H., et al., *Development of a Liquid Chromatography-Tandem Mass Spectrometric Method for Quantification of Mycophenolic Acid and Its Glucuronides in Dried Blood Spot Samples.* Ther Drug Monit, 2017. **39**(6): p. 648-653.
71. Martial, L.C., et al., *Dried Blood Spot Sampling for Tacrolimus and Mycophenolic Acid in Children: Analytical and Clinical Validation.* Ther Drug Monit, 2017. **39**(4): p. 412-421.

72. Ferreira, P.C.L., et al., *Comparison of plasma and oral fluid concentrations of mycophenolic acid and its glucuronide metabolite by LC-MS in kidney transplant patients.* Eur J Clin Pharmacol, 2019. **75**(4): p. 553-559.
73. Brooks, E., et al., *Investigation of the Association Between Total and Free Plasma and Saliva Mycophenolic Acid Concentrations Following Administration of Enteric-Coated Mycophenolate Sodium in Adult Kidney Transplant Recipients.* Clin Drug Investig, 2019. **39**(12): p. 1175-1184.
74. Alsmadi, M.M., et al., *The development of a population physiologically based pharmacokinetic model for mycophenolic mofetil and mycophenolic acid in humans using data from plasma, saliva, and kidney tissue.* Biopharm Drug Dispos, 2019. **40**(9): p. 325-340.
75. Mendonza, A.E., R.Y. Gohh, and F. Akhlaghi, *Analysis of mycophenolic acid in saliva using liquid chromatography tandem mass spectrometry.* Ther Drug Monit, 2006. **28**(3): p. 402-6.
76. Wiesen, M.H., et al., *Liquid chromatography-tandem mass spectrometry method for the quantification of mycophenolic acid and its phenolic glucuronide in saliva and plasma using a standardized saliva collection device.* J Chromatogr A, 2012. **1241**: p. 52-9.
77. Shen, B., et al., *Determination of total, free and saliva mycophenolic acid with a LC-MS/MS method: application to pharmacokinetic study in healthy volunteers and renal transplant patients.* J Pharm Biomed Anal, 2009. **50**(3): p. 515-21.
78. Teshima, D., et al., *High-performance liquid chromatographic method for mycophenolic acid and its glucuronide in serum and urine.* J Clin Pharm Ther, 2003. **28**(1): p. 17-22.
79. Benoit-Biancamano, M.O., et al., *Sensitive high-performance liquid chromatography-tandem mass spectrometry method for quantitative analysis of mycophenolic acid and its glucuronide metabolites in human plasma and urine.* J Chromatogr B Analyt Technol Biomed Life Sci, 2007. **858**(1-2): p. 159-67.
80. Zheng Jiao, Y.Z., Jie Shen, Yun-qiu Yu, *Simple High-Performance Liquid Chromatographic Assay, with Post-Column Derivatization, for Simultaneous Determination of Mycophenolic Acid and its Glucuronide Metabolite in Human Plasma and Urine.* Chromatographia, 2005. **62**: p. 363-371.
81. Yau, W.P., et al., *Simple reversed-phase ion-pair liquid chromatography assay for the simultaneous determination of mycophenolic acid and its glucuronide metabolite in human plasma and urine.* J Chromatogr B Analyt Technol Biomed Life Sci, 2004. **805**(1): p. 101-12.
82. Karin M. Hold, D.d.B., Jan Zuidema, Robert A.A. Maes, *Saliva as an Analytical Tool in Toxicology.* 1996. **Volume 1**.
83. PubChem, N.L.o.M. *Mycophenolic acid*. 2005 [cited 2022; Mycophenolic acid: Compound summary]. Available from: https://pubchem.ncbi.nlm.nih.gov/compound/446541.
84. PubChem, N.L.o.M. *Mycophenolic acid glucuronide*. 2006; Mycophenolic acid glucuronide: Compound summary]. Available from: https://pubchem.ncbi.nlm.nih.gov/compound/6442661.
85. PubChem, N.L.o.M. *Mycophenolic Acid Carboxybutoxy Ether*. 2013 [cited 2022 August]; Mycophenolic Acid Carboxybutoxy Ether - Compound summary]. Available from: https://pubchem.ncbi.nlm.nih.gov/compound/71750878.

86. PubChem, N.L.o.M. *p-Cresol*. 2004; *p*-Cresol: Compound summary]. Available from: https://pubchem.ncbi.nlm.nih.gov/compound/2879.
87. PubChem, N.L.o.M. *p-cresol sulfate*. *p*-cresol sulfate, 2005 [cited 2022 August]; p-Cresol sulfate: Compound summary]. Available from: https://pubchem.ncbi.nlm.nih.gov/compound/4615423.
88. Chemical, C., *Product information - p-Cresol Glucuronide (Item No. 35113)*. 2021, Cayman Chemical: U.S.A.
89. PubChem, N.L.o.M. *2,4-Dimethylphenol*. 2005 [cited 2022 August]; 2,4-Dimethylphenol: Compound summary]. Available from: https://pubchem.ncbi.nlm.nih.gov/compound/7771.
90. Chemical, C., *Product information - Mycophenolic acid glucuronide (Item No. 19078)*. 2021: U.S.A.
91. Poesen, R., et al., *Metabolism, Protein Binding, and Renal Clearance of Microbiota-Derived p-Cresol in Patients with CKD.* Clin J Am Soc Nephrol, 2016. **11**(7): p. 1136-44.
92. U.S. Department of Health and Human Services, F.a.D.A., *Bioanalytical Method Validation Guidance for Industry*, U.S.D.o.H.a.H. Services, Editor. 2018, Center for Drug Evaluation and Research (CDER): Maryland, U.S.A. p. 1-44.
93. Gupta, K. and R. Mahajan, *Applications and Diagnostic Potential of Dried Blood Spots.* Int J Appl Basic Med Res, 2018. **8**(1): p. 1-2.
94. Gallant, J., J. Wichart, and T.K.L. Kiang, *Predictability of Capillary Blood Spot Toward Venous Whole Blood Sampling for Therapeutic Drug Monitoring of Tacrolimus in Solid Organ Transplant Recipients.* Eur J Drug Metab Pharmacokinet, 2019. **44**(6): p. 729-741.
95. Wilhelm, A.J., et al., *Analysis of mycophenolic acid in dried blood spots using reversed phase high performance liquid chromatography.* J Chromatogr B Analyt Technol Biomed Life Sci, 2009. **877**(30): p. 3916-9.
96. Mino, Y., et al., *Simultaneous determination of mycophenolic acid and its glucuronides in human plasma using isocratic ion pair high-performance liquid chromatography.* J Pharm Biomed Anal, 2008. **46**(3): p. 603-8.
97. Bahrami, G. and B. Mohammadi, *An isocratic high performance liquid chromatographic method for quantification of mycophenolic acid and its glucuronide metabolite in human serum using liquid-liquid extraction: application to human pharmacokinetic studies.* Clin Chim Acta, 2006. **370**(1-2): p. 185-90.
98. Shen, J., et al., *Quantification of total and free mycophenolic acid in human plasma by liquid chromatography with fluorescence detection.* J Chromatogr B Analyt Technol Biomed Life Sci, 2005. **817**(2): p. 207-13.
99. Hosotsubo, H., et al., *Rapid and simple determination of mycophenolic acid in human plasma by ion-pair RP-LC with fluorescence detection.* J Pharm Biomed Anal, 2001. **24**(4): p. 555-60.
100. Zhong, Y., Z. Jiao, and Y. Yu, *Simultaneous determination of mycophenolic acid and valproic acid based on derivatization by high-performance liquid chromatography with fluorescence detection.* Biomed Chromatogr, 2006. **20**(4): p. 319-26.
101. Zivanovic, L., et al., *Application of experimental design in optimization of solid phase extraction of mycophenolic acid and mycophenolic acid glucuronide from human urine and plasma and SPE-RP-HPLC method validation.* J Pharm Biomed Anal, 2008. **47**(3): p. 575-85.

102. Sugioka, N., et al., *Determination of a new immunosuppressant, mycophenolate mofetil, and its active metabolite, mycophenolic acid, in rat and human body fluids by high-performance liquid chromatography.* J Chromatogr B Biomed Appl, 1994. **654**(2): p. 249-56.
103. Wiwattanawongsa, K., et al., *Determination of mycophenolic acid and its phenol glucuronide metabolite in human plasma and urine by high-performance liquid chromatography.* J Chromatogr B Biomed Sci Appl, 2001. **763**(1-2): p. 35-45.
104. Kagaya, H., et al., *Quantification and 24-hour monitoring of mycophenolic acid by high-performance liquid chromatography in Japanese renal transplant recipients.* Yakugaku Zasshi, 2006. **126**(12): p. 1357-62.
105. Kolaci, M., et al., *Therapeutic monitoring of mycophenolic acid in renal transplanted patients by a validated HPLC method.* Folia Med (Plovdiv), 2021. **63**(5): p. 768-774.
106. Seebacher, G., et al., *A simple HPLC method for monitoring mycophenolic acid and its glucuronidated metabolite in transplant recipients.* Clin Chem Lab Med, 1999. **37**(4): p. 409-15.
107. Syed, M. and N.R. Srinivas, *A comprehensive review of the published assays for the quantitation of the immunosuppressant drug mycophenolic acid and its glucuronidated metabolites in biological fluids.* Biomed Chromatogr, 2016. **30**(5): p. 721-48.
108. Sahu, P.K., et al., *An overview of experimental designs in HPLC method development and validation.* J Pharm Biomed Anal, 2018. **147**: p. 590-611.
109. Liu, Y., et al., *Validated LC-MS/MS method for quantitation of total and free mycophenolic acid concentration and its application to a pharmacokinetic study in pediatric renal transplant recipients.* Biomed Chromatogr, 2021. **35**(2): p. e4989.
110. PubChem, N.L.o.M. *Formic acid*. Formic acid: Compound summary [cited 2022; Available from: https://pubchem.ncbi.nlm.nih.gov/compound/284.
111. Zegarska, J., et al., *Mycophenolic Acid Metabolites Acyl-Glucuronide and Glucoside Affect the Occurrence of Infectious Complications and Bone Marrow Dysfunction in Liver Transplant Recipients.* Ann Transplant, 2015. **20**: p. 483-92.
112. Kawanishi, M., et al., *Sensitive and validated LC-MS/MS methods to evaluate mycophenolic acid pharmacokinetics and pharmacodynamics in hematopoietic stem cell transplant patients.* Biomed Chromatogr, 2015. **29**(9): p. 1309-16.
113. Nguyen Thi, M.T., et al., *Mycophenolic acid quantification in human peripheral blood mononuclear cells using liquid chromatography-tandem mass spectrometry.* Clin Biochem, 2013. **46**(18): p. 1909-11.
114. Tszyrsznic, W., et al., *Two rapid ultra performance liquid chromatography/tandem mass spectrometry (UPLC/MS/MS) methods with common sample pretreatment for therapeutic drug monitoring of immunosuppressants compared to immunoassay.* J Chromatogr B Analyt Technol Biomed Life Sci, 2013. **928**: p. 9-15.
115. Delavenne, X., et al., *UPLC MS/MS method for quantification of mycophenolic acid and metabolites in human plasma: Application to pharmacokinetic study.* Clin Chim Acta, 2011. **412**(1-2): p. 59-65.
116. Elbarbry, F.A. and A. Shoker, *Simple high performance liquid chromatographic assay for mycophenolic acid in renal transplant patients.* J Pharm Biomed Anal, 2007. **43**(2): p. 788-92.
117. Indjova, D., L. Kassabova, and D. Svinarov, *Simultaneous determination of mycophenolic acid and its phenolic glucuronide in human plasma using an isocratic*

high-performance liquid chromatography procedure. J Chromatogr B Analyt Technol Biomed Life Sci, 2005. **817**(2): p. 327-30.
118. Md Dom, Z.I., et al., *Validation of an LC-MS/MS method for the quantification of mycophenolic acid in human kidney transplant biopsies.* J Chromatogr B Analyt Technol Biomed Life Sci, 2014. **945-946**: p. 171-7.
119. Daurel-Receveur, M., et al., *Fully automated analytical method for mycophenolic acid quantification in human plasma using on-line solid phase extraction and high performance liquid chromatography with diode array detection.* Ther Drug Monit, 2006. **28**(4): p. 505-11.
120. Kunicki, P.K. and A. Wrobel, *Validated Simple HPLC-UV Method for Mycophenolic Acid (MPA) Monitoring in Human Plasma. Internal Standardization: Is It Necessary?* Molecules, 2021. **26**(23).
121. Mathew, J., P. Sankar, and M. Varacallo, *Physiology, Blood Plasma*, in *StatPearls*. 2022: Treasure Island (FL).
122. Kuhn, J., et al., *Measurement of mycophenolic acid and its glucuronide using a novel rapid liquid chromatography-electrospray ionization tandem mass spectrometry assay.* Clin Biochem, 2009. **42**(1-2): p. 83-90.
123. Benech, H., et al., *Development and validation of an LC/MS/MS assay for mycophenolic acid in human peripheral blood mononuclear cells.* J Chromatogr B Analyt Technol Biomed Life Sci, 2007. **853**(1-2): p. 168-74.
124. Kiang, T.K.L. and M.H.H. Ensom, *Exposure-Toxicity Relationships of Mycophenolic Acid in Adult Kidney Transplant Patients.* Clin Pharmacokinet, 2019. **58**(12): p. 1533-1552.
125. Rong, Y., V. Patel, and T.K.L. Kiang, *Recent lessons learned from population pharmacokinetic studies of mycophenolic acid: physiological, genomic, and drug interactions leading to the prediction of drug effects.* Expert Opin Drug Metab Toxicol, 2021. **17**(12): p. 1369-1406.
126. Kiang, T.K. and M.H. Ensom, *Therapeutic drug monitoring of mycophenolate in adult solid organ transplant patients: an update.* Expert Opin Drug Metab Toxicol, 2016. **12**(5): p. 545-53.
127. Kiang, T.K.L. and M.H.H. Ensom, *Population Pharmacokinetics of Mycophenolic Acid: An Update.* Clin Pharmacokinet, 2018. **57**(5): p. 547-558.
128. Resendiz-Galvan, J.E., et al., *Determination of mycophenolic acid in human plasma by ultra-performance liquid chromatography-tandem mass spectrometry and its pharmacokinetic application in kidney transplant patients.* Biomed Chromatogr, 2019. **33**(12): p. e4681.
129. Al-Uzri, A., et al., *Longitudinal study on the use of dried blood spots for home monitoring in children after kidney transplantation.* Pediatr Transplant, 2017. **21**(6).
130. Veenhof, H., et al., *Clinical Validation of Simultaneous Analysis of Tacrolimus, Cyclosporine A, and Creatinine in Dried Blood Spots in Kidney Transplant Patients.* Transplantation, 2017. **101**(7): p. 1727-1733.
131. Cheung, C.Y., et al., *Dried blood spot measurement: application in tacrolimus monitoring using limited sampling strategy and abbreviated AUC estimation.* Transpl Int, 2008. **21**(2): p. 140-5.
132. Hoogtanders, K., et al., *Therapeutic drug monitoring of tacrolimus with the dried blood spot method.* J Pharm Biomed Anal, 2007. **44**(3): p. 658-64.

133. Hoogtanders, K., et al., *Dried blood spot measurement of tacrolimus is promising for patient monitoring.* Transplantation, 2007. **83**(2): p. 237-8.
134. Koop, D.R., et al., *Analysis of tacrolimus and creatinine from a single dried blood spot using liquid chromatography tandem mass spectrometry.* J Chromatogr B Analyt Technol Biomed Life Sci, 2013. **926**: p. 54-61.
135. Moradi, M., et al., *Simple Determination of p-Cresol in Plasma Samples Using Fluorescence Spectroscopy Technique.* Iran J Pharm Res, 2021. **20**(2): p. 68-78.
136. Niwa, T., *Phenol and p-cresol accumulated in uremic serum measured by HPLC with fluorescence detection.* Clin Chem, 1993. **39**(1): p. 108-11.
137. Moradi, M., J. Soleymani, and A. Jouyban, *A combination of amino-functionalized fibrous silica (KCC-1-NH2)/effectively and efficiently oxidized graphene oxide (EEGO) nanocomposite for dispersive solid-phase extraction, pre-concentration and fluorescence determination of total para-cresol in plasma samples of chronic kidney disease patients.* J Pharm Biomed Anal, 2022. **214**: p. 114746.
138. Hitzmann, B., *Measurement, Modeling and Automation in Advanced Food Processing*, ed. T. Scheper. Institute of Food Science and Biotechnology, University of Hohenheim, Stuttgart, Germany.: Springer. 201.
139. Korytowska, N., et al., *Development of the LC-MS/MS method for determining the p-cresol level in plasma.* J Pharm Biomed Anal, 2019. **167**: p. 149-154.
140. De Smet, R., et al., *A sensitive HPLC method for the quantification of free and total p-cresol in patients with chronic renal failure.* Clin Chim Acta, 1998. **278**(1): p. 1-21.
141. Vanholder, R., et al., *The uremic toxicity of indoxyl sulfate and p-cresyl sulfate: a systematic review.* J Am Soc Nephrol, 2014. **25**(9): p. 1897-907.
142. Martinez, A.W., et al., *Removal of P-cresol sulfate by hemodialysis.* J Am Soc Nephrol, 2005. **16**(11): p. 3430-6.